University of Strathclyde

Strathclyde Institute of Pharmacy and Biomedical Sciences

A system approach to determine how *Toxoplasma gondii* infection causes neuropsychiatric disease

By

Aisha A Abdelati Abdelsalam

A thesis submitted to University of Strathclyde in partial fulfillment of the requirements for the degree of Doctor of Philosophy

2019

This thesis is the result of the author's original research. It has been composed by the author and has not been previously submitted for examination which has led to the award of a degree.

Signed:

Date

Acknowledgements

First and foremost, I would like to thank Allah (SWT) so much for giving me the strength to perform my experiments and finish my work. Secondly, I would like to express my sincere gratitude to my supervisor Professor Craig Roberts for the continuous support of my Ph.D. study and research, for his patience, motivation, and immense knowledge. His guidance helped me in all the time of research and writing of this thesis. I could not have imagined having a better supervisor and mentor for my Ph.D. study. I would like to thank Dr. Gareth Westrop, Dr. Stuart Wood and Dr. Benjamin Pickard for sharing with me their expertise in mass spectrometry, molecular work and different lab procedures. I would like also to thank Dr. David Thomson, for sharing with me his expertise in animal Behavioural Studies and Dr. Selina Henriquez for her Ph.D. thesis which enriched my research. My sincere thanks also goes to all the staff and members of the BPU, from which their technical advice on animal care following the guidance of the Home Office procedures was a big contribution towards the fulfillment of this PhD study. Sharing my time and work with all the members of the Roberts laboratory, especially Rasha, has made the achievement of my PhD a rich and complete experience, from the scientific learning to the personal growth, and for this I would like to express my true thankfulness. Finally but not least I would like to thank my family: my husband (Mahmoud) and our children for supporting me spiritually throughout writing this thesis and my life in general. I also wish

to extend my thanks to my mother and sister for their prayers and giving me the strength to achieve such success.

Dedications

To my Mother and the Soul of my Father

Abstract

T. gondii infection acquired during life has been associated with psychoneurological disease in humans and behavioural changes in mice. However, less is known about the potential of congenitally acquired *T. gondii* infection, or for maternal *T. gondii* infection induced immune activation, to cause psychoneurological disease. The studies described herein, using LCMS (Liquid chromatography–mass spectrometry) demonstrate that adult acquired infection alters the neurochemistry and transcriptome of the brains of BALB/c mice. Notable changes to tryptophan, purine, arginine and carnitine metabolism were observed in infected mice. Congenitally infected and mice exposed to the maternal immune response to *T. gondii*, but not congenitally infected were found to have decreased mobility compared with control mice. Congenital *T. gondii* infection resulted in similar alterations in the neurochemistry of mice as seen in adult acquired infections. Some of these changes were observed, including tryptophan metabolism in mice exposed to the maternal immune response to *T. gondii*, but not congenitally infected. Both adult acquired *T. gondii* and congenital infection altered the brain transcriptome of mice relative to control uninfected mice with notable changes seen to transcripts of many immunologically important genes and enzymes in some of the metabolic pathways identified by LCMS. In addition, both adult acquired *T. gondii* infection, congenital infection and maternal exposure to different degrees were found to induce changes in a number of additional transcripts previously associated with psychoneurological diseases. These results

demonstrate that maternal exposure to *T. gondii* infection during pregnancy induces a subset of neurochemical and transcriptomic changes found in mice with adult acquired and congenital *T. gondii* infection. The results therefore reinforce the potential of maternal immune activation to affect psychoneurological diseases and implicate *T. gondii* as a potential aetiological agent of this process.

Abbreviations

5-HT	5-hydroxytryptamine (serotonin)
AD	Alzheimer's disease
AIDS	Acquired Immune Deficiency Syndrome
ALS	amyotrophic lateral sclerosis
AMP	Adenosine Monophosphate
APC	Antigen presenting cells
Arg1	Arginase-1
ATG5	Autophagy protein 5
ATP	Adenosine triphosphate
CD	Cluster of differentiation
CNS	Central Nervous System
CRP	C-reactive protein
DCs	Dendritic cells
DEGS	Differentially expressed genes
DMEM	Dulbecco’s Modified Eagle Medium
ELISA	Enzyme-linked immunosorbent assay
FCS	Foetal Calf Serum
FDR	False Discovery Rate (adjusted p-value)

FFHs	Foreskin Fibroblast cells
FPKM	Fragments Per Kilobase of transcript per Million mapped reads
FTD	frontotemporal dementia
GABA	Gamma-aminobutyric acid
GBPs	Guanylate Binding Proteins
GM-CSF	Granulocyte-macrophage colony-stimulating factor
GPI	glycosyl phosphatidylinositol
GST	Glutathione-S-transferases
HPLC	High-Performance Liquid Chromatography
IDO	Indoleamine 2,3-dioxygenase
IFN	Interferon
IFNγR	Interferon γ Receptor
Ig	Immunoglobulin
IL	interleukin
InDel	Insertion/Deletion polymorphism
INF-γ	Interferon Gamma
iNOS	inducible nitric oxide synthetase
KLRG1	Killer cell lectin-like receptor G1
KYNA	kynurenic acid
LCMS	Liquid Chromatography Mass Spectrometry
L-DOPA	L-3,4-dihydroxyphenylalanine

LPS	Lipopolysaccharides
MHC	Major Histocompatibility Complex
MPEC	memory precursor effector cells
NF-kB	Nuclear Factor Kappa-light-chain-enhancer of activated B cells
NK cells	Natural Killer cells
NO	Nitric oxide
OPLS-DA	orthogonal partial least squares discriminant analysis
P value	Probability value
PAI-1	Plasminogen activator inhibitor 1
PAMPS	pathogen associated molecular patterns
PBS	Phosphate Buffered Saline
PCA	principal components analysis
PD	Parkinson's disease
PDCs	plasmacytoid dendritic cells
PPS	Pathway Perturbation Score
PRRS	pattern recognition receptors
PV	parasitophorous vacuole
RNA	Ribonucleic Acid
ROI	Reactive Oxygen Intermediates
SLEC	Selective short-lived effector cells
SNP	Single nucleotide polymorphism

STAT	Signal Transducer and Activator of Transcription
TDO	Tryptophan 2,3 dioxygenase (TDO)
TGF-β	Transforming growth factor beta
TgPRF	*T. gondii* protein profilin
Th	T Helper cells
TIMP-1	Tissue inhibitor of metalloproteinase 1
TLA	Toxoplasma Lysate Antigen preparation
TLRs	toll like receptors
TNF	Tumor Necrosis Factor
Tregs	Regulatory T cells
VCAM-1	Vascular cell adhesion molecule 1
VIP	Variable Importance for the Projection

Table of Contents

LIST OF FIGURES

LIST OF TABLES

1 Introduction

1.1 *Toxoplasma gondii*

T. gondii is an obligative intracellular parasitic protozoan, which was accidently discovered in 1908, by Nicolle and Manceaux (Ajioka and Morrissette, 2009, Innes, 2010). At the same time, Alfonso Splendore working in Sao Paulo discovered a similar parasite in rabbits (Dubey, 2010, Innes, 2010). The name Toxoplasma means is derived from 'toxo' meaning 'arc form' in Greek and reflects the crescent-shaped morphology of the tachyzoite and bradyzoite stages of the organism. *Gondii* is taken from rodent *Ctenodactylus gondii* from which it was first isolated (Dubey, 2008, Innes, 2010). Thirty years later *T.gondii* was identified as a causative agent of an infectious disease (Robert-gangneux and Dardé, 2012), but it was not until the 1970s that the life cycle was fully understood (Dubey et al., 1970). *T. gondii* infections have been found in many mammals including humans, wild animals, domestic animals and farm animals such as birds (Hill et al., 2005, Sukthana, 2006). These hosts are termed, intermediate or secondary hosts, as sexual reproduction does not occur within these animals (Dubey, 2010, Fuller Torrey and Yolken, 2013, Tenter et al., 2000). Members of the Felidae including domestic cats are the definitive host as sexual reproduction occurs exclusively in their intestines (Hutchison et al., 1969). *T. gondii* is a part of the phylum of Apicomplexa that consists of more than 5000 species of protozoa that includes other human parasitic infections including members of *Plasmodia* (the causative agent of malaria) and *Cryptosporidia* that cause diarrheal disease. All these species have a unique organelle complex at the apical tip, which gave the phylum its name (Dubey, 2010, Kim and Weiss, 2004).

1.2 Toxoplasmosis

1.2.1 Etiology

Toxoplasmosis is an anthropozoonic disease resulting from infection with the obligate intracellular parasites *Toxoplasma gondii* (Montoya and Liesenfeld, 2004, Sukthana, 2006, Dubey et al., 2014). This parasite infects over one third of the world's population (Henriquez et al., 2009, Weiss and Dubey, 2009, Halonen et al., 2014). This infectious disease is significant medical and veterinary importance due to its ability to cause abortion, serious congenital disease and non-congenital acquired disease (Torgerson and Macpherson, 2011). Toxoplasmosis may produce different diseases and syndromes when postnatally acquired in humans, ranging from flu-like symptoms to serious ocular disease in immunocompetent individuals, largely depending on the strain of *T. gondii* responsible for infection. In immunocompromised individuals, disease can be severe and life-threatening if untreated and manifest as toxoplasmic encephalitis or systemic disease (Innes, 2010, Dubey, 2010).

T. gondii is considered to be the most successful known parasite, owing to the high number of people and diversity and number of animals it infects. Arguably this is in least part due to its ability to manipulate the immune responses of host cells to facilitate chronic infections (Saeij et al., 2005). There was once thought to be three major lineages of *T. gondii* (Types I, II and III), but with increased sampling of more geographical regions, this has been revised to at least 5 lineages. These different genetic lineages are associated with different geographical regions and differ in their preponderance in intermediate hosts

(Halonen et al., 2014, Saeij et al., 2005, Wendte et al., 2011). The virulence and disease manifestation are known to vary in both humans and rodents. Type I strains such the RH strain are virulent in mice while the Type II and Type III lineages exemplified by Beverly and Veg strains, respectively are less virulent (Halonen et al., 2014). Type I strains, such as the RH strain, cause severe clinical outcomes in congenital toxoplasmosis, ocular toxoplasmosis and immune supressed patients (Halonen et al., 2014, Saeij et al., 2005). Type II strains are associated with chronic toxoplasmosis (Vaudaux et al., 2010, Xiao et al., 2011). Type III strains are often present in the reservoir of the animal hosts. Types IV and V lineages of *T. gondii* often referred to as atypical strains that are recombinant strains derived from type I, II and III that may result from atypical allele combinations. These types are usually found in hosts from Africa and South America (Saeij et al., 2005). The success of *T. gondii* is often attributed to its multiple modes of transmission including the transmission via oocysts released in cat feces that often contaminate vegetables and water, the transmission via ingestion of tissue cysts in undercooked meats and the transplacental route of transmission (Ajzenberg, 2011, Hide et al., 2009).

1.2.2 *Toxoplasma gondii* life cycle

The life cycle of *T. gondii* consists of two phase, namely a sexual or direct life cycle and asexual or indirect life cycle. The intestinal phase which contains a sexual cycle happens only in the intestine of the definitive host (one of Felidae family members) following ingestion of oocysts or tissue cysts from the intermediate host. Following ingestion of oocysts, gastric enzymes destroy the cyst wall and leads to the release of sporozoites which infect intestinal endothelial cells. Similarly ingestion of tissue cysts from the meat of the intermediate hosts, bradyzoites are released and infect the intestinal endothelial cells. The parasite initially multiplies asexually by endopolygeny (a modified version of schizogony) before undergoing gametogony to produce male microgametes and female macrogametes. These haploid forms combine to give rise to diploid zygotes, which develop into oocysts which are eventually released in the feces of the cat. Oocyts, are produced only in the intestine of the definitive hosts. An asexual cycle occurs in different tissues of intermediate hosts (all warm blooded organisms) following ingestion of oocysts or tissue cysts, both of which are infective to intermediate hosts including humans (Dubey, 2010, Fuller Torrey and Yolken, 2013, Tenter et al., 2000). The infectious cat can shed a huge number of oocysts, which can survive in the external environment for a year (Dubey, 2010). After ingestion, oocysts or tissue cysts release sporozoites or bradyzoites, respectively which develop into tachyzoites (rapidly multiplying stage) and disseminate throughout the body. Tachyzoites can cause tissue destruction as they spread throughout the body. They may be found in virtually all tissues and body fluids such as blood, urine, saliva and milk (Tenter et al., 2000). Although there is a low risk of transmission through

body fluid, transmission might happen via milk from mothers to offspring (Dass et al., 2011). Tachyzoites also have the ability to infect the foetus in pregnant women through the placenta. In addition, they can be transmitted through blood transfusion and organ transplantation(Singh and Sehgal, 2010). Tachyzoites localise in muscle and neural tissue and subsequently convert to bradyzoites (slow dividing forms) which develop into cysts that can contain many bradzoites (Sibley et al., 2009, Tenter, 2009) Figure1.1. Bradyzoites can convert back into tachyzoites within a chronically infected host and give rise to disease reactivation as most evident in the immunosuppressed and in the retinas of congenitally infected individuals (Dubey, 2010).

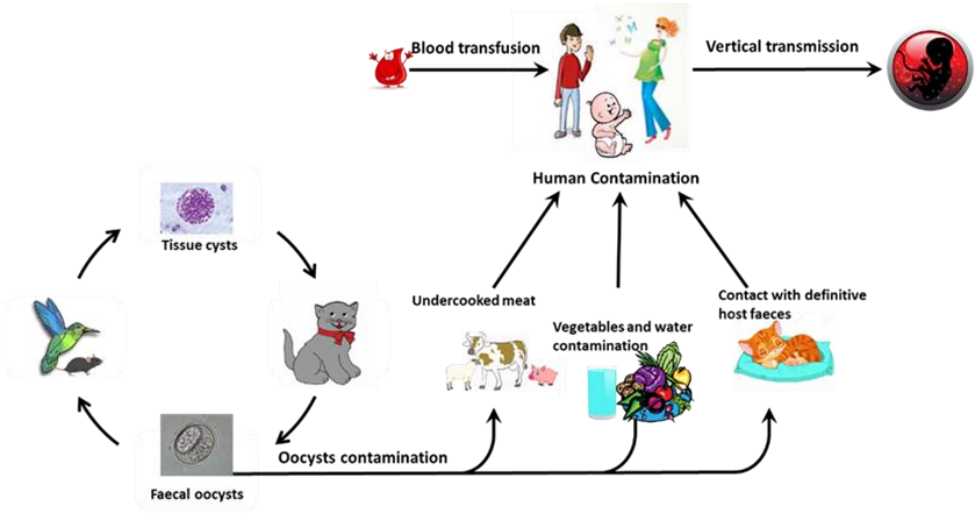

Figure 1.1 Transmission of *Toxoplasma gondii* infection.

The sexual stage of *T. gondii* occurs only inside one of the Felidae family members (definitive host). When the cat ingests the tissue cysts or oocysts, they invade the small intestine (epithelial layer) of the cat where an asexual followed by a sexual cycle are undergone and after that they form oocysts which are released and excreted.

1.3 Congenital toxoplasmosis

Congenital toxoplasmosis occurs when infection of the developing fetus occurs through placental passage of parasites from an infected mother. In 1928 congenital toxoplasmosis was reported by Janku (an ophthalmologist) in an infant with congenital hydrocephalus and microphthalmia. He had previously recognised the first human case of ocular disease in 1923 and three years later he suggested a possible connection between congenital hydrocephalus and toxoplasmosis (Remington et al., 2006). In the communities with high prevalence of *T. gondii* parasites, congenital toxoplasmosis is considered as a significant problem with the most serious manifestations of *T. gondii* infection (Dubey, 2004, Montoya and Rosso, 2005, Torgerson and Macpherson, 2011). The risk of congenital infection varies significantly according to the primary infection time of pregnant mother (Dunn, 1999) Figure 1.2. The risk of congenital infection reaches 20% during the first trimester of pregnancy and 90% during the third trimester of pregnancy. However, the severity of congenital manifestations in the new-born is the highest and most serious when maternal infection is acquired during the first trimester and the lowest when maternal infection is acquired in the third trimester of pregnancy (Dubey, 2008, Jones et al., 2001). Overall, around 30% of women who are infected with *T. gondii* during their pregnancy transmit the parasite through the placenta to their fetus in contrast the rest of them give birth to normal uninfected infants. Congenital toxoplasmosis has a wide range of clinical signs and symptoms. However, around 80% of infected infants are asymptomatic in the new-born periods (Wilson et al., 1980). Moreover, reactivation of infection in

immunosuppressed women before pregnancy has also been reported to lead to congenital toxoplasmosis, however it is not common (Dubey, 2010, Dubey et al., 2014).

Maternal *T. gondii* infection during pregnancy can also lead to spontaneous abortion, prematurity and stillbirth. Most infected infants show no clinical manifestation during the new-born period, but more than 80% of them will present ocular impairment in their lives, and around 50% will develop neurological disorders (Dubey, 2004, Remington et al., 2006). Central nervous system (CNS) involvement is considered as a hallmark of congenital toxoplasmosis. Congenitally infected new-borns with severe manifestations often display one or more components of the "classic triad" of symptoms, namely hydrocephalus, intracranial calcification and more often bilateral retinochoroditis (Dubey, 2004, Montoya and Rosso, 2005, Torgerson and Macpherson, 2011).

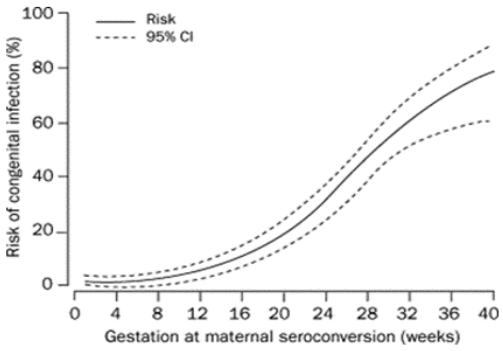

pregnancy gestation	The risk of congenital infection	Severity of congenital manifestations
First Trimester	Low	High
Third Trimester	High	Low

Figure 1.2 Risk of congenital infection by duration of gestation at maternal seroconversion. (Adapted from Dunn et al, 1999).

1.4 Immune response to *T. gondii*

The immune response to this parasite is a particularly complicated process due to the ability of *T. gondii* to spread in all the body tissues and the ability of the parasite to undergo a stage switch from the tachyzoite to the bradyzoite stage. A variety of clonal lineages of *T. gondii* exist with variable virulence and evolved mechanisms that subvert or modulate the immune response. In addition, the immune response can have unique aspects in each organ, especially the CNS and the eye which are immune privileged and the placenta which has a complex immune system within that has evolved to facilitate a successful nurture of a partial allograft (Filisetti and Candolfi, 2004). Primary *T. gondii* infection induces both humoral and cellular immune responses in immunocompetent individuals. The initial immune response leads to significant reduction in the number of parasites, but stage switching to the bradyzoite stage allows the development of the cyst form of parasite which is found predominantly in the brain and muscles for the life of the host. Specific immunity is long lasting and is generally believed to prevent reinfection (Klaren and Kijlstra, 2002). Although there are some differences between animal and human toxoplasmosis, the careful selection and use of experimental murine models has facilitated study of the vast majority of the physiological host parasite interaction occurring naturally in humans (Sher et al., 2016).

1.4.1 Cell-mediated response

Cell-mediated responses are divided into a nonspecific innate cell responses and a specific responses reliant on T cells and B cells.

1.4.1.1 Innate immune response

Interaction between *T. gondii* and the innate immune response plays a crucial role in determining the outcome of infection in the murine model. Cellular immune response is the key component of the host's immunity in the case of *T. gondii* infection. *T. gondii* has a number of pathogen associated molecular patterns (PAMPS) that bind a number of toll like receptors (TLRs). Ligation of these TLRs initiate a cascade of signaling events that culminate in the production of a number of cytokines and immunological mediators including the pro-inflammatory cytokines interleukin 12 (IL-12) and IFN-γ which are crucial for the control *T. gondii* infection.

In the murine models, TLR 11 has been demonstrated as one of the important receptors and a strong inducer of (IL-12) from DCs (Pifer et al., 2011). TLR11 recognises the *T. gondii* protein profilin (TgPRF) which is believed to be important to induce IL-12 from DCs. Deficiency in either TLR11 or TgPRF leads to a decreased in the IL-12 response in infected mice and increased susceptibility to infection (Hunter and Sibley, 2012, Pifer et al., 2011). In addition, TLR 12 also recognises TgPRF by plasmacytoid dendritic cells (pDCs). TLR11 and TLR12 are both required in macrophages and conventional DCs to respond to TgPRF. TLR12-dependent induction of IL-12 and IFNγ in pDCs leads to production of IFN-γ by natural killer cells (NK). TLR12 deficiency has been shown to increase susceptibility to infection in murine models of *T. gondii* infection (Hunter and Sibley, 2012, Koblansky et al., 2013). TLR2- and TLR4-mediate detection of glycosyl phosphatidylinositol (GPI)-anchored *T. gondii* proteins. They stimulate macrophages to

produce IL-12 and also TNF-α, which contribute to immune killing mechanisms of *T. gondii* (Hunter and Sibley, 2012).

Thus early in infection, neutrophils, macrophages and dendritic cells (DCs) produce IL-12, which activates NK cells to release interferon-γ (IFNγ). IFNγ is an essential mediator of resistance to *T. gondii* and is fundamental for the stimulation of a variety of antimicrobial activities, in both haematopoetic and non-haematopoetic cells, which limit parasite replication in the acute stage of infection and prevent the development of toxoplasmic encephalitis in late stage of infection (Hunter and Sibley, 2012, Suzuki, 2004, Tait and Hunter, 2009). Both IFNγ and IFNα stimulate the production of nitric oxide (NO), which is a significant in controlling the chronic infection. IFNγ also activates the reactive oxygen intermediates (ROI) and induces iron depravation in order to reduce parasite growth (Dimier and Bout, 1998, Filisetti and Candolfi, 2004). Neutrophils are a fundamental component of control *T. gondii* infection in early stages as they act as antimicrobial agents and produce reactive oxygen intermediates (ROI) and nitric oxide (NO). Neutrophils also have the ability to produce cytokines (IL-12) and chemokines (Van Gisbergen et al., 2005).

IFNγ production in infected hosts induces a variety of mechanisms that kill *T. gondii* or curtail its multiplication. For example, IFNγ up regulates the expression of the indoleamine 2, 3 dioxygenase (IDO), an enzyme which catalyses the degradation of the essential amino acid tryptophan (Pfefferkorn et al., 1986a, Pfefferkorn et al., 1986b). As *T. gondii* is a tryptophan auxotroph this IDO mediated depletion of host tryptophan curtails its growth (Fujigaki et al., 2002). This pathway of tryptophan degradation is also

likely to play a role in control of the immune response and inflammation as tryptophan is necessary for the optimum function of immune cells and kynurenine (a product of tryptophan degradation) also expands Treg cells which are known to limit inflammation during *T. gondii* infection (Rodriguez Cetina Biefer et al., 2017).

In response to IFNγ, haematopoietic and non-haematopoietic cells activate two families of defense proteins immunity relates GTPases (IRGs) and p67 guanylate binding proteins (GBPs), which are recruited to the parasitophorous vacuole (PV) and kill parasites. The function of IRGS and GBPs depends on (ATG5) autophagy protein5 (Hunter and Sibley, 2012). IRGs proteins contribute as potent effectors to regulate infection of *T. gondii* in mice (Butcher et al., 2005). Different IRGs are believed to provide an early defense in acute and chronic infection (Howard et al., 2011).

In human, TLR 11 is represented only by a non-functional pseudogene. The significance of TLR11 deficiency in humans is less clear given that infected individuals are capable of developing protective immunity upon infection. An analysis of wild type mice and TLR11−/− mice infected orally with the parasite could provide a possible benefit of TLR11 deficiency in humans (Benson et al., 2009). TLR11−/− mice are fully protected from parasitic infection as a result of gut commensal driven immunity against *T. gondii*. Remarkably, TLR11−/− mice infected orally with the parasite were not only able to control the pathogen, but were largely free from the intestinal pathology seen in wild type animals (Benson et al., 2009). For this reason, the authors speculate that a balanced immune response in humans can be achieved in the absence of TLR11 via indirect immunostimulation by gut commensals (Benson et al., 2009, Pifer and Yarovinsky, 2011).

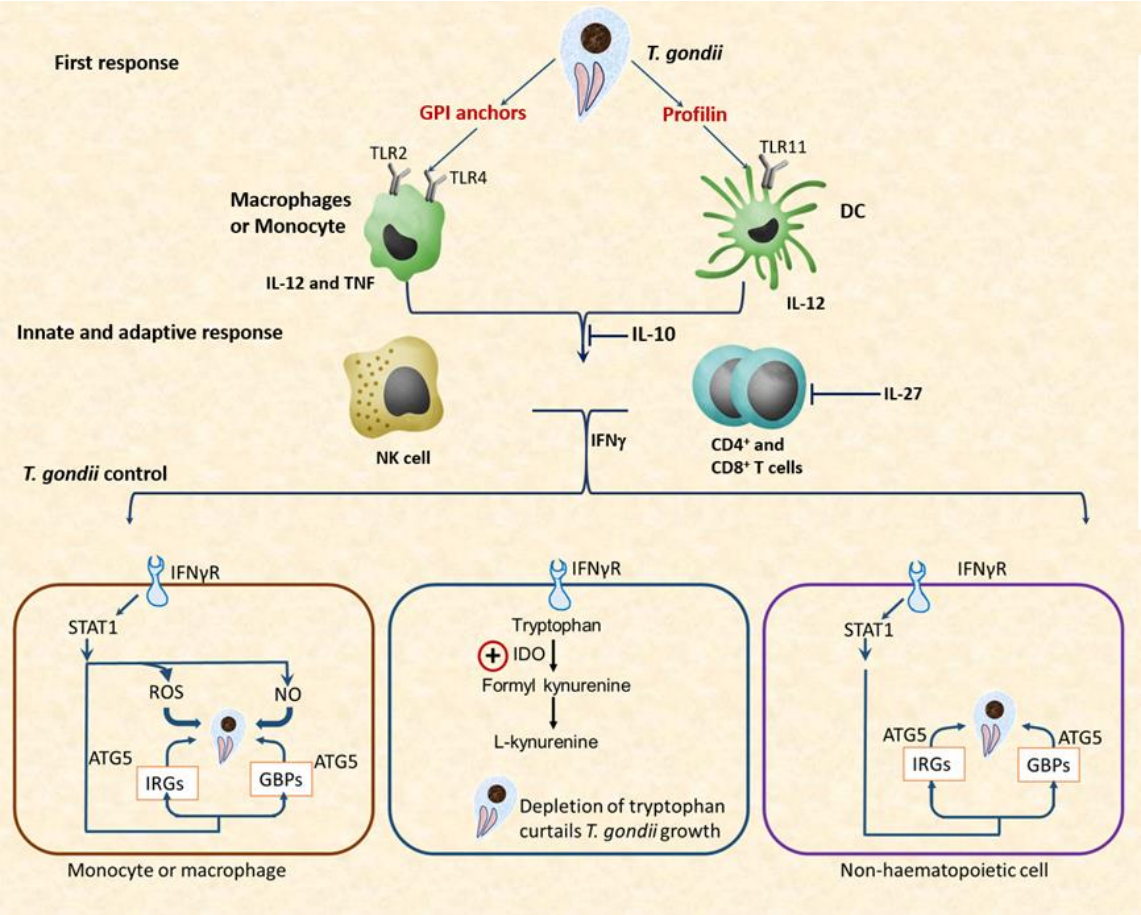

Figure 1.3 Immune responses to *Toxoplasma gondii* during infection in mice.

At the beginning of infection, DCs, monocytes and macrophages are the first cells respond. The *T. gondii* produce profilin which interact with Toll-like receptor 11 (TLR11) on DCs leading to IL-12 production. In contrast, macrophages activate IL-12 production and also stimulate TNF production, which is a cofactor in antimicrobial activity, in response to TLR2- and TLR4-mediated detection of glycosyl phosphatidylinositol (GPI)-anchored parasite proteins.

Innate and adaptive immunity play an important role to reduce the pathology of this infection. NK cells are stimulated by the innate immune response to produce IFNγ while CD4+ and CD8+ T cells are stimulated by adaptive immune response to also produce IFNγ. At the same time IL-10 and IL-27 paly essential roles in these pathways to prevent the overproduction of T helper 1 type cytokines.

IFNγ is responsible for stimulating cells to control *T. gondii* infection. IFNγ transmits a signal through IFNγ receptor (IFNγR) to stimulate STAT1 (signal transducer and activator of transcription 1). Macrophages and monocytes then up regulate the production of NO and ROS (reactive oxygen

species) which participate to control growth of intracellular parasites. In addition, haematopoietic and non-haematopoietic cells activate two families of defense proteins IRGs (immunity relates GTPases) and GBPs (p67 guanylate binding proteins, which are recruited to the PV (parasitophorous vacuole) and are involved in parasite clearance. The function of IRGS and GBPs depends on (ATG5) autophagy protein5.

1.4.1.2 A specific T cell response

The expansion and qualities of the developing T cell response is influenced by the mediators produced during the innate immune response (Hunter and Sibley, 2012).

CD4+ and CD8+ T cells both play critical roles to resist *T. gondii* infection, control the accompanying inflammatory response and prevent reactivation of infection.

Th1 and Th2 responses

$CD4^+$ T helper 1 (Th1) and 2 (Th2), determine the balance between cell-mediated and humoral immune responses. Th1 polarization is characteristically driven by a strong antigen stimulus in the presence of the cytokine IL-12 (Zhu et al., 2010). They are also stimulated by antigen presenting cells (APC) to produce pro-inflammatory cytokines such as IFNγ and IL-2. IL-2 induces lymphokine-activated killer cells of either NK-cell or T-cell phenotype, which are cytotoxic for target cells infected with *T. gondii* (Denkers and Gazzinelli, 1998) and IFNγ and TNF promote the activation of macrophages in intracellular infection (Wan and Flavell, 2009). Conversely, Th2 polarization is initiated by a weak antigen stimulus and IL-2/STAT5 signaling. Cytokines produced by Th2 cells, such as IL-4, IL-5, IL-10 and IL-13, induce IgE class switching in B cells, as well as the activation of eosinophils, both of which are required to restrain parasitic infections (Zhu et al., 2010). Dysregulated Th cell function often leads to inefficient clearance of pathogens and causes inflammatory diseases and autoimmunity (Hirahara et al., 2013).

Treg and Th17 responses

T-helper 17 (Th17) and T-regulatory (Treg) cells have been shown to play significant roles in hosts infected with *T. gondii*. Tregs are capable of producing IL-10 and TGF-β so they probably act as anti-inflammatory mediators (Bettelli et al., 2006). Th17 cells are differentiated by TGF-β and IL-6 as well as by IL-21 and later stabilised by IL-23 (Bettelli et al., 2007). Th17 cells have also been reported to play a crucial role in clearing specific pathogens and inducing autoimmune tissue inflammations (Awasthi and Kuchroo, 2009, Yan et al., 2015). Thus Th17/Treg cell balance is critical to prevent autoimmune disease and also in the mobilisation and generation of neutrophils during responses to the pathogens through the production of IL-17 (Bettelli et al., 2007, Sakaguchi, 2000, Lee, 2018).

CD8 cytotoxic cells

The protective activity of $CD8^+$ T cells is mediated partly through production of cytokines, such as IFNγ, but a direct cytotoxic effect on the parasite has also been reported, as well as major histocompatibility complex (MHC) class I-restricted cytotoxicity for *T. gondii* infected cells (Bliss et al., 1999, Miller et al., 2009, Roberts and McLeod, 1999).

CD8 T cells as mentioned previously are essential for control of *T. gondii* infection. Once activated they differentiate into 2 phenotypes. Selective short-lived effector cells (SLEC) and memory precursor effector cells (MPEC) which are distinguished based on their surface expression of Killer cell lectin-like receptor G1 (KLRG1) and IL-7Rα (IL-7R). SLECs are defined as being ($KLRG1^{hi}$) and $IL\text{-}7R^{Io}$ while MPECs are $KLRG1^{Io}$ $IL\text{-}7R^{hi}$.

(Joshi et al., 2007, Gigley et al., 2011). Despite differing in phenotype, both effector cells possess similar functions in term of their cytotoxic activity and proliferation (Wilson et al., 2008). Once immune control has been initiated, the memory $CD8^+$ T cell populations regulate the chronic phase of *T. gondii* infection. Interestingly, the level of IL-12 has been shown to have an effect on the development of $CD8^+$ cell populations. A previous studies has been demonstrated that the absence or low level of IL-12 led to increase the differentiation of $CD8^+$ T cells into more long-lived effector memory cells after infection with *Listeria monocytogenes* (Pearce and Shen, 2007).

In the murine model, it has been shown that IL-12 is required in *T. gondii* infection for generation of SLEC $CD8^+$ T cell and this is independent of $CD4^+$ T cells. SLECs were more producible than MPECs in the $CD8^+$ T cell populations (Wilson et al., 2008). Interestingly, a study on BALB/c mice indicates that $CD8^+$ T lymphocytes from *T. gondii*-infected mice are the principal mediators of resistance to *T. gondii*, although $CD4^+$ T cells appear to be involved during the acute phase of infection (Parker et al., 1991).

1.4.2 Humoral immune response

T. gondii infection stimulates B cells to produce several antibodies. These antibodies do not eliminate the parasite. Nevertheless, infection stimulates production of many classes of immunoglobulin including IgG, IgM, IgA and IgE (Correa et al., 2007, Filisetti and Candolfi, 2004). These antibodies act on the extracellular tachyzoites released following lysis or egress of infected cells. They reduce multiplication of *T. gondii*, by lysing the

parasites in the presence of complement. They are also active via opsonisation which facilitates phagocytosis by macrophages and also induce phagosome lysosome fusion in macrophages (Filisetti and Candolfi, 2004, Roberts and McLeod, 1999). As mentioned previously, these mechanisms do not protect the host against the live parasites which are already intracellular. However, secretory IgA interferes with the initial interaction of the parasite with the host cell at mucous membranes (Roberts and McLeod, 1999). Furthermore, the detection of IgA in hosts with congenital toxoplasmosis is particularly important, hence these antibodies can be detected in the absence of IgM. IgA has the ability to cross the placenta while IgM does not, so they are useful in the diagnosis of toxoplasmosis (Filisetti and Candolfi, 2004). IgM also plays a significant role in limiting systemic dissemination of tachyzoites during the early acute *T. gondii* infection (Couper et al., 2005). The most important antibodies for protecting the foetus are IgG as they are able to cross the placenta. Although IgE is correlated with the onset of complications, such as chorioretinitis, adenopathies and infection reactivation in immunosuppressed host, the analysis of its presence is only useful when it is combined with analysis of IgM and IgA (Filisetti and Candolfi, 2004, Pinon et al., 2001). In general, the available evidence suggests that antibodies play a minor role in term of protection against *T. gondii* infection but play the essential role in term of infection diagnosis in humans (Filisetti and Candolfi, 2004).

1.4.3 Brain immune response

Following *T. gondii* infection, the parasites enter macrophages and dendritic cells, which are believed to migrate by the blood vessels to the brain. In the chronic stage, bradyzoites are isolated from the host immune response by a cyst wall and have the ability to persist in chronically infected hosts. The parasite can infect a variety of brain cells, such as astrocytes, neurons and microglia. However, the vast majority of the literature suggests that ultimately the cysts stages are predominately, if not exclusively found in neurons (Ferguson and Hutchison, 1987a, Ferguson and Hutchison, 1987b, Carruthers and Suzuki, 2007). There is a strong immune response to *T. gondii* in the brain and the production of many cytokines including IL-1β, IL-2, IL-4, IL-6, GM-CSF, TNFα and IFNγ as a response to infection (Carruthers and Suzuki, 2007, Wilson and Hunter, 2004, Hunter et al., 1992). Although the dogma in the literature suggested that cysts persist for the life of the host, studies now suggest that cyst numbers vary in mice with time and point towards a dynamic situations where rupture of cysts is a natural process occurring in the brain. In immunocompetent mice or humans, the immune response is likely to deal with this by killing the resultant extracellular parasites. However, immunocompromised subjects incapable of this cannot prevent disease reactivation, which leads to serious complications, such as toxoplasmic encephalitis in AIDS patients (Denkers and Gazzinelli, 1998). Both CD4+ and CD8+ T cells are important in preventing reactivation of the parasite and are likely to be important in dealing with the result of cysts rupture. The brain immune response is an important process to keep *T. gondii* infection inactive as

a result alteration of cytokine level could influence neuromodulator levels and host behaviour (Gatkowska et al., 2012, Rassoulpour et al., 2005).

Control of *T. gondii* infection is complex and depends on the genetic background of the host, his immune status and parasite factors, including virulence.

1.5 Behavioural changes in hosts infected with *T. gondii*

In the chronic phase of *T. gondii* infection, tachyzoites can localise in neural tissue and brain, which subsequently convert to cysts or bradyzoites (Sibley et al., 2009, Tenter, 2009). The predilection of *T. gondii* for the brain of their intermediate hosts sets this parasite in a prime position to manipulate the host's behaviour (Adamo, 2013, Carruthers and Suzuki, 2007, Hill et al., 2005, Webster, 1994).

1.5.1 Behavioural changes in rats

It has been reported that the *T. gondii* parasite is associated with higher activity level in infected wild and wild laboratory hybrid rats (*Rattus norvegicus*) than in uninfected rats (Webster, 1994). In addition, wild brown rats (*Rattus norvegicus*) have shown lower neophobia in an infected group with *T. gondii* than in an uninfected group (Webster et al., 1994). It has been suggested that these differences arise from pathological changes caused by *T. gondii* cysts in the brains of infected rats. Such behavioural changes may have evolved to facilitate transmission to the definitive hosts by increasing the possibility of predation (Webster et al., 1994, Berdoy et al., 1995). Another study supports the hypothesis that the *T. gondii* parasite manipulates the behaviour of its intermediate host in order to increase its chance of being predated by cats, thereby ensuring the completion of

its life cycle. This study showed that *T. gondii* infection appeared to change the rat's perception of cat predation risk, and in some cases turned their innate aversion into an attraction (Berdoy et al., 2000). Moreover, these changes were highly specific and did not result from destruction of olfactory region of the brain (Webster et al., 1994). Other studies strongly supported the previous hypothesis and they demonstrated that *T. gondii* infection associated with behavioural changes were specific to feline definitive host by testing the reaction of infected and uninfected Lister hooded laboratory rats to feline and other predatory animals such as dog and mink (Kannan et al., 2010, Lamberton et al., 2008). Furthermore, lower anxiety level has been reported using a standard anxiety test elevated plus maze among Wister rats infected with *T. gondii* compared with uninfected counterparts (Gonzalez et al., 2007). Wistar rats were inoculated intraperitoneally with several doses of *T. gondii* tachyzoites and tested, increased change was detected in open arm exploration and social interaction levels without a change in motor activity measurements. However, when the dose was increased locomotor activity a significant decrease was reported. This decrease in motor activity of infected rats prevented the detection of an anxiolytic effect. This has suggested that *T. gondii* activates an anxiolytic effect on rats at specific levels of infection as high levels of infection may lead to pathology which cover the behavioural changes that occur at lower levels of infection. According to serological and histological tests, the anxiolytic effects are associated with anti-*T. gondii* IgG levels in serum and with the position of their brain(Gonzalez et al., 2007). The dominant invasion of limbic areas and the damage of glial and neural cells may also participate in the anxiolytic mechanism (Gonzalez et al., 2007, McConkey et al.,

2013). In addition, rats infected with *T. gondii* appear to have behavioural change in their aversion to cat odour and their sexual attractiveness to females (House et al., 2011, Hughes, 2013, Knight, 2013, Vyas, 2015).

1.5.2 Behavioural changes in mice

A study in C57BL/6J female mice indicated that chronically infected mice with brain cysts display behavioural changes, such as increased exploratory locomotion, more risky behaviours and reduced unconditioned fear (Afonso et al., 2012). Another study in C57BL/6 mice chronically infected with type II strain of *T. gondii* has demonstrated widespread brain pathology, motor coordination and sensory deficits. while cognitive function, anxiety levels, social behaviour and the motivation to explore novel objects were normal (Gulinello et al., 2010). Early studies indicated that behavioural changes were only transient and disappeared before the 12th week post inoculation. These results suggested that the behavioural changes in infected mice which was reported and observed could be nonspecific by products of pathological symptoms of toxoplasmosis rather than specific products of manipulation activity by the parasite (Hrdá et al., 2000). In outbred mice, chronic, adult acquired *T. gondii* infection causes neurologic and behavioural abnormalities secondary to inflammation and loss of brain parenchyma and inflammation of perivascular region is common (Hermes et al., 2008). This suggests that the persistence of *T. gondii* cysts in the brain can develop inflammation or neurodegeneration in genetically susceptible mice (Hermes et al., 2008). Other studies showed that infected mice display increased general movement, but decreased digging and rearing movement

(Hutchinson et al., 1980). In addition, adult infected mice showed increased immobility, while congenitally infected mice showed decreased immobility (Hay et al., 1984b). Other studies have shown that infected mice explored novel area of apparatus more than uninfected mice (Hay et al., 1984a).

The impact of *T. gondii* parasite on its intermediate hosts is highly variable. Differences between observations are probable due to differences in the parasite strain, host species (strain, age and sex of the host), the time of exposure and the level of infection. Genetic differences in the host's susceptibility to the parasite could play a significant role (Hermes et al., 2008, Worth et al., 2013).

1.5.3 Behavioural changes in humans

There is a growing body of evidence to suggest that *T. gondii* infection may also affect human behaviour in different ways (Flegr, 2007, Flegr, 2012, Flegr, 2013). Some studies have examined the personality characteristics using Cattell's questionnaire in *T. gondii* seropositive and seronegative cases from normal populations (Flegr et al., 1996). These studies reported that the differences between infected and uninfected cases are significantly affected by gender, as a result infected males showed lower superego strength and higher vigilance and infected females showed higher superego strength and higher warmth (Flegr et al., 1996, Lindová et al., 2006). Furthermore, another piece of evidence showed that individuals with latent toxoplasmosis have considerably increased risk of road traffic accidents than the uninfected individual (Flegr et al., 2002, Yereli et al., 2006, Galvan-Ramirez Mde et al., 2013, Kocazeybek et al., 2009). Furthermore, this

infection could reduce psychomotor performance in infected cases, as it has been reported that adults with latent toxoplasmosis performed worse than uninfected adults (Flegr, 2007).

1.5.3.1 Schizophrenia

Beside the behavioural changes described above, further evidence indicates that *T. gondii* infection might increase the risk of schizophrenia development (Brown et al., 2005, Dickerson et al., 2007, Dickerson et al., 2014, Holub et al., 2013, Pearce et al., 2013, Torrey et al., 2007, Torrey and Yolken, 2007, Torrey and Yolken, 2003, Wang et al., 2006). Despite significant progress having been made in treatment of psychiatric disorders, the causes of these diseases generally remain imprecise and indeed are likely to be multifactorial, including host genetics and environmental factors. Many theories have linked infectious agents with mental illness and behavioural changes, for example the protozoa – *Plasmodium*, *Trypanosoma*, and *T. gondii*. These agents have the ability to chronically infect human brain cells and affect structure and or function of the host's brain due to their position in the central nervous system (Torrey and Yolken, 2007). Strong evidence was produced by Torrey (Torrey et al., 2007) when a meta-analysis found a significant increase in the prevalence of *T. gondii* antibodies in schizophrenic patients compared with a control group. In schizophrenic individuals seropositivity for *T. gondii* would appear to be an important environmental factor that interact with genetic factors to result in an increased risk for psychiatric susceptibility and is likely to be dependent on immunomodulation which results in modulation of the neurotransmitter systems (Hinze-

Selch et al., 2007). In addition, another study has examined the association with clinical and demographic factors and mortality. Although schizophrenic individuals seropositive for *T. gondii* were more likely to be female, and shown to have high risk of dying from natural causes, all other demographic factors did not show association with *T. gondii* infection (Dickerson et al., 2007). Further evidence has shown that early *T. gondii* infection as foetus or infant could increase the risk of schizophrenia development in the adulthood period and this risk might interact with other factors to produce this disorder (Mortensen et al., 2007b). However, it is not always easy to separate cause from effect and it has been suggested that the characteristics of the schizophrenic patient such as lack of personal hygiene might participate in transmission of *T. gondii* infection (Wang et al., 2006). However, one study has demonstrated that the prevalence of seropositive *T. gondii* antibodies was significantly higher in new cases of schizophrenia than a control group. This indicates that *T. gondii* infection is recorded at the beginning of the disorder itself (Yolken et al., 2001). A recent study was done to identify a set of biomarkers that might share within the pathophysiological pathway of schizophrenia such as C-reactive protein (CRP), interleukin-1 beta (IL-1β), interferon gamma (IFNγ), plasminogen activator inhibitor 1 (PAI-1), tissue inhibitor of metalloproteinase 1 (TIMP-1), and vascular cell adhesion molecule 1 (VCAM-1). These biomarkers could provide a main point to understand their specific contributions to pathogenesis (Tomasik et al., 2016).

1.5.3.2 Other neuropsychological disorders

Other studies indicate an association between *T. gondii* infection and mood disorder. Individuals with depression were significantly more likely to be seropositive for *T. gondii* than control groups (Delgado Garcia and Rodriguez Perdomo, 1980). Studies are often conflicting. A study has shown no significant relationship between *T. gondii* infection and suicide attempt status, number of prior suicide attempts, and recurrent mood disorder diagnosis (Arling et al., 2009). In contrast, it has been suggested that a significant relationship between rates of *T. gondii* infection and suicide is apparent in women of postmenopausal period (Ling et al., 2011). Further studies are required to confirm this relationship. Furthermore, the association between toxoplasmosis and depression has been reported in a case report. Depressed patient with seropositive *T. gondii* did not response to the antidepressant medicines until the patient received adequate treatment for *T. gondii* infection. This case has illustrated that in some way there is association between this infection and neuropsychiatric diseases (Kar and Misra, 2004). As a result, more studies are required to answer this question and identify the pathways of interaction between *T. gondii* infection and neuropsychiatric diseases.

1.6 Potential mechanisms of *T. gondii* action and its behavioural manipulation

There are at least three potential mechanisms whereby *T. gondii* infection might cause behavioural changes in hosts when acquired after birth. It has been suggested that the parasite's effects on the brain may be (i) indirect via the action of the immune response of

hosts or (ii) a direct pathological effect due to its localisation within a specific brain region, or (iii) by releasing molecules that affect host cell transcription or modulate neurotransmitter levels directly (Schwarcz and Hunter, 2007). Epigenetic modifications could play a significant mechanistic role in this area (Dixon et al., 2010).

1.6.1 Indirect effects of immune response

As mentioned above, local immune responses in the brain are essential to resist *T. gondii* that may change cytokine levels. This might subsequently influence neuromodulator levels and host behaviour (Miller et al., 2009, Novotná et al., 2005). Furthermore, production of IFNγ by immune cells is a key component of the body's defenses against *T. gondii* by stimulation of a variety of antimicrobial activities using macrophages and lymphocytes. Production of IFNα in response to *T. gondii* infection in high levels has been shown to be associated with behavioural alterations such as increased biting behaviour and decreased emotionality in mice (Kustova et al., 1998, Robertson et al., 1997). *T. gondii* infection has also been shown to increase kynurenic acid in the host brain which is associated with decreases levels of dopamine in the striatum (Rassoulpour et al., 2005, Schwarcz and Hunter, 2007, Wu et al., 2007). In contrast, increased kynurenic acid might stimulate the activity of dopaminergic neurons (Erhardt et al., 2001). As a result, this immune response to the *T. gondii* parasite could indirectly affect neuromodulators in the brain and thereby host behaviours.

1.6.2 Localisation in the brain as a direct effect

T. gondii manipulation of host behaviour could result from its localisation in brain areas, with high prevalence in neuronal cells (McConkey et al., 2013, Webster et al., 2006). As a result, *T. gondii* infection could directly affect neuronal function and thus explain neuropsychological disorders. For example, in rodents infected with *T. gondii* behavioural changes and neurodegeneration signs have been shown and this was related to nonspecific pathology which might be due to interference with the function of infected neurons (McConkey et al., 2013). An explanation for alteration in the behaviour of infected hosts might be the potential preferential localisation in specific brain regions, such as the amygdala, the olfactory bulbs and the nucleus accumbens which have been recognised as areas where cysts are frequently found (Berenreiterova et al., 2011). A study reported the mechanism that accounts for 'fatal feline attraction' might be mediated by pathways that stimulate the amygdala (Berdoy et al., 2000, House et al., 2011). The amygdala plays a significant role in fear processing which can be seen in rats with amygdala pathologies. When these animals are housed with sedated cats, instead of evading the cat they in fact approach the cat (Berdoy et al., 2000, Davis, 1998, McConkey et al., 2013, Vyas et al., 2007). Another study has suggested that the attraction of infected rats to feline odour could be resulting from inhibition to specific olfactory receptors that can detect feline odour, this is supported by the fact that different predators stimulate particular olfactory brain areas in rats (Staples et al., 2008). Although the direct effect of *T. gondii* caused by its location in the brain regions is possible, different location in the host's brain is inconsistent between studies (McConkey et al., 2013). This potentially could be the result of different

parasite strains, which might have possibly pleiotrophisms and therefore have different abilities to manipulate the intermediate host.

1.6.3 Neurotransmitter modulation in hosts infected with *T. gondii*

Neural activity within the brain is a balance of excitatory and inhibitory neurotransmission. In chronic *T. gondii* infection, the cysts directly affect neuromodulator levels of the host brain by increasing levels of dopamine which changes host behaviour (Vyas, 2015). The *T. gondii* parasites have the ability to disrupt dopamine signaling in the host brain. The genome of this parasite contains two genes (AAH1 and AAH2) which encode for tyrosine hydroxylase. This enzyme produces (3,4-dihydroxyphenylalanine) L-DOPA, which is a precursor of dopamine (Gaskell et al., 2009). Tyrosine hydroxylase in mammal catalyses both tyrosine and phenylalanine, with a substrate preference for tyrosine. Phenylalanine is catabolised to tyrosine and tyrosine is then catabolised to L-DOPA. This reaction is a rate limiting step in synthesis of dopamine. In contrast, the enzyme produced by the *T. gondii* parasite has similar characteristics to the mammals' enzyme. This has the potential to lead to increased dopamine signaling in the brain of hosts infected with *T. gondii* which may alter their innate behavioural profile (Prandovszky et al., 2011, Salamone and Correa, 2012, Vyas, 2015). These reported changes in neurochemicals in mice infected with *T. gondii*, might vary between acute and chronic phases of infection. The increase in dopamine levels were found in brains of rodents with chronic *T. gondii* infection (Stibbs, 1985). Furthermore, another hypothesis is that L-DOPA participates in the formation of the tissue cyst wall which is supported by

evidence of *Eimeria maxima* containing L-DOPA on its oocyst wall glycoproteins (Belli et al., 2003). The most interesting hypothesis is that high levels of dopamine during chronic infection is linked to behavioural alteration in animals and humans. As dopamine is involved in reward seeking and motivational behaviours manipulation of host levels could have profound effects on behaviour (Bressan and Crippa, 2005). In addition, the genome of *T. gondii* contains a protein mimic of the human protein called 14-3-3 protein. This protein has the ability for phosphorylation activity during combination with different molecules and seems to participate in the regulation of tyrosine hydroxylase reactions (Assossou et al., 2004).

1.6.4 Epigenetic Changes

Epigenetic modifications could result from environmental factors such as infection, diet habits, exercise and medication. There is a growing body of evidence suggesting that protozoan parasites such as *Leishmania* (McMaster et al., 2016) and *T. gondii* may lead to epigenetic changes in the host genome (Flegr and Markoš, 2014). The changes in DNA methylation which result from epigenetic modification can affect gene expression and hence the phenotype of the host. Furthermore, infectious agents or the immune response can affect neurodevelopment in utero during the infection process. This impact seems to be different according to the host's immunity, time of infection and genetic susceptibility to specific infection (Meyer, 2013).

In humans, a cohort study has been shown that ocular and brain manifestations in congenital toxoplasmosis were associated with polymorphisms in ABCA4 encoding ATP-

binding cassette transporter. In contrast, polymorphisms at COL2A1 encoding type II collagen were associated only with ocular manifestation. This association between clinical manifestation of congenital toxoplasmosis and polymorphisms for both ABCA4 and COL2A1 indicate potential epigenetics changes in the hosts (Jamieson et al., 2009, Jamieson et al., 2008).

Rats infected with *T. gondii* have shown their attraction to cat odours instead of the natural fear of cats. This change in animal behaviour seems to increase the probability of parasite transmission to definitive hosts. These rats have been shown to have DNA hypo-methylation of arginine vasopressin in the amygdala. This hypo-methylation has been suggested to be responsible for the observed changes to their behaviour and specifically to their natural fear of cats (Hari Dass and Vyas, 2014). These results may demonstrate that this infection has the ability to induce epigenetic changes, which directly affect the host's behaviour.

1.7 Maternal infection and psychiatric disorders in offspring

Several studies focused on infection during pregnancy and the consequences for development schizophrenia and other mental disorders in offspring. A study was conducted to test the association between maternal infections and psychiatric disorder in adulthood (Buka, 2001). Another two cohort studies have shown the association between offspring of pregnant mothers infected with *T. gondii* and schizophrenia and other psychotic illness (Mortensen et al., 2007a, Mortensen et al., 2007b). Although the association between *T. gondii* maternal infection and schizophrenia has been shown in

these studies, it is still unclear if there is any causative relationship between them. More studies were conducted and these studies conclude the same as previous results (Blomstrom et al., 2016, Blomstrom et al., 2015, Wang et al., 2011). Another study has shown that this relationship is changed according to levels of *T. gondii* specific IgG antibodies as mothers with high level of IgG antibodies have a significantly elevated risk of developing schizophrenia (Giørtz Pedersen et al., 2011).

1.8 Aims and objectives

T. gondii infection acquired during life has been associated with psychoneurological disease in humans. However, less is known about the potential of congenitally acquired *T. gondii* infection to cause psychoneurological disease. Recent studies have demonstrated that at least certain maternal infections are associated with increased risk of psychiatric disorders in the offspring of humans. In addition, maternal immune reactions induced by TLR3 ligands have been demonstrated to induce certain behavioural changes in the offspring of rodents. Previous work in the Roberts Laboratory demonstrated that BALB/c mice infected with *T. gondii* behave differently from control uninfected mice in the open field test and using LCMS changes to the neurochemistry of brains in infected mice were observed. Therefore the studies herein, have the objectives of expanding these findings by: (i) examining *T. gondii* induced changes to the transcriptome of BALB/c mice. In addition the studies will evaluate the effects of congenital *T. gondii* infection and the maternal immune response it induces to (ii) modify the behaviour (iii) alter the

neurochemistry and (iv) alter the transcriptome of the brain of BALB/c mice. The overall aim is to determine how adult acquired *T. gondii* and congenital infection affects the transcriptome and metabolome of mice and establish if maternal immune activation caused by *T. gondii* infection has any effects on these parameters.

2 Material and Methods

2.1 Animal Procedure

All animal procedures were carried out according to guidelines from The Home Office of the UK Government. All work was covered by Home Office License: PPL60/4568. Group sizes were determined on the basis of Roberts's laboratory previous experience and all experiments were conducted with sufficient sample sizes. Experimental groups consisted of at least 5 mice per group to provide meaningful statistical analysis by the students t test, the Mann Whitney U test and other statistical analysis where appropriate using Ideom v19 worksheet (Creek et al., 2012), SPSS statistics software, SIMCA 14 (Umetrics, Sweden), MetaboAnalyst (Chong and Xia, 2018), and Prism 7 statistical analysis software (GraphPad Prism, USA).

2.2 Mice and caging

A study has shown that vertical *T. gondii* infection transmission, which occurs in BALB/c mice infected for the first time during pregnancy, mimics what occurs in human congenital toxoplasmosis (Roberts and Alexander, 1992). Therefore, BALB/c dams were selected as a model of congenital toxoplasmosis. All mice were provided by The Biological Procedures Unit (BPU) at University of Strathclyde, which is an ethical multispecies conventional unit licensed to house animals for use in Medical research. The cages were provided with bedding, water and food ad libitum. The rooms where the animals were held were on a cycle of 12 hours' light and 12 hours' dark.

2.3 Experimental design

A single male was paired with 3 females. Each day the females were checked twice for vaginal plugs as a sign of a possible pregnancy, and then if successfully found the females would be separated from the male. These females with vaginal plugs were checked daily for increasing weight and dams with no weight increase were excluded from the experiments.

The dams were infected orally at 12th day of gestation to mimic human infection, which often happens due to ingesting undercooked infected meat (Sukthana, 2006), by gavage with a concentration of 10 cysts of *T. gondii Beverley Strain* (Type II) per animal in 200µl of 1X PBS sterile (Phosphate Buffered Saline) (Invitrogen, UK).

The time of infection, the second trimester of gestation, was selected to reduce the risk of abortion and increase the incidence of parasite transmission to the embryo (Roberts and Alexander, 1992). A number of pregnant dams were not infected to provide sufficient numbers of offspring for the control group.

Once the litters were born, both control and congenital infected groups were fostered. New mothers carried out the fostering for all groups. Studies have been demonstrated that fostering is associated with altered emotional behaviour which could be a risk factor in development of behavioural disorders (Matthews et al., 2011). Thereby, this factor was maintained in both groups in order to demonstrate that any behavioural differences observed would have been caused by the additional factors of the parasite infection and not by the fostering effect of the offspring in adulthood.

The infected mice were sacrificed after giving birth. This protocol was followed twice at separated times.

2.4 Open field behavioural study

At 14 weeks old, open field study was carried out in a control room with monitoring the temperature, light and the noise between each test to reduce variation. Mice were carried to the test room in their home cages and were handled by the base of their tails at all times. Mice were placed on one of the four corners of the open field arena, which is 40cm x 40cm x 40cm black Perspex walls, and allowed to explore the apparatus for 30 minutes Figure 2.1. Locomotor behaviour of these mice was tracked using Ethovision software program which recorded by digital video file. After the 30 minutes' test, mice were returned in their home cages and the arena was cleaned and dried between tests. The parameters were studied for each mouse: the total distance moved in the arena, frequencies of centre square entries, duration of time spent in centre square and frequencies of head rotation.

Behavioural Statistics

SPSS software was used for statistical analysis. As the data was not normally distributed the one way non-parametric ANOVA was used to compare the three groups: control, congenital infected and the exposed non-infected group. The p value of <=0.05 indicated a significant difference between individual groups. To identify any significant differences between individual groups the post hoc value Bonferroni-Dunn test was performed.

A

B

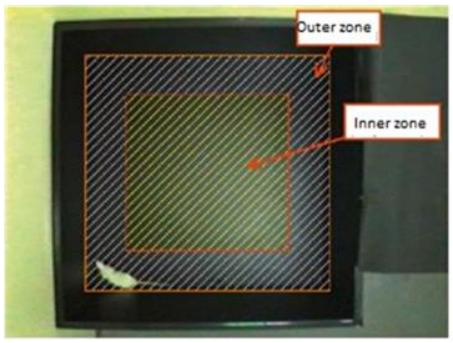

Figure 2.1 Open Field test:

A) It illustrates the open field box (40x40x40cm).

B) Green area demonstrates the inner zone of open field test and blue area demonstrates the outer zone of open field test.

2.5 Antibody ELISA (enzyme-linked immunosorbent assay)

2.5.1 Tail bleeding and Sera preparation

When the open field study has finished, tail bleeding procedure were performed on mice born from infected dams during pregnancy to collect blood samples. Antibody ELISA was performed to distinguish the infected group from the uninfected group. The blood was collected using capillary column. The blood samples were centrifuged at 4000 rpm for 5 minutes. The sera were collected and stored at -20°C.

2.5.2 Maintenance of *T. gondii* RH strain in *vivo* and *in vitro*

In vivo RH *T. gondii* were maintained in BALB/c mice. Mice were infected intraperitoneally with RH *T. gondii* tachyzoites. A few days later the mice were sacrificed

using CO_2 inhalation. The intraperitoneal cavity of the mice was washed out using 1ml of PBS to harvest the tachyzoites.

In vitro Human foreskin fibroblast cells (HFFs) were infected with RH *T. gondii* tachyzoites. HFFs were grown in 10ml DMEM, Dulbecco's Modified Eagle Medium (Invitrogen, UK), 10% foetal calf serum (FCS), 100U/ml Amphotericin B, 100U/ml penicillin/streptomycin and100U/ml µg L-glutamine (Gibco), in $75cm^3$ tissue culture flasks at 37^0C in 5% CO_2.

2.5.3 Toxoplasma Lysate Antigen preparation (TLA)

Antigen preparation was achieved in vitro by infecting Human Foreskin Fibroblast cells (HFF) with RH *T. gondii* tachyzoites. HFFs were grown in DMEM (Invitrogen, UK) supplemented with 1% penicillin/streptomycin (Gibco), 1% Amphotericin B, 1% L-glutamine (Gibco) and 10% Foetal calf serum (FCS) in $75cm^3$ flasks (Corning, UK). When the *T. gondii* had multiplied and invaded 90% of HFFs, the flasks were then scraped and the content of the flasks were centrifuged at 1500rpm for 10 minutes at 4^0C and the pellet was resuspended in 500µl of distilled water. The preparation was frozen, sonicated then defrosted at 60^0C and passed through a 25-gauge needle 10 times. This process was repeated eight times, 4500µl 1X PBS was then added. The protein concentration was measured using protein quantification assay (Bradford assay).

2.5.4 Optimisation of the Antibody ELISA

IgG1 and IgG2a antibody were optimised. Then levels of these antibodies were measured for all blood samples of mice from infected mothers during pregnancy in order to

distinguish whether the offspring were congenitally infected with *T. gondii* or maternally exposed but not infected. IgG antibody production occur in the adulthood period and when the immune system is fully developed. For this reason, the blood was collected from all experimental mice at the end of the study, as well as collecting the blood samples at that time would not influence the possible behaviour changes in the experimental groups.

2.5.5 ELISA

96 well ELISA plates (Greiner Bio-One Ltd, UK) were coated with 100 µl per well of 5µl/ml of *T. gondii* antigen, which diluted in coating buffer pH 9 and incubated at 4^{o}C overnight. Wash buffer (1X PPS pH 7, 1:20 Tween 20) was used to wash plates three times. 150 µl of blocking solution (5% (w/v) of dried skimmed milk, wash buffer) was added to each well. The plates were then incubated at 37^{o}C for one hour, followed by washing three times by wash buffer. 200 µl of the serum samples, which were diluted 1/500, 1/1000 and 1/2000 in 2.5% (w/v) milk and wash buffer, were added per well. The plates were incubated at 37^{o}C for one hour. All samples were made in duplicates. The plates were washed five times using wash buffer. 100µl of conjugate solution of two antibodies (IgG1 1/5000 in 1X PBS pH 7.4 and 2.5% (w/v) of dried skimmed milk and IgG2a 1/2500 in 1X PBS pH 7.4 and 2.5% (w/v) of dried skimmed milk. The plates were incubated for one hour, then were washed five times. 100µl of substrate prepared by 10ml of sodium acetate pH 5.5, 100 µl of TMB, and 5µl of H_2O_2 was added to each well. The plates were then incubated at room temperature for 30-40 minutes. 50µl of 10% (v/v)

H_2SO_4 was added to stop the colorimetric reaction. The plates were then read at 450nm of the Spectramax spectrophotometer (Molecular Devices, UK).

2.6 Metabolomics Extraction

At the end of the congenital experiment the mice were sacrificed and the brains were extracted to undergo metabolomics and molecular analysis.

In this experiment, 19 congenitally infected mice, 30 mice exposed to the infection during pregnancy but serologically uninfected and 12 control mice were sacrificed.

All mice brains were then analysed using Liquid Chromatography Mass Spectrometry (LCMS) (Thermo Fisher Scientific Inc., UK).

2.6.1 Sample preparation for metabolomics analysis:

The right hemisphere of the brain was extracted and stored in 0.1% of formic acid. Methanol/Chloroform/Water two step extraction protocol was followed. Tissue samples were homogenised with a blender in 4ml/g cold (0^{o}C) methanol (Fisher, Optima LC/MS Grade), and 0.85ml/g cold (0^{o}C) water. Homogenates were transferred into chilled tubes then 4ml/g chloroform (Fisher Chemical) and 2ml/g water were added to the homogenate. The sample preparation was then centrifuged at 1200rpm for 5 minutes at 4^{O}C to produce a biphasic mix. The upper polar phase was then put into HPLC vials and stored at -80 until analysis.

2.6.2 LCMS analysis

After metabolite extraction, LCMS was used by expert Dr. Gareth Westrop to detect and quantify metabolite production. The samples were analysed by an Orbitrap Classic mass spectrometer to obtain high resolution and provide the highest accuracy data available. For metabolic profiling the LC-MS platform consisted of an Accela 600 HPLC system in combination with an Exactive (Orbitrap) mass spectrometer (Thermo Fisher Scientific, Bremen, Germany). Two columns, with complementary abilities were used [zwitterionic ZIC-pHILLIC column (150 mm × 4.6 mm; 3.5 μm, Merck, Germany) and the reversed phase ACE C18-AR column (150 mm × 4.6 mm; 3.5 μm, Hichrom)]. An injection volume of 10 μl and a flow rate of 0.3 ml/min were employed. A gradient of mobile phase A, 20 mM ammonium carbonate pH 9.2, and mobile phase B, acetonitrile (ACN) was used to elute the ZIC-pHILLIC column. The concentration of buffer A was increased from 20% to 80% over 30 min and then maintained at 92% for 5 mins, before equilibrating at 20%. The mobile phases for the reverse phase column consisted of: A, 0.1% (v/v) formic acid in H20; B, 0.1% (v/v) formic acid in ACN. Buffer A was decreased from 95% to 10% over 30 min and maintained at 10% for 5 min.

Data processing

Raw data files of metabolite standard solution were processed using ToxID 2.1 (Thermo Fisher Scientific Inc., Hemel Hempstead, UK). After visual evaluation of extracted ion chromatograms, the retention times of the standards were used to calibrate IDEOM v19. Briefly, raw files of sample metabolites were processed and converted to mzXML open

format using msConvert (ProteoWizard). Chromatograms were extracted using XCMS and stored in PeakML before aligning replicate peaks and combining them using mzMatch.R. After noise filtering and gap filling a CSV file was generated and imported into IDEM v19 for metabolite identification based on accurate mass (± 3ppm) and retention time prediction. The lipids and peptides were excluded from the lists of putatively identified metabolites in the biological samples. The reason for that the lipid profile is subject to frequent alterations in the mouse brain and therefore it difficult to detect changes and to maintain consistent between mice groups in any experiment (Rappley et al., 2009).

2.6.3 Metabolite identification

The majority of metabolite identities were confirmed by accurate mass and in addition either by matching the sample retention time to that of an authentic standard (± 0.2 min) or by obtaining MS2 spectra. The confirmed metabolites correspond to the metabolic standards initiative (MSI) level 1. Metabolites putatively identified by accurate mass and predicted retention time correspond to MSI level 2.

2.6.4 Metabolomics Statistics

The file produced by mzMatch were further analysed by IDEOM v19, and the student t test was performed to establish the presence of possible significant differences between the metabolites detected in different groups. Further analysis was carried out using SIMCA 14 (Umetrics, Sweden) software, for processing principal components analysis (PCA), partial least squares discriminant analysis (PLS-DA) and orthogonal partial least

squares discriminant analysis (OPLS-DA), which were carried out to visualize the maximal metabolic alterations between each group in all experiments. MetaboAnalyst server and the BioCyc collection of Pathway/Genome Databases was used for further analysis.

2.7 Molecular Analysis

The sagittal section of the left hemisphere of the brain was stored in RNA *later* at -80°C in order to carry out the molecular analysis (RNA extraction).

2.7.1 Isolation and extraction of total RNA from mouse brain

RNeasy purification kit (Qiagen) was used to extract total RNA from mouse brain. RNA *later* stabiliser reagent was removed and the mouse brain was then weighed. 10µl of β-mercaptoethanol was added to RLT plus buffer per ml. 15-20 mg of brain tissue was mixed with 600µl of RLT-plus buffer, the mixture was then homogenised. After that, the cell lysate was pipetted into a QIAshredder column in a 2 ml collection tube, it was then centrifuged at 15000 rpm for 2 minutes which was repeated at maximum speed for 3 minutes. The supernatant was transferred to a gDNA eliminator column to spin at 10000 rpm for 1 minute, the supernatant was then used to purify total RNA using an RNeasy spin column. The total volume of supernatant was checked by a pipette and an equal volume of 70% ethanol was added and mixed well by pipetting. 700µl of the mix was put into an RNeasy spin column to centrifuge at 10000 rpm for 15 seconds and the flow-through was discard, and this step was repeated for the reminder of mix. 700µl of RW1 buffer was then

added to the column and centrifuged at 10000 rpm for 15 seconds and the flow-through discarded.

500µl of RPE buffer was then added and centrifuged at 10000 rpm for 15 seconds and 500µl of RPE buffer was added again and centrifuged at 10000 rpm for 2 minutes. The column was transferred to a new 2ml collection tube and centrifuged at 10000 rpm for 1 minute. The column was then transferred to a new 1.5ml collection tube and 50µl of RNAse free water was added and eluted RNA by centrifugation at 10000 rpm for 1 minute. The RNA samples were stored at -20^{o}C.

2.7.2 The integrity and concentration of RNA

The integrity and concentration of RNA was checked using a Bio-analyser kit (Agilent RNA 6000 Nano Bio-analyser). The Agilent Bioanalyser software creates an electropherogram graph, which diagrams fluorescence over time. Smaller molecules are pulsed through the separation channel quicker than larger ones and will therefore appear on the left side of the electropherogram. For each sample the software creates a gel image to accompany the graph. Expect 5-10µg of RNA from 10mg tissue in 50µl so concentration is about 100-200ng/µl. Following this processes, the samples were sent to GTCA Biotech for RNA Transcriptomics and RNA sequencing data analysis.

2.7.3 GATC service Processes

2.7.3.1 Samples of chronic infection experiment

Samples from previous *T. gondii* acquired infection experiment were analysed to investigate the transcriptomic changes that may occur and compared with congenital infection. Therefore, the samples was divided into two groups, Uninfected (Control) group and Infected with *T. gondii* group. Each group has three biological replicates. See table 2.1.

Table 2.1 Name of the (replicate) groups and their assigned samples used in the analysis (PE= paired end)

Group	**Assigned samples**	**Read Type**
Infected	D2, D3, D4	PE
Uninfected	B1, B3, B4	PE

2.7.3.2 Samples of congenital infection experiment

Samples from the congenital *T.gondii* infection were divided into three groups, Uninfected (control) group, congenitally infected group, exposed uninfected group. See table 2.2.

Table 2.2 Name of the (replicate) groups and their assigned samples used in the analysis (SE = Single end).

Group	Assigned samples	Read Type
Congenitally infected	I25, I26, I27	SE
Exposed uninfected	U35, U36, U37	SE
Control	C10, C11, C12	SE

2.7.3.3 Reference

Organism: Mouse, Genome: mm10 / GRCm38, Ensembl, Annotations: v85 Ensembl.

2.7.3.4 Workflow

The workflow for transcriptomic analyses is summarised in Figure 2.2

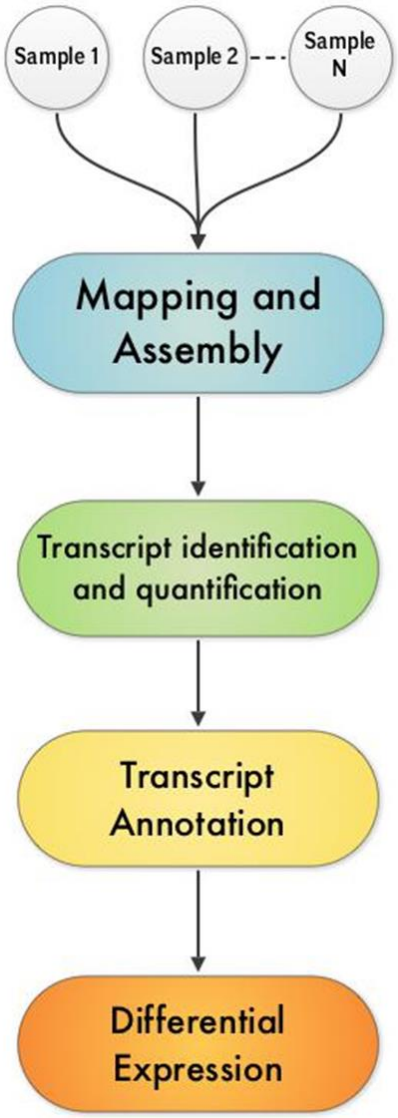

Figure 2.2 RNA-Seq Workflow

2.7.3.5 Expression Analysis

The RNA-Seq reads are aligned to the reference genome or reference transcriptome using Bowtie generating genome / transcriptome alignments. TopHat identifies the potential exon-exon splice junctions of the initial alignment. Then Cufflinks identifies and quantifies the transcripts from the preprocessed RNA-Seq alignment-assembly. After this, Cuffmerge merges the identified transcript pieces to full length transcripts and annotates the transcripts based on the given annotations. Finally, three biological replicates for each group were averaged then transcripts from samples / conditions are compared using Cuffdiff to determine the differential expression levels at transcript and gene level including a measure of significance between samples / conditions. Cuffdiff program calculates the FPKM fold change to determine which genes are differentially regulated between experimental groups. Cuffdiff also calculates p-value and q-value to determine if the fold change is significant. Each brain was treated as a biological replicate in Cuffdiff and therefore variation between replicates was considered when assigning a p-value. A p-value and q-value <0.05 were considered significant.

2.7.3.6 Variant Analysis

The SNP and InDel calling is done using GATK's Haplotype Caller (DePristo et al., 2011, McKenna et al., 2010). Variants detected are annotated based on their gene context using snpEff. Several metrics, that are used to evaluate the quality of a variant, are annotated using GATK's Variant Annotator module. Customised filters are applied to the variants to filter false positive variants using GATK's Variant Filtration module.

3 Metabolomics profile for BALB/c mice brain in adulthood infected with *T. gondii*

3.1 Introduction

In the last decades a large body of evidence has emerged to highlight a relationship between infection and the development of neuropsychiatric diseases (Patterson, 2009). A meta-analysis of studies has shown that infection by some agents, such as Human *Herpes*virus, Borna Disease Virus, *Chlamydophila pneumonia* and *T. gondii* may be associated with development of psychiatric disorders (Arias et al., 2012). These data illustrate that the incidence of at least some infectious agents are increased in psychiatric patients compared with other people. It is difficult to demonstrate a causative relationship between any infectious agent and neuropsychiatric diseases in humans. However, there is a large amount of literature and many studies that connect some diseases such as toxoplasmosis with behavioural changes or neuropsychiatric disease in humans (Flegr et al., 2002, Flegr, 2007, Flegr et al., 2009). In addition, *T. gondii* infection has been shown to have the ability to manipulate rodent behaviours under laboratory conditions (Hay et al., 1984a, Webster et al., 1994, Gonzalez et al., 2007, Berdoy et al., 1995, Gulinello et al., 2010, Skallova et al., 2006). After infection, *T.gondii* may be located anywhere in the brain (McConkey et al., 2013) because it has the ability to reach the central nervous systems by the immune cells (Ueno and Lodoen, 2015). *T. gondii* infection has the potential to directly interfere with neuronal cell function, but the immune processes during chronic infection may also lead to alterations in neuronal connectivity, synaptic plasticity and brain function (Parlog et al., 2015, Klein et al., 2017). The precise mechanisms, immunological mediators and their consequences have not been extensively studied,

however new technologies offer opportunities to advance knowledge. For example, metabolomics is a rapidly emerging field of "omics" research and can provide a global analysis of the metabolic changes in biological systems in response to external stimuli (Nicholson et al., 1999). Metabolomics has been as a powerful method to profile metabolic alterations associated with microbial infections. Identification of molecular changes associated with chronic *T. gondii* infection could provide better understanding of its contributions to develop neuropsychiatric diseases.

3.2 Results

At week 4 after infection, adult female BALB/c mice were sacrificed, the right hemisphere of brain extracted to preform metabolomic analyses as described in chapter 2.

3.2.1 Global metabolomic changes in adult mice brain with *T. gondii* infection

In this study, LC-MS based metabolomic analysis were used to identify characteristics of the entire metabolite profiles of the entire brain of mice infected with *T. gondii* as adults and to determine the alterations which discriminate infected animals from non-infected animals. It was decided that the lipid profile in the mouse brain would not be taken into consideration for the metabolomics analysis in this study. The reasons for this are: (i) the lipid profile is subject to frequent alterations in the mouse brain and therefore it is difficult to detect changes and to maintain consistent conditions between mice groups in any experiment (Rappley et al., 2009) and (ii) the LC-MS systems used are not optimised for lipidomics. Initial principal component analysis (PCA) of LCMS outputs from the pHILLIC and C18-PFP columns confirmed that infected and non-infected mouse brains

formed distinct groups. Orthogonal partial least squares discriminant analysis (OPLS-DA) was performed to identify metabolites associated with acquired *T. gondii* infection. OPLS-DA is a supervised pattern recognition process that allows identification and ranking of metabolites that are associated with mouse infection status. This allowed ranking of metabolites by VIP (Variable Importance for the Projection) scores. The OPLS-DA plots show that infected groups clearly separate from the corresponding controls Figure 3.2. Tables were produced allowing easy comparisons of (VIP≥1) and the P-value of student's t-test for each metabolite. These identified metabolites include amino acids, carbohydrates, cofactors and vitamins, and are known to contribute to a wide range of biological processes and pathways. The statistically significant metabolites detected in this experiment, using pHILLIC column (primary column) that was augmented with C18-PFP Column to obtain important missing metabolites. The pHILLIC column, following manual curation and filtration successfully identified 232 metabolites with high confidence and the C18-PFP column identified 159 metabolites with high confidence. 70 of these metabolites were identified using both columns adding an additional degree of confidence (Figure 3.1). The formula, fold change (FC) and *P*- value for each metabolite are shown in Tables 3.1 and 3.2 respectively.

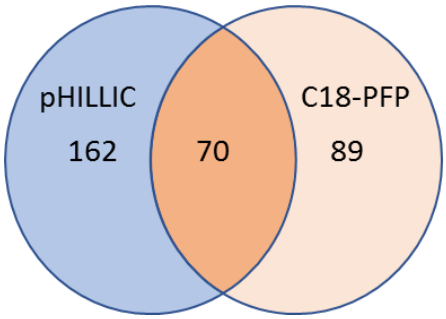

Figure 3.1 Venn diagram shows the number of metabolites that were detected by pHILLIC Column, C18-PFP Column or Both columns in adult mice experiment. For the details of these metabolites see appendix 3.

Different analysis methods was used and same results that are presented in this chapter were obtained. For different analysis see appendix 3.

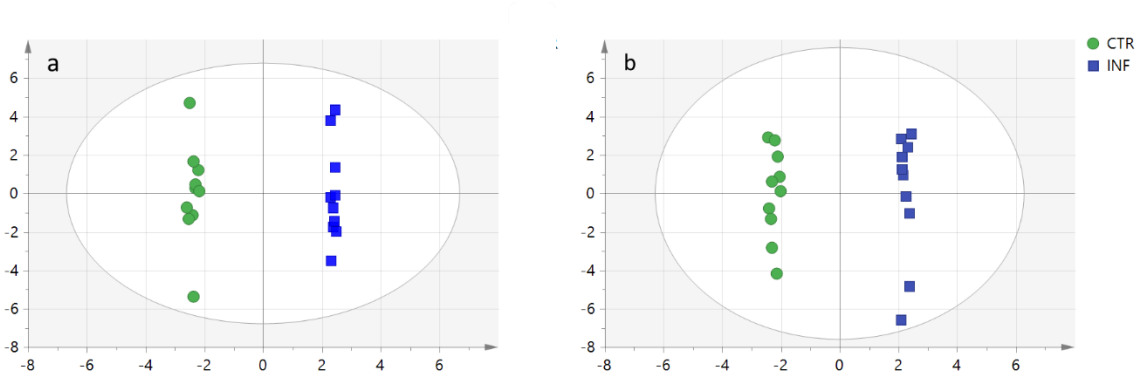

Figure 3.2 Orthogonal Partial Least Square Discriminant Analysis (OPLS-DA) score plot shows an excellent separation between infected mice group and control groups, each data point represents one mouse brain sample. (a)The metabolites were detected using pHILLIC Column in LC-MS. (b) the metabolites were detected using C18-PFP Column.

Table 3.1 List of differentially expressed metabolites identified by pHILLIC Column according to VIP score or p values ≤ 0.05. The metabolites highlight by yellow color corresponding to standard metabolites that are used. FC Inf/Ctr: Fold Change of Infected group compared with Control group.

VIP	Formula	Identification	FC Inf/Ctr	*P*-value
2.80	C10H12N2O3	L-Kynurenine	**4.07**	7.39E-06
2.69	C5H4N4O3	Urate	**3.24**	7.74E-05
2.14	C7H8N2O	1-Methylnicotinamide	**2.44**	2.88E-05
2.00	C12H23NO4	N-(octanoyl)-L-homoserine	**2.15**	8.23E-04
1.97	C8H17NO6	N-acetyl -D- glucosaminitol	**2.1**	5.57E-05
1.94	C7H15NO3	L-Carnitine	**2.05**	2.67E-05
1.92	C5H12O4	D-Apiitol	**2.03**	9.40E-05
1.80	C9H17NO4	O-Acetylcarnitine	**1.87**	6.15E-05
1.78	C4H6N4O3	Allantoin	**1.85**	8.35E-05
1.77	C12H21NO4	Tiglylcarnitine	**1.85**	1.46E-03
1.73	C7H15N3O3	L-Homocitrulline	**1.9**	1.20E-03
1.62	C11H19NO6	Lotaustralin	**1.69**	1.14E-05
1.60	C3H9N3O3S	Taurocyamine	**1.67**	6.60E-05
1.58	C8H17NO2	DL-2-Aminooctanoicacid	**2.13**	1.30E-02
1.51	C7H14N2O4S	L-Cystathionine	0.8	5.20E-01
1.49	C14H18N2O2	Hypaphorine	**1.7**	4.80E-03
1.45	C9H16N2O5	N2-Succinyl-L-ornithine	**0.64**	8.14E-04
1.41	C7H13NO3	5-Acetamidopentanoate	**1.52**	7.58E-04
1.41	C8H13NO5	N2-Acetyl-L-aminoadipate	**0.67**	3.59E-05
1.39	C15H24N5O17P3	ADPribose 2'-phosphate	**1.47**	3.45E-03
1.35	C2H4O5S	Sulfoacetate	**0.68**	5.19E-03
1.31	C7H15O9P	1-Deoxy-D-altro-heptulose 7-phosphate	**0.61**	2.75E-02
1.29	C10H15N3O4	5-Methyl-2'-deoxycytidine	**1.46**	5.47E-03
1.27	C4H7NO4	L-Aspartate	0.72	1.37E-01
1.27	C16H25N5O14P2	GDP-3,6-dideoxy-D-galactose	**1.46**	1.26E-02
1.27	C3H5O6P	3-Phosphonopyruvate	**0.7**	1.45E-03
1.26	C6H10N2O3	4-Methylene-L-glutamine	**1.38**	1.19E-04
1.25	C5H5N5O	Guanine	1.34	2.26E-01
1.25	C23H45NO5	3-Hydroxyhexadecanoylcarnitine	**1.46**	4.70E-02
1.21	C3H5O6P	Phosphoenolpyruvate	**1.38**	1.37E-02
1.17	C8H16N2O3	N6-Acetyl-L-lysine	**1.36**	4.04E-03
1.17	C20H32N6O12S2	Glutathione disulfide	0.73	1.81E-01
1.17	C5H11NO3S	L-Methionine S-oxide	1.33	6.58E-02

1.15	C10H17NO6	Linamarin	**1.34**	6.24E-04
1.15	C4H4N2O2	**Uracil**	**1.33**	1.28E-02
1.14	C17H26O4	[6]-Gingerol	**0.65**	4.04E-02
1.14	C4H10N3O5P	**Phosphocreatine**	**1.45**	1.78E-02
1.13	C3H7N3O2	Guanidinoacetate	**1.35**	7.80E-03
1.12	C11H15N5O3S	**5'-Methylthioadenosine**	1.12	5.72E-01
1.11	C6H9N3O2	L-Histidine	**0.74**	7.35E-03
1.11	C7H8N2O2	N1-Methyl-2-pyridone-5-carboxamide	**1.4**	2.34E-02
1.11	C3H8NO6P	O-Phospho-L-serine	**1.33**	4.92E-02
1.10	C10H13N5O4	**Adenosine**	**0.77**	5.03E-03
1.10	C6H6N2O	**Nicotinamide**	1.31	6.07E-02
1.07	C3H7NO3	**L-Serine**	**0.78**	5.02E-03
1.06	C6H9NO6	Nitrilotriacetic acid	**1.32**	4.05E-02
1.05	C8H15N3O4	N-Acetyl-L-citrulline	0.71	1.09E-01
1.05	C7H10O7	2-Hydroxybutane-1,2,4-tricarboxylate	0.78	5.34E-02
1.04	C20H26O8	Glaucarubolone	**0.7**	3.98E-02
1.03	C9H17NO8	Neuraminic acid	**0.77**	4.77E-03
1.03	C6H12O4S	5-Methylthio-D-ribose	**1.26**	4.80E-02
1.01	C9H14N4O3	**Carnosine**	0.75	1.04E-01
0.99	C6H14O6	**D-Sorbitol**	**0.81**	2.25E-03
0.97	C21H27N7O14P2	**NAD+**	**0.83**	2.46E-02
0.95	C7H8N2O3	2,3-Diaminosalicylic acid	**0.82**	3.26E-02
0.95	C5H10O2	Pentanoate	**0.77**	2.69E-02
0.94	C5H14NO4P	Choline phosphate	**1.21**	3.62E-02
0.94	C15H23N5O14P2	Phosphoribosyl-AMP	**1.25**	2.52E-02
0.91	C6H9NO2	2,3,4,5-Tetrahydropyridine-2-carboxylate	**1.22**	1.74E-02
0.90	C6H12O7	**D-Gluconic acid**	**1.20**	5.91E-03
0.90	C11H17NO8	2,7-Anhydro-alpha-N-acetylneuraminic acid	**0.83**	7.56E-03
0.89	C2H5O4P	Phosphonoacetaldehyde	**1.20**	1.08E-02
0.87	C5H9NO4	L-Glutamate	**0.83**	1.04E-02
0.87	C6H12O5	L-Rhamnose	**0.82**	3.58E-02
0.86	C9H18N4O4	N2-(D-1-Carboxyethyl)-L-arginine	**1.24**	3.94E-02
0.84	C9H13N5O3	6-Lactoyl-5,6,7,8-tetrahydropterin	**1.20**	1.94E-02
0.84	C13H25NO3	N-Undecanoylglycine	**0.78**	4.54E-02
0.82	C5H12O5	**Xylitol**	**0.84**	2.71E-02
0.81	C11H19N3O6S	gamma-L-Glutamyl-L-cysteinyl-beta-alanine	**0.86**	1.28E-02
0.78	C6H8N2O3	4-Imidazolone-5-propanoate	**0.86**	3.23E-02

0.77	C10H17NO5	Suberylglycine	**0.84**	3.00E-02
0.76	C21H29N7O14P2	NADH	**1.16**	1.21E-02
0.68	C10H14N5O7P	**AMP**	**0.91**	3.99E-02

Table 3.2 List of differentially expressed metabolites identified by C18-PFP Column according to VIP score p values ≤ 0.05. The metabolites highlight by yellow color corresponding to standard metabolites that are used. FC Inf/Ctr: Fold Change of Infected group compared with Control group.

VIP	FORMULA	Identification	FC Inf/Ctr	*P*-value
2.81	C10H13NO3	L-Tyrosine methyl ester	0.85	4.36E-01
2.47	C11H10O5	2-Succinylbenzoate	0.77	1.42E-01
2.31	C10H12N2O3	L-Kynurenine	**3.34**	1.39E-07
2.14	C23H41NO4	9,12-Hexadecadienoylcarnitine	0.83	4.13E-01
1.94	C12H23NO4	2-Methylbutyroylcarnitine	**2.39**	2.56E-05
1.79	C4H12N2	Putrescine	**2.19**	1.32E-04
1.74	C5H9N3	1H-Imidazole-4-ethanamine	**0.48**	1.32E-05
1.69	C9H15N3O2S	Ergothioneine	**2.16**	5.39E-04
1.50	C7H15NO3	L-Carnitine	**1.74**	2.30E-05
1.46	C10H19NO4	O-Propanoylcarnitine	**1.71**	3.69E-05
1.44	C13H25NO4	Hexanoylcarnitine	**1.68**	1.43E-02
1.39	C8H11NO2	Dopamine	**0.63**	4.84E-03
1.39	C10H14N2O4	Porphobilinogen	**1.67**	7.78E-03
1.35	C8H17NO2	Methacholine	**1.86**	1.33E-02
1.28	C3H7N3O2	Guanidinoacetate	**1.53**	3.34E-05
1.27	C7H16N4O2	Homoarginine	**1.6**	3.27E-03
1.27	C6H13NO5	D-Glucosamine	**1.73**	2.67E-02
1.23	C6H11NO2	L-Pipecolate	**1.87**	2.21E-02
1.19	C3H7O5P	Propanoyl phosphate	1.41	3.27E-01
1.18	C4H4N2O2	Uracil	**1.47**	9.57E-04
1.15	C8H16N2O5	N-Acetyl-beta-D-glucosaminylamine	1.26	5.26E-01
1.11	C5H5N5O	Guanine	**1.42**	3.12E-02
1.08	C14H17N5O8	Succinyladenosine	1.28	4.30E-01
1.07	C10H13N5O5	Guanosine	1.23	4.43E-01
1.06	C9H13NO2	3-Methoxytyramine	0.81	1.81E-01
1.05	C11H11NO3	Indolelactate	**1.51**	4.70E-02
1.05	C11H15N5O3S	5'-Methylthioadenosine	1.1	7.45E-01
1.04	C6H13NO2S	S-Methyl-L-methionine	**1.33**	1.32E-02
1.04	C9H13N3O5	Cytidine	1.3	1.79E-01
1.03	C10H17N3O6S	Glutathione	0.9	6.34E-01
1.00	C5H14NO4P	Choline phosphate	**1.34**	5.96E-03
0.62	C2H6O4S	2-Hydroxyethanesulfonate	**1.17**	1.52E-02

0,91	C7H15NO2	4-Trimethylammoniobutanoate	**0.78**	1.95E-02
0.98	C6H11N3O3	5-Guanidino-2-oxopentanoate	**1.35**	1.16E-03
0.51	C10H14N5O7P	AMP	**0.93**	2.07E-02
0.97	C4H9O7P	D-Erythrose 4-phosphate	**0.73**	8.97E-03
0.83	C6H10O8	D-Glucarate	**1.27**	1.37E-02
0.61	C5H11O8P	D-Ribose 5-phosphate	**1.17**	4.81E-02
0.85	C4H4O4	Fumarate	**1.27**	1.26E-02
0.87	C5H4N4O	Hypoxanthine	**1.24**	1.77E-02
0.84	C10H12N4O5	Inosine	**1.24**	2.14E-02
0.9	C6H13N3O3	L-Citrulline	**1.28**	2.31E-02
0.83	C6H14N2O2	L-Lysine	**1.22**	2.67E-04
0.84	C5H9NO2	L-Proline	**1.23**	3.59E-03
0.81	C11H19NO9	N-Acetylneuraminate	**0.85**	1.93E-03
0.9	C7H14N2O3	N-Acetylornithine	**1.29**	1.04E-02
0.44	C3H9O6P	sn-Glycerol 3-phosphate	**1.10**	4.06E-02
0.83	C5H4N4O2	Xanthine	**1.23**	4.99E-03

3.2.2 Variations in metabolic pathways of adult mice brain infected with *T. gondii*

An indication of the metabolic pathways most differentially affected by infection was visualised using BioCyc Pathway Database Collection. The BioCyc software orders pathways according to pathway perturbation scores (PPS) as a means to identify pathways that are most affected. Metabolic pathways most affected between the infected group and their controls included those involved in purine metabolism, tryptophan metabolism, arginine metabolism and L-carnitine biosynthesis. Metabolites from these pathways also scored high in terms of their VIP score and were often individually statistically significant between infected and non-infected control samples.

3.2.2.1 Purine Degradation Pathway

Purine metabolism were found to have high PPS valuse (see Table 3.4 in appendix 3). Mice infected with *T. gondii* were found to have statistically significant decreased levels of adenosine (p= 0.005), but incresed levels of inosine (p= 0.02), xanthine (p= 0.0004), guanine (P= 0.03), urate (P= 0.00007) and allantoin (P= 0.00008). These metabolites also had VIP scores of 1 or greater adenosine (VIP: 1.1), guanine (VIP: 1.25), urate (VIP: 2.69) and allantoin (VIP: 2.69). Overall these data indicate that *T. gondii* infection induces purine degradation in the brains of mice.

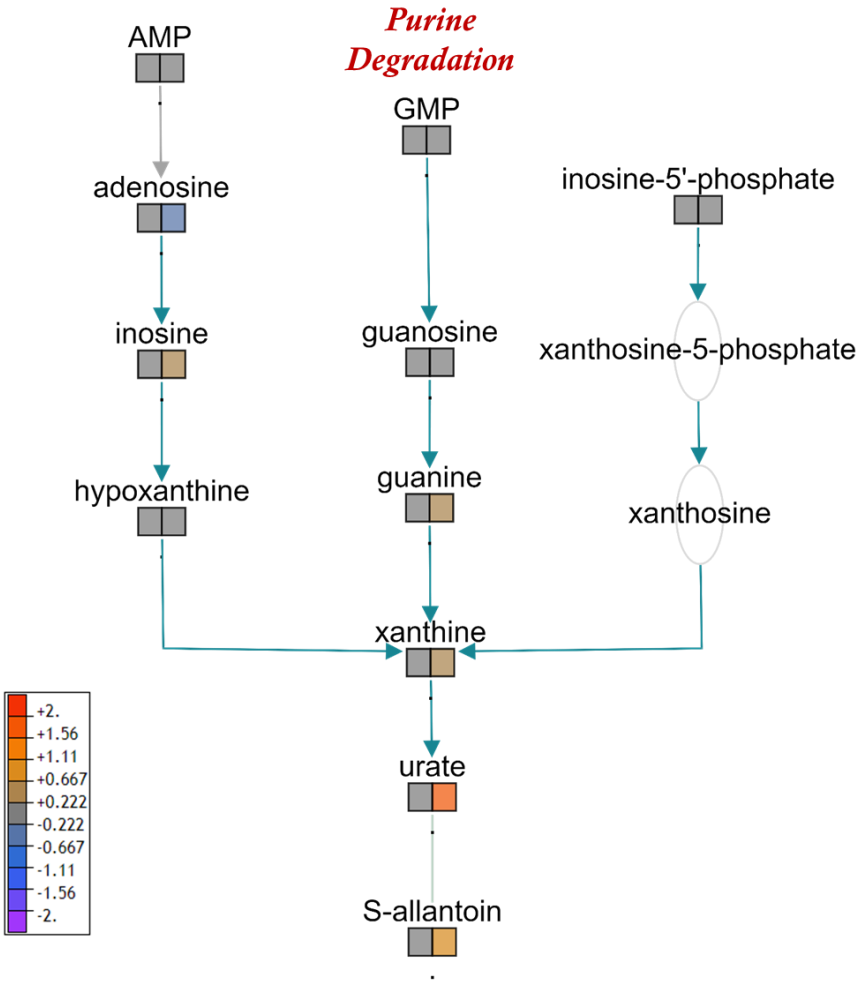

Figure 3.3 Purine Degradation Pathway. Metabolites which were detected in this pathway are represented by two squares. First square represents control group and second square represents infected group (log 2 transformed) are visualised as a color spectrum scaled from least abundant to highest range is from -2 to 2. Purple indicates low expression, while red indicates high expression of the changed metabolites. Metabolites that were found to be significantly different between infected and non-infected mice are adenosine (p=0.005), inosine (p=0.002), xanthine (p=0.0004), guanine (p=0.03), urate (p=0.00007) and allantoin (p=0.00008).

3.2.2.2 Tryptophan Degradation Pathway

Pathways associated with tryptophan metabolism were found to have high PPS values (see Table 3.4 in appendix 3). Mice infected with *T. gondii* were found to have statistically significant increased levels of kynurenine (p= 0.00007) and N-methylnicotinamide (p= 0.00002). Metabolites in these pathways also had VIP scores of 1 or greater kynurenine (VIP: 2.8), N-methylnicotinamide (VIP: 2.14) and Nicotinamide (VIP: 1.1). This data indicates that *T. gondii* infection directs tryptophan metabolism towards kynurenine rather than serotonin in the brains of mice.

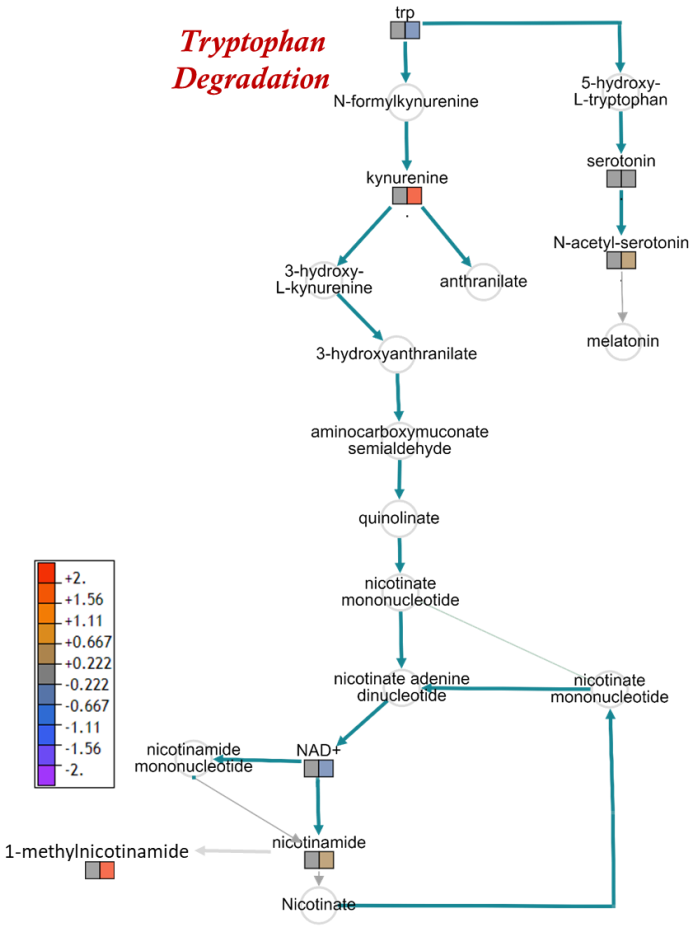

Figure 3.4 Tryptophan Degradation Pathway. Metabolites which were detected in this pathway are represented by two squares. First square represents control group and second square represents infected group (log 2 transformed) are visualised as a color spectrum scaled from least abundant to highest range is from -2 to 2. Purple indicates low expression, while red indicates high expression of the changed metabolites. Metabolites that were found to be significantly different between infected and non-infected mice are kynurenine (p=0.00007) and N-methylnicotinamide (p=0.00002).

3.2.2.3 Dopamine Pathway

Mice infected with *T. gondii* were found to have statistically significant decreased levels of dopamine (p= 0.004). Dopamine and 3-methoxytyramine had high VIP scores of 1 or greater dopamine (VIP: 1.4) and 3-methoxytyramine (VIP: 1.1).

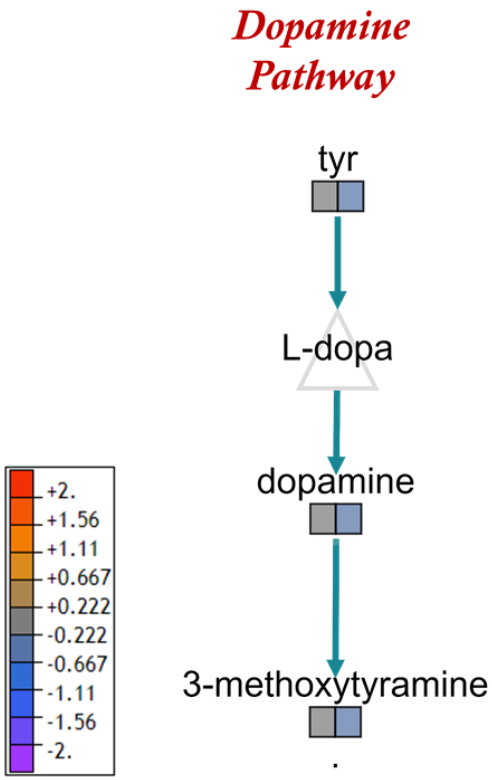

Figure 3.5 Dopamine Pathway. Metabolites which were detected in this pathway are represented by two squares. First square represents control group and second square represents infected group (log 2 transformed) are visualised as a color spectrum scaled from least abundant to highest range is from -2 to 2. Purple indicates low expression, while red indicates high expression of the changed metabolites. Metabolite that was found to be significantly different between infected and non-infected mice is dopamine (p=0.004).

3.2.2.4 Arginine and Proline Biosynthesis with other amino acids degradation.

Mice infected with *T. gondii* were found to have statistically significant increased levels of putresine (p= 0.0001), guanidinoacetate, L-Citrulline (p=0.002), (p= 0.007), creatine-phosphate (phosphocreatine) (p= 0.01), but decreased levels of L-serine (p= 0.005).These metabolites also had VIP scores of 1 or greater putrescine (VIP: 1.8), guanidinoacetate VIP: 1.13), creatine-phosphate (VIP: 1.14) and L-serine (VIP: 1.07). In addition, other metabolites associated with arginine and proline biosynthesis including L- cystathionine (VIP: 1.51) and glutathione disulfide (VIP: 1.17) were reduced in the brains of infected mice. These data indicate that *T. gondii* infection alter arginine and induces putrescine accumulation in the brains of mice.

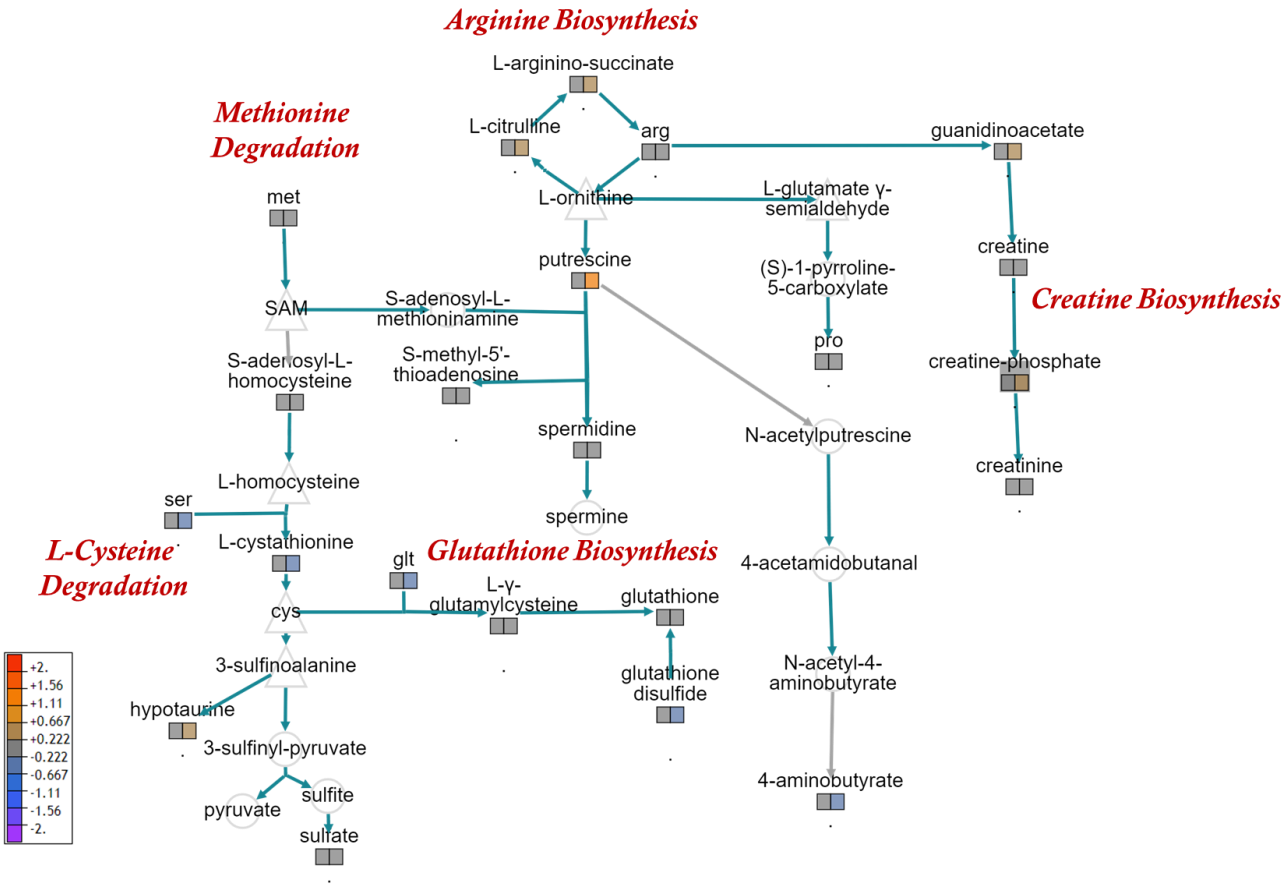

Figure 3.6 Arginine and Proline Biosynthesis and other pathways. Metabolites which were detected in these pathways are represented by two squares. First square represents control group and second square represents infected group (log 2 transformed) are visualised as a color spectrum scaled from least abundant to highest range is from -2 to 2. Purple indicates low expression, while red indicates high expression of the changed metabolites. Metabolites that were found to be significantly different between infected and non-infected mice are Putrescine (p=0.0001), guanidinoacetate (p=0.007), L-Citrulline (p=0.002), creatine-phosphate (p= 0.01) and L-serine (p= 0.005).

3.2.2.5 Glycolysis and Pentose phosphate pathways

Mice infected with *T. gondii* were found to have statistically significant increased levels of 3-phospho-L-serine (0-phospho-L-serine) (p= 0.04), phosphoenolpyruvate (p= 0.01), but decreased levels of L-serine (p= 0.005).These metabolites also had VIP scores of 1 or greater 3-phospho-L-serine (VIP: 1.11), phosphoenolpyruvate (VIP: 1.21), and L-serine (VIP: 1.07).

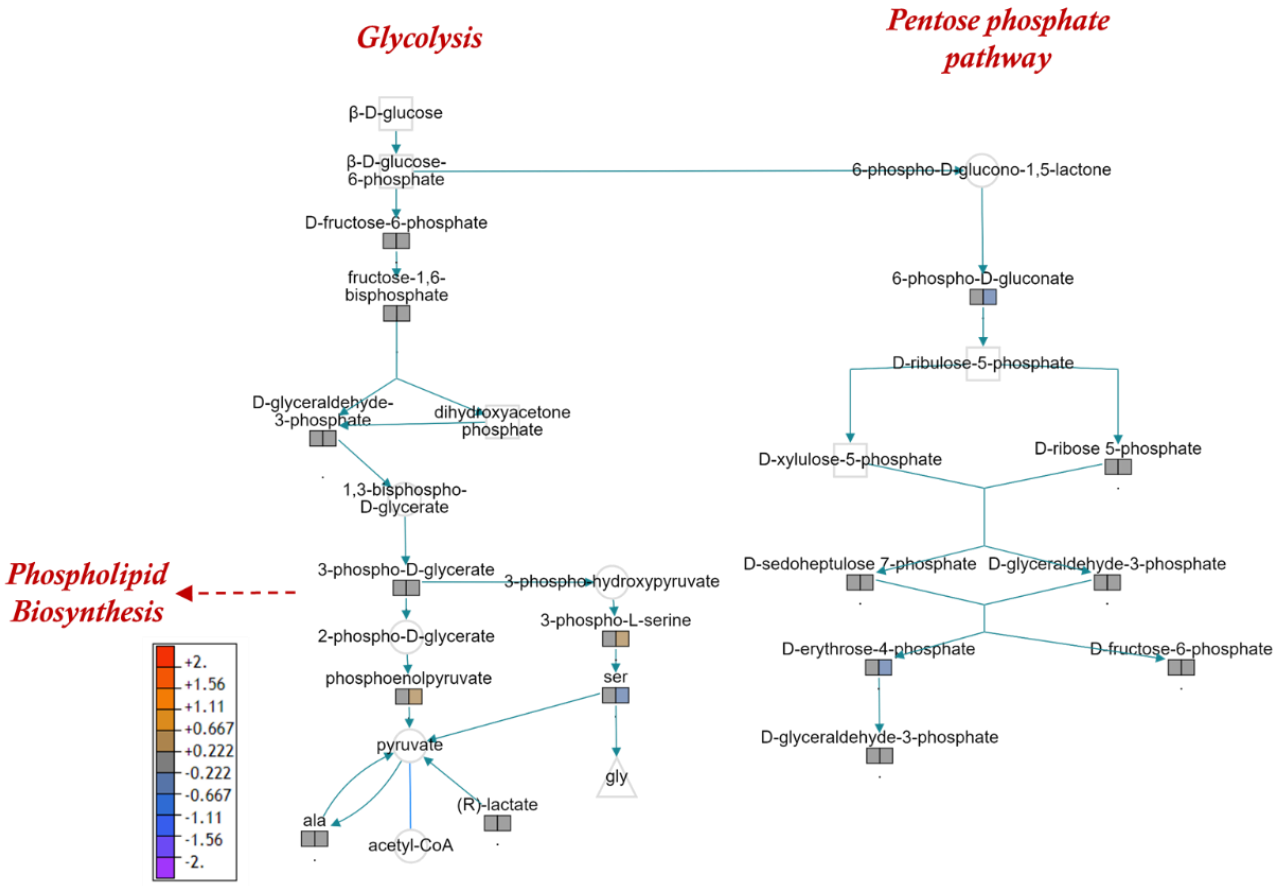

Figure 3.7 Glycolysis and Pentose phosphate pathways. Metabolites which were detected in these pathways are represented by two squares. First square represents control group and second square represents infected group (log 2 transformed) are visualised as a color spectrum scaled from least abundant to highest range is from -2 to 2. Purple indicates low expression, while red indicates high expression of the changed metabolites. Metabolites that were found to be significantly different between infected and non-infected mice are 3-phospho-L-serine (0-phospho-L-serine) (p=0.04), phosphoenolpyruvate (p=0.01) and L-serine (p= 0.005).

3.2.2.6 L-Carnitine Biosynthesis

Mice infected with *T. gondii* were found to have statistically significant increasd levels of L-carnitine (p= 0.00002). L-carnitine had high VIP scores of 1 or greater dopamine (VIP: 1.94).

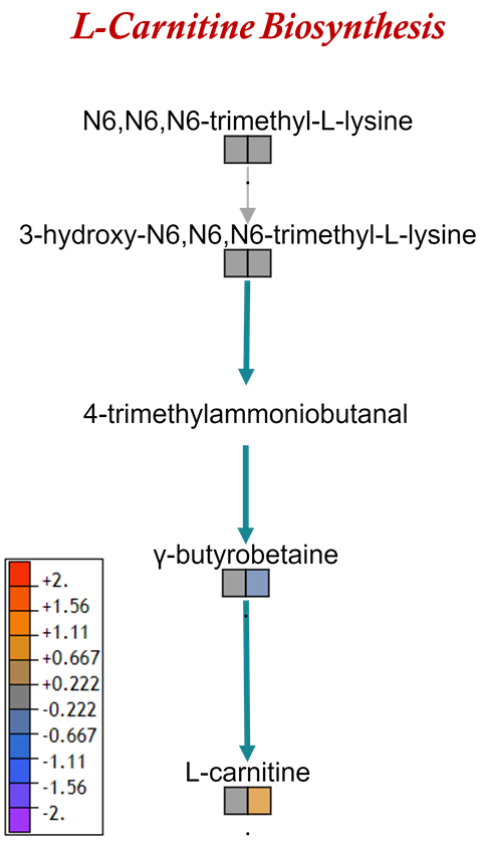

Figure 3.8 L-Carnitine Biosynthesis. Metabolites which were detected in these pathways are represented by two squares. First square represents control group and second square represents infected group (log 2 transformed) are visualised as a color spectrum scaled from least abundant to highest range is from -2 to 2. Purple indicates low expression, while red indicates high expression of the changed metabolites. Metabolites that was found to be significantly different between infected and non-infected mice is L-carnitine (p= 0.00002).

3.3 Conclusion

The results presented in this chapter demonstrate that there is significant alteration in metabolism of adult mice infected with *T. gondii*. In this study, an untargeted approach was used to determine metabolites and thus pathway that *T. gondii* infection influenced. Two different columns pHILLIC and C18-PFP were used to detect polar and nonpolar metabolites, respectively. This approach was found to facilitate identification of more and an increased diversity of metabolites than reported in many previous studies.

A number of methods were used to quality control data and identify pathways most affected by *T. gondii* infection. PCA of LCMS outputs from both pHILLIC and C18-PFP columns distinct separation of infected and non-infected mouse brain. This allowed the data to be analysed by OPLS-DA to identify and rank metabolites associated with acquired *T. gondii* infection by VIP scores. These scores were used in concert with p values obtained using IDEOM (Creek et al., 2012). BioCyc Pathway Database Collection was used to simultaneously evaluate multiple metabolites in interacting biochemical pathways, yielding pathway perturbation scores. Notably, metabolites with significant p values generally also had high VIP scores and the pathways in which they are produced identified as having a high pathway perturbation score using BioCyc Pathway Database Collection. Overall this process highlights many pathways, specifically purine, tryptophan, dopamine, arginine and L-carnitine pathways as being altered in the brains of mice with *T. gondii* infection.

In theory these changes represent changes to the entire tissue including any parasites present, but the contribution of parasite metabolites is likely to be very small as there are few parasite present in the brains of BALB/c mice. However, the changes observed can be viewed as host evolved mechanisms derived to mediate protection of the host or parasite evolved mechanisms that manipulate the host to allow parasite survival and transmission. Consequently, some changes result from the immune response against *T. gondii* while others are likely to be induced from parasite secreted molecules that interfere with host metabolism. Transcriptomics studies are used in next chapter to deconvolute these scenarios and provide a clearer picture of the mechanism responsible for these alterations.

4 Transcriptomics profile for BALB/c mice brain in adulthood infected with *T. gondii.*

4.1 Introduction

In the previous chapter of this thesis, alterations in the metabolomic profile of the brains from mice infected with *T. gondii* was demonstrated. However, metabolomic approaches can only detect a relatively small amount of the overall changes occurring and do not differentiate between murine and parasite produced metabolites. For example metabolomics do not directly detect canonical immunological mediators. To gain a wider understanding of the changes that *T. gondii* infection induces in the brains of mice other 'omics' approaches can be used. In recent years, transcriptomics and proteomics approaches have been employed to study the interaction between *T. gondii* and its host. Systemic infection with *T. gondii* is efficiently controlled by the cellular immune response. However, in chronic infections, parasites within neurons can directly cause neuronal death and atrophy of neuronal processes, while inflammation resulting from production of nitric oxide (NO) and inflammatory cytokines from microglia or other immune cells which could contribute to the death of neighboring neurons (Hermes et al., 2008).

In this study, we investigated the transcriptomic profile of mouse brains infected with *T. gondii* using the whole transcriptome sequencing approach RNA sequencing in order to understand the functional changes in central nervous system and the alterations of the metabolomics profile in chronic infection with *T. gondii*. These changes are also correlated with the metabolomic changes observed in the previous chapter

4.2 Results

4.2.1 Global Transcriptomics changes in the brain of mice infected with *T. gondii*.

4.2.1.1 Electropherograms for RNA extraction samples.

All chosen samples in adult mice brain experiment show high quality RNA electropherograms, which illustrate a clear 28S and 18S peaks. There is low noise between the peaks and minimal low molecular weight contamination (Figure 4.1). An excellent RNA concentration and high RNA integrity number is shown in table 4.1.

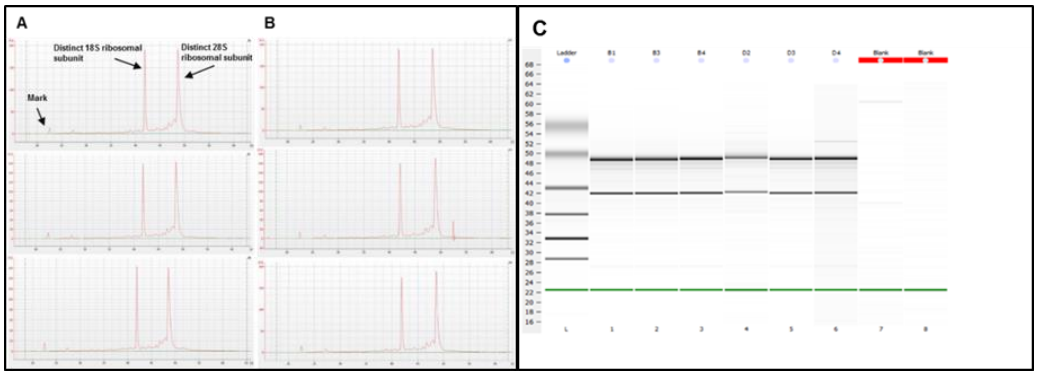

Figure 4.1 Illustration of electropherograms demonstrating the high quality RNA extracted from infected and control brain samples (A) and (B). There are clear 28S and 18S peaks and low noise between the peaks and minimal low molecular weight contamination. (C) Bioanalyzer gel image showing RNA extracted from 6 samples. The first three are extracted from the brain of female mice infected with *T. gondii* and the three after are extracted from the brain of uninfected female mice and the last two samples are blank.

Table 4.1 Samples chosen for sequencing based on RNA concentration, RNA ratio and RNA integrity numbers (RIN). Uninfected group= Control Group.

Sample	Group	RNA concentration (ng/µl)	RNA Ratio [28s / 18s]	RIN
B1	Uninfected	378	1.3	8.8
B3	Uninfected	305	1.3	8.8
B4	Uninfected	317	1.3	8.8
D2	Infected	377	1.4	8.9
D3	Infected	242	1.4	8.8
D4	Infected	336	1.3	8.7

4.2.1.2 Read Statistics

The total amount of raw sequence data and the results of the quality filtering is collected and reported in table 4.2.

Table 4.2 Quality control statistics per sample in acquired infection experiment. (CTR=Control group, INF= Infected group).

Sample	Total Reads	Discarded Reads	Clean Reads (single)	Clean Reads
B1-CTR	64,929,820	1,879,909 (2.9 %)	1,469,703 (2.3 %)	61,580,208 (94.8 %)
B3-CTR	70,834,158	2,246,211 (3.2 %)	1,794,709 (2.5 %)	66,793,238 (94.3 %)
B4-CTR	60,094,238	2,022,316 (3.4 %)	1,601,114 (2.7 %)	56,470,808 (94.0 %)
D2-INF	61,708,738	1,539,423 (2.5 %)	1,218,169 (2.0 %)	58,951,146 (95.5 %)
D3-INF	68,405,108	2,156,796 (3.2 %)	1,721,768 (2.5 %)	64,526,544 (94.3 %)
D4-INF	72,589,950	2,208,305 (3.0 %)	1,811,693 (2.5 %)	68,569,952 (94.5 %)

Single reads are reads without mates (discarded poor quality mate reads). They are not included in further analysis.

The following table contains the number of reads mapped to the reference genome/ transcriptome for each of the samples. The accuracy of the reference (genome/

transcriptome) and higher the quality of mapped reads lead to a higher percentage of reads mapped to the reference. Approximately 98% of reads were successfully mapped to the mouse reference transcriptome (Genome: mm10 / GRCm38, Ensembl, Annotations).

Table 4.3 Mapped read statistics observed per sample in acquired infection experiment.

Sample	QC Passed Reads	Mapped Reads	% Mapped
B1	61,580,208	60,406,719	98.1
B3	66,793,238	65,519,139	98.1
B4	56,470,808	55,322,271	98.0
D2	58,951,146	57,833,036	98.1
D3	64,526,544	63,219,398	98.0
D4	68,569,952	67,090,913	97.8

4.2.1.3 Volcano plots (Infected vs. Uninfected) in acquired infection experiment.

Volcano plots highlight the genes that significantly differ between the conditions tested based on the fold change and test statistics performed on the RNA-Seq data between conditions. They are generated based on expression data of genes using the cummeRbund package. Volcano plots can be used for displaying the relationship between conditions at gene expression level.

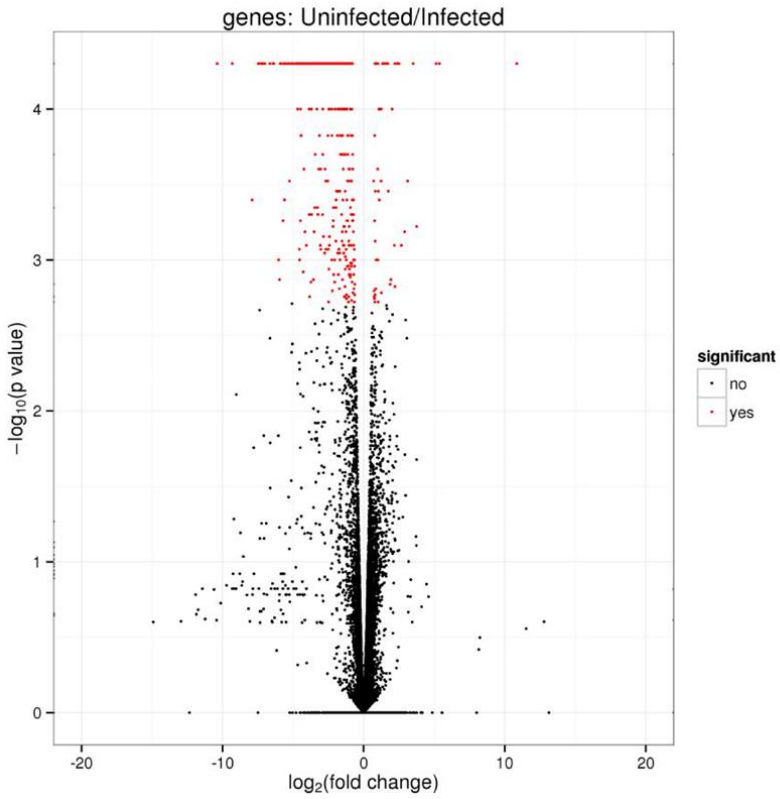

Figure 4.2 Volcano plot for infected group versus Uninfected (control) group in acquired infection experiment. The red circles represent the significant genes expression above the threshold. Note both fold changes and *P*-values are log transformed. The further its position away from the (0, 0), the more significant the feature is.

In the current study, 701 known differentially expressed genes (DEGs) were detected based on having more than 2-fold change and a corrected p value of <0.05. 17 genes were excluded because the gene name was unknown. From the total of DEGs 629 genes were upregulated and 55 genes were downregulated when compared with the control group. Top 50 significant genes were shown in tables 4.4 and 4.5.

4.2.2 Genes associated with microglial activation and antioxidant responses

Transcripts of particular genes that associated with *T. gondii* infection were significantly upregulated in the infected group compared with the non-infected control group. These genes and their fold change are SOCS1, 6.2-fold; CD36, 4.3-fold; C1qa, 7.8-fold; C1qb, 7.9-fold; C1qc, 8.2-fold; GFAP, 2.6-fold; Ifi30, 3-fold; Gbp2, 30.7-fold; Gbp3, 23-fold; Gbp4, 13.7-fold; Gbp5, 18.5-fold; Gbp7, 19.1-fold; Gbp11, 13.8-fold.

Transcripts of genes that are known to be associated with microglia activity were significantly upregulated in infected mice compared with non-infected mice. These genes and their fold change are TLR-2, 8.4-fold; TLR-4, 2.4-fold; TNF, 0.6*-fold; IL-1β, 15.5-fold; CD68, 2.5-fold; Cx3cr1, 2.4; TREM2, 3.9-fold; Tmem119, 3.8-fold.

Transcripts associated with antioxidant responses were altered in mice infected with *T. gondii*. Glutathione-S-transferases enzymes (GST) have been reported to have a significant role in cellular detoxification processes and regulation of redox homeostasis. Transcripts for two members of the family of enzymes were significantly downregulated in infected mice compared with non-infected mice. These genes and their fold change are GSTM1, 0.6-fold and GSTM3, 0.6-fold.

Table 4.4 Top 50 genes significantly (>2-fold change and FDR of <0.05) upregulated in the acquired *T. gondii* infection experiment.

Gene	Description	Average FPKM		Fold Change	FDR	Ensembl ID
		Inf (n=3)	Ctr (n=3)			
Igkc	immunoglobulin kappa constant	3483.4	2.6	1340.1	0.002	ENSMUSG00000076609
Jchain	immunoglobulin joining chain	193.9	0.3	634.3	0.002	ENSMUSG00000067149
Zbp1	Z-DNA binding protein 1	20.6	0.1	239.0	0.013	ENSMUSG00000027514
H2-Eb1	histocompatibility 2, class II antigen E beta	316.9	1.8	176.5	0.002	ENSMUSG00000060586
Cd74	CD74 antigen (invariant polypeptide of major histocompatibility complex, class II antigen-associated)	700.1	4.1	170.7	0.002	ENSMUSG00000024610
Gm12250	predicted gene 12250	24.0	0.2	153.1	0.002	ENSMUSG00000082292
H2-Aa	histocompatibility 2, class II antigen A, alpha	274.9	1.9	147.1	0.002	ENSMUSG00000036594
Gm5970	predicted gene 5970	80.7	0.6	140.5	0.002	ENSMUSG00000085977
Iigp1	interferon inducible GTPase 1	80.7	0.6	140.5	0.002	ENSMUSG00000054072
H2-Ea-ps	histocompatibility 2, class II antigen E alpha, pseudogene	256.1	2.0	128.1	0.002	ENSMUSG00000036322
Cxcl10	chemokine (C-X-C motif) ligand 10	23.6	0.2	99.6	0.002	ENSMUSG00000034855
H2-Ab1	histocompatibility 2, class II antigen A, beta 1	258.7	3.0	85.3	0.002	ENSMUSG00000073421
Igtp	interferon gamma induced GTPase	145.0	1.8	82.5	0.002	ENSMUSG00000078853
Irgm2	immunity-related GTPase family M member 2	145.0	1.8	82.5	0.002	ENSMUSG00000069874
Ifi202b	interferon activated gene 202B	4.9	0.1	65.4	0.028	ENSMUSG00000026535
Itgax	integrin alpha X	1.8	0.0	62.7	0.037	ENSMUSG00000030789
Oasl2	2'-5' oligoadenylate synthetase-like 2	71.5	1.2	60.0	0.002	ENSMUSG00000029561
Batf2	basic leucine zipper transcription factor, ATF-like 2	5.5	0.1	58.9	0.002	ENSMUSG00000039699
Nlrc5	NLR family, CARD domain containing 5	3.7	0.1	57.5	0.002	ENSMUSG00000074151
BC023105	cDNA sequence BC023105	2.9	0.1	52.3	0.017	ENSMUSG00000063388

Psmb9	proteasome (prosome, macropain) subunit, beta type 9 (large multifunctional peptidase 2)	66.5	1.3	50.3	0.002	ENSMUSG00000096727
Gimap3	GTPase, IMAP family member 3	3.0	0.1	48.7	0.013	ENSMUSG00000039264
C3	complement component 3	9.2	0.2	46.1	0.002	ENSMUSG00000024164
Gbp2b	guanylate binding protein 2b	38.5	0.8	46.0	0.002	ENSMUSG00000040264
Psmb8	proteasome (prosome, macropain) subunit, beta type 8 (large multifunctional peptidase 7)	105.2	2.6	41.2	0.002	ENSMUSG00000024338
Ly6a	lymphocyte antigen 6 complex, locus A	147.3	3.6	40.5	0.002	ENSMUSG00000075602
Ifi44	interferon-induced protein 44	11.3	0.3	38.9	0.002	ENSMUSG00000028037
Hcar2	hydroxycarboxylic acid receptor 2	2.8	0.1	38.1	0.010	ENSMUSG00000045502
Ifi44l	interferon-induced protein 44 like	5.2	0.1	34.9	0.002	ENSMUSG00000039146
AB124611	cDNA sequence AB124611	4.4	0.1	34.9	0.002	ENSMUSG00000057191
Ifi204	interferon activated gene 204	3.6	0.1	34.6	0.002	ENSMUSG00000073489
H2-DMb1	histocompatibility 2, class II, locus Mb1	14.2	0.4	33.8	0.002	ENSMUSG00000079547
H2-DMb2	histocompatibility 2, class II, locus Mb2	14.2	0.4	33.8	0.002	ENSMUSG00000037548
Gbp2	guanylate binding protein 2	35.1	1.1	30.7	0.002	ENSMUSG00000028270
Ltb	lymphotoxin B	8.9	0.3	27.8	0.002	ENSMUSG00000024399
Ighv1-7	immunoglobulin heavy variable V1-7	100403.0	0	100403*	0.002	ENSMUSG00000095200
Ighv1-81	immunoglobulin heavy variable 1-81	52894.7	0	52894.7*	0.002	ENSMUSG00000094689
Ighv1-55	immunoglobulin heavy variable 1-55	34399.8	0	34399.8*	0.002	ENSMUSG00000095589
Ighv1-56	immunoglobulin heavy variable 1-56	29368.4	0	29368.4*	0.039	ENSMUSG00000094862
Ighv7-3	immunoglobulin heavy variable 7-3	22087.2	0	22087.2*	0.002	ENSMUSG00000076652
Ighv7-4	immunoglobulin heavy variable 7-4	22087.2	0	22087.2*	0.002	ENSMUSG00000076668
Ighv1-39	immunoglobulin heavy variable 1-39	16743.1	0	16743.1*	0.002	ENSMUSG00000095130
Ighv5-1	immunoglobulin heavy variable V5-1	9502.9	0	9502.9*	0.002	ENSMUSG00000102901

Ighv1-2	immunoglobulin heavy variable 1-2	6141.7	0	6141.7*	0.002	ENSMUSG00000102524
Igkv3-11	immunoglobulin kappa variable 3-11	4698.5	0	4698.5*	0.049	ENSMUSG00000105499
H2-Bl	histocompatibility 2, blastocyst	2514.7	0	2514.7*	0.002	ENSMUSG00000073406
Ighv1-42	immunoglobulin heavy variable V1-42	1130.7	0	1130.7*	0.002	ENSMUSG00000094652
Ighv1-66	immunoglobulin heavy variable 1-66	234.6	0	234.6*	0.002	ENSMUSG00000095519
Ighv8-8	immunoglobulin heavy variable 8-8	234.5	0	234.5*	0.002	ENSMUSG00000104452
Igkv8-21	immunoglobulin kappa variable 8-21	200.6	0	200.6*	0.002	ENSMUSG00000076586

Table 4.5 All significant genes (FDR of <0.05) downregulated in the acquired *T. gondii* experiment.

Gene	Description	Average FPKM		Fold Change	FDR	Ensembl ID
		Inf (n=3)	Ctr (n=3)			
Srsf5	serine/arginine-rich splicing factor 5	52.6	86.0	0.6	0.010	ENSMUSG00000021134
2900052N01Rik	RIKEN cDNA 2900052N01 gene	10.9	18.2	0.6	0.042	ENSMUSG00000099696
Kcng4	potassium voltage-gated channel, subfamily G, member 4	7.2	12.1	0.6	0.046	ENSMUSG00000045246
Serpinb1a	serine (or cysteine) peptidase inhibitor, clade B, member 1a	6.3	10.8	0.6	0.047	ENSMUSG00000044734
Gstm1	glutathione S-transferase, mu 1	69.8	119.8	0.6	0.005	ENSMUSG00000058135
Gstm3	glutathione S-transferase, mu 3	69.8	119.8	0.6	0.005	ENSMUSG00000004038
Resp18	regulated endocrine-specific protein 18	70.9	121.8	0.6	0.017	ENSMUSG00000033061
Cbln1	cerebellin 1 precursor protein	47.0	81.6	0.6	0.049	ENSMUSG00000031654
Calb2	calbindin 2	42.0	73.4	0.6	0.002	ENSMUSG00000003657
Epha8	Eph receptor A8	2.4	4.1	0.6	0.045	ENSMUSG00000028661
Sparc	secreted acidic cysteine rich glycoprotein	205.9	363.2	0.6	0.022	ENSMUSG00000018593
AW047730	expressed sequence AW047730	22.9	40.5	0.6	0.011	ENSMUSG00000097428
Paqr6	progestin and adipoQ receptor family member VI	4.3	7.8	0.6	0.041	ENSMUSG00000041423
En2	engrailed 2	6.2	11.3	0.6	0.041	ENSMUSG00000039095
Itih3	inter-alpha trypsin inhibitor, heavy chain 3	19.1	35.2	0.5	0.002	ENSMUSG00000006522
Kirrel2	kirre like nephrin family adhesion molecule 2	2.2	4.0	0.5	0.028	ENSMUSG00000036915
Etnppl	ethanolamine phosphate phospholyase	7.5	14.0	0.5	0.002	ENSMUSG00000019232
Cdhr1	cadherin-related family member 1	2.3	4.6	0.5	0.008	ENSMUSG00000021803
Hbb-bs	hemoglobin, beta adult s chain	90.3	180.9	0.5	0.002	ENSMUSG00000052305
Gm12966	predicted gene 12966	7.5	15.0	0.5	0.028	ENSMUSG00000070729
Dmpk	dystrophia myotonica-protein kinase	2.4	4.8	0.5	0.049	ENSMUSG00000030409
Cartpt	CART prepropeptide	10.3	21.9	0.5	0.004	ENSMUSG00000021647

Nts	Neurotensin	4.7	10.0	0.5	0.013	ENSMUSG00000019890
Ngb	Neuroglobin	4.2	9.2	0.5	0.004	ENSMUSG00000021032
Dlk1	delta like non-canonical Notch ligand 1	6.7	14.8	0.5	0.004	ENSMUSG00000040856
Sp8	trans-acting transcription factor 8	0.9	2.0	0.4	0.010	ENSMUSG00000048562
Ccdc153	coiled-coil domain containing 153	1.7	4.0	0.4	0.044	ENSMUSG00000070306
Gpx3	glutathione peroxidase 3	11.7	29.6	0.4	0.002	ENSMUSG00000018339
Avp	arginine vasopressin	30.2	81.9	0.4	0.002	ENSMUSG00000037727
Trh	thyrotropin releasing hormone	3.6	10.2	0.4	0.002	ENSMUSG00000005892
Gal	Galanin	4.2	13.1	0.3	0.002	ENSMUSG00000024907
Hcrt	Hypocretin	12.9	42.4	0.3	0.002	ENSMUSG00000045471
Spint1	serine protease inhibitor, Kunitz type 1	0.3	1.1	0.3	0.011	ENSMUSG00000027315
Cldn3	claudin 3	0.3	1.1	0.3	0.039	ENSMUSG00000070473
Tmem30b	transmembrane protein 30B	0.2	0.6	0.3	0.037	ENSMUSG00000034435
Pou1f1	POU domain, class 1, transcription factor 1	0.3	1.0	0.2	0.004	ENSMUSG00000004842
Lhx3	LIM homeobox protein 3	0.2	0.8	0.2	0.023	ENSMUSG00000026934
Oxt	Oxytocin	26.4	122.7	0.2	0.002	ENSMUSG00000027301
Gnb3	guanine nucleotide binding protein (G protein), beta 3	0.2	0.9	0.2	0.040	ENSMUSG00000023439
Stoml3	stomatin (Epb7.2)-like 3	0.3	1.8	0.2	0.002	ENSMUSG00000027744
Parpbp	PARP1 binding protein	3.0	17.0	0.2	0.002	ENSMUSG00000035365
Six6	sine oculis-related homeobox 6	0.1	0.6	0.2	0.023	ENSMUSG00000021099
Cldn9	claudin 9	0.1	1.1	0.1	0.019	ENSMUSG00000066720
Fcrls	Fc receptor-like S, scavenger receptor	0.1	1.0	0.1	0.010	ENSMUSG00000015852
Epcam	epithelial cell adhesion molecule	0.4	4.1	0.1	0.002	ENSMUSG00000045394
Pitx1	paired-like homeodomain transcription factor 1	0.1	1.0	0.1	0.018	ENSMUSG00000021506
Lhb	luteinizing hormone beta	0.2	8.3	0.03	0.002	ENSMUSG00000100916
Pomc	pro-opiomelanocortin-alpha	2.2	90.2	0.02	0.002	ENSMUSG00000020660
Gh	growth hormone	1.0	1820.7	0.001	0.002	ENSMUSG00000020713
Fshb	follicle stimulating hormone beta	0.0	6.4*	6.4	0.002	ENSMUSG00000027120

Pyy	peptide YY	0.0	0.9*	0.9	0.007	ENSMUSG00000017311
Prl	Prolactin	0.0	0.8*	0.8	0.002	ENSMUSG00000021342
Gnrhr	gonadotropin releasing hormone receptor	0.0	0.7*	0.7	0.002	ENSMUSG00000029255
Gm14617	predicted gene 14617	0.0	0.6*	0.6	0.002	ENSMUSG00000084795

4.2.3 Human - Mouse: Disease Connection

The DEGs that were detected in this study were uploaded to the Mouse Genome Database Informatics (MGI) (Blake et al., 2000) to determine potential connections between our data and the literature in terms of phenotypes and diseases. The sources of human gene to disease annotations are from the National Center for Biotechnology Information (NCBI) and Online Mendelian Inheritance in Man (OMIM). Human phenotype to disease annotations are from Human Phenotype Ontology (HPO). Mouse gene to disease and gene to phenotype annotations are from MGI.

In this study, 491 genes were associated with 214 diseases and phenotypes. However, filters were applied to detect genes associated with behaviour, neurological changes, nervous system diseases and diseases of mental health as these are pertinent to the aims of the study. These genes which associated with human disease are illustrated in the Table 4.6.

Table 4.6 Human - Mouse genes in chronic infected mice brain connected with nervous system diseases.

	Organism	Gene Symbol	ID	Associated Human Diseases	Abnormal Mouse Phenotypes
1	Mouse Human	Ctsc	MGI:109553	schizophrenia	behaviour/neurological nervous system
2	Mouse Human	Nr4a2	MGI:1352456	Parkinson's disease schizophrenia	behaviour/neurological aging /nervous system
3	Mouse Human	Hcrt	MGI:1202306	narcolepsy	behaviour/neurological nervous system
4	Mouse Human	Cd86	MGI:101773	Guillain-Barre syndrome	behaviour/neurological nervous system
5	Mouse Human	Grn	MGI:95832	Grn-related frontotemporal lobar degeneration with Tdp43 inclusions nephrogenic diabetes insipidus	behaviour/neurological mortality/aging nervous system/ vision/eye
6	Mouse Human	Trem2	MGI:1913150	frontotemporal dementia	nervous system
7	Mouse Human	C1qa	MGI:88223	epilepsy systemic lupus erythematosus	behaviour/neurological aging / nervous system
8	Mouse Human	Ctss	MGI:107341	Duchenne muscular dystrophy	behaviour/neurological
9	Mouse	Tg(ACTA1-Ctss)1Jmol	MGI:5765990	Duchenne muscular dystrophy	behaviour/neurological
10	Mouse Human	En2	MGI:95390	autism spectrum disorder	behaviour/neurological nervous system
11	Mouse Human	Gstm1	MGI:95860	autism spectrum disorder	behaviour/neurological nervous system
12	Human Mouse	PIK3R5	23533	ataxia with oculomotor apraxia type 3	Immune system
13	Mouse Human	Cx3cr1	MGI:1333815	age related macular degeneration 12	behaviour/neurological nervous system/vision/eye
14	Mouse Human	Ccr2	MGI:106185	age related macular degeneration	behaviour/neurological nervous system/ vision/eye
15	Human Mouse	ALOX5AP	241	cerebral infarction	Homeostasis/Metabolism

4.2.4 Transcriptomics variations in pathways of the brains of mice infected with *T. gondii.*

Transcript of the DEGs were uploaded with the metabolites from adult metabolome experiment in previous chapter to BioCyc pathway Database Collection. This step was done to obtain a more complete picture for the following pathways.

4.2.4.1 Purine degradation pathway

Transcripts for 2 genes in the purine degradation pathway, adenosine deaminase (ADA) and xanthine dehydrogenase (XDH) were found to be significantly upregulated ($p = 0.013$ and 0.002 respectively) in the brains on *T. gondii*-infected mice relative to non-infected control mouse brains. These results are consistent with the depletion of adenosine and accumulation of inosine, xanthine, uric acid and allantoin in the brains of mice infected with *T. gondii* as measured by LCMS (Figure 4.3)

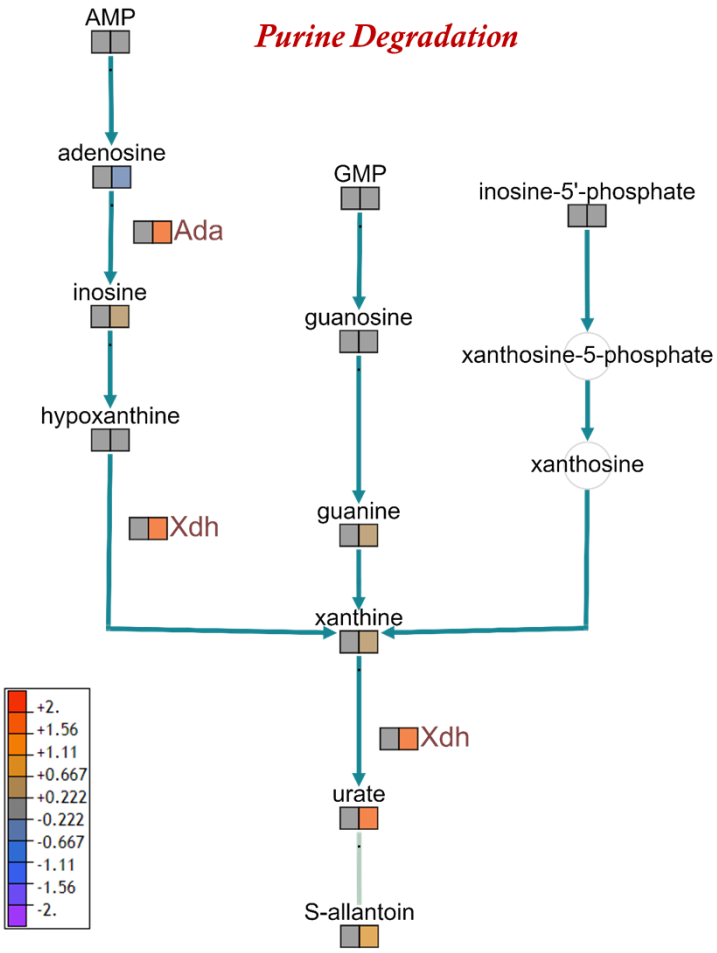

Figure 4.3 Purine pathway degradation. Metabolites and transcript which were detected in this pathway are represented by two squares. The first square represents the control group and Second Square represents the infected group. The log 2 transformed data are visualised as a color spectrum scaled from least to most abundant from -2 to 2. Purple indicates low expression, while red indicates high expression of the changed metabolites and transcripts. The transcripts that were found to be significantly different between infected and non-infected mice are Ada (adenosine deaminase) (p= 0.013) and Xdh (xanthine dehydrogenase) (p= 0.002).

4.2.4.2 Tryptophan degradation pathway.

Transcripts for one gene in the tryptophan degradation pathway, arylformamidase (Afmid) were found to be significantly upregulated ($p = 0.029$) in the brains on *T. gondii*-infected mice relative to non-infected control mouse brains. This result is consistent with the accumulation of kynurenine in the brains of mice infected with *T. gondii* as measured by LCMS.

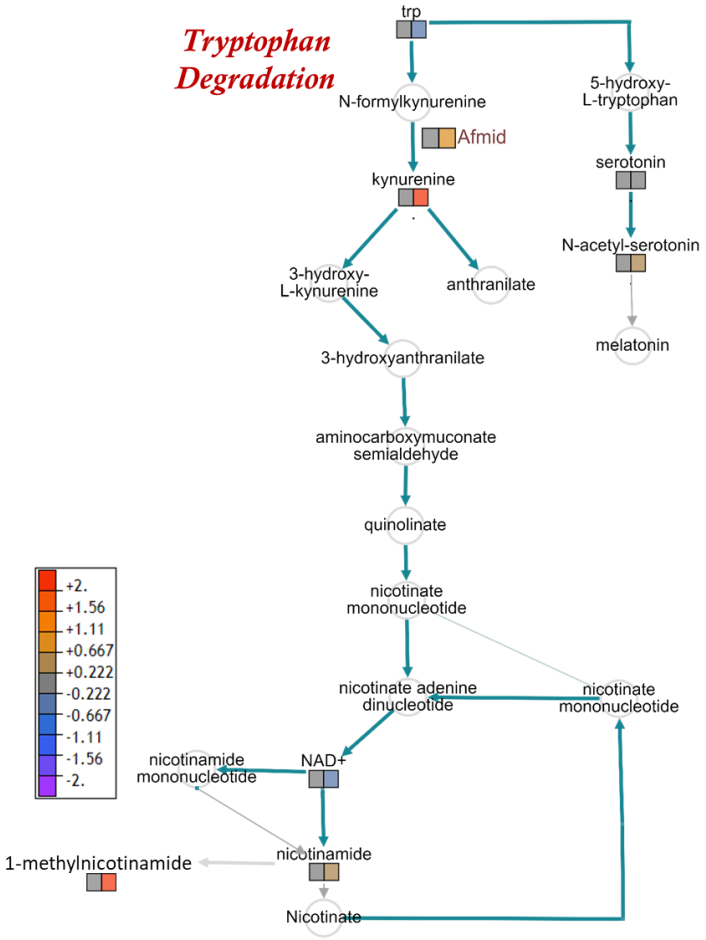

Figure 4.4 Tryptophan degradation Pathway. Metabolites and transcript which were detected in this pathway are represented by two squares. The first square represents the control group and Second Square represents the infected group. The log 2 transformed data are visualised as a color spectrum scaled from least to most abundant from -2 to 2. Purple indicates low expression, while red indicates high expression of the changed metabolites and transcripts. The transcript that was found to be significantly different between infected and non-infected mice is Afmid (arylformamidase) (p= 0.029).

4.2.4.3 Citrulline nitric oxide cycle.

Transcripts of nitric oxide synthase 2 (NOS2) was found to be significantly upregulated (p= 0.002) in the brains on *T. gondii*-infected mice relative to non-infected control mouse brains.

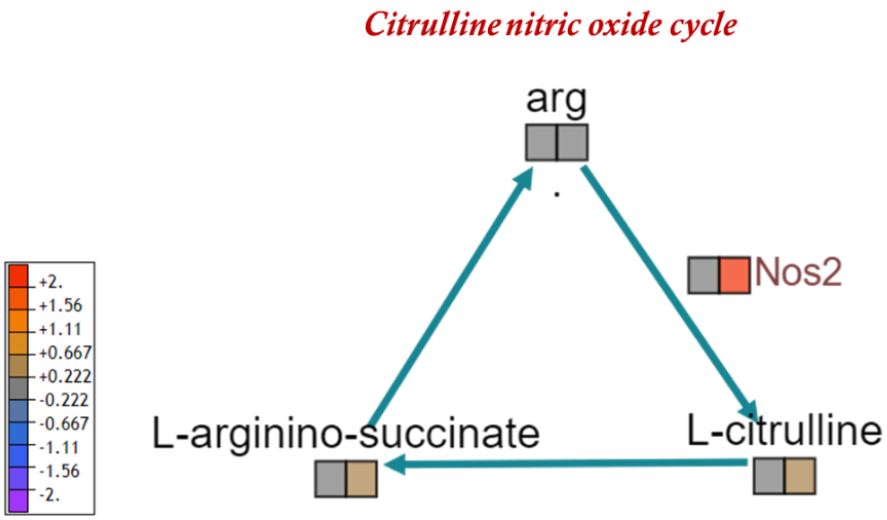

Figure 4.5 Citrulline nitric oxide cycle. Metabolites and transcript which were detected in this pathway are represented by two squares. The first square represents the control group and Second Square represents the infected group. The log 2 transformed data are visualised as a color spectrum scaled from least to most abundant from -2 to 2. Purple indicates low expression, while red indicates high expression of the changed metabolites and transcripts. The transcript that was found to be significantly different between infected and non-infected mice is Nos2 (nitric oxide synthase 2) (p= 0.002).

4.2.4.4 Cyclic AMP biosynthesis and Pyrimidine ribonucleosides degradation.

Transcripts for 5 genes in the pyrimidine ribonucleosides degradation pathway, Apobec1 (apolipoprotein B mRNA editing enzyme, catalytic polypeptide 1), Dock8 (dedicator of cytokinesis 8), Gna15 (guanine nucleotide binding protein, alpha 15), Adap2 (ArfGAP with dual PH domains 2) and Arhgap (Rho GTPase activating protein) were found to be significantly upregulated (p= 0.002, 0.002, 0.002, 0.002 and 0.004 respectively) in the brains of *T. gondii*-infected mice relative to non-infected control mouse brains.

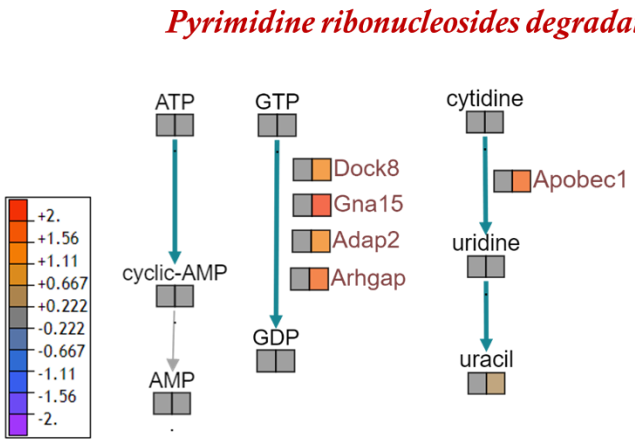

Figure 4.6 Cyclic AMP biosynthesis and Pyrimidine ribonucleosides degradation. Metabolites and transcripts which were detected in this pathway are represented by two squares. The first square represents the control group and Second Square represents the infected group. The log 2 transformed data are visualised as a color spectrum scaled from least to most abundant from -2 to 2. Purple indicates low expression, while red indicates high expression of the changed metabolites and transcripts. The transcript that was found to be significantly different between infected and non-infected mice are Apobec1 (apolipoprotein B mRNA editing enzyme, catalytic polypeptide 1) (p= 0.002), Dock8 (dedicator of cytokinesis 8) (p= 0.002), Gna15 (guanine nucleotide binding protein, alpha 15) (p= 0.002), Adap2 (ArfGAP with dual PH domains 2) (p= 0.002) and Arhgap (Rho GTPase activating protein) (p= 0.004).

4.3 Conclusion

The studies described in this chapter aimed to augment the metabolomic data obtained in the previously chapter with transcriptomic data. Significant alteration in the transcriptome was observed between the infected and non-infected mouse brains. The majority of genes highly expressed in infected mouse brains compared with the brains from non-infected mice are involved in immune responses and immune cell activation. Our findings are consistent with an ongoing immune and inflammatory process involving immunoglobulin and B cells and interferon gamma production. These results are expected as *T. gondii* is known to induce a robust immune response and many immunological transcripts have been previously demonstrated to be upregulated (Hunter et al., 1992, Hunter et al., 1993). While the primary function of these gene products is host immunity, it is now recognized that some of these immunological mediators can also affect behavior or even contribute to psychoneurological disease (Berger, 2016, Sankowski et al., 2015, Khandaker et al., 2015). Some changes were also seen to transcripts encoding enzymes involved in host metabolism including some of the pathways implicated in the previous chapter.

In addition, to the above mentioned transcripts associated with ongoing immunological responses, a number of DEGS in this study are involved in the development and function of the brain such as regulation of pre-synapse and postsynaptic assembly, synaptic membrane, nervous system development, neuron projection development, peroxidase activity and mitochondrial activity. These changes might be important and could assist in

elucidation of the mechanism underlying neurological changes and psychoneurological disease observed in some *T. gondii*-infected hosts.

5 Discussion of metabolomic and transcriptomic changes in the brains of mice infected with *T. gondii.*

5.1 The integration of transcriptomic and of metabolic profiles of chronic infected mice brain with *T. gondii*

Integration of transcriptomic and metabolomic data provides a powerful way to investigate complex disease processes involving biological pathways. Using these two techniques gives a more complete view of the effects of infection and in combination can provide greater confidence in processes that are affected.

5.1.1 Purine Catabolism Pathway

Purine metabolites are essential precursors for nucleic acid synthesis, but they also act as metabolic signals, provide energy, control cell growth, form part of essential coenzymes, contribute to sugar transport and donate phosphate groups in phosphorylation reactions (Handford et al., 2006). Purine metabolites such as (Adenosine triphosphate) ATP and adenosine have been demonstrated as significant neuronal co-transmitters with GABA, acetylcholine, glutamate, noradrenaline and dopamine (Poelchen et al., 2001). In this study, the results showed that *T. gondii* infection increases purine catabolism, leading to a reduction in adenosine and accumulation of uric acid and allantoin in the brains of infected mice. Consistent with these observations the transcriptomic data found transcripts for adenosine deaminase and xanthine dehydrogenase to be raised in the brains of infected mice. Changes to purine levels could have neurological consequences as adenosine is known to have neuromodulatory effects throughout the brain, affecting fundamental

processes such as normal neuronal signaling, learning and memory, astrocytic function, anxiety and stress response (Burnstock et al., 2011). Along with these normal physiological processes, adenosine and its receptors are also involved in neuropathologies such as Parkinson's disease (Schwarzschild et al., 2006) and schizophrenia (Hirota and Kishi, 2013). Therefore a reduction in adenosine levels in the brains of infected mice could have profound effects. In addition, a previous study has demonstrated that purine catabolism might contribute to mitochondrial antioxidant defense by uric acid (Kristal et al., 1998). These authors reported that failure to maintain elevated xanthine and uric acid occurred contemporaneously with progressive mitochondrial dysfunction (Kristal et al., 1998). Therefore, purine catabolism appears to be a homeostatic response of mitochondria to oxidant stress and may protect against progressive mitochondrial dysfunction in certain disease states (Kristal et al., 1998).

Alteration of purine levels could also have direct effects on *T. gondii* as it is a purine auxotroph and therefore relies on scavenging host cell purines. Although it has the capability to use host adenine, hypoxanthine, xanthine, guanine, guanosine and inosine, adenosine is thought to be the most important salvaged purine (Krug et al., 1989, Ngo et al., 2000, Chaudhary et al., 2004). Thus degradation of purine might deprive *T. gondii* of this essential resource. Importantly studies in different organs of mice demonstrate that IFNγ is capable of inducing xanthine oxidase (XO) which catalyzes the oxidation of xanthine to uric acid (Ghezzi et al., 1984). Consequently, purine degradation might represent a host evolved mechanism to limit *T. gondii* growth.

Previous studies assessed the purine levels and Ada activity in the brain of mice (BALB/c) experimentally infected with *T. gondii* and the results of chronic infection were similar to our results, since purine metabolites were catabolized and uric acid was accumulated and increased, Ada activity also was increased in the chronic stage (Tonin et al., 2014).

Ada has been demonstrated to be involved in the development and maintenance of the immune system in mammals including humans and associated with differentiation of epithelial and monocytes (Moriwaki et al., 1999). A study has implicated abnormalities of immune functions including T cell activation in people with Parkinson's Disease with high serum Ada activity (Chiba et al., 1995). Thus increased levels of Ada induced as a consequence of the immune responses to *T. gondii* infection could promote or accelerate neurodegenerative diseases.

In our experiments, transcripts for the purinergic receptors that adenosine A3 receptor (Adora3); purinergic receptor P2X, ligand-gated ion channel, 7 (P2rx7); and pyrimidinergic receptor P2Y, G-protein coupled, 6 (p2ry6) were increased by *T. gondii* infection. Recent studies have demonstrated that microglia p2y6 receptors were highly expressed in patients with Parkinson's disease compared with healthy control people. P2ry6 is also known to be upregulated in microglial cell line BV2 cells following stimulation of TLR4 with LPS (Yang et al., 2017). For this reason, p2ry6 might be increased in infected mice brain due to the direct effect of *T. gondii* ligands for TLR4.

In addition, P2x7 receptor is directly involved in T cell activation during adaptive immune response and has for example been shown to modulate the balance between Th17 and Treg lymphocytes (Yip et al., 2009). P2X7 receptor-mediated killing of an intracellular *T. gondii*, by human and murine macrophages (Lees et al., 2010). P2X7 receptor activation can generate both protective and deleterious responses depending on the type of pathogen, virulence, and severity of infection (Savio et al., 2018). Increased expression and prolonged activation of P2x7 receptor might contribute to the pathogenesis of several inflammatory and neurodegenerative diseases by stimulating microglia activation for long time (Savio et al., 2018). In addition, a recent study suggests that the structural connectivity between the hippocampus and lateral parietal regions in the brain is relevant to the development of episodic memory (Ngo et al., 2017).

5.1.2 Tryptophan degradation pathway

Tryptophan metabolism is important for production of the neurotransmitters, serotonin and tryptamine and the neurotransmitter-like substance, melatonin. Tryptophan can also be degraded through the kynurenine metabolism in the brain to give rise to a number of products, some of which are known to be neuro-active or even neurotoxic. In a number of studies, depletion of tryptophan has been demonstrated to result in reduction of brain serotonin levels and depression (Ruddick et al., 2006). Intracellular tryptophan levels were generally reduced in infected mice although this did not reach statistical significance, compared with control mice. In the current study serotonin levels were not found to be

altered which is consistent with a previous study of *T. gondii*-infected (Stibbs, 1985). However, levels of kynurenine were found to be significantly increased in the brains of infected mice compared with control mice indicating degradation of tryptophan via the kynurenine pathway. Consistent with this transcripts for arylformamidase (Afmid) were raised in the brains of infected mice compared with brains from control non-infected mice. In the literature, there is a growing body of evidence that the kynurenine metabolite can contribute to the pathophysiology of several diseases such as acquired immunodeficiency syndrome (AIDS)-related dementia, Alzheimer's disease and schizophrenia (Baran et al., 1999, Erhardt et al., 2001, Koola, 2016, Nilsson et al., 2005, Schwarcz et al., 2001, Schwieler et al., 2015). These studies showed that overproduction of kynurenic acid (KYNA), another kynurenine derived metabolite, is associated with cognitive impairment in brain diseases. The kynurenine pathway is initiated by the oxidative ring opening of tryptophan by either indoleamine 2, 3-dioxygenase (IDO) or tryptophan 2, 3 dioxygenase (TDO). Importantly, in the context of *T. gondii* infection, IDO is known to be induced by IFNγ and the process of tryptophan degradation has been implicated in host defense as *T. gondii* is a tryptophan auxotroph (Pfefferkorn et al., 1986a, Pfefferkorn et al., 1986b). In the brain, the L-kynurenine is enzymatically converted in microglial cells and astrocytes. In schizophrenia, there is a persistent reduction of microglial kynurenine 3-monooxygenase activity, along with increased L-kynurenine influx from the circulation. This results in increased kynurenic acid formation in astrocytes which leads to inhibition of α-7 nicotinic (α7nAch) and the N-methyl-D-aspartate (NMDA) receptors which leads to cognitive impairments (Schwarcz and Stone, 2017). Thus, *T. gondii* infection through

stimulation of inflammatory cytokines such as IFNγ would appear to stimulate tryptophan degradation to kynurenine leading to accumulation of kynurenic acid which in turn could contribute to brain dysfunction and disease (Figure 5.1).

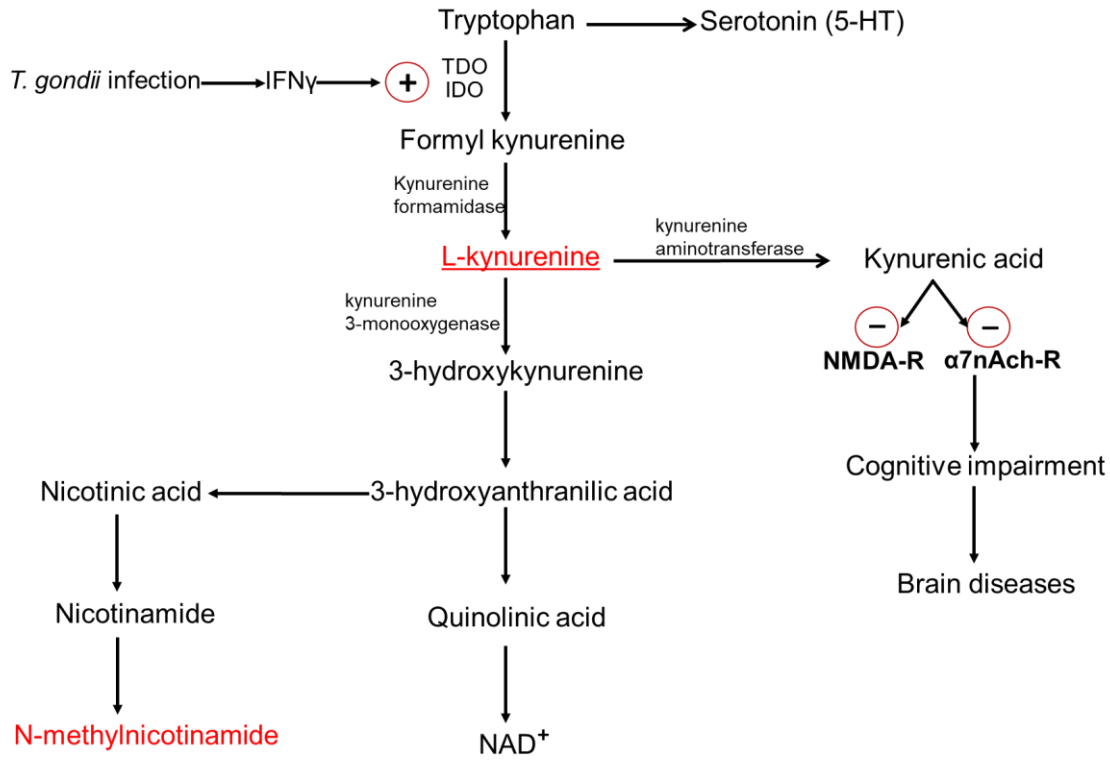

Figure 5.1 Tryptophan degradation through kynurenine metabolism and its effect on NMDA-R and α7nAch-R which leads to cognitive impairment in neuropsychiatric disorders. The metabolites written in red color are statistically significant metabolites in our experiment.

N-methylenicotinamide is a metabolite of niacin (also termed, nicotinic acid) or nicotinamide which can also be produced from the kynurenine pathway as shown in Figure 5.1. N-methylenicotinamide is known to inhibit choline transport and reduce choline clearance out of the brain (Koppen et al., 1993). Furthermore, choline has been shown to exert neuroprotective effects in both animals and humans. In several animal models of neuronal dysfunction including that resulting from ageing, seizures and genetic disorders have shown that choline administration provides neuroprotective mechanism to reduce cognitive impairments (Meck et al., 2007, Nag and Berger-Sweeney, 2007, Yang et al., 2000). In our study, choline was not changed in infected mice compared with control mice. This stability in the choline level in the brains of infected mice could result from overproduction of N-methylenicotinamide and could be neuroprotective in the context of *T. gondii* infection. Failure to maintain choline levels can have detrimental consequences as downregulation of N-methylenicotinamide has been associated with reduction in choline level in bipolar disorder (Zheng et al., 2013c, Chen et al., 2014a).

Induction of the kynurenine pathway during *T. gondii* infection is a likely result of the immune response and IFNγ production. The resultant tryptophan degradation is likely to be host protective through depriving the parasite of tryptophan, but the accumulation potentially neurotoxic metabolites could be responsible for adverse effects and trigger brain diseases and dysfunction.

Several studies have been shown that some of the metabolites associated with purine, and tryptophan metabolism are potential metabolomics biomarkers of neuropsychiatric disorders and neurodegenerative diseases. The overlap between these studies results and our results is demonstrated in Table 5.1.

Table 5.1 Summary of potential urinary biomarkers of neuropsychiatric disorders and neurodegenerative diseases from urine in literature, the metabolites written in red was detected with significant alteration in our experiments.

Disease	Method	Species	Potential Biomarkers		References
			Upregulated	Downregulated	
Major depressive disorder	NMR-based metabolomics	Human	Formate, alanine	Malonate, N-methylenicotinamide, m-hydroxyphenylacetate	(Zheng et al., 2013b)
	GC-MS-based metabolomics	Human	Sorbitol, uric acid, azelaic acid	Hippuric acid, quinolinic acid, tyrosine	(Zheng et al., 2013a)
Bipolar disorder	NMR and GC-MS-based metabolomics	Human	Azelaic acid, β-alanine, α-hydroxybutyrate	Pseudouridine, 2,4-dihydroxypyrimidine	(Chen et al., 2014b)
	GC-MS-based metabolomics	Human		2,4-dihydroxypyrimidine	(Xu et al., 2014)
	NMR-based metabolomics	Human	α-Hydroxybutrate, isobutyrate	Choline, N-methylenicotinamide	(Zheng et al., 2013c)
	NMR-based metabolomics	Human	α-Hydroxybutrate, formate (males) α-Hydroxybutrate (females)	Choline, N-methylenicotinamide (males) Oxaloacetate, acetone, N-methylenicotinamide (females)	(Chen et al., 2014a)
Autism spectrum disorder	NMR-based metabolomics	Human	N-methy-2-pyridone-5-carboxamide, N-methyl nicotinic acid, taurine, N-methylenicotinamide	Glutamate	(Yap et al., 2010)
	NMR-based metabolomics	Human	3-(3-Hydroxyphenyl)-3-hydroxypropanoic, 3,4-dihydroxybutyric acid, glycolic acid, glycine, cis-aconitic acid	Fructose, 1,2,3-butanetriol, propylene glycol	(Noto et al., 2014)
	GC-MS-based metabolomics	Human	Oxalic acid, β-hydroxybutyric acid, ribonic acid, m-hydroxybenzoic acid	Phosphoric acid, sebacic acid	(Kałużna-Czaplińska et al., 2014)
Schizophrenia	MS/MS, UPLC-MS and NMR-based metabolomics	Human	Uric acid, pregnanediol, valine, glycine, glucose	Creatinine, hippurate, creatine	(Cai et al., 2012)
	GC-TOF and NMR-based metabolomics	Human	β-Hydroxybutyrate	Citrate, α-Ketoglutaric acid, taurine, trimethylamine-N-oxide	(Yang et al., 2013)
Alzheimer's disease	NMR-based metabolomics	Mouse	3-Hydroxkynurenine, homogentisate, allantoin	Dimethylamine, trimethylamine	(Fukuhara et al., 2013)
	LC-MS-based metabolomics	Mouse	Methionine, desaminotyrosine	N1-acetylspermidine, 5-hydroxindoleacetic acid	(Peng et al., 2014)

5.1.3 Arginine metabolism

The arginine metabolism pathway (including polyamine biosynthesis) was identified as being affected by *T. gondii* infection using the multivariate analyses. The polyamines (spermidine and spermine) and their precursor (putrescine) pathway plays an important role in many cellular functions and has been implicated in mental disorders (Fiori and Turecki, 2008). Of note, putrescine was increased in the brains of infected compared with control mouse brains. Whether putrescine is a causative agent of neurological dysfunction or simply a marker of disease remains to be determined. However, upregulation of this pathway starting with increased Arg1 expression has been implicated in host protection as it deprives *T. gondii* of arginine (Woods et al., 2013).

NOS2 (nitric oxide synthase 2), the inducible form of this enzyme was upregulated in infected mice group. NOS2 was originally described as an enzyme that is expressed in activated macrophages, it converts the amino acid L-arginine into NO and L-Citrulline, and thereby contributes to the control of replication or killing of intracellular microbial pathogens. Its expression is induced by cytokines such as IFNγ, IL-1 or TNF-α (Coleman, 2001). In our transcriptomics data these cytokines were upregulated in the infected mouse group compared with control mice. These cytokines are characteristic neuroinflammation a process that controls parasite growth, but can be harmful if unchecked. A high concentration of NO has been shown to induce apoptotic cell damage in neuronal cells and thus leads to neuronal dysfunction (Wei et al., 2000).

5.1.4 Dopamine and other pathways

The dopamine synthesis pathway involves several enzymes and cofactors, any one of which could be manipulated to yield alteration in dopamine levels. A previous study in the literature demonstrated that *T. gondii* has the ability to directly up regulate the dopamine levels of infected neuronal cells (Prandovszky et al., 2011). However, in the current study, dopamine was significantly decreased in the brains of infected mice. Differences between these studies might reflect the timing of sampling.

5.1.5 Glycolysis, phospholipid biosynthesis and L-carnitine biosynthesis

It is acknowledged that the glucose is the primary energy source for the brain. However, under some conditions such as fasting, fatty acids work as an alternative energy metabolism for the brain. Significant alterations of carnitines and phospholipids indicate variation of fatty acids oxidations metabolism. In this experiment, L-carnitine and its derivative, 2-methylbutyroylcarnitine, hexanoylcarnitine, 3-Hydroxyhexadecanoyl-carnitine, tiglycarnitine, Acetyl carnitine and o-propanoylcarnitine were found to be increased in the brains of infected mice. Acetyl-carnitine regulates the activity of many mitochondrial enzymes which are involved in the citric acid cycle, the gluconeogenesis, the urea cycle and the fatty acids oxidation, as its acetyl groups are incorporated into brain lipid metabolism (Ricciolini et al., 1998, Steiber et al., 2004). In addition, acetyl carnitine plays a significant role in neuroprotection and has beneficial effects in major depressive disorders and Alzheimer's disease (Pettegrew et al., 2000).

In contrast, 3-phosphonopyruvate was significantly decreased, but phosphoenolpyruvate was significantly increased in the brains of infected mice. This is consistent with increased glycolytic flux. An increase in glycolysis in aerobic conditions termed, aerobic glycolysis or the Warburg Effect. This is generally associated with immune activation and *T. gondii* has recently been shown to induce this in murine dendritic cells (Hargrave et al., 2019).

No obvious differences in the levels of transcripts were found in the enzymes involved in glycolysis, phospholipid biosynthesis or L-carnitine biosynthesis. This might suggest that changes to these transcripts are limited to a small number of cells and hence do not make the threshold of a log2 FC employed in this study. Nonetheless the results demonstrate a benefit to using metabolomics in parallel with transcriptomics.

5.1.6 Enzymes involved in biological pathways and immune responses

In our study, Apobec1, Apobec3, Dock1, Dock2, Dock8, and adap2 were upregulated in infected mice. Polynucleotide editing enzymes, apolipoprotein B mRNA editing enzyme catalytic polypeptide 1 and 3 (Apobec1, Apobec3) catalyze the deamination of cytidine to uridine. However, no changes to the substrate or product were found in the LCMS data. It is potentially significant that these enzymes also play roles in a variety of host defense mechanisms. These enzymes act in innate and adaptive immune responses by modifying host transcripts that encode immune effectors and their regulators. Apobec1-mediated

RNA editing in microglia is required for maintaining the balance between CNS homeostasis and activated immune function of microglia to keep normal neurological and behavioral function throughout the life span. This is supported by the neuropathology and abnormal behavioral findings in Apobec1 knockout mouse model (Cole et al., 2017). Similarly, the LCMS data did not find any alteration to GTP or GDP following *T. gondii* infection. This again implies potential immunological functions for dedicator of cytokinesis 8 (Dock8), and dedicator of cytokinesis 2 (Dock2) proteins. These Dock proteins are known to regulate diverse cellular functions in multiple immune cell types (Kearney et al., 2017). Furthermore, ArfGAP Domain-Containing Protein 2 (ADAP2), which can also affect GTP and GDP metabolism also regulates both interferon and NF-κB responses by several pattern recognition receptors located at different sites within host cells so its activation during infection is crucial for host immune system (Bist et al., 2017). Consequently, these gene products normally involved in pyrimidine metabolism might have host important host protective immunological roles.

5.2 Transcripts associated with microglial activation are upregulated in mice infected with *T. gondii*

In a previous study, gene expression analysis of female Swiss Webster mice brain infected with *T. gondii* using full genome microarrays demonstrated that expression of genes such as those encoding suppression of cytokine signaling 1 (SOCS1), CD36, complement component 1 (C1q), and glial fibrillary acidic protein (GFAP) were highly expressed

(Hermes et al., 2008). Another analysis of gene expression of female BALB/c mice brain infected with *T. gondii* using RNA-seq showed that a similar set of genes SOCS1, CD36, C1q and GFAP were increased (Tanaka et al., 2013). Consistent with these findings, our results demonstrated that particular genes were upregulated (SOCS1, CD36, C1qa, C1qb, C1qc, and GFAP) in infected group compared with controls. These results reflect the astrocyte response to neuronal cell injury (Hermes et al., 2008).

Transcripts for IFN-inducible GTPase families and chemokines were increased following *T. gondii* infection. Studies have suggested that IFN-γ-inducible p65 GTPases such as Gbp1, Gbp2, Gbp3, Gbp5 and Gbp7 provide important roles in anti-*T. gondii* host defense (Yamamoto et al., 2012). Consistent with these findings, the results of this study showed that particular genes were highly expressed (Ifi30, Gbp2, Gbp3, Gbp4, Gbp5, Gbp7 and Gbp11).

More generally and not just pertinent to *T. gondii* infection, glia cells, including astrocytes, oligodendrocytes and microglia, play vital roles in brain functions, such as modulation of homeostatic functions, synaptic functions, nerve signal propagation and responses to neural injury, during development and disease (Herculano-Houzel, 2014, Zuchero and Barres, 2015). An inflammatory process in CNS is believed to play a significant role in the pathway leading to neural cell death in a number of neurodegenerative diseases such as Parkinson's disease (PD), Alzheimer's disease (AD), frontotemporal dementia (FTD) and HIV-dementia. Notably, in the current study, TREM2 was found to upregulated in the

brains of mice infected with *T. gondii*. TREM2 (triggering receptor expressed on myeloid cells 2) is a major microglia-specific gene in CNS (Hickman and El Khoury, 2014). Under normal conditions, TREM2 stimulates phagocytosis, proliferation and survival. However, mutations in TREM2 impairs the normal function and interferes with phagocytosis and may be a risk factor of neurodegenerative diseases. In addition, TREM2 has been detected in human cerebrospinal fluid, where it was increased in patients with multiple sclerosis and CNS inflammation (Piccio et al., 2008). A recent meta-analysis has also reported that multiple variants in TREM2 have associated with the onset of AD, FTD, and PD in North Americans (Zhou et al., 2019).

Another interesting gene has been linked to AD, ALS (Amyotrophic lateral sclerosis) and ischemic changes in the brain is Cx3cr1 (chemokine (C-X3-C motif) receptor 1). The current study finds that transcripts for this gene are upregulated in the brains of mice with *T. gondii* infection. This gene product is involved in microglial migration and Cx3cr1 deficient mice have reduced neuronal loss following inflammatory insult compared with control animals (Fuhrmann et al., 2010, Lopez-Lopez et al., 2014, Cisbani et al., 2018). A recent study has reported that upregulation of Cx3cr1 in ischemic neurons is associated with neuronal apoptotic cell death following stroke (Wang et al., 2018).

We also find that transcripts for CD33, a transmembrane receptor mainly expressed by microglial cells in the brain that regulates innate immune responses are upregulated in the brains of mice with *T. gondii* infection. Upregulation of this receptor has been correlated

with high risk of AD. In mouse models of AD an increase in CD33 levels has been shown to slow microglial phagocytosis by increasing plaque deposition in the brain (Griciuc et al., 2013, Jiang et al., 2014). A meta-analysis in human studies has demonstrated that different variants in CD33 were associated with AD (Jiang et al., 2018).

Microglial phenotype regulation is mainly dependent on their interaction with molecules released by surrounding cells or associated with pathogens, through membrane bound pattern recognition receptors (PRRs) (Venegas and Heneka, 2017). TLRs are a major family of PRRs, and many of them are expressed by microglia. TLR-mediated signaling has been suggested to be both beneficial and detrimental depending on the receptor involved in the response (Downer, 2013). For instance, TLR9 stimulation has a positive role to reduce neurodegenerative pathology in mice (Scholtzova et al., 2014). However, chronic microglia activation through ligation of TLR4 expressed on microglia, increases neuroinflammation and pathology (Vincenti et al., 2015). In contrast, TLR4 may play a protective role in AD and enhance cognitive function (Michaud et al., 2013). These conflicting results regarding TLR4 could be explained by understanding other parameters in its function and whether it is in complex with TLR2 or co-receptors CD14 and CD36 and thus how it initiates an intracellular signal cascade, leading to the expression of the pro-inflammatory molecules. Of note, TLR2 and 4 are both upregulated in the brains of *T. gondii*-infected mice.

Collectively, the data obtained demonstrates that microglial activation is a feature of *T. gondii* infection. Besides the genes mentioned above, other genes that have been reported to be involved in microglial activation such as Aif-1 (allograft inflammatory factor 1), CD68, and Tmem119 (transmembrane protein 119) were found to be upregulated (Ito et al., 1998, Hoogland et al., 2015, Bennett et al., 2016). Importantly, some of these gene products are known to be important in control of *T. gondii* infection. However, there is increasing evidence that many are also associated with neuropathology and neurological diseases and dysfunction.

In summary, it has been reported that microglia activation is associated with an upregulation of TLRs (TLR-2 and TLR-4), TNF, IL-1β, CD68, Cx3cr1, TREM2, and Tmem119. In the current study, all these genes were significantly increased in infected mice compared with non-infected control mice.

5.3 Transcripts associated with antioxidant responses are altered in mice infected with *T. gondii*

Another interesting point in the literature is that oxidative stress might be a part of the pathology in schizophrenia, AD, PD, stroke and epilepsy (Boskovic et al., 2011, Kumar et al., 2017). The CNS is highly sensitive to oxidative stress because of low levels of antioxidant enzymes. The brain is highly metabolically active in nature making it susceptible to oxidative stress. Additionally, Glutathione-S-transferases enzymes (GST) which have been reported to have a significant role in cellular detoxification process and

regulation of redox homeostasis, may be involved in the development of several brain diseases. For instance, a murine model of autism using GSTM1 knockout mice demonstrated that GSTM1 (glutathione S-transferase, mu 1) may play a protection role in neuronal death (Yochum et al., 2010). Furthermore, a case control study demonstrated that deletion polymorphism in GSTM1 gene are associated with early onset of mental disorder in humans at younger ages (Pejovic-Milovancevic et al., 2016). Thus, decreased GSTs levels might reduce the antioxidant process leading to neural loss which is involved in several brain disorders. In the current study, the level of GSTM1 and GSTM3 transcripts were significantly downregulated in infected mice group compared with its controls. From the points discussed above and this study data, it would be suggested that chronic *T. gondii* infection has the ability to stimulate microglia cells and other brain cells and promote oxidative stress. At the beginning, this activation could be protective as part of killing mechanism against the *T. gondii* parasite. However, chronic microglia activation, associated with persistent infection and other micro-environmental factors could work together to induce neural impairment and damage associated with neuropathological diseases (Figure 5.2). This suggestion may be emphasized by the finding that viruses such as *cytomegalovirus* and *Herpes simplex* which have been suggested to be risk factor for neuropsychiatric disorders and neuropathological diseases, induce similar immune changes in their hosts.

A good analysis tool that was used in this study was Human - Mouse disease connection which detects genes associated with behaviour, neurological changes, nervous system diseases and diseases of mental health and illustrated in Table 4.6. This table contains

some of the genes already discussed (such as, Trem2, Cx3cr1, and Gstm1) as well as others that have been implicated in neurological disease in humans and mice.

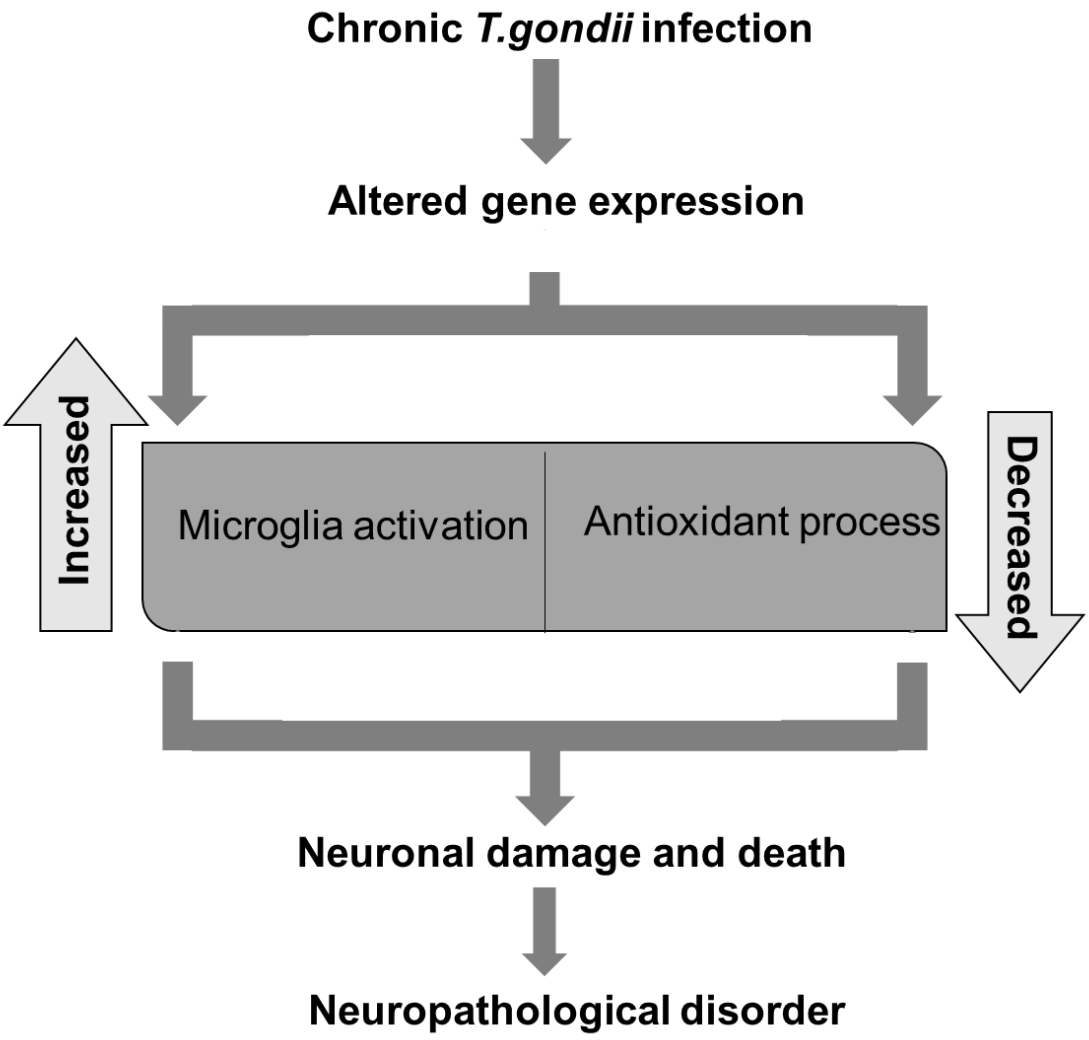

Figure 5.2 Chronic *T. gondii* infection and Neuropathological disorders. According to this study's data, chronic *T. gondii* infection alters transcriptomics profile of its host by two ways. Increased microglia activation and decreased antioxidant process which are both involved in neuronal damage and progress into neuropathological disorders.

6 The effect of *T. gondii* congenital infection or maternal exposure on the metabolomic profile of brain.

6.1 Introduction

In humans a recent large serological study provides evidence that exposure to *T. gondii* might be a contributing causal factor for developing schizophrenia and serious psychiatric disorders (Burgdorf et al., 2019). Furthermore, *T. gondii* infections have been suggested to be associated with cognitive deficits and behavior alteration in humans. Prenatal exposure to a range of infections including *T. gondii* may be associated with increased risk of adult schizophrenia. The mechanisms would appear to be the dependent on the immune response to these infections since increased pro-inflammatory cytokines during pregnancy were also associated with risk (Khandaker et al., 2013). However, congenital toxoplasmosis most likely also leads to mental retardation and development of neurological diseases directly through tissue destruction (Dubey, 2004, Remington et al., 2006). Animal models are required to investigate the effects of prenatal infections on neurodevelopment and neurological disease. Despite the large volume of literature that details the effects of adult acquired *T. gondii* infection on psychoneurological disease, little is known about the potential of congenitally acquired *T. gondii* infection to affect neurological parameters. Furthermore, animal models have demonstrated that other maternal infections are associated with increased risk of psychiatric disorders in offspring (Estes and McAllister, 2016, Brown and Meyer, 2018). These affects have been attributed to the immune response as maternal immune activation (MIA) induced by TLR3 ligands has been demonstrated to induce certain behavioural changes in the offspring of rodents. Therefore, the aim of this project is to evaluate the effects of congenital *T. gondii* infection and the maternal immune response it induces to (i) modify the behaviour (ii) alter the

neurochemistry. To achieve this aim the BALB/c murine model of congenital *T. gondii* infection will be used (Roberts and Alexander, 1992). This model results in approximately 50% of offspring being congenitally infected and logically the remaining approximately 50% uninfected, but exposed to the maternal immune response. Thus this model allows simultaneous study of *T. gondii* congenital infection and maternal immune activation.

6.2 Results

6.2.1 ELISA results

Seropositive evaluation of IgG1 and IgG2a levels in the serum of offspring was achieved by ELISA. 19 out of 49 pups born to 12 mothers were seropositive having both IgG1 and IgG2a specific for *T. gondii* and thus were congenitally infected, whereas 30 out of 49 pups were congenitally exposed but not infected (Figure 6.1).

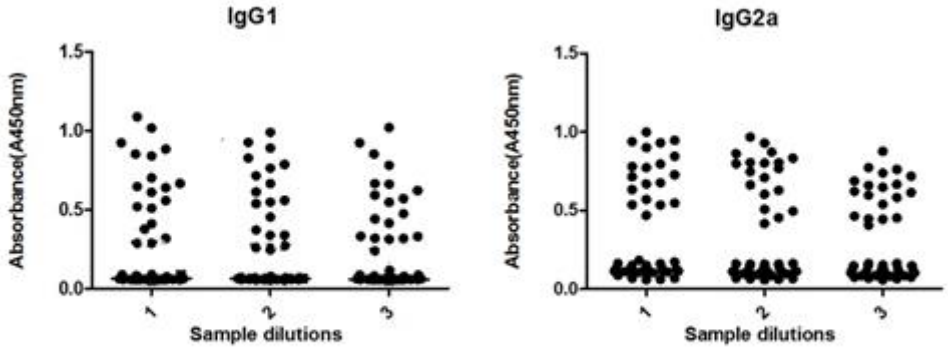

Figure 6.1 Absorbance at 450 nm of plasma samples of 49 of congenital run. (Which were diluted 1/500, 1/1000, 1/2000 in a solution of 2.5% (w/v) milk and washing buffer) tested by ELISA.

6.2.2 Open Field Test

All mice were assessed in the open field study at 14 weeks of age (Figure 6.2).

Total distances moved (cm) in mice congenitally infected and mice born to infected mothers, but uninfected (maternally exposed) were significantly decreased compared to control mice ($p= 0.0420$ and 0.0166, respectively) for the whole 30 minutes of the study. The data is shown as 10 min periods in the apparatus. No difference was observed in the total distance moved in the open field between the congenitally infected mice and maternally exposed mice (Figure 6.2.A).

The number of entries (n) into centre of the arena of the open field did not differ between the congenital infected mice and the maternally exposed mice or the control mice group (Figure 6.2.B). The time spent in the centre of the open field at 14 weeks of the age was not significantly different between the three groups of mice (Figure 6.2.C). The rotation frequency of mice in the arena of the open field was not significantly different between the three groups of mice (Figure 6.2.D).

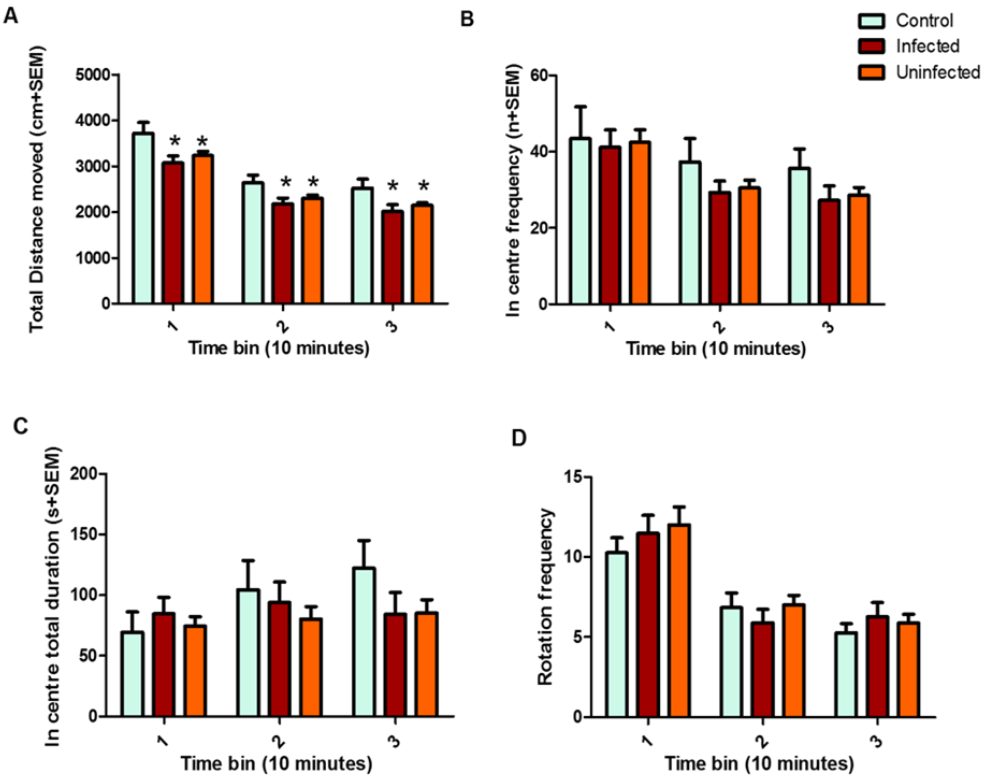

Figure 6.2 represents the performance of 12 control BALB/c mice (6 males and 6 females), 19 congenitally infected BALB/c with *T. gondii* Beverley (10 males, 9 females), and 30 uninfected litter mate mice (13 males, 17 females) in the open field task for a 30 minute trial at 14 weeks of age.

A) Represents the average of total distance travelled (cm) in the arena of the field during the 30-minutes task.
B) Represents the average number of entries (n) at the centre zone of the arena for each group.
C) Represents the average of the time spent (s) in the centre zone of the arena for each group.
D) Represents the average of rotation frequency for each group.

6.2.3 Global metabolomics changes in congenitally infected and maternally exposed uninfected mice brain with *T. gondii*.

In this study, non-targeted LC-MS based metabolomic analyses were used to identify characteristics of the metabolite profiles of congenitally infected and maternally exposed uninfected mice. The goal was to determine if congenitally infected animals had similar changes to the mice with adult acquired infections and to understand if maternally exposed non-infected animals had metabolic changes in comparison with control animals. The same approach described in the third chapter was used in this study.

The OPLS-DA plots show that infected groups clearly separate from the corresponding controls (Figure 5.4). Tables were produced allowing easy comparisons of (VIP≥1) and the P-value of student's t-test for each metabolite. The statistically significant metabolites detected in this experiment, using the pHILLIC column (primary column) that was augmented with C18-PFP Column to obtain important missing metabolites. The pHILLIC column, following manual curation and filtration successfully identified 196 metabolites with high confidence and the C18-PFP column identified 121 metabolites with high confidence. 68 of these metabolites were identified using both columns adding an additional degree of confidence (Figure 6.3). The formula, fold change (FC) and *P*- value for each metabolite are shown in Tables 6.1 and 6.2 respectively.

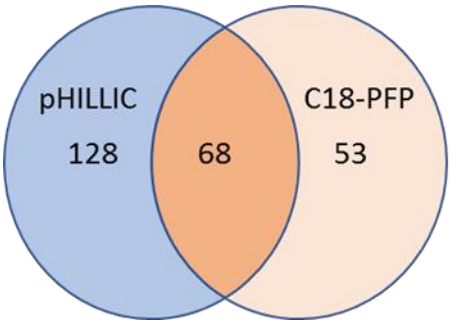

Figure 6.3 Venn diagram shows the number of metabolites that were detected by pHILLIC Column, C18-PFP Column or Both columns in the congenital experiment. For the details of these metabolites see appendix 6.1.

Additional, different analysis methods to visualize the data were used and similar results to those presented in this chapter were obtained. These are presented in appendix 6.

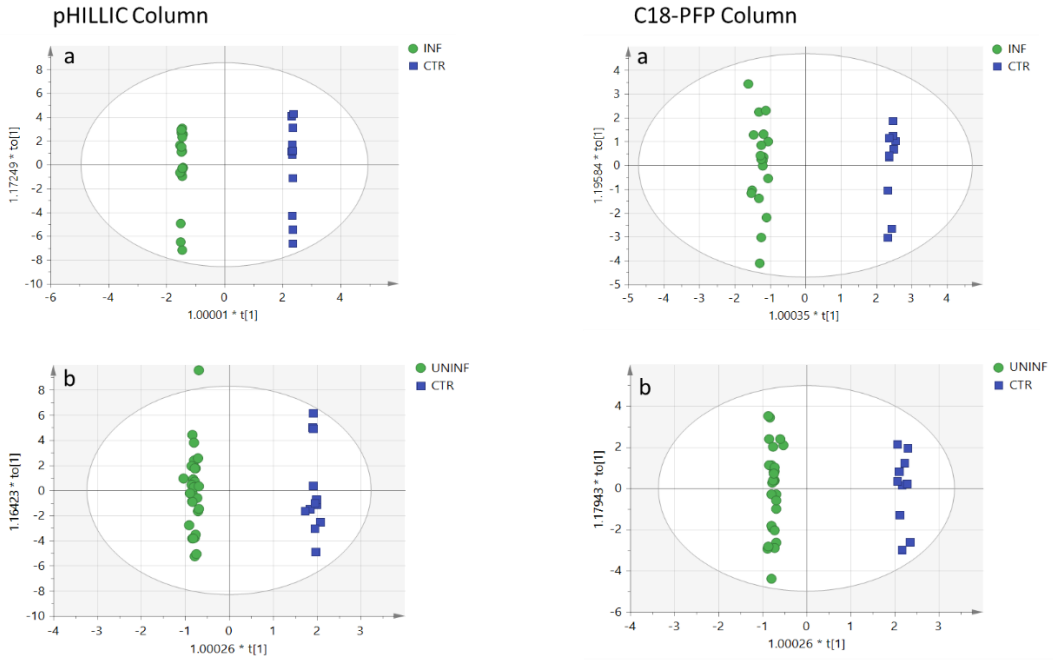

Figure 6.4 Orthogonal Partial Least Square Discriminant Analysis (OPLS-DA) score plot shows an excellent separation between congenital experiment groups. pHILLIC Column was used as primary column to detect the metabolites a and b. it then was augmented with C18-PFP Column a and b to obtain important missing metabolites. CTR= control group, INF= congenitally infected group. UNINF= maternally exposed uninfected group.

Table 6.1 List of differentially expressed metabolites between control group and congenitally infected group or maternally exposed uninfected group identified by pHILLIC Column according to VIP score or p values ≤ 0.05. The metabolites highlighted by yellow color corresponding to standard metabolites that were used. FC: Fold Change.

		Congenitally infected samples			Maternally exposed uninfected samples		
FORMULA	**Identification**	**VIP**	**FC INF/CTR**	**ttest**	**VIP**	**FC Uninf/CTR**	**ttest**
C5H4N4O3	**Urate**	2.31	**2.36**	2E-05	0.74	**0.87**	5E-01
C8H12N2O4	Dihydroclavaminic acid	2.07	**0.46**	2E-03	1.91	**0.61**	1E-02
C11H20N2O5	L-gamma-glutamyl-L-leucine	1.76	**0.56**	2E-04	1.69	**0.7**	5E-03
C10H16N5O14P3	GTP	1.73	**1.73**	3E-02	1.29	1.09	7E-01
C10H12N2O3	**L-Kynurenine**	1.71	**2.14**	4E-03	0.71	1.04	8E-01
C4H6N4O3	**Allantoin**	1.63	**1.63**	2E-04	0.68	1.00	1E+00
C10H16N5O13P3	**ATP**	1.62	1.57	8E-02	1.32	1.14	6E-01
C12H23NO4	2-Methylbutyroylcarnitine	1.58	**1.62**	2E-04	0.81	1.04	7E-01
C21H30N7O17P3	NADPH	1.49	**1.77**	7E-03	1.43	1.07	7E-01
C9H17NO4	**O-Acetylcarnitine**	1.48	**1.48**	2E-03	0.80	0.99	9E-01
C20H32N6O12S2	**Glutathione disulfide**	1.47	**1.52**	1E-02	1.23	1.22	3E-01
C10H13N4O9P	Xanthosine 5'-phosphate	1.47	**1.65**	2E-03	0.66	1.06	7E-01
C11H21NO5	Hydroxybutyrylcarnitine	1.45	**1.5**	8E-05	0.71	1.01	9E-01
C7H13NO3	5-Acetamidopentanoate	1.42	**1.5**	4E-03	0.84	1.00	1E+00
C3H5O6P	**Phosphoenolpyruvate**	1.42	**1.6**	3E-02	1.17	1.09	7E-01
C9H14N2O12P2	**UDP**	1.39	1.38	2E-01	1.20	1.11	6E-01
C10H15N5O11P2	**GDP**	1.39	**1.43**	1E-02	0.99	1.03	8E-01
C24H50NO7P	1-Palmitoylglycerophosphocholine	1.37	**1.44**	6E-04	0.67	1.08	5E-01
C9H15N3O11P2	**CDP**	1.37	1.39	9E-02	1.17	1.13	5E-01
C15H22N2O18P2	UDP-glucuronate	1.35	**1.39**	2E-02	0.99	1.00	1E+00
C8H14N2O6	L-beta-aspartyl-L-threonine	1.35	**0.71**	2E-02	1.17	0.81	8E-02
C21H29N7O14P2	NADH	1.33	**1.5**	2E-02	1.03	1.06	7E-01
C8H17NO6	N-acetyl -D-glucosaminitol	1.32	**1.37**	6E-04	0.77	1.00	1E+00
C7H11N3O2	**N(pi)-Methyl-L-histidine**	1.31	**1.39**	6E-03	0.78	1.06	6E-01
C10H15N5O10P2	**ADP**	1.28	**1.37**	2E-02	0.99	1.11	4E-01
C8H9NO3	**Pyridoxal**	1.25	**0.73**	2E-02	1.63	**0.71**	1E-02
C14H18N5O11P	N6-(1,2-Dicarboxyethyl)-AMP	1.22	1.31	8E-02	0.96	0.99	9E-01
C7H14N2O4	N5-acetyl-N5-hydroxy-L-ornithine	1.22	**0.72**	1E-02	1.20	**0.79**	4E-02
C11H14N4O5	8-Oxocoformycin	1.22	**1.35**	2E-03	0.64	0.99	9E-01
C7H15NO3	L-Carnitine	1.20	**1.32**	4E-04	0.69	0.97	6E-01
C3H7O7P	3-Phospho-D-glycerate	1.18	1.35	9E-02	0.90	1.02	9E-01

C21H39NO4	cis-5-Tetradecenoylcarnitine	1.18	**1.31**	8E-03	0.62	1.01	9E-01
C11H15N3O6	N4-Acetylcytidine	1.17	1.24	3E-01	1.01	1.01	9E-01
C21H35N7O13P2S	Dephospho-CoA	1.15	**0.77**	1E-02	1.30	**0.79**	2E-02
C12H21NO6	Glutarylcarnitine	1.14	**0.74**	5E-02	0.65	1.04	7E-01
C11H15NO10	beta-Citryl-L-glutamic acid	1.13	1.21	2E-01	0.97	0.90	5E-01
C6H13O10P	**6-Phospho-D-gluconate**	1.13	1.23	2E-01	1.02	1.02	9E-01
C6H14O12P2	D-Fructose 1,6-bisphosphate	1.09	0.86	5E-01	1.09	0.82	4E-01
C10H17N3O6	Gamma-Glutamylglutamine	1.08	**1.34**	4E-03	0.84	1.11	3E-01
C10H12N4O4	Deoxyinosine	1.04	0.91	3E-01	1.30	**0.79**	2E-02
C10H13N5O3	Deoxyadenosine	1.04	**0.80**	1E-02	0.86	0.88	1E-01
C7H14N2O4S	**Cystathionine**	1.03	1.24	2E-02	0.74	0.99	9E-01
C11H15N5O3S	5'-Methylthioadenosine	1.02	1.25	1E-01	0.66	0.94	7E-01
C5H9NO2	**L-Proline**	1.02	**1.24**	1E-03	0.61	1.01	9E-01
C7H15NO2	4-Trimethylammoniobutanoate	1.02	**1.27**	1E-03	0.56	1.01	9E-01
C26H52NO7P	1-Oleoylglycerophosphocholine	1.00	**1.23**	3E-02	0.62	1.02	8E-01
C10H13N5O5	**Guanosine**	0.99	**0.81**	2E-02	1.10	**0.84**	4E-02
C2H6O4S	2-Hydroxyethanesulfonate	0.97	**1.20**	1E-02	0.71	0.94	4E-01
C6H8O6	Ascorbate	0.97	**1.22**	2E-02	0.67	0.98	8E-01
C6H6O6	trans-Aconitate	0.97	**1.23**	3E-02	0.70	0.94	5E-01
C10H17N3O11P2	2'-Deoxy-5-hydroxymethylcytidine-5'-diphosphate	0.95	**1.22**	2E-02	0.54	1.02	8E-01
C10H18N4O6	N-(L-Arginino)succinate	0.95	**1.22**	2E-02	0.65	0.95	5E-01
C12H17N5O5	N2-N2-Dimethylguanosine	0.95	**1.21**	2E-02	0.65	1.03	7E-01
C9H14N2O6	5-6-Dihydrouridine	0.94	**1.19**	3E-02	0.62	1.01	9E-01
C7H15O10P	D-Sedoheptulose 7-phosphate	0.93	**0.80**	3E-02	0.84	0.87	2E-01
C6H11NO4	N-Methyl-L-glutamate	0.92	**0.81**	5E-02	0.62	0.98	8E-01
C17H21N4O9P	FMN	0.9	**1.18**	4E-02	0.68	1.00	1E+00
C9H11NO3	L-Tyrosine	0.89	**1.19**	1E-02	0.65	1.07	3E-01
C9H10O4	3-(4-Hydroxyphenyl)lactate	0.88	**1.20**	8E-03	0.68	1.06	3E-01
C9H11NO2	L-Phenylalanine	0.88	**1.17**	2E-02	0.63	0.97	6E-01
C17H27N3O17P2	UDP-N-acetyl-D-glucosamine	0.88	**1.17**	3E-02	0.68	1.01	9E-01
C6H11NO2	N4-Acetylaminobutanal	0.87	1.01	1E+00	1.05	0.89	4E-01
C17H20N4O6	**Riboflavin**	0.86	0.88	2E-01	1.21	**0.81**	5E-02
C11H23N2O7PS	Pantetheine 4'-phosphate	0.84	0.86	2E-01	1.11	0.82	7E-02
C3H7O5P	Propanoyl phosphate	0.84	**1.17**	4E-02	0.56	1.01	9E-01
C3H7N3O2	Guanidinoacetate	0.83	**1.18**	3E-03	0.49	0.97	5E-01

CH5O4P	Hydroxymethylphosphonate	0.83	1.27	1E-01	1.72	**1.64**	8E-04
C3H10NO5P	serinol phosphate	0.82	**1.17**	4E-02	0.59	1.01	9E-01
C5H14NO6P	sn-glycero-3-Phosphoethanolamine	0.82	**1.15**	4E-02	0.61	1.00	9E-01
C8H14N2O5	gamma-L-Glutamyl-D-alanine	0.81	**1.20**	4E-02	0.51	1.05	5E-01
C2H8NO4P	Ethanolamine phosphate	0.79	**1.14**	2E-02	0.59	0.97	5E-01
C2H7NO3S	Taurine	0.79	**1.13**	4E-03	0.46	0.99	8E-01
C8H16N2O4	γ-glutamyl-L-alaninol	0.75	1.11	3E-01	1.02	**0.83**	1E-01
C4H4N2O2	**Uracil**	0.75	1.13	7E-02	1.14	**0.84**	9E-03
C6H12O7	D-Gluconic acid	0.75	**1.15**	4E-02	0.55	1.03	7E-01
C3H9NO	Trimethylamine N-oxide	0.73	1.11	4E-01	1.12	0.80	7E-02
C10H13N5O4	Adenosine	0.71	**0.89**	4E-02	0.51	0.98	8E-01
C10H12N4O5	**Inosine**	0.64	0.91	2E-01	1.06	**0.85**	4E-02
C12H16N4OS	**Thiamin**	0.59	0.93	3E-01	1.09	**0.85**	4E-02
C20H22O4	Pulverochromenol	0.59	**1.09**	2E-02	0.61	1.08	5E-02
C5H4N4O	**Hypoxanthine**	0.55	0.97	6E-01	1.07	**0.86**	2E-02
C5H11N3O2	4-Guanidinobutanoate	0.54	1.05	6E-01	1.05	**0.84**	5E-02
C5H4N4O2	**Xanthine**	0.54	0.93	2E-01	1.02	**0.86**	2E-02
C4H7N3O	Creatinine	0.54	1.06	2E-01	0.76	**0.92**	5E-02

Table 6.2 List of differentially expressed metabolites between control group and congenitally infected group or maternally exposed uninfected identified by C18-PFP Column according to VIP score p values ≤ 0.05. The metabolites highlight by yellow color corresponding to standard metabolites that were used. FC: Fold Change.

		Congenitally infected samples			Maternally exposed uninfected samples		
FORMULA	**Identification**	**VIP**	**FC INF/CTR**	**ttest**	**VIP**	**FC UNIF/CTR**	**ttest**
C3H7NO2S	L-Cysteine	3.20	**0.51**	2E-02	2.59	**0.57**	3E-02
C14H22N6O3S	S-Adenosylmethioninamine	2.02	**0.4**	6E-04	1.43	0.73	7E-02
C5H14N2	Cadaverine	1.87	**0.46**	6E-05	1.27	0.82	1E-01
C10H12N2O3	L-Kynurenine	1.82	**3.26**	9E-03	1.17	**1.54**	2E-02
C10H23N3O3	Hypusine	1.82	**0.52**	2E-03	1.53	**0.7**	3E-02
C13H21N3O8S	(R)-S-Lactoylglutathione	1.76	**2.54**	1E-03	1.90	**2.03**	7E-03
C13H22N4O8S2	S-glutathionyl-L-cysteine	1.58	2	6E-02	1.95	**2.29**	2E-02
C8H16N2O4	N6-Acetyl-N6-hydroxy-L-lysine	1.49	**0.58**	3E-03	1.11	0.8	1E-01
C9H21N3O	N1-Acetylspermidine	1.44	**0.63**	1E-02	1.32	**0.72**	3E-02
C10H19NO4	O-Propanoylcarnitine	1.42	**1.63**	1E-04	0.8	1.14	3E-01
C6H11N3	N-Methylhistamine	1.36	**0.6**	2E-03	0.96	0.78	6E-02
C14H18N5O11P	N6-(1,2-Dicarboxyethyl)-AMP	1.35	**1.66**	5E-03	1.16	1.32	1E-01
C12H21NO6	Glutarylcarnitine	1.27	**0.65**	5E-02	0.89	1.01	1E+00
C8H7NO2	5,6-Dihydroxyindole	1.23	**0.66**	1E-02	1.05	0.77	7E-02
C4H6O4	Succinate	1.22	**1.5**	4E-02	1.31	**1.45**	4E-02
C4H4O2	3-Butynoate	1.21	**1.54**	4E-03	0.93	1.08	5E-01
C4H12N2	Putrescine	1.12	0.87	5E-01	1.38	**0.7**	1E-02
C9H15N3O2S	Ergothioneine	1.10	**1.47**	5E-04	0.75	1.14	2E-01
C11H21NO4	O-Butanoylcarnitine	1.08	**1.39**	6E-03	0.66	1.04	7E-01
C27H33N9O15P2	FAD	1.07	**1.43**	6E-04	1.05	**1.30**	5E-03
C10H16N2O7	GammaGlutamylglutamic acid	1.05	**1.48**	2E-04	1.07	**1.41**	6E-04
C10H13N5O5	Guanosine	1.04	**0.75**	1E-02	0.73	0.90	2E-01
C11H21NO5	Hydroxybutyrylcarnitine	1.03	**1.36**	1E-02	0.7	1.03	8E-01
C9H11NO3	L-Tyrosine	1.02	**1.34**	4E-03	1.18	**1.35**	3E-03
C10H18N2O3	Dethiobiotin	1.00	**0.74**	3E-02	0.79	0.85	2E-01
C8H15NO6	N-Acetyl-D-glucosamine	0.95	**0.77**	6E-03	1.13	**0.78**	7E-03
C10H12N5O6P	3'_5'-Cyclic AMP	0.67	1.15	2E-01	1.00	**1.28**	3E-02
C10H23N3O3	Hypusine	1.8	**0.52**	2E-03	1.53	**0.7**	3E-02
C5H11N3O2	4-Guanidinobutanoate	0.33	0.97	6E-01	0.77	**0.86**	3E-02

C5H8N2O2	5,6-Dihydrothymine	0.49	1.09	1E-01	0.75	**1.16**	1E-02
C10H13N5O4	Adenosine	0.54	0.90	1E-01	0.77	**1.15**	3E-02
C10H17N3O6	Gamma-Glutamylglutamine	0.69	**1.23**	3E-02	0.7	**1.23**	3E-02
C6H11NO4	L-2-Aminoadipate	0.56	0.89	2E-01	0.79	**1.17**	4E-02
C12H23NO10	Lactosamine	0.66	1.06	6E-01	0.85	**1.24**	2E-02
C4H8N2O3	L-Asparagine	0.33	1.00	1E+00	0.76	**1.15**	5E-02
C4H7NO4	L-Aspartate	0.35	1.01	9E-01	0.64	**1.09**	2E-02
C6H13N3O3	L-Citrulline	0.92	**1.30**	5E-04	0.82	**1.18**	2E-02
C3H7NO3	L-Serine	0.48	0.92	3E-01	0.75	**1.15**	4E-02
C11H19NO9	N-Acetylneuraminate	0.75	**0.81**	3E-02	0.93	**0.84**	3E-02
C3H9O6P	sn-Glycerol 3-phosphate	0.69	0.90	1E-01	0.78	**0.88**	5E-02
C9H17NO4	O-Acetylcarnitine	1.40	**1.64**	4E-05	0.86	**1.18**	4E-02
C9H13NO2	3-Methoxytyramine	0.97	**0.78**	2E-02	0.75	0.91	3E-01
C6H8O6	Ascorbate	0.86	**1.26**	2E-03	0.65	1.09	2E-01
C6H11O10P	D-Glucuronate 1-phosphate	0.86	**1.27**	2E-02	0.69	1.09	3E-01
C8H11NO2	Dopamine	0.98	**0.77**	4E-04	0.5	0.92	1E-01
C3H7N3O2	Guanidinoacetate	0.8	**1.22**	2E-02	0.42	1.04	6E-01
C10H13N4O8P	IMP	0.86	**1.23**	1E-02	0.82	1.15	8E-02
C7H15NO3	L-Carnitine	0.98	**1.28**	4E-04	0.34	1.01	8E-01
C9H11NO2	L-Phenylalanine	0.97	**1.28**	3E-02	0.98	1.20	7E-02
C5H9NO2	L-Proline	0.71	**1.14**	2E-02	0.84	1.03	6E-01
C5H11NO2	L-Valine	0.83	**1.21**	5E-02	0.84	1.17	6E-02
C21H27N7O14P2	NAD+	0.73	**0.85**	5E-02	0.55	0.93	3E-01
C9H13N2O9P	UMP	0.85	**1.24**	3E-02	0.76	1.14	6E-02

6.2.4 Variations in metabolic pathways of mice brain congenitally infected and maternally exposed uninfected with *T. gondii.*

An indication of the metabolic pathways most differentially affected by infection was visualised using BioCyc which software orders pathways according to pathway perturbation scores (PPS).

6.2.4.1 Purine degradation pathway

Purine metabolism was found to have high PPS values (see Table 6.7 in appendix 6). Mice congenitally infected with *T. gondii* were found to have statistically significant increased levels of xanthosine-5-phosphate (p= 0.002), urate (p= 0.00002) and allantoin (p= 0.0002), but decreased levels of guanosine (p= 0.01). These metabolites also had VIP scores of 1 or greater of xanthosine-5-phosphate (VIP: 1.47), urate (VIP: 2.31) allantoin (VIP: 1.63) and guanosine (VIP: 1.04). Mice maternally exposed but uninfected were found to have statistically significant decreased levels of inosine (p= 0.039), hypoxanthine (p= 0.021), xanthine (P= 0.025), and guanosine (p= 0.038), but increased levels of adenosine (p= 0.028) relative to control uninfected mice. These metabolites also had VIP scores of 1 or greater of inosine (VIP: 1.06), hypoxanthine (VIP: 1.07), xanthine (VIP: 1.02), guanosine (VIP: 1.10), and adenosine (VIP: 1.08).

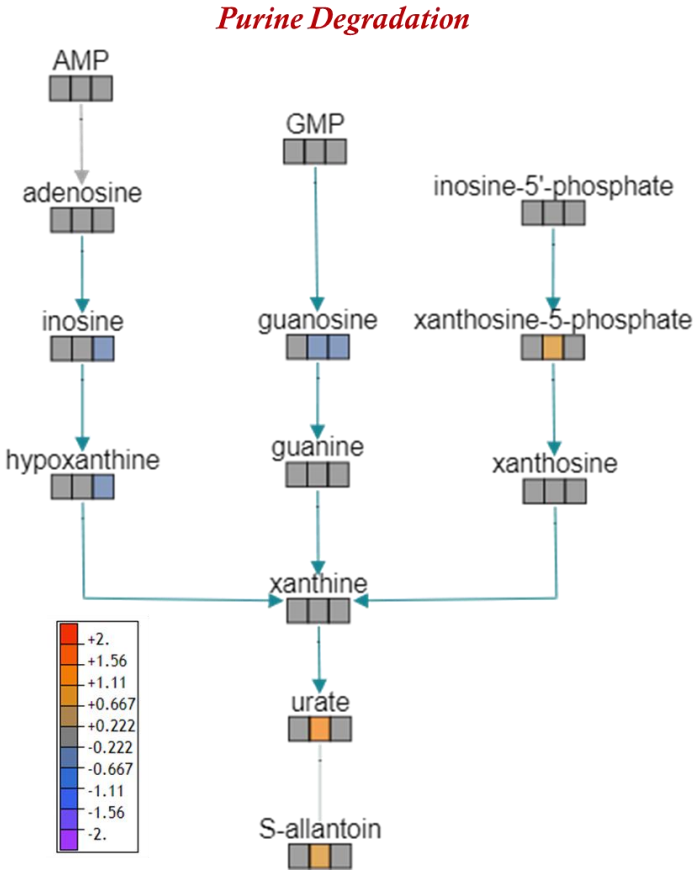

Figure 6.5 Purine degradation pathway. Metabolites which were detected in this pathway are represented by three squares. First square represents control group, second square represents congenitally infected group, and third square represents maternally exposed uninfected group (log 2 transformed) are visualised as a color spectrum scaled from least abundant to highest range is from -2 to 2. Purple indicates low expression, while red indicates high expression of the changed metabolites. In congenitally infected mice, metabolites that were found to be significantly different between congenitally infected and control mice are xanthosine-5-phosphate (p= 0.002), urate (p= 0.00002), allantoin (p= 0.0002) and guanosine (p= 0.01). In maternally exposed uninfected mice, metabolites that were found to be significantly different between maternally exposed uninfected mice and control mice are adenosine (p= 0.028), inosine (p= 0.039), hypoxanthine (p= 0.021), xanthine (0.025), and guanosine (p= 0.038).

6.2.4.2 Tryptophan Degradation Pathway

Pathways associated with tryptophan metabolism were found to have high PPS values (see Table 6.7 in appendix 6). Mice congenitally infected with *T. gondii* were found to have statistically significant incresed levels of kynurenine (p= 0.0003). This metabolite also had VIP scores of 1 or greater kynurenine (VIP: 1.71). Mice maternally exposed but uninfected were also found to have statistically significant increased levels of kynurenine (p= 0.016) and (VIP: 1.17). This data indicates that *T. gondii* infection directs tryptophan metabolism towards kynurenine rather than serotonin in the brains of mice.

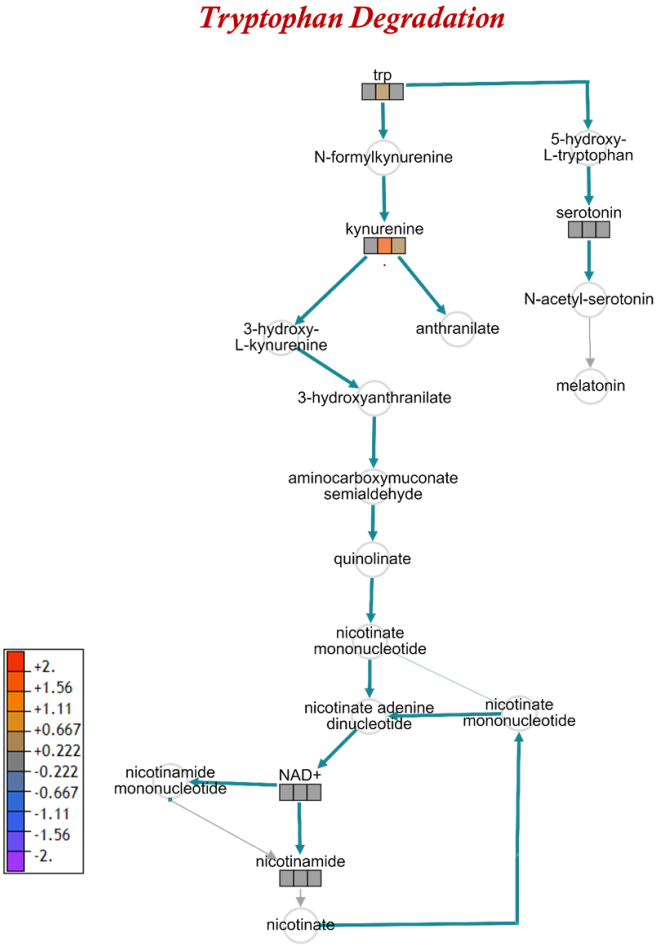

Figure 6.6 Tryptophan Degradation Pathway. Metabolites which were detected in this pathway are represented by three squares. First square represents control group, second square represents congenitally infected group, and third square represents maternally exposed uninfected group (log 2 transformed) are visualised as a color spectrum scaled from least abundant to highest range is from -2 to 2. Purple indicates low expression, while red indicates high expression of the changed metabolites. In congenitally infected mice, metabolite that was found to be significantly different between congenitally infected and control mice is Kynurenine (p= 0.0003). In maternally exposed uninfected mice, the metabolite that was found to be significantly different between maternally exposed uninfected mice and control mice is Kynurenine (p= 0.016).

6.2.4.3 Dopamine Pathway

Mice congenitally infected with *T. gondii* were found to have statistically significant increased levels of L-tyrosine (p= 0.004). This metabolite also had a VIP scores 1.02. Mice maternally exposed uninfected were found to have statistically significant increased levels of L-tyrosine (p= 0.003) and (VIP: 1.18). Dopamine levels were significantly decreased in congenitally infected mice relative to control mice (P= 0.048), but uninfected mice born to infected mothers.

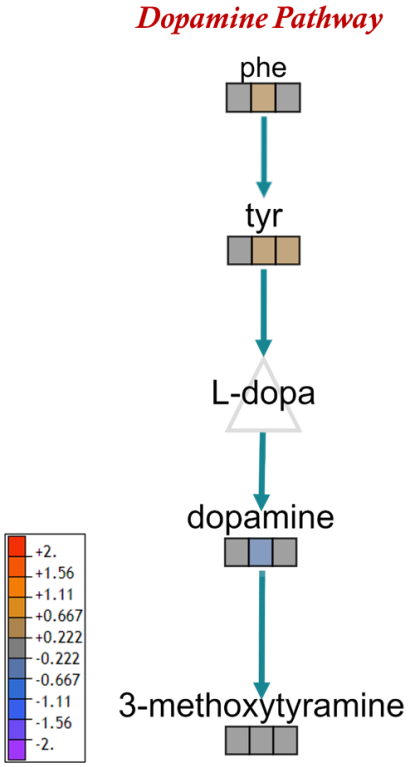

Figure 6.7 Dopamine Pathway. Metabolites which were detected in this pathway are represented by three squares. First square represents control group, second square represents congenitally infected group, and third square represents maternally exposed uninfected group (log 2 transformed) are visualised as a color spectrum scaled from least abundant to highest range is from -2 to 2. Purple indicates low expression, while red indicates high expression of the changed metabolites. In congenitally infected group, the metabolites that were found to be significantly different between congenitally infected and control mice are L-tyrosine (p= 0.004) and dopamine (p= 0.048). In maternally exposed uninfected mice, metabolite that was found to be significantly different between maternally exposed uninfected mice and control mice is L-tyrosine (p= 0.003).

6.2.4.4 Arginine and Proline Biosynthesis with other amino acids degradation.

Mice congenitally infected with *T. gondii* were found to have statistically significant incresed levels of L- proline (p= 0.03), L- cystathionine (P= 0.002), and Glutathione disulfide (p= 0.02), but decreased levels of S-Adenosyl-L-methioninamine (p= 0.001) and L-Cysteine (P= 0.02). These metabolites also had VIP scores of 1 or greater proline (VIP: 1.02), S-Adenosyl-L-methioninamine (VIP: 2.02), L- cystathionine (VIP: 1.03), L-Cysteine (VIP: 3.2) and Glutathione disulfide (VIP: 1.47). Mice maternally exposed but uninfected were found to have statistically significant decreased levels of putrescine (p= 0.011) and L-Cysteine (p= 0.033). These metabolites also had VIP scores of 1 or greater putrescine (VIP: 1.38) and L-Cysteine (VIP: 2.59).

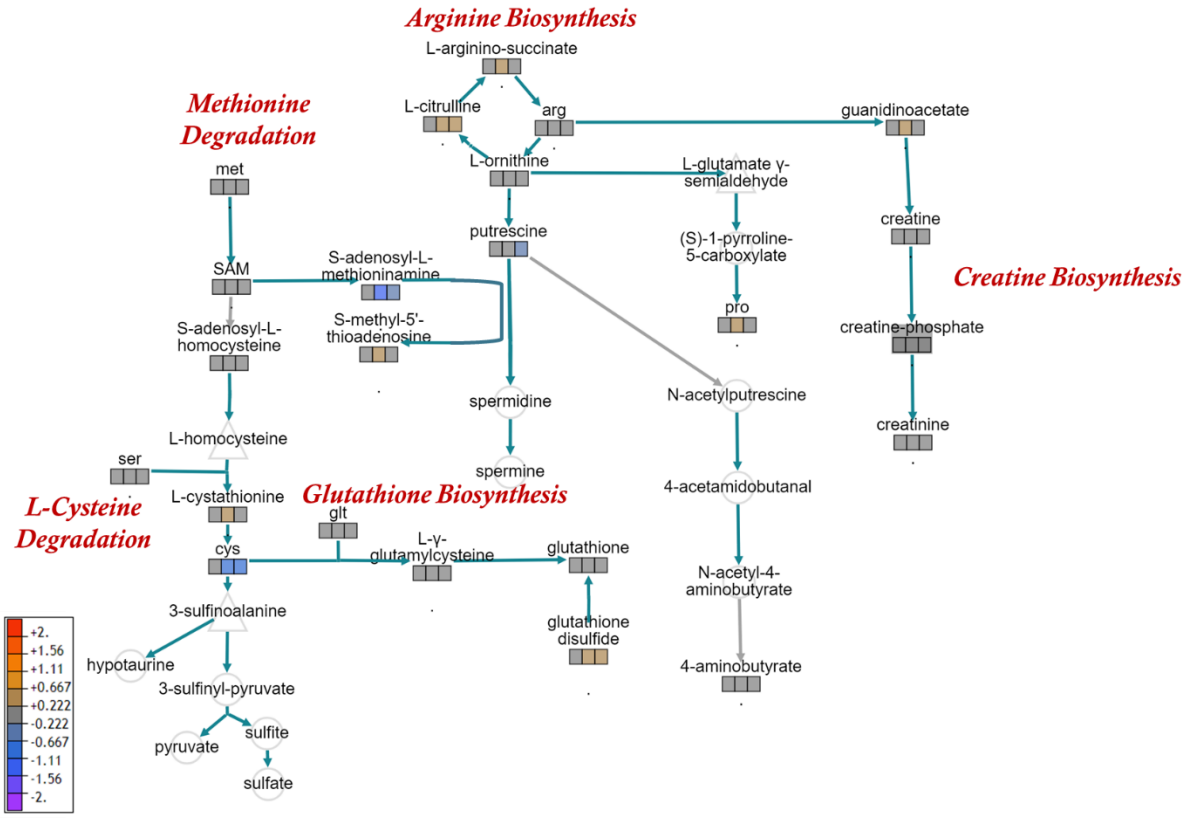

Figure 6.8 Arginine and Proline Biosynthesis with other amino acids degradation. Metabolites which were detected in this pathway are represented by three squares. First square represents control group, second square represents congenitally infected group, and third square represents maternally exposed uninfected group (log 2 transformed) are visualised as a color spectrum scaled from least abundant to highest range is from -2 to 2. Purple indicates low expression, while red indicates high expression of the changed metabolites. In congenitally infected group, metabolites that were found to be significantly different between infected mice and control mice are proline (p= 0.03), S-Adenosyl-L-methioninamine (p= 0.001), L- cystathionine (0.002), L-Cysteine (0.021) and Glutathione disulfide (p= 0.01). In maternally exposed uninfected group, metabolites that were found to be significantly different between maternally exposed uninfected mice and control mice are putrescine (p= 0.011) and L-Cysteine (p= 0.033).

6.2.4.5 Glycolysis and Pentose phosphate pathways

Mice congenitally infected with *T. gondii* were found to have statistically significant incresed levels of Phosphoenolpyruvate (p= 0.0003). This metabolite also had a VIP score 1.42. In addition, metabolites including 3-phospho-D-glycerate (VIP: 1.18) and 6-phospho-D-gluconate (VIP: 1.13) were increased in the brains of congenitally infected mice, but D-fructose 1, 6-bisphoshate (VIP: 1.13) was decreased.

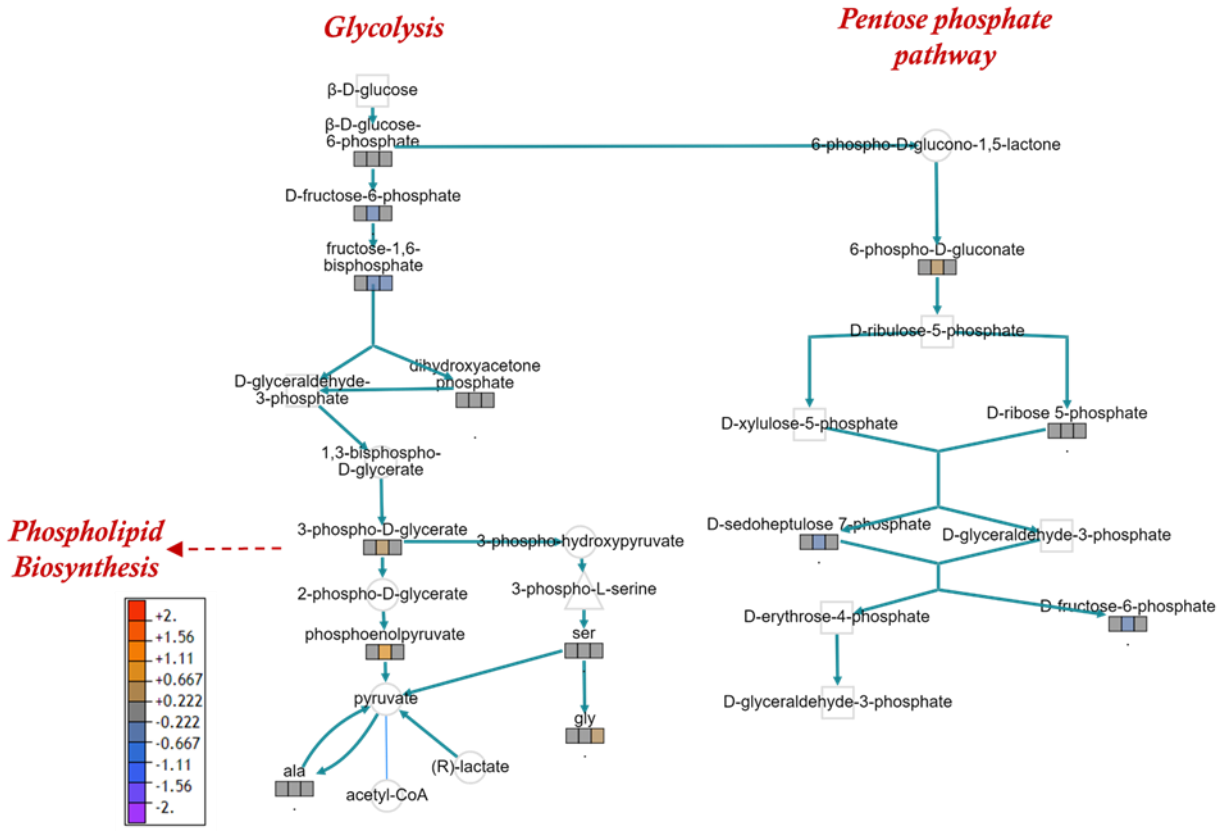

Figure 6.9 Glycolysis and Pentose phosphate pathways. Metabolites which were detected in this pathway are represented by three squares. First square represents control group, second square represents congenitally infected group, and third square represents maternally exposed uninfected group (log 2 transformed) are visualised as a color spectrum scaled from least abundant to highest range is from -2 to 2. Purple indicates low expression, while red indicates high expression of the changed metabolites. In congenitally infected group, metabolites that was found to be significantly different between infected mice and control mice is Phosphoenolpyruvate (p= 0.0003).

6.3 Conclusion and discussion of behavioural data

The Open Field test is considered to be a suitable measure of the anxiety level of an animal, which provides a good evaluation of locomotor activity in relation to anxiety as well as assessing the natural behaviour of exploration (Walsh and Cummins, 1976). A high frequency of crossing to the central part of the open field arena and mobility behaviours indicate increased locomotion and exploration and/or a lower level of anxiety. The number of central square entries and the duration of time spent in the central square are measures of exploratory behaviour and anxiety. A high frequency and duration of these behaviours indicates high exploratory behaviour and low anxiety levels (Rogério dos Santos and Alex Soares de Souza, 2014). Postnatal and congenital infection was associated with increased activity of rats and mice (Hutchinson et al., 1980, Hay et al., 1984b, Webster et al., 1994). In the current study, from the analysis between the congenitally infected mice, the uninfected litter mates and the control mice, the only statistically significant difference observed on the behaviour was decreased activity of the congenitally infected mice and uninfected litter mates compared to the control. Both congenitally infected mice and exposed uninfected mice travelled a similar distance in the field, but less than control mice group. That means the hypo-activity was obvious in both congenitally infected mice and exposed uninfected mice. The results reported here for congenitally infected mice appear to be in contrast to those reported previously. However, the previous murine studies used outbred mice and different behavioural tests to measure activity.

From the analysis, congenitally infected mice and exposed uninfected litter mates did not show statistically significant differences in terms of exploration behaviour compared to control mice group. Rotation frequency another parameter was used to assess any neurological abnormality among the congenitally infected and exposed uninfected mice groups. However, no differences were recorded in terms of rotation frequency in our study. A previous study compared the effects of infection of adult mice with the Me49 and VEG strains of *T. gondii* in BALB/c mice using the open field test. An effect was found in the VEG strain infected mice at 6 weeks, but not 16 weeks post infection (Bezerra et al., 2019). Thus the importance of the strain of *T. gondii* and duration are important determinants of outcome in adult mice and are likely to also be important in congenitally acquired disease where the timing of infection during pregnancy would be another potential confounding factor. In addition, the mouse strain and sex of mice may contribute to outcome. For instance, even healthy female C57BL/6J mice show lower levels of anxiety and higher levels of activity than female BALB/c during the open field (An et al., 2011).

7 Transcriptomics profile for BALB/c mice brains which were congenitally infected with *T. gondii* or exposed to the parasite during intrauterine period.

7.1 Introduction

In the previous chapter a number of changes to brain metabolism were characterised in mice congenitally infected with *T. gondii*. Many of these were similar to those observed in mice with adult acquired *T. gondii* infection including increased purine degradation and tryptophan degradation. In addition, more modest changes to the metabolism of mice born to infected mothers were observed. This suggests that maternal *T. gondii* infection has the ability to alter neurochemical events in the brains of developing pups that are maintained postnatally. The ability of maternal infections and even simply maternal immune activation to affect the behaviour of rodents is now well documented. Animal models have demonstrated that at least certain maternal infections are associated with increased risk of psychiatric disorders in the offspring (Estes and McAllister, 2016, Brown and Meyer, 2018) and more animal models are required to investigate the effects of prenatal infections on neurodevelopment. The ability of maternal *T. gondii* infection to mediate such effects could have important implications for humans. Indeed, a number of epidemiological studies have suggested an association between prenatal infections, maternal immune activation and development of impaired adult behaviour (Canetta and Brown, 2012). Primary infection with the *T. gondii* parasite in pregnant woman can cause abortion or severe and disabling disease in the developing fetus depending on time of infection. However, a number of new-borns have no obvious symptoms and they may be infected or uninfected with the parasite. The potential influence of maternal *T. gondii* infection on the likelihood of them developing psychoneurological diseases or behavioural deficits is

unknown although recent findings indicate that latent toxoplasmosis may play different roles in the etiology of different mental disorders (Canetta and Brown, 2012). However, considerably less is known about the potential of congenitally acquired *T. gondii* infection to cause psychoneurological disease. In this study, a transcriptomics approach has been employed to study the interaction between congenital *T. gondii* and its host. These results will be interpreted with the finding of the metabolomics profile for BALB/c mice brains which were congenitally infected with *T. gondii* or exposed to the parasite during intrauterine period (previous chapter results). Furthermore, the transcriptomics approach will also provide additional information regarding other aspects of the brain affected by congenital infection or maternal exposure to *T. gondii*.

7.2 Results

7.2.1 Global Transcriptomics changes in mice brains congenitally infected or exposed to *T. gondii*.

7.2.1.1 Electropherograms for RNA extraction samples

All chosen samples from congenitally infected and maternally exposed uninfected and control mice showed high quality RNA electropherograms, which illustrate clear 28S and 18S peaks. There is low noise between the peaks and minimal low molecular weight contamination Figure 7.1. All extracted RNA samples had high concentration and high RNA integrity number (Table 7.1).

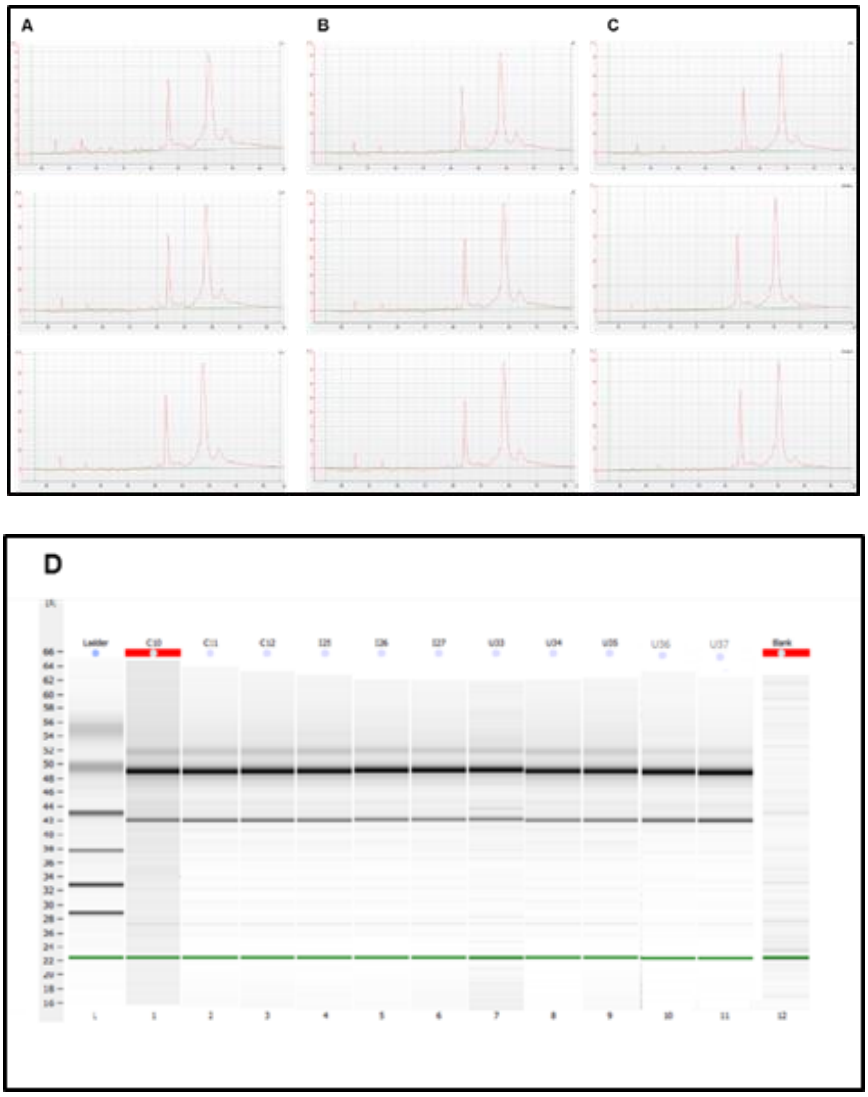

Figure 7.1 Illustrates the electropherograms from high quality RNA for congenitally infected, congenitally exposed uninfected and control samples (A), (B) and (c) respectively. There are clear 28S and 18S peaks and low noise between the peaks and minimal low molecular weight contamination. (D) Bioanalyzer gel image showing RNA extracted from 9 samples. The first three is extracted from the brain of female uninfected control mice and the three after is extracted from the brain of female mice congenitally infected with *T. gondii* and the rest is extracted from female mice congenitally exposed to *T. gondii* but uninfected. The last sample is blank.

Table 7.1 Samples chosen for sequencing based on RNA concentration, RNA ratio and RNA integrity numbers (RIN).

Samples	Group	RNA Concentration (ng/µl)	RNA Ratio [28s / 18s]	(RIN)
C10	Control	236 ng/µl	2.9	9.8
C11	Control	249 ng/µl	2.7	9.9
C12	Control	216 ng/µl	2.7	10
I25	Congenitally infected	259 ng/µl	2.8	10
I26	Congenitally infected	245 ng/µl	2.7	10
I27	Congenitally infected	143 ng/µl	2.8	10
U35	Exposed uninfected	237 ng/µl	2.7	10
U36	Exposed uninfected	225 ng/µl	2.7	10
U37	Exposed uninfected	502 ng/µl	2.7	10

7.2.1.2 Read Statistics

The total amount of raw sequence data and the results of the quality filtering is collected and reported in Table 7.2.

Table 7.2 Quality control statistics per sample in congenital infection experiment (CTR= Control group, INF= Infected group, UNINF= exposed uninfected group).

Sample	Total Reads	Discarded Reads	Clean Reads
C10_CTR	35,943,891	381,885 (1.1 %)	35,562,006 (98.9 %)
C11_CTR	40,451,973	639,787 (1.6 %)	39,812,186 (98.4 %)
C12_CTR	35,198,105	698,680 (2.0 %)	34,499,425 (98.0 %)
I25_INF	43,666,876	669,709 (1.5 %)	42,997,167 (98.5 %)
I26_INF	35,675,284	564,057 (1.6 %)	35,111,227 (98.4 %)
I27_INF	37,900,606	569,092 (1.5 %)	37,331,514 (98.5 %)
U35_UNINF	37,912,069	555,972 (1.5 %)	37,356,097 (98.5 %)
U36_UNINF	42,924,540	637,435 (1.5 %)	42,287,105 (98.5 %)
U37_UNINF	71,056,844	749,952 (1.1 %)	70,306,892 (98.9 %)

Single reads are reads without mates (discarded poor quality mate reads). They are not included in further analysis.

The number of reads mapped to the reference genome/ transcriptome for each of the samples. The accuracy of the reference (genome/ transcriptome) and better quality of mapped reads lead to a higher percentage of reads mapped to the reference Table 7.3.

Table 7.3 Mapped read statistics observed per sample in congenital infection experiment.

Sample	**QC Passed Reads**	**Mapped Reads**	**% Mapped**
C10_CTR	35,562,006	34,820,914	97.9
C11_CTR	39,812,186	38,935,805	97.8
C12_CTR	34,499,425	33,639,270	97.5
I25_INF	42,997,167	41,875,234	97.4
I26_INF	35,111,227	34,233,342	97.5
I27_INF	37,331,514	36,428,722	97.6
U35_UNINF	37,356,097	36,501,708	97.7
U36_UNINF	42,287,105	41,245,646	97.5
U37_UNINF	70,306,892	68,940,898	98.1

7.2.1.3 Volcano plots (Control vs. Infected and Control vs. Uninfected) in congenital infection experiment.

Volcano plots highlight the genes that significantly differ between the conditions tested based on the fold change and test statistics performed on the RNA-Seq data between conditions. They are generated based on expression data of genes using the cummeRbund package. Volcano plots can be used for displaying the relationship between conditions at gene expression level.

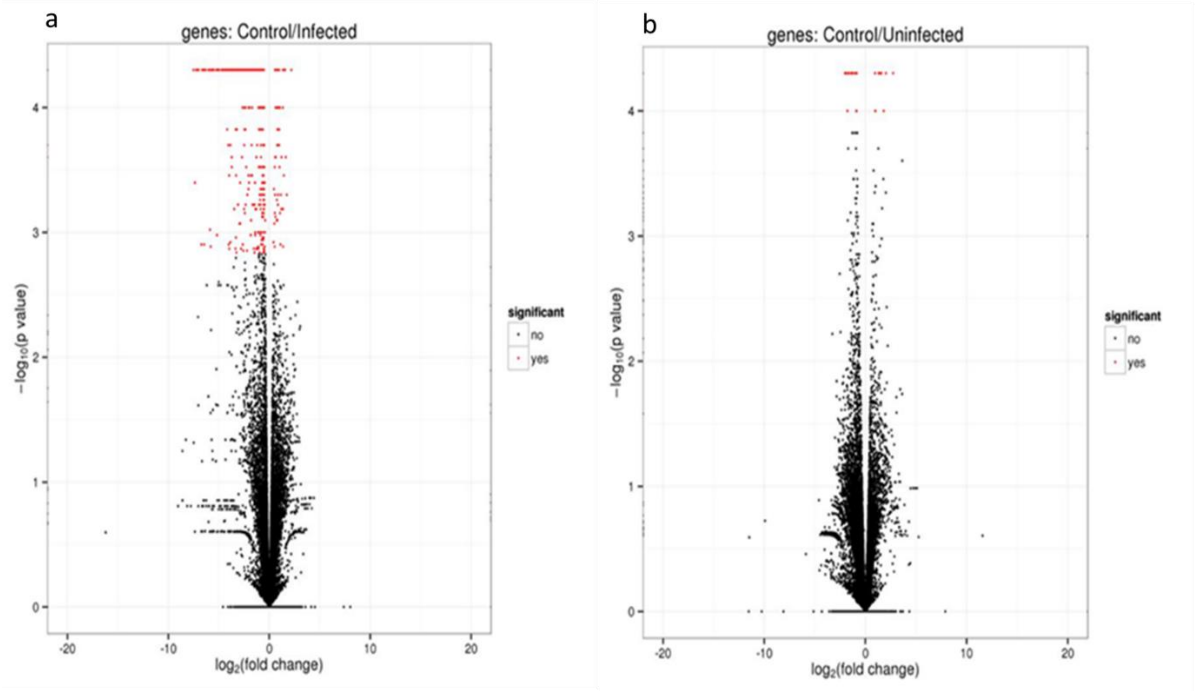

Figure 7.2 Volcano plot of congenital infection experiment. (a) Congenitally infected group versus control and (b) Maternally exposed uninfected group versus control. The red circles represent significant genes expression above the threshold. Note both fold changes and *P*-values are log transformed. The further its position away from the (0, 0), the more significant the feature is.

A number of genes are currently not annotated in the mouse genome and were excluded from further analysis. 721 genes were found to be significantly differentially expressed in the congenitally infected mice compared with control mice. 663 genes of these were upregulated and 58 genes downregulated. The top 50 significant genes were shown in Tables 7.4 and 7.5. The remaining genes are tabulated in appendix 7.

In the same experiment, 38 genes were found to be differentially expressed in the maternally exposed uninfected mice brains. 20 of these genes were upregulated and 18 downregulated. All significant genes are shown in Tables 7.6 and 7.7.

7.2.2 Genes associated with microglial activation and antioxidant responses

Transcripts of particular genes that are associated with *T. gondii* infection were significantly upregulated in the congenitally infected group compared with the non-infected control group. These genes and their fold change are SOCS1, 4.2-fold; CD36, 62-fold; C1q, 4.2-fold; GFAP, 2.3-fold; Ifi30, 2.9-fold; Gbp2b, 31.3-fold; Gbp2, 21.7-fold; Gbp3, 17.3-fold; Gbp5, 14.7-fold; Gbp7, 14.5-fold; Gbp10, 58.6-fold; and Gbp11, 6.4-fold.

Transcripts of genes that are known to be associated with microglia activity were significantly upregulated in congenitally infected mice compared with non-infected control mice. These genes and their fold change are TLR-2, 3.2-fold; TLR-4, 2-fold; TNF such as Tnfsf10, 5.1-fold and Tnfaip2, 2.1-fold; IL-1β, 8.6-fold; CD68, 1.8-fold; Cx3cr1, 2.1; TREM2, 2.2-fold; Tmem119, 2.6-fold.

Table 7.4. Top 50 genes significantly (>2-fold change and FDR of <0.05) upregulated in congenitally infected mice brain with *T. gondii*.

Gene	Description	Average FPKM		Fold Change	FDR	Ensembl ID
		Infected (n=3)	Control (n=3)			
Ighg1	immunoglobulin heavy constant gamma 1 (G1m marker)	78.8	0.4	182.8	0.002	ENSMUSG00000069518
Igkv8-21	immunoglobulin kappa variable 8-21	78.0	0.5	166.0	0.016	ENSMUSG00000056501
H2-Eb1	histocompatibility 2, class II antigen E beta	177.0	1.2	153.8	0.002	ENSMUSG00000030124
Zbp1	Z-DNA binding protein 1	20.6	0.1	149.5	0.002	ENSMUSG00000079293
Cd74	CD74 antigen (invariant polypeptide of major histocompatibility complex, class II antigen-associated)	497.4	3.3	149.1	0.002	ENSMUSG00000024610
H2-Ea-ps	histocompatibility 2, class II antigen E alpha, pseudogene	66.2	0.5	139.9	0.002	ENSMUSG00000045730
Iigp1	interferon inducible GTPase 1	42.4	0.3	134.1	0.002	ENSMUSG00000043157
Ighg2b	immunoglobulin heavy constant gamma 2B	28.8	0.2	127.5	0.002	ENSMUSG00000038055
Ccl5	chemokine (C-C motif) ligand 5	23.2	0.2	106.4	0.043	ENSMUSG00000038642
Gm12250	predicted gene 12250	19.6	0.2	101.6	0.002	ENSMUSG00000042096
H2-Aa	histocompatibility 2, class II antigen A, alpha	142.8	1.4	98.9	0.002	ENSMUSG00000069515
Jchain	immunoglobulin joining chain	22.6	0.2	93.9	0.002	ENSMUSG00000079018
Gm12185	predicted gene 12185	1.2	0.01	87.3	0.043	ENSMUSG00000002944
Cxcl9	chemokine (C-X-C motif) ligand 9	7.0	0.1	85.7	0.002	ENSMUSG00000076518
Igha	immunoglobulin heavy constant alpha	138.5	1.7	82.8	0.002	ENSMUSG00000020638
Igkc	immunoglobulin kappa constant	337.0	4.2	80.6	0.002	ENSMUSG00000061080
Irgm2	immunity-related GTPase family M member 2	109.2	1.4	79.3	0.002	ENSMUSG00000076655
Nlrc5	NLR family, CARD domain containing 5	3.6	0.1	66.0	0.002	ENSMUSG00000030789
Hcar2	hydroxycarboxylic acid receptor 2	2.4	0.04	58.6	0.034	ENSMUSG00000020713
Gbp10	guanylate-binding protein 10	26.8	0.5	58.6	0.002	ENSMUSG00000092021
Gm43302	predicted gene 43302	26.8	0.5	58.6	0.002	ENSMUSG00000045102
Plac8	placenta-specific 8	6.4	0.1	55.5	0.045	ENSMUSG00000027792
H2-DMb1	histocompatibility 2, class II, locus Mb1	9.3	0.2	53.9	0.002	ENSMUSG00000052926
F830016B08Rik	RIKEN cDNA F830016B08 gene	2.2	0.04	53.3	0.002	ENSMUSG00000030048

H2-Ab1	histocompatibility 2, class II antigen A, beta 1	137.4	2.6	52.0	0.002	ENSMUSG00000035208
Gm4841	predicted gene 4841	2.5	0.1	48.5	0.002	ENSMUSG00000075602
Batf2	basic leucine zipper transcription factor, ATF-like 2	5.0	0.1	46.8	0.002	ENSMUSG00000046718
Ciita	class II transactivator	2.6	0.1	46.4	0.002	ENSMUSG00000020932
Oasl2	2'-5' oligoadenylate synthetase-like 2	40.1	0.9	44.8	0.002	ENSMUSG00000022014
Cd8a	CD8 antigen, alpha chain	2.0	0.1	38.0	0.002	ENSMUSG00000090215
Fcgr4	Fc receptor, IgG, low affinity IV	7.8	0.2	37.7	0.002	ENSMUSG00000095210
Psmb9	proteasome (prosome, macropain) subunit, beta type 9 (large multifunctional peptidase 2)	36.8	1.0	36.5	0.002	ENSMUSG00000028015
Igkv1-117	immunoglobulin kappa variable 1-117	13.9	0.4	36.2	0.037	ENSMUSG00000018008
Ighg3	Immunoglobulin heavy constant gamma 3	12.8	0.4	36.0	0.002	ENSMUSG00000026031
Psmb8	proteasome (prosome, macropain) subunit, beta type 8 (large multifunctional peptidase 7)	91.5	2.7	34.3	0.002	ENSMUSG00000027514
Ighv3-7	immunoglobulin heavy variable V3-7	362.8	0	362.8*	0.002	ENSMUSG00000000942
Ighv1-23	immunoglobulin heavy variable V1-23	127.2	0	127.2*	0.002	ENSMUSG00000028037
Ighv7-4	immunoglobulin heavy variable 7-4	66.2	0	66.2*	0.002	ENSMUSG00000105096
Cd36	CD36 molecule	62.4	0	62.4*	0.002	ENSMUSG00000104713
Ighv8-11	immunoglobulin heavy variable V8-11	51.7	0	51.7*	0.002	ENSMUSG00000073403
Ighj3	immunoglobulin heavy joining 3	46.7	0	46.7*	0.002	ENSMUSG00000083041
Igkv4-79	immunoglobulin kappa variable 4-79	31.3	0	31.3*	0.002	ENSMUSG00000038253
Igkv4-55	immunoglobulin kappa variable 4-55	30.9	0	30.9*	0.002	ENSMUSG00000075588
Ighv5-1	immunoglobulin heavy variable V5-1	28.4	0	28.4*	0.002	ENSMUSG00000037405
Ighv1-15	immunoglobulin heavy variable 1-15	27.0	0	27.0*	0.002	ENSMUSG00000000732
Igkv4-70	immunoglobulin kappa chain variable 4-70	23.1	0	23.1*	0.002	ENSMUSG00000031549
Ighv8-12	immunoglobulin heavy variable V8-12	22.5	0	22.5*	0.002	ENSMUSG00000026535
Ighv8-8	immunoglobulin heavy variable 8-8	19.8	0	19.8*	0.002	ENSMUSG00000021208
Igkv8-24	immunoglobulin kappa chain variable 8-24	19.5	0	19.5*	0.002	ENSMUSG00000079017
Ighv2-3	immunoglobulin heavy variable 2-3	19.4	0	19.4*	0.002	ENSMUSG00000079017

Table 7.5 The significant genes (FDR of <0.05) downregulated in congenitally infected mice brain with *T. gondii*.

Gene	Description	Average FPKM		Fold Change	FDR	Ensembl ID
		Inf (n=3)	Ctr (n=3)			
Grm4	glutamate receptor, metabotropic 4	26.7	36.6	0.7	0.017	ENSMUSG00000063239
Cbln1	neuronal regeneration related protein	49.5	70.2	0.7	0.030	ENSMUSG00000031654
Nrep	neuronal regeneration related protein	64.5	95.3	0.7	0.002	ENSMUSG00000042834
Gm37917	predicted gene, 37917	48.1	71.2	0.7	0.019	ENSMUSG00000103276
Enpp2	ectonucleotide pyrophosphatase/ phosphodiesterase 2	97.0	145.0	0.7	0.002	ENSMUSG00000022425
Lamp5	lysosomal-associated membrane protein family, member 5	36.3	55.2	0.7	0.002	ENSMUSG00000027270
Gm28925	predicted gene 28925	65274.0	100418.0	0.7	0.004	ENSMUSG00000099383
Ipcef1	interaction protein for cytohesin exchange factors 1	9.4	12.6	0.7	0.042	ENSMUSG00000064065
Serpinb1a	serine (or cysteine) peptidase inhibitor, clade B, member 1a	8.9	13.0	0.7	0.025	ENSMUSG00000044734
Eomes	Eomesodermin	3.1	4.8	0.7	0.027	ENSMUSG00000032446
Glra1	glycine receptor, alpha 1 subunit	5.8	9.0	0.6	0.010	ENSMUSG00000000263
Kl	Klotho	3.5	5.5	0.6	0.002	ENSMUSG00000058488
Bche	butyrylcholinesterase	0.6	1.0	0.6	0.029	ENSMUSG00000027792
Slc4a5	solute carrier family 4, sodium bicarbonate cotransporter, member 5	0.7	1.2	0.6	0.021	ENSMUSG00000068323
Sostdc1	sclerostin domain containing 1	5.2	8.8	0.6	0.004	ENSMUSG00000036169
Fat2	FAT atypical cadherin 2	2.5	4.3	0.6	0.002	ENSMUSG00000055333
Dao	D-amino acid oxidase	3.2	5.4	0.6	0.008	ENSMUSG00000042096
Sp8	trans-acting transcription factor 8	1.0	1.8	0.6	0.006	ENSMUSG00000048562
Bbox1	butyrobetaine (gamma), 2-oxoglutarate dioxygenase 1 (gamma-butyrobetaine hydroxylase)	1.6	2.8	0.6	0.006	ENSMUSG00000041660
F5	coagulation factor V	0.5	0.9	0.6	0.019	ENSMUSG00000026579
Prokr2	prokineticin receptor 2	0.5	0.9	0.6	0.022	ENSMUSG00000050558
Ttr	Transthyretin	419.1	765.1	0.5	0.002	ENSMUSG00000061808
Mybpc1	myosin binding protein C, slow-type	3.0	5.4	0.5	0.002	ENSMUSG00000020061

Folr1	folate receptor 1 (adult)	4.3	7.9	0.5	0.004	ENSMUSG00000001827
Pax2	paired box 2	0.6	1.2	0.5	0.004	ENSMUSG00000004231
Haus3	HAUS augmin-like complex, subunit 3	2.9	5.7	0.5	0.008	ENSMUSG00000079555
Poln	DNA polymerase N	2.9	5.7	0.5	0.008	ENSMUSG00000045102
Slc6a5	solute carrier family 6 (neurotransmitter transporter, glycine), member 5	5.6	11.1	0.5	0.002	ENSMUSG00000039728
1500015O10Rik	RIKEN cDNA 1500015O10 gene	6.0	11.9	0.5	0.002	ENSMUSG00000026051
Gkn3	gastrokine 3	2.6	5.1	0.5	0.006	ENSMUSG00000030048
Col2a1	collagen, type II, alpha 1	0.3	0.5	0.5	0.012	ENSMUSG00000022483
Scgn	secretagogin, EF-hand calcium binding protein	0.8	1.8	0.5	0.025	ENSMUSG00000021337
Rln3	relaxin 3	2.0	4.3	0.5	0.004	ENSMUSG00000045232
Hoxc4	homeobox C4	0.8	1.7	0.5	0.043	ENSMUSG00000075394
Hoxb2	homeobox B2	0.7	1.6	0.4	0.024	ENSMUSG00000075588
Hoxd3	homeobox D3	0.7	1.6	0.4	0.010	ENSMUSG00000079277
Hoxd4	homeobox D4	0.7	1.6	0.4	0.010	ENSMUSG00000101174
Kcne2	potassium voltage-gated channel, Isk-related subfamily, gene 2	1.6	3.9	0.4	0.002	ENSMUSG00000039672
Hoxb3os	homeobox B3 and homeobox B2, opposite strand	0.7	1.8	0.4	0.024	ENSMUSG00000084844
Tmem72	transmembrane protein 72	0.3	0.8	0.4	0.045	ENSMUSG00000048108
Hoxa4	homeobox A4	0.4	1.0	0.4	0.014	ENSMUSG00000000942
Hoxa5	homeobox A5	0.6	1.6	0.4	0.002	ENSMUSG00000038253
Hoxb5	homeobox B5	1.1	3.4	0.3	0.002	ENSMUSG00000038700
Mpz	myelin protein zero	0.3	1.1	0.3	0.010	ENSMUSG00000056569
Fcrls	Fc receptor-like S, scavenger receptor	0.4	1.8	0.2	0.002	ENSMUSG00000015852
Tmem63a	transmembrane protein 63a	0.0	59.5	59.5*	0.002	ENSMUSG00000026519
Stard13	StAR-related lipid transfer (START) domain containing 13	0.0	52.6	52.6*	0.004	ENSMUSG00000016128
Lsamp	limbic system-associated membrane protein	0.0	20.9	20.9*	0.002	ENSMUSG00000061080
Plekhs1	pleckstrin homology domain containing, family S member 1	0.0	15.4	15.4*	0.002	ENSMUSG00000035818
Col15a1	collagen, type XV, alpha 1	0.0	8.4	8.4*	0.021	ENSMUSG00000028339
Hoxb3os	homeobox B3 and homeobox B2, opposite strand	0.0	4.9	4.9*	0.010	ENSMUSG00000084844

Gm44398	predicted gene, 34933	0.0	2.3	2.3*	0.004	ENSMUSG00000107714
Gpr35	G protein-coupled receptor 35	0.0	1.9	1.9*	0.014	ENSMUSG00000026271
Gm12439	predicted gene 12439	0.0	1.5	1.5*	0.002	ENSMUSG00000080850
Lipf	lipase, gastric	0.0	1.4	1.4*	0.008	ENSMUSG00000107714
Gm44398	predicted gene, 34933	0.0	1.4	1.4*	0.002	ENSMUSG00000107714
Kmo	kynurenine 3-monooxygenase	0.0	0.9	0.9*	0.002	ENSMUSG00000039783
Bpifb1	BPI fold containing family B, member 1	0.0	0.8	0.8*	0.002	ENSMUSG00000027485

Table 7.6. All significant genes (FDR of <0.05) upregulated in congenitally exposed uninfected with *T. gondii*.

Gene	Description	Average FPKM		Fold change (Uninf vs CTR)	FDR	Ensembl ID
		Uninfected (n=3)	Control (n=3)			
Rpe65	retinal pigment epithelium 65	20.3	0.0	20.3	0.048	ENSMUSG00000028174
Gm16011	predicted gene 16011	7.7	0.0	7.7	0.048	ENSMUSG00000081303
Zcchc8	zinc finger, CCHC domain containing 8	4.9	0.0	4.9	0.030	ENSMUSG00000029427
Gm6728	predicted gene 6728	4.6	0.0	4.6	0.030	ENSMUSG00000091408
Prl	prolactin	65.9	16.1	4.1	0.030	ENSMUSG00000021342
Oxt	oxytocin	41.7	11.1	3.8	0.030	ENSMUSG00000027301
Aloxe3	arachidonate lipoxygenase 3	5.2	1.5	3.4	0.048	ENSMUSG00000020892
Gh	growth hormone	24.2	7.8	3.1	0.030	ENSMUSG00000020713
Pomc	pro-opiomelanocortin-alpha	7.3	2.7	2.7	0.030	ENSMUSG00000020660
Cntnap5b	contactin associated protein-like 5B	2.7	1.1	2.5	0.030	ENSMUSG00000067028
Fat2	FAT atypical cadherin 2	10.7	4.3	2.5	0.030	ENSMUSG00000055333
Cntnap5b	contactin associated protein-like 5B	3.0	1.3	2.4	0.030	ENSMUSG00000067028
Gm44398	predicted gene, 34933	0.0	2.3	2.3	0.030	ENSMUSG00000107714
Cnpy1	canopy FGF signaling regulator 1	11.6	5.7	2.0	0.030	ENSMUSG00000044681
Samd4	sterile alpha motif domain containing 4	7.2	3.7	2.0	0.030	ENSMUSG00000021838
Atp2a3	ATPase, Ca++ transporting, ubiquitous	20.6	11.0	1.9	0.048	ENSMUSG00000020788
Fam107b	family with sequence similarity 107, member B	21.8	11.9	1.8	0.048	ENSMUSG00000026655
Mir124a-1hg	Mir124-1 host gene (non-protein coding)	15.7	8.7	1.8	0.030	ENSMUSG00000097545
Gm26910	predicted gene, 26910	1.7	0.0	1.7	0.030	ENSMUSG00000097835
Scn1b	sodium channel, voltage-gated, type I, beta	1.1	0.0	1.1	0.030	ENSMUSG00000019194

Table 7.7 All significant genes (FDR of <0.05) downregulated in congenitally exposed uninfected with *T. gondii*.

Gene	Description	Average FPKM		Fold change (Uninf vs CTR)	FDR	Ensembl ID
		Uninfected (n=3)	Control (n=3)			
Tmem63a	transmembrane protein 63a	0.0	60.0	60.0*	0.030	ENSMUSG00000026519
Dnah10	dynein, axonemal, heavy chain 10	0.0	1.1	1.0*	0.030	ENSMUSG00000038011
Ttr	transthyretin	401.3	770.5	0.5	0.030	ENSMUSG00000061808
Abi3bp	ABI gene family, member 3 (NESH) binding protein	1.2	2.3	0.5	0.048	ENSMUSG00000035258
Sp8	trans-acting transcription factor 8	0.7	1.8	0.4	0.030	ENSMUSG00000048562
Shisa3	shisa family member 3	0.5	1.3	0.4	0.030	ENSMUSG00000050010
Kcne2	potassium voltage-gated channel, Isk-related subfamily, gene 2	1.5	3.9	0.4	0.030	ENSMUSG00000039672
Cdhr1	cadherin-related family member 1	1.1	3.4	0.3	0.030	ENSMUSG00000021803
Scgn	secretagogin, EF-hand calcium binding protein	0.5	1.8	0.3	0.048	ENSMUSG00000021337
Igkc	immunoglobulin kappa constant	1.0	4.2	0.2	0.030	ENSMUSG00000076609
Igha	immunoglobulin heavy constant alpha	0.3	1.7	0.2	0.030	ENSMUSG00000095079
Ccdc62	coiled-coil domain containing 62	3.6	0.0	3.6*	0.030	ENSMUSG00000061882
Denr	density-regulated protein	3.6	0.0	3.6*	0.030	ENSMUSG00000023106
Gm44257	predicted gene, 44257	2.5	0.0	2.5*	0.030	ENSMUSG00000107815
Clcn1	chloride channel, voltage-sensitive 1	2.0	0.0	2.0*	0.048	ENSMUSG00000029862
Prrg4	proline rich Gla (G-carboxyglutamic acid) 4 (transmembrane)	1.1	0.0	1.0*	0.030	ENSMUSG00000027171
1810010D01Rik	RIKEN cDNA 1810010D01 gene	0.8	0.0	0.8*	0.030	ENSMUSG00000109305
E230016M11Rik	RIKEN cDNA E230016M11 gene	0.7	0.0	0.7*	0.030	ENSMUSG00000087231

7.2.3 Human - Mouse: Disease Connection

Genes that were differentially expressed in congenitally infected mice brains detected in this study were uploaded to the MGI for particular analysis to determine possible connections between our data and the literature in term of phenotypes and diseases. The sources of human gene to disease annotations are from NCBI and OMIM. Human phenotype to disease annotations are from HPO. Mouse gene to disease and gene to phenotype annotations are from MGI.

In this study, 535 genes were associated with 63 diseases and phenotypes. However, filters were applied to detect genes associated with behaviour, neurological changes, nervous system diseases and diseases of mental health as this is the aim of the study. These genes which associated with human disease are illustrated in the Table 7.8.

Table 7.8 Human - Mouse genes in congenital infected mice brain connected with nervous system diseases.

	Organism	Gene Symbol	ID	Associated Human Diseases	Abnormal Mouse Phenotypes
1	Mouse Human	Hcrt	MGI:1202306	narcolepsy	behaviour/neurological nervous system
2	Mouse Human	Cd86	MGI:101773	Guillain-Barre syndrome	behaviour/neurological nervous system
3	Mouse Human	Grn	MGI:95832	Grn-related frontotemporal lobar degeneration with Tdp43 inclusions nephrogenic diabetes insipidus	behaviour/neurological mortality/aging nervous system/ vision/eye
4	Mouse Human	Trem2	MGI:1913150	frontotemporal dementia	nervous system
5	Mouse Human	C1qa	MGI:88223	epilepsy systemic lupus erythematosus	behaviour/neurological aging / nervous system
6	Mouse Human	Ctss	MGI:107341	Duchenne muscular dystrophy	behaviour/neurological
7	Human Mouse	PIK3R5	23533	ataxia with oculomotor apraxia type 3	Immune system
8	Mouse Human	Cx3cr1	MGI:1333815	age related macular degeneration 12	behaviour/neurological nervous system/vision/eye
9	Human Mouse	ALOX5AP	241	cerebral infarction	Homeostasis/Metabolism
10	Mouse	Drd2	MGI:94924	Parkinson's disease	behaviour/neurological

Genes that were significantly expressed in maternally exposed uninfected mice brains detected in this study were uploaded to the MGI and table 7.9 generated.

Table 7.9 Human - Mouse genes in maternity exposed uninfected mice brain connected with nervous system diseases.

	Organism	Gene Symbol	ID	Associated Human Diseases	Abnormal Mouse Phenotypes
1	Mouse Human	Scn1b	MGI:98247	early infantile epileptic encephalopathy generalized epilepsy with febrile seizures plus	behaviour/neurological nervous system
2	Mouse Human	Clcn1	MGI:88417	myotonia congenita	behaviour/neurological nervous system
3	Human	FAT2	2196	spinocerebellar ataxia 45	
4	Mouse	Oxt	MGI:97453		behaviour/neurological nervous system
5	Mouse	Prl	MGI:97762		behaviour/neurological nervous system
6	Mouse	Denr	MGI:1915434		behaviour/neurological nervous system

7.2.4 Transcriptomics variations in pathways of mice brain congenitally infected with *T. gondii* maternally exposed to the infection.

7.2.4.1 Purine degradation pathway.

Transcripts for one gene in the purine degradation pathway, xanthine dehydrogenase (XDH) was found to be significantly upregulated ($p = 0.002$) in the brains of congenitally infected mice relative to non-infected control mice.

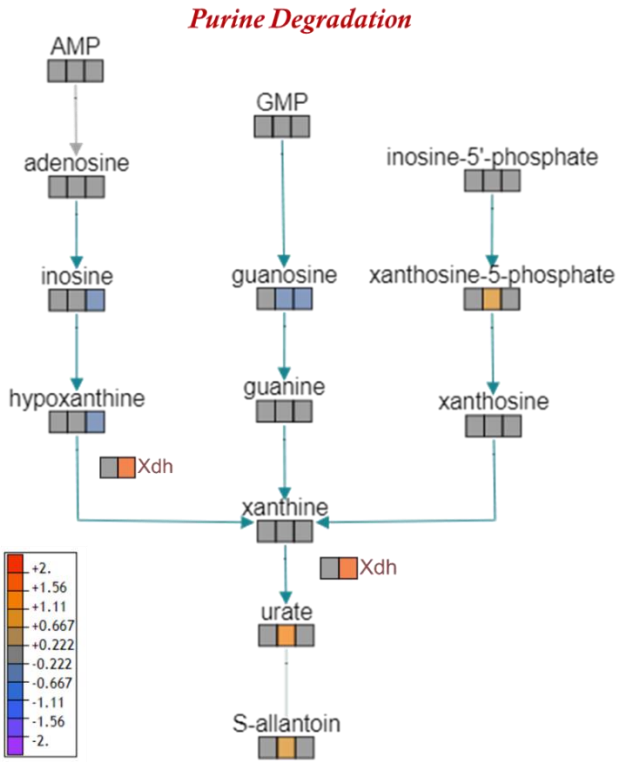

Figure 7.3 Purine degradation pathway. Metabolites which were detected in this pathway are represented by three squares. First square represents control group, second square represents congenitally infected group, and third square represents congenitally uninfected group (log 2 transformed) are visulaised as a color spectrum scaled from least abundant to highest range is from -2 to 2. Purple indicates low expression, while red indicates high expression of the changed metabolites. In congenitally infected group, p value of xanthosine-5-phosphate, urate and allantoin are 0.002, 0.00002, and 0.0002 respectively. The p-value of Xdh (xanthine dehydrogenase) is 0.002. In congenitally uninfected group, p value of adenosine, inosine, hypoxanthine, xanthine, and guanosine are 0.028, 0.039, 0.021, 0.025, and 0.038 respectively.

7.2.4.2 Tryptophan degradation pathway.

Transcripts for three genes in the tryptophan degradation pathway, indoleamine 2, 3-dioxygenase 1 (IDO1), arylformamidase (Afmid) and kynurenine 3-monooxygenase (kmo) were found to be significantly upregulated ($p = 0.002$, 0.002 and 0.0023 respectively) in the brains of congenitally infected mice relative to non-infected control mouse brains.

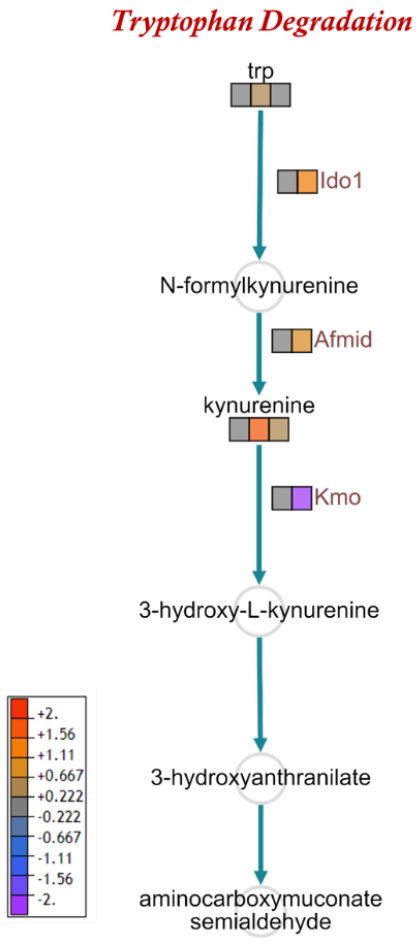

Figure 7.4 Tryptophan degradation pathway. Tryptophan Degradation Pathway. Metabolites which were detected in this pathway are represented by three squares. First square represents control group, second square represents congenitally infected group, and third square represents congenitally uninfected group (log 2 transformed) are visulaised as a color spectrum scaled from least abundant to highest range is from -2 to 2. Purple indicates low expression, while red indicates high expression of the changed metabolites. In congenitally infected group, p value of Kynurenine is 0.008. P-values of IDO1 (indoleamine 2, 3-dioxygenase 1), Afmid (arylformamidase), and kmo (kynurenine 3-monooxygenase) are 0.002, 0.002 and 0.0023. In congenitally uninfected group, p value of Kynurenine is 0.015.

7.2.4.3 Urea Cycle pathway.

Transcripts of arginase 1 (Arg1) was found to be significantly upregulated (p = 0.0023) in the brains of congenitally infected mice relative to non-infected control mouse brains.

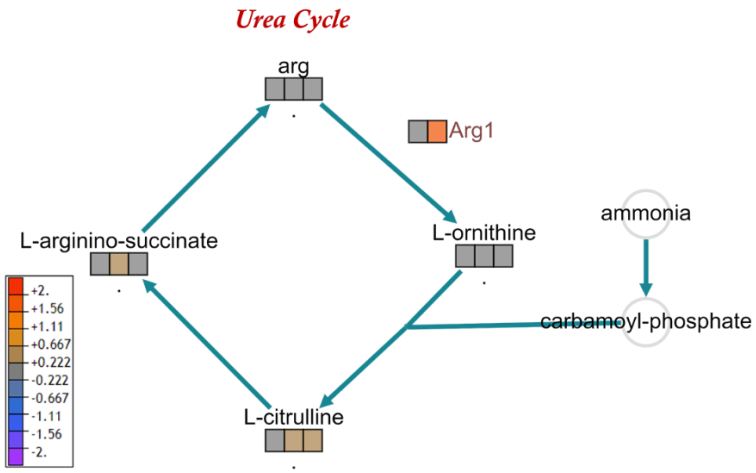

Figure 7.5 Urea cycle pathway. Metabolites which were detected in this pathway are represented by three squares. First square represents control group, second square represents congenitally infected group, and third square represents congenitally uninfected group (log 2 transformed) are visulaised as a color spectrum scaled from least abundant to highest range is from -2 to 2. Purple indicates low expression, while red indicates high expression of the changed metabolites. In congenitally infected mice group, P-value of Arg1 (arginase 1) is 0.0023.

7.2.4.4 Cyclic AMP biosynthesis and Pyrimidine ribonucleosides degradation.

Transcripts for 4 genes in the pyrimidine ribonucleosides degradation pathway, Apobec1 (apolipoprotein B mRNA editing enzyme, catalytic polypeptide 1), Gna15 (guanine nucleotide binding protein, alpha 15), Adap2 (ArfGAP with dual PH domains 2) and Arhgap 9 (Rho GTPase activating protein 9) were found to be significantly upregulated ($p= 0.002, 0.002, 0.002, 0.002$ and 0.004 respectively) in the brains of congenitally infected mice relative to non-infected control mouse brains.

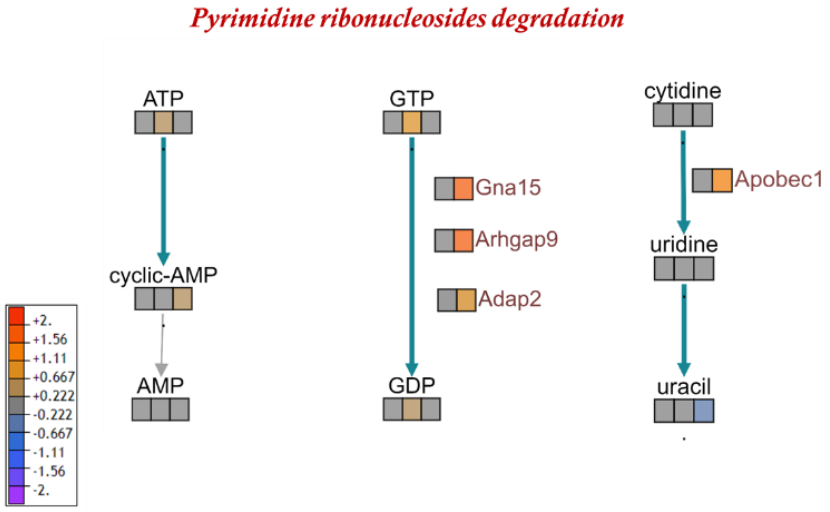

Figure 7.6 Cyclic AMP biosynthesis and Pyrimidine ribonucleosides degradation. Metabolites which were detected in this pathway are represented by three squares. First square represents control group, second square represents congenitally infected group, and third square represents congenitally uninfected group (log 2 transformed) are visulaised as a color spectrum scaled from least abundant to highest range is from -2 to 2. Purple indicates low expression, while red indicates high expression of the changed metabolites. In congenitally infected group, p value of GTP and GDP are 0.03 and 0.01. P-values of Apobec1 (apolipoprotein B mRNA editing enzyme, catalytic polypeptide 1) Gna15 (guanine nucleotide binding protein, alpha 15), Adap2 (ArfGAP with dual PH domains 2) and Arhgap 9 (Rho GTPase activating protein 9) are 0.002, 0.002, 0.002 and 0.002 respectively. In congenitally uninfected group, p value of Uracil is 0.009.

7.3 Conclusion

The transcriptomics studies performed in this chapter successfully identified transcripts that are upregulated in congenitally infected mice and their non-infected littermates that were exposed to the maternal infection. These are discussed in conjunction with the metabolomic data obtained in chapter 6 of this thesis in the following chapter.

8 Discussion of metabolomic and transcriptomic changes in the brains of mice congenitally infected with *T. gondii.*

8.1 The effect of congenital *T. gondii* and exposure to maternal *T. gondii* infection on brain metabolites and transcripts

To determine the ability of *T. gondii* congenital infection or maternal exposure to *T. gondii* to affect brain metabolism and neurochemistry LCMS and RNAseq were used in a similar fashion as described for the adult infection studies in chapters 3 and 4 of this thesis. The results demonstrate that there is significant alteration in metabolomic and transcriptomic profiles between the congenitally infected mice and control non-infected mice. These data also allow comparison of the effects of congenital infection with the effects of adult infection with *T. gondii*. In the congenital experiment, it is noticeable that the brains show global changes to metabolites and transcripts involving multiple biochemical pathways.

8.1.1 Purine Metabolites

As reported for adult mice in the previous chapters differences were observed in purine metabolism in congenitally infected mice. In particular, levels of xanthosine-5-phosphate, urate and allantoin were found to be higher in the congenitally infected brain samples by compared to controls. In contrast, levels of adenosine were found to be higher and inosine, hypoxanthine, xanthine and guanosine were found to be lower in uninfected mice exposed to a maternal infection. In keeping with these changes in purine metabolism detected by LCMS in congenitally infected mice, transcripts for XO/Xdh involved in purine metabolism was also found to be altered following congenital infection. Xanthine dehydrogenase and xanthine oxidase are the product of a single gene, the specific activity of which can be altered reversibly by sulfhydryl oxidation or by irreversible proteolytic

modification. However, the presence of increased levels of urate and allantoin suggests that this gene product is functioning as the dehydrogenase. XO/Xdh might play pathophysiological roles through generation of ROS (Honorat et al., 2013). This could have important implications as elevated oxidative stress which is suggested to be a risk factor in etiology of neurodegenerative diseases. As reported in the previous chapters for adult infected mice, transcripts for P2ry6 were raised in congenitally infected mice brain compared to uninfected litter mates and control mice.

8.1.2 Tryptophan and kynurenine pathways

As discussed previously, in the context of adult acquired infection, dysregulation or over activation of kynurenine pathway can lead to immune activation and accumulation of potentially neurotoxic metabolites. Kynurenine levels were increased in the brains of congenitally infected and also in the brains of their uninfected litter mates compared with control uninfected mice. In addition, kynurenine upregulation in the brains of uninfected mice exposed to a maternal infection in utero demonstrates a long-lasting effect of maternal immune activation on offspring. The kynurenine pathway is initiated by IDO and TDO enzymes which are stimulated by inflammatory cytokines and IFN-γ and converted tryptophan to formyl kynurenine. Transcripts for IDO1 were increased in the brains of congenitally infected mice compared with control mice. Transcripts for Afmid the enzyme responsible for the conversion of formyl kynurenine to kynurenine were also increased in the brains of congenitally infected mice brain compared with uninfected litter

mates and control mice. In contrast, transcripts for kynurenine 3-monooxygenase (KMO) were decreased in congenitally infected mice compared to the other two groups. In schizophrenia, there is a persistent reduction of microglial kynurenine 3-monooxygenase activity, along with increased L-kynurenine influx from the circulation. This results in increased kynurenic acid formation in astrocytes which leads to inhibition of α-7 nicotinic (α7nAch) and the N-methyl-D-aspartate (NMDA) receptors which leads to cognitive impairments (Schwarcz and Stone, 2017). The results suggest that the immune response to *T. gondii* alters tryptophan metabolism and could be a risk factor in the etiology of neurodegenerative diseases. See also additional discussion points in chapter 5.

8.1.3 Dopamine, arginine and other pathways

Dopamine levels were decreased in the brains of congenitally infected mice as reported for mice with adult acquired infection. Consistent with this L-tyrosine and phenylalanine, the precursors for dopamine were increased in the brains of congenitally infected mice. Whether these alterations were directly contributed to *T. gondii* infection in the brain or as are as a result of complex neuro-immunological interactions is not known. None of the transcripts associated with dopamine biosynthesis were significantly affected by infection.

In the brains from congenitally infected mice, S-Adenosyl-L-methioninamine and L-Cysteine levels were decreased while proline, Glutathione disulfide and L-cystathionine levels were increased compared with control mice. In the brains of mice exposed to maternal infection but uninfected, L-Cysteine levels were decreased relative to the control mice. Changes to the levels of cysteine and methionine metabolism could reflect the defense mechanism of the host against the infection and could impact oxidative stress levels in the brains of these mice (Klein Geltink and Pearce, 2019).

8.1.4 Glycolysis, phospholipid biosynthesis and L-carnitine biosynthesis

Significant alterations of carnitines and phospholipids indicate variation of fatty acid oxidation and changes to energy metabolism. Previous studies have demonstrated that *T. gondii* infection alters the metabolism of dendritic cells resulting in oxidative glycolysis (Hargrave et al., 2019). In this experiment, L-carnitine and its derivatives, 4-Trimethylammoniobutanoate, Hydroxybutyrylcarnitine, o-Acetylcarnitine, cis-5-Tetradecenoylcarnitine, 2-Methylbutyroylcarnitine, and 0-Propanoylcarnitine were found to be increased in the brains of congenitally infected mice compared to their uninfected litter mates and control mice. Whereas, Glutarylcarnitine was found decreased in the congenitally infected mice group compared to uninfected litter mates and controls. Acetyl-carnitine regulates the activity of many mitochondrial enzymes which are involved in the citric acid cycle, gluconeogenesis, the urea cycle and the fatty acids oxidation and its acetyl groups are incorporated into brain lipid metabolism (Ricciolini et al., 1998, Steiber

et al., 2004). In addition, acetyl carnitine plays a significant role in neuroprotection and beneficial effects have been seen in major depressive disorders and Alzheimer's disease (Pettegrew et al., 2000). In addition, phosphoenolpyruvate was significantly increased in the brains of the congenitally infected mouse group compared to uninfected litter mates and control mice. These results were similar to those observed in mice with adult acquired infection.

8.1.5 Arginine and Urea Cycle pathway

Transcripts for Arginase 1 (Arg1) were upregulated in the brains of congenitally infected mice compared to control mice. As a part of the urea cycle, arginase catalyzes L-arginine to urea and L-ornithine. Ornithine is then used in polyamine biosynthesis where it is converted to putrescine, spermidine and spermine. Consistent with increase arginine degradation, levels of putrescine were higher in the brains of congenitally infected mice relative to control mice. It has been reported that arg1 has a neuroprotective role in an *in vitro* model of neuronal oxidative stress, however persistent raised arg1 could indicate prolonged immune activation and associated high levels of oxidative stress which ultimately could lead to brain dysfunction (Lange et al., 2004).

8.1.6 Enzymes involved in biological pathways and immune responses

In congenitally infected mice brains, we found Apobec1, Apobec3, Dok1, Dock2, Adp2, and gna15 were highly expressed compared to uninfected and control mice. These results are consistent with the findings in mice with adult acquired infection and indicate immune activation as discussed in chapter 5.

8.2 Transcripts associated with microglial activation are upregulated in mice congenitally infected with *T. gondii*

We found significant alterations in the transcriptome profiles of congenitally infected mice and uninfected mice exposed to maternal infection compared to their control mice. In the congenitally infected mice brain samples, the findings are consistent with an inflammatory process involving immunoglobulin and B cells and interferon gamma production. Thus, the majority of genes involved in immune responses and cell activation were highly expressed in congenitally infected mice brains compared with controls. In contrast, a number of significant genes in this study involved in other functions, such as fatty acid beta-oxidation, synaptic membrane, brain development, neuron projection development, and mitochondrial activity were low expressed. These important findings are consistent with the results obtained in the mice with adult acquired infection (Chapter 5). Changes to transcript levels for 419 genes were found to be similarly affected in mice that were congenitally infected and mice that acquired infection as adults and may assist in elucidation of the mechanism underlying neurological changes in infected hosts. Different murine experiments have demonstrated a range of similarity in gene expressions of mice brains infected with *T. gondii* (Hermes et al., 2008, Tanaka et al., 2013). Many of these genes are associated with inflammatory processes that although often necessary to control infection, can lead to microglia activation which can be considered in etiology of neuropsychiatric and mental disorders. In addition, these genes have been linked to neuropsychiatric diseases (discussed in Chapter 5).

The CNS is highly sensitive to oxidative stress because of low levels of antioxidant enzymes, but highly susceptible to oxidative stress due to its metabolic nature. In chapter 5, we discussed the role of GST enzymes in the regulation of redox homeostasis and we found reduced expression levels of these genes in infected mice. This would be consistent with oxidative stress. However, these changes were not observed in congenitally infected mice. However, the changes to purine catabolism pathway could affect redox homeostasis in congenitally infected mice as discussed above.

There is consistent epidemiological evidence connecting maternal immune activation with neurobehavioral alteration and molecular dysfunction of offspring in their adulthood. The epidemiological studies have suggested maternal immune activation is a risk factor for neuropsychiatric diseases, such as schizophrenia, autism spectrum disorder, depression, and bipolar disorder (Brown and Meyer, 2018). Thus, maternal immune activation independently from the infection itself, can be responsible for adverse outcomes in offspring (Boksa, 2010, Bauman et al., 2014). Thus, gene expression profiling of mice brains from mice exposed to maternal *T. gondii* induced immune activation was investigated. In comparison to congenitally infected mice, those exposed to maternal immune activation, but uninfected has distinct, but overlapping transcriptomic profiles (Figure 8.1 and Table 8.1)

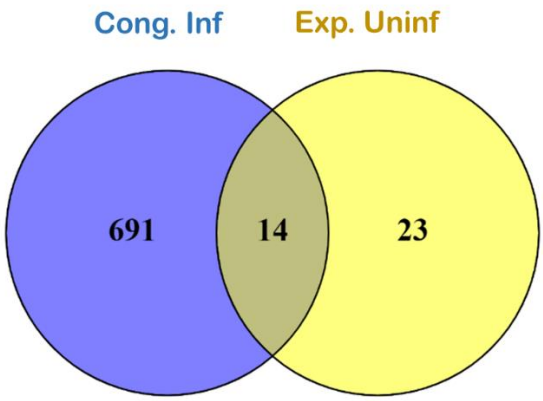

Figure 8.1 Venn diagram illustrates the number of common genes between Cong. Inf (congenitally infected group) and their Exp. Uninf (maternally exposed uninfected litter mate).

Table 8.1 Common genes between congenitally infected mice group and their maternally exposed uninfected litter mates. FC = Fold Change.

Gene Symbol	**Name**	**FC Cong.infected/CTR**	**FC Maternally exposed uninfected/CTR**
Igha	immunoglobulin heavy constant alpha	82.8	0.2
Igkc	Immunoglobulin kappa constant	80.6	0.2
Prl	Prolactin	6.5	4.1
Gh	growth hormone	5.1	3.1
Pomc	pro-opiomelanocortin-alpha	3.2	2.7
Oxt	Oxytocin	1.8	3.8
Fat2	FAT atypical cadherin 2	0.6	2.5
Sp8	trans-acting transcription factor 8	0.6	0.4
Ttr	Transthyretin	0.5	0.5
Scgn	secretagogin, EF-hand calcium binding protein	0.5	0.3
Kcne2	potassium voltage-gated channel, Isk-related subfamily, gene 2	0.4	0.4
Tmem63a	transmembrane protein 63a	59.5	60
Gm44398	predicted gene, 34933	2.3	2.3
Gm44257	predicted gene, 44257	1.3	2.5

A number of transcripts that were altered in the brains of uninfected mice born to mothers infected with *T. gondii* are involved in a number of pathways, such as Neuroactive ligand-receptor interaction, cAMP signaling pathway, Jak-STAT signaling pathway and Cytokine-cytokine receptor interaction. It has been reported that neuroactive ligand-receptor interaction pathway is associated with AD (Yan et al., 2019). Furthermore, Jak-STAT signaling pathway is one of key regulators of pro-gliogenesis during brain development and thus alteration to this pathway may contribute in abnormal development of the brain (Lee et al., 2019). In addition, three genes (Oxt, Scn1b and Kcne2) involved in the regulation of homeostatic processes were affected. Alteration of expression levels of these genes may indicate a response to infection to maintain homeostasis and reduce oxidative stress. These results demonstrate alteration to pathways as a result of maternal immune activation.

9 Comparison between the effects of adult acquired infection, congenital infection and maternal exposure to *T. gondii* infection during prenatal period.

In this comparison, only the significant metabolites, that were detected according to VIP score or p value ≤0.05 (as tabulated in the third and sixth chapters), were used to find the overlap between the three groups (Figure 9.1).

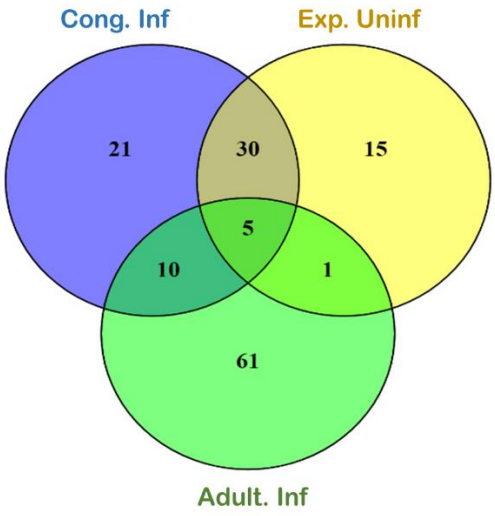

Figure 9.1 Venn diagram showing the overlap of significant metabolites detected by VIP score between three groups of two experiments. Cong.inf = congenitally infected mice group, Exp. uninf= maternally exposed uninfected litter mates, Adult.inf = adult mice brain sample infected with *T.gondii.*

Metabolomics studies

Metabolomic profiles of the experimental brain samples from adult acquired chronic infection, congenital infection and the maternally exposed uninfected litter mates, indicates important alterations present compared to their controls (Table 9.1).

Table 9.1 Significant metabolites in the metabolomics brain profiling of the three experimental groups: FC = Fold change, Cong.inf = congenitally infected mice group, Exp. uninf= maternally exposed uninfected litter mates, Adult.inf = adult mice brain sample infected with *T.gondii* compared to their controls groups.

FORMULA	Identification	FC (Cong.INF/CTR)	FC (Exp.Uninf/CTR)	FC (Adult inf/CTR)	p-value: Cong. Inf	p-value: Cong.uninf	p-value: adult inf
C10H12N2O3	**L-Kynurenine**	**2.14**	**1.54**	**4.07**	4E-03	2E-02	7E-06
C5H4N4O3	**Urate**	**2.36**	0.87	**3.24**	2E-05	5E-01	8E-05
C12H23NO4	2-Methylbutyroylcarnitine	**1.62**	1.04	**2.39**	2E-04	7E-01	3E-05
C4H12N2	Putrescine	0.87	**0.7**	**2.19**	5E-01	1E-02	1E-04
C9H15N3O2S	Ergothioneine	**1.47**	1.14	**2.16**	5E-04	2E-01	5E-04
C8H17NO6	N-acetyl -D-glucosaminitol	**1.37**	0.92	**2.1**	6E-04	4E-01	6E-05
C7H15NO3	L-Carnitine	**1.32**	0.97	**2.05**	4E-04	6E-01	3E-05
C9H17NO4	**O-Acetylcarnitine**	**1.48**	0.99	**1.87**	2E-03	9E-01	6E-05
C4H6N4O3	**Allantoin**	**1.63**	1	**1.85**	2E-04	1E+00	8E-05
C10H19NO4	O-Propanoylcarnitine	**1.63**	1.14	**1.71**	1E-04	3E-01	4E-05
C7H13NO3	5-Acetamidopentanoate	**1.5**	1	**1.52**	4E-03	1E+00	8E-04
C3H5O6P	**Phosphoenolpyruvate**	**1.6**	1.09	**1.38**	3E-02	7E-01	1E-02
C4H4N2O2	**Uracil**	1.13	**0.84**	**1.33**	7E-02	9E-03	1E-02
C10H13N5O5	Guanosine	**0.75**	**0.84**	1.23	1E-02	4E-02	4E-01
C11H15N5O3S	5'-Methylthioadenosine	1.25	0.94	1.12	1E-01	7E-01	6E-01
C20H32N6O12S2	**Glutathione disulfide**	**1.52**	1.22	0.73	1E-02	3E-01	2E-01

A number of pathways are affected in the brain of all experimental groups and there is clear similarity between adult acquired chronic infection brain samples and congenital infection brain samples. This is an indication of the ability of the *T. gondii* parasite, which is transmitted at different time points (prenatal or postnatal) during life, to change the biological pathways of its host. For instance, kynurenine metabolites in kynurenine pathway was significantly increased in all experimental groups which is a likely result IFNγ produced as part of the immune response and maternal immune activation, as discussed above increased kynurenine may lead to accumulation of kynurenic acid that leads to inhibition of α7nAch and NMDA receptors which leads to cognitive impairments. Other examples, include the purine catabolism pathway and the L-carnitine pathway which were affected in both adult acquired chronic infection brain samples and congenital infection brain samples. Purine metabolism is involved in the upregulation of inflammatory responses during brain infection and this catabolism could also be explained as immune response to *T. gondii* which promotes antioxidant defense system by producing uric acid and/or associated with stimulation of adenosine deaminase. In addition, acetyl carnitine plays a significant role in neuroprotection and has been noted to have beneficial effects in major depressive disorders and Alzheimer's disease (Pettegrew et al., 2000). Thus, the metabolic and immune environment of the infected brain samples have been directly or/and indirectly affected by the presence of the *T. gondii.*

Overall, *T. gondii* infection can lead to chronic inflammation which is a component of many psychoneurological disease. This inflammation can disrupt brain homeostasis as observed in numerous other neurological diseases. Although each neurological disease has unique malfunctions, they all share components of inflammation, microglia activation, the release of pro-inflammatory cytokines, such as TNF-α, IL-1β, and IL-6, and increased oxidative stress or decreased antioxidant process. Our data support the hypothesis that *T. gondii* induces microglia dysfunction which is an important contributing factor in neurodegenerative disease and brain disorders. These changes could be a result of the presence of the *T. gondii* parasites within neurons and potentially occasional cyst rupture induced immune responses. Our finding has been illustrated in Figures 9.2 and 9.3. These unifying principles could apply to both adult and congenitally acquired *T. gondii* infection.

An additional important finding is that *T. gondii* induced maternal immune activation has the ability to alter the gene transcription and metabolism/neurochemistry of the brains of offspring. The mechanism responsible for this remains to be determined, but epigenetic changes induced by maternal immune activation are one likely possibility. Another outstanding question is to what extent are similar changes observed in humans and if so how do they affect the likelihood of developing psychoneurological diseases.

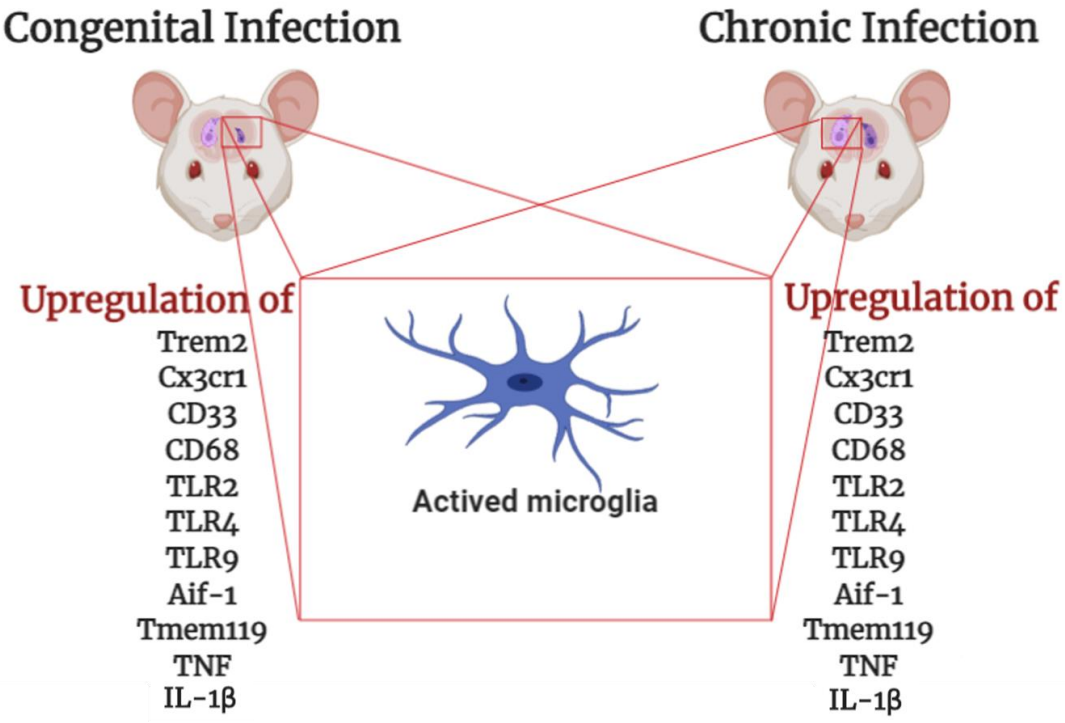

Figure 9.2 *T. gondii* parasite in congenital and/or chronic infection lead to high expressions of the same genes which associated with microglia activation.

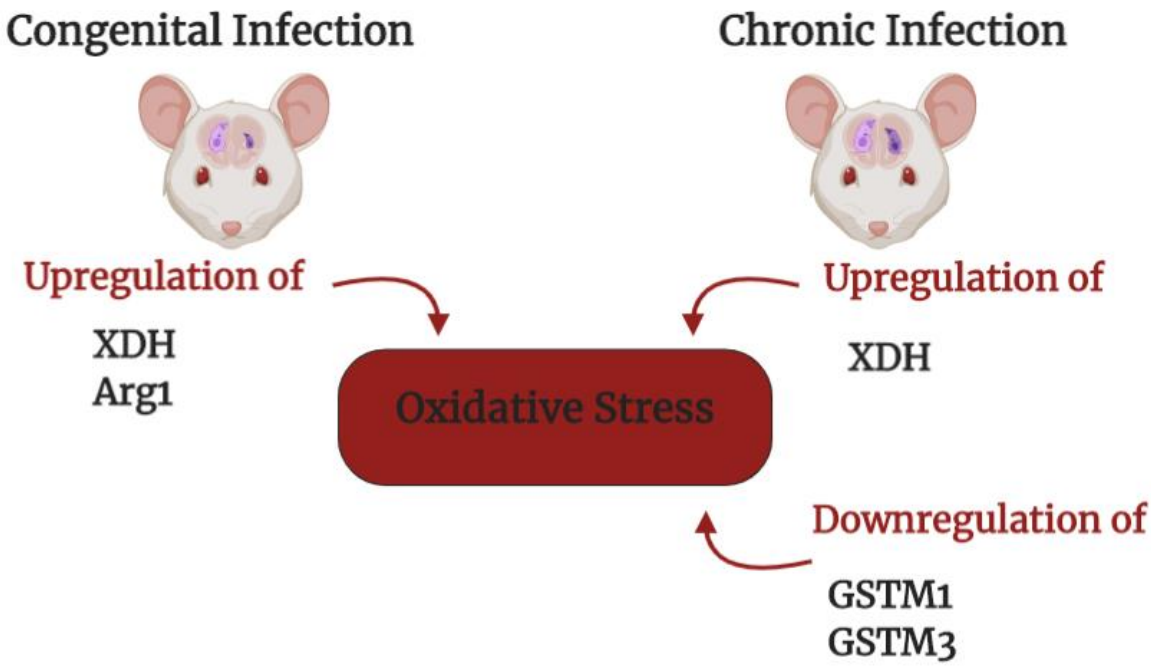

Figure 9.3 *T. gondii* parasite in congenital and/or chronic infection lead to alteration in some genes that may induce oxidative stress.

Future Work

Further work is required to confirm the effect of *T. gondii* on specific metabolic pathways and transcripts using BV-2 microglial cells which are used as a model of neuroinflammation. In addition, work on human samples to find the similarity between our murine experiments and chronic or congenital human infection.

References

ADAMO, S. A. 2013. Parasites: evolution's neurobiologists. *J Exp Biol,* 216**,** 3-10.

AFONSO, C., PAIXÃO, V. B. & COSTA, R. M. 2012. Chronic toxoplasma infection modifies the structure and the risk of host behavior. *PLoS ONE,* 7.

AJIOKA, J. W. & MORRISSETTE, N. S. 2009. A century of Toxoplasma research.

AJZENBERG, D. 2011. Unresolved questions about the most successful known parasite. *Expert review of anti-infective therapy,* 9**,** 169-71.

AN, X.-L., ZOU, J.-X., WU, R.-Y., YANG, Y., TAI, F.-D., ZENG, S.-Y., JIA, R., ZHANG, X., LIU, E.-Q. & BRODERS, H. 2011. Strain and sex differences in anxiety-like and social behaviors in C57BL/6J and BALB/cJ mice. *Experimental Animals,* 60**,** 111-123.

ARIAS, I., SORLOZANO, A., VILLEGAS, E., DE DIOS LUNA, J., MCKENNEY, K., CERVILLA, J., GUTIERREZ, B. & GUTIERREZ, J. 2012. Infectious agents associated with schizophrenia: a meta-analysis. *Schizophr Res,* 136**,** 128-36.

ARLING, T. A., YOLKEN, R. H., LAPIDUS, M., LANGENBERG, P., DICKERSON, F. B., ZIMMERMAN, S. A., BALIS, T., CABASSA, J. A., SCRANDIS, D. A., TONELLI, L. H. & POSTOLACHE, T. T. 2009. Toxoplasma gondii antibody titers and history of suicide attempts in patients with recurrent mood disorders. *The Journal of nervous and mental disease,* 197**,** 905-908.

ASSOSSOU, O., BESSON, F., ROUAULT, J. P., PERSAT, F., FERRANDIZ, J., MAYENÇON, M., PEYRON, F. & PICOT, S. 2004. Characterization of an excreted/secreted antigen form of 14-3-3 protein in Toxoplasma gondii tachyzoites. *FEMS Microbiology Letters,* 234**,** 19-25.

AWASTHI, A. & KUCHROO, V. K. 2009. Th17 cells: From precursors to players in inflammation and infection. *International Immunology,* 21**,** 489-498.

BARAN, H., JELLINGER, K. & DEECKE, L. 1999. Kynurenine metabolism in Alzheimer's disease. *Journal of Neural Transmission,* 106**,** 165-181.

BAUMAN, M. D., IOSIF, A. M., SMITH, S. E., BREGERE, C., AMARAL, D. G. & PATTERSON, P. H. 2014. Activation of the maternal immune system during pregnancy alters behavioral development of rhesus monkey offspring. *Biol Psychiatry,* 75**,** 332-41.

BELLI, S. I., WALLACH, M. G., LUXFORD, C., DAVIES, M. J. & SMITH, N. C. 2003. Roles of tyrosine-rich precursor glycoproteins and dityrosine- and 3,4-dihydroxyphenylalanine-mediated protein cross-linking in development of the oocyst wall in the coccidian parasite Eimeria maxima. *Eukaryotic Cell,* 2**,** 456-464.

BENNETT, M. L., BENNETT, F. C., LIDDELOW, S. A., AJAMI, B., ZAMANIAN, J. L., FERNHOFF, N. B., MULINYAWE, S. B., BOHLEN, C. J., ADIL, A., TUCKER, A., WEISSMAN, I. L., CHANG, E. F., LI, G., GRANT, G. A., HAYDEN GEPHART, M. G. & BARRES, B. A. 2016. New tools for studying microglia in the mouse and human CNS. *Proc Natl Acad Sci U S A,* 113**,** E1738-46.

BENSON, A., PIFER, R., BEHRENDT, C. L., HOOPER, L. V. & YAROVINSKY, F. 2009. Gut commensal bacteria direct a protective immune response against Toxoplasma gondii. *Cell Host Microbe,* 6**,** 187-96.

BERDOY, M., WEBSTER, J. P. & MACDONALD, D. W. 1995. Parasite-altered behaviour: is the effect of Toxoplasma gondii on Rattus norvegicus specific? *Parasitology*, 403-9.

BERDOY, M., WEBSTER, J. P. & MACDONALD, D. W. 2000. Fatal attraction in rats infected with Toxoplasma gondii. *Proceedings of the Royal Society B,* 267**,** 1591-1594.

BERENREITEROVA, M., FLEGR, J., KUBENA, A. A. & NEMEC, P. 2011. The distribution of Toxoplasma gondii cysts in the brain of a mouse with latent toxoplasmosis: implications for the behavioral manipulation hypothesis. *PLoS One,* 6**,** e28925.

BERGER, T. 2016. Immunological processes related to cognitive impairment in MS. *Acta Neurol Scand,* 134 Suppl 200**,** 34-8.

BETTELLI, E., CARRIER, Y., GAO, W., KORN, T., STROM, T. B., OUKKA, M., WEINER, H. L. & KUCHROO, V. K. 2006. Reciprocal developmental pathways for the generation of pathogenic effector TH17 and regulatory T cells. *Nature,* 441**,** 235-8.

BETTELLI, E., KORN, T. & KUCHROO, V. K. 2007. Th17: the third member of the effector T cell trilogy. *Curr Opin Immunol,* 19**,** 652-7.

BEZERRA, E. C. M., DOS SANTOS, S. V., DOS SANTOS, T. C. C., DE ANDRADE, H. F. J. & MEIRELES, L. R. 2019. Behavioral evaluation of BALB/c (Mus musculus) mice infected with genetically distinct strains of Toxoplasma gondii. *Microb Pathog,* 126**,** 279-286.

BIST, P., KIM, S. S., PULLOOR, N. K., MCCAFFREY, K., NAIR, S. K., LIU, Y., LIN, R. & KRISHNAN, M. N. 2017. ArfGAP Domain-Containing Protein 2 (ADAP2) Integrates Upstream and Downstream Modules of RIG-I Signaling and Facilitates Type I Interferon Production. *Mol Cell Biol,* 37.

BLAKE, J. A., EPPIG, J. T., RICHARDSON, J. E. & DAVISSON, M. T. 2000. The Mouse Genome Database (MGD): expanding genetic and genomic resources for the laboratory mouse. The Mouse Genome Database Group. *Nucleic Acids Res,* 28**,** 108-11.

BLISS, S. K., ZHANG, Y. & DENKERS, E. Y. 1999. Murine neutrophil stimulation by Toxoplasma gondii antigen drives high level production of IFN-gamma-independent IL-12. *Journal of immunology (Baltimore, Md. : 1950),* 163**,** 2081-8.

BLOMSTROM, A., GARDNER, R. M., DALMAN, C., YOLKEN, R. H. & KARLSSON, H. 2015. Influence of maternal infections on neonatal acute phase proteins and their interaction in the development of non-affective psychosis. *Transl Psychiatry,* 5**,** e502.

BLOMSTROM, A., KARLSSON, H., GARDNER, R., JORGENSEN, L., MAGNUSSON, C. & DALMAN, C. 2016. Associations Between Maternal Infection During Pregnancy, Childhood Infections, and the Risk of Subsequent Psychotic Disorder--A Swedish Cohort Study of Nearly 2 Million Individuals. *Schizophr Bull,* 42**,** 125-33.

BOKSA, P. 2010. Effects of prenatal infection on brain development and behavior: a review of findings from animal models. *Brain Behav Immun,* 24**,** 881-97.

BOSKOVIC, M., VOVK, T., KORES PLESNICAR, B. & GRABNAR, I. 2011. Oxidative stress in schizophrenia. *Curr Neuropharmacol,* 9**,** 301-12.

BRESSAN, R. A. & CRIPPA, J. A. 2005. The role of dopamine in reward and pleasure behaviour--review of data from preclinical research. *Acta Psychiatrica Scandinavica. Supplementum,* 111**,** 14-21.

BROWN, A. S. & MEYER, U. 2018. Maternal Immune Activation and Neuropsychiatric Illness: A Translational Research Perspective. *Am J Psychiatry,* 175**,** 1073-1083.

BROWN, A. S., SCHAEFER, C. A., QUESENBERRY, C. P., LIU, L., BABULAS, V. P. & SUSSER, E. S. 2005. Maternal exposure to toxoplasmosis and risk of schizophrenia in adult offspring. *American Journal of Psychiatry,* 162**,** 767-773.

BUKA, S. L. 2001. Maternal Infections and Subsequent Psychosis Among Offspring. *Archives of General Psychiatry,* 58**,** 1032-1037.

BURGDORF, K. S., TRABJERG, B. B., PEDERSEN, M. G., NISSEN, J., BANASIK, K., PEDERSEN, O. B., SORENSEN, E., NIELSEN, K. R., LARSEN, M. H., ERIKSTRUP, C., BRUUN-RASMUSSEN, P., WESTERGAARD, D., THORNER, L. W., HJALGRIM, H., PAARUP, H. M., BRUNAK, S., PEDERSEN, C. B., TORREY, E. F., WERGE, T., MORTENSEN, P. B., YOLKEN, R. H. & ULLUM, H. 2019. Large-scale study of Toxoplasma and Cytomegalovirus shows an association between infection and serious psychiatric disorders. *Brain Behav Immun,* 79**,** 152-158.

BURNSTOCK, G., KRÜGEL, U., ABBRACCHIO, M. P. & ILLES, P. 2011. Purinergic signalling: From normal behaviour to pathological brain function.

BUTCHER, B. A., GREENE, R. I., HENRY, S. C., ANNECHARICO, K. L., WEINBERG, J. B., ERIC, Y., SHER, A., TAYLOR, G. A. & DENKERS, E. Y. 2005. p47 GTPases Regulate Toxoplasma gondii Survival in Activated Macrophages p47 GTPases Regulate Toxoplasma gondii Survival in Activated Macrophages. *Society,* 73**,** 3278-3286.

CAI, H. L., LI, H. D., YAN, X. Z., SUN, B., ZHANG, Q., YAN, M., ZHANG, W. Y., JIANG, P., ZHU, R. H., LIU, Y. P., FANG, P. F., XU, P., YUAN, H. Y., ZHANG, X. H., HU, L., YANG, W. & YE, H. S. 2012. Metabolomic analysis of biochemical changes in the plasma and urine of first-episode neuroleptic-naive schizophrenia patients after treatment with risperidone. *J Proteome Res,* 11**,** 4338-50.

CANETTA, S. E. & BROWN, A. S. 2012. Prenatal Infection, Maternal Immune Activation, and Risk for Schizophrenia. *Transl Neurosci,* 3**,** 320-327.

CARRUTHERS, V. B. & SUZUKI, Y. 2007. Effects of Toxoplasma gondii infection on the brain.

CHAUDHARY, K., DARLING, J. A., FOHL, L. M., SULLIVAN, W. J., JR., DONALD, R. G., PFEFFERKORN, E. R., ULLMAN, B. & ROOS, D. S. 2004. Purine salvage pathways in the apicomplexan parasite Toxoplasma gondii. *J Biol Chem,* 279**,** 31221-7.

CHEN, J. J., HUANG, H., ZHAO, L. B., ZHOU, D. Z., YANG, Y. T., ZHENG, P., YANG, D. Y., HE, P., ZHOU, J. J., FANG, L. & XIE, P. 2014a. Sex-specific urinary biomarkers for diagnosing bipolar disorder. *PLoS ONE,* 9.

CHEN, J. J., LIU, Z., FAN, S. H., YANG, D. Y., ZHENG, P., SHAO, W. H., QI, Z. G., XU, X. J., LI, Q., MU, J., YANG, Y. T. & XIE, P. 2014b. Combined application of NMR- and GC-MS-based metabonomics yields a superior urinary biomarker panel for bipolar disorder. *Sci Rep,* 4**,** 5855.

CHIBA, S., MATSUMOTO, H., SAITOH, M., KASAHARA, M., MATSUYA, M. & KASHIWAGI, M. 1995. A correlation study between serum adenosine deaminase activities and peripheral lymphocyte subsets in Parkinson's disease. *J Neurol Sci,* 132**,** 170-3.

CHONG, J. & XIA, J. 2018. MetaboAnalystR: an R package for flexible and reproducible analysis of metabolomics data. *Bioinformatics,* 34**,** 4313-4314.

CISBANI, G., LE BEHOT, A., PLANTE, M. M., PREFONTAINE, P., LECORDIER, M. & RIVEST, S. 2018. Role of the chemokine receptors CCR2 and CX3CR1 in an experimental model of thrombotic stroke. *Brain Behav Immun,* 70**,** 280-292.

COLE, D. C., CHUNG, Y., GAGNIDZE, K., HAJDAROVIC, K. H., RAYON-ESTRADA, V., HARJANTO, D., BIGIO, B., GAL-TOTH, J., MILNER, T. A., MCEWEN, B. S., PAPAVASILIOU, F. N. & BULLOCH, K. 2017. Loss of APOBEC1 RNA-editing function in microglia exacerbates age-related CNS pathophysiology. *Proc Natl Acad Sci U S A,* 114**,** 13272-13277.

COLEMAN, J. W. 2001. Nitric oxide in immunity and inflammation. *Int Immunopharmacol,* 1**,** 1397-406.

CORREA, D., CAÑEDO-SOLARES, I., ORTIZ-ALEGRÍA, L. B., CABALLERO-ORTEGA, H. & RICO-TORRES, C. P. 2007. Congenital and acquired toxoplasmosis: Diversity and role of antibodies in different compartments of the host. *Parasite Immunology,* 29**,** 651-660.

COUPER, K. N., ROBERTS, C. W., BROMBACHER, F., ALEXANDER, J. & JOHNSON, L. L. 2005. Toxoplasma gondii-Specific Immunoglobulin M Limits Parasite Dissemination by Preventing Host Cell Invasion. *INFECTION AND IMMUNITY,* 73**,** 8060-8068.

CREEK, D. J., JANKEVICS, A., BURGESS, K. E., BREITLING, R. & BARRETT, M. P. 2012. IDEOM: an Excel interface for analysis of LC-MS-based metabolomics data. *Bioinformatics,* 28**,** 1048-9.

DASS, S. A. H., VASUDEVAN, A., DUTTA, D., SOH, L. J. T., SAPOLSKY, R. M. & VYAS, A. 2011. Protozoan Parasite Toxoplasma gondii Manipulates Mate Choice in Rats by Enhancing Attractiveness of Males. *PLoS ONE,* 6**,** e27229-e27229.

DAVIS, M. 1998. Are different parts of the extended amygdala involved in fear versus anxiety? *Biological Psychiatry,* 44**,** 1239-1247.

DELGADO GARCIA, G. & RODRIGUEZ PERDOMO, E. 1980. [Reactivity of toxoplasmin intradermal test in neurotic and manic-depressive patients]. *Rev Cubana Med Trop,* 32**,** 35-39.

DENKERS, E. Y. & GAZZINELLI, R. T. 1998. Regulation and Function of T-Cell-Mediated Immunity during Toxoplasma gondii Infection Regulation and Function of T-Cell-Mediated Immunity during Toxoplasma gondii Infection. *Clinical Microbiology reviews,* 11**,** 569-588.

DEPRISTO, M. A., BANKS, E., POPLIN, R., GARIMELLA, K. V., MAGUIRE, J. R., HARTL, C., PHILIPPAKIS, A. A., DEL ANGEL, G., RIVAS, M. A., HANNA, M., MCKENNA, A., FENNELL, T. J., KERNYTSKY, A. M., SIVACHENKO, A. Y., CIBULSKIS, K., GABRIEL, S. B., ALTSHULER, D. & DALY, M. J. 2011. A framework for variation discovery and genotyping using next-generation DNA sequencing data. *Nat Genet,* 43**,** 491-8.

DICKERSON, F., BORONOW, J., STALLINGS, C., ORIGONI, A. & YOLKEN, R. 2007. Toxoplasma gondii in individuals with schizophrenia: Association with clinical and demographic factors and with mortality. *Schizophrenia Bulletin,* 33**,** 737-740.

DICKERSON, F., STALLINGS, C., ORIGONI, A., VAUGHAN, C., KATSAFANAS, E., KHUSHALANI, S. & YOLKEN, R. 2014. Antibodies to Toxoplasma gondii in individuals with mania. *Bipolar Disorders,* 16**,** 129-136.

DIMIER, I. H. & BOUT, D. T. 1998. Interferon-γ-activated primary enterocytes inhibit Toxoplasma gondii replication: A role for intracellular iron. *Immunology,* 94**,** 488-495.

DIXON, S. E., STILGER, K. L., ELIAS, E. V., NAGULESWARAN, A. & SULLIVAN, W. J. 2010. A decade of epigenetic research in Toxoplasma gondii. NIH Public Access.

DOWNER, E. J. 2013. Toll-Like Receptor Signaling in Alzheimer's Disease Progression. *Journal of Alzheimer's Disease & Parkinsonism,* S10.

DUBEY 2004. Toxoplasmosis – a waterborne zoonosis. *Veterinary Parasitology***,** 57---72.

DUBEY, J. P. 2008. The history of Toxoplasma gondii--the first 100 years. *The Journal of Eukaryotic Microbiology,* 55**,** 467-475.

DUBEY, J. P. 2010. *Toxoplasmosis of animals and humans,* CRC Press.

DUBEY, J. P., HOTEA, I., OLARIU, T. R., JONES, J. L. & DĂRĂBUȘ, G. 2014. Epidemiological review of toxoplasmosis in humans and animals in Romania. *Parasitology,* 141**,** 311-25.

DUBEY, J. P., MILLER, N. L. & FRENKEL, J. K. 1970. The Toxoplasma gondii oocyst from cat feces. *The Journal of experimental medicine,* 132**,** 636-662.

DUNN, D. W., M. PEYRON, F. PETERSEN, E. PECKHAM, C. GILBERT, R. 1999. Mother-to-child transmission of toxoplasmosis: risk estimates for clinical counselling. *Lancet,* 353**,** 1829-33.

ERHARDT, S., BLENNOW, K., NORDIN, C., SKOGH, E., LINDSTRÖM, L. H. & ENGBERG, G. 2001. Kynurenic acid levels are elevated in the cerebrospinal fluid of patients with schizophrenia.

ESTES, M. L. & MCALLISTER, A. K. 2016. Maternal immune activation: Implications for neuropsychiatric disorders. *Science,* 353**,** 772-7.

FERGUSON, D. J. & HUTCHISON, W. M. 1987a. The host-parasite relationship of Toxoplasma gondii in the brains of chronically infected mice. *Virchows Arch A Pathol Anat Histopathol,* 411**,** 39-43.

FERGUSON, D. J. & HUTCHISON, W. M. 1987b. An ultrastructural study of the early development and tissue cyst formation of Toxoplasma gondii in the brains of mice. *Parasitol Res,* 73**,** 483-91.

FILISETTI, D. & CANDOLFI, E. 2004. Immune response to Toxoplasma gondii. *Ann Ist Super Sanita,* 40**,** 71-80.

FIORI, L. M. & TURECKI, G. 2008. Implication of the polyamine system in mental disorders. *J Psychiatry Neurosci,* 33**,** 102-10.

FLEGR, J. 2007. Effects of Toxoplasma on human behavior. *Schizophrenia Bulletin,* 33**,** 757-760.

FLEGR, J. 2012. Influence of latent Toxoplasma infection on human personality, physiology and morphology: pros and cons of the Toxoplasma–human model in studying the manipulation hypothesis. *Journal of Experimental Biology,* 216.

FLEGR, J. 2013. Influence of latent Toxoplasma infection on human personality, physiology and morphology: pros and cons of the Toxoplasma–human model in studying the manipulation hypothesis. *Journal of Experimental Biology,* 216**,** 127-133.

FLEGR, J., HAVLÍCEK, J., KODYM, P., MALÝ, M. & SMAHEL, Z. 2002. BMC Infectious Diseases Increased risk of traffic accidents in subjects with latent toxoplasmosis: a retrospective case-control study. *BMC Infectious Diseases,* 2.

FLEGR, J., KLOSE, J., NOVOTNA, M., BERENREITTEROVA, M. & HAVLICEK, J. 2009. Increased incidence of traffic accidents in Toxoplasma-infected military drivers and protective effect RhD molecule revealed by a large-scale prospective cohort study. *BMC Infect Dis,* 9**,** 72.

FLEGR, J. & MARKOŠ, A. 2014. Masterpiece of epigenetic engineering - How Toxoplasma gondii reprogrammes host brains to change fear to sexual attraction. *Molecular Ecology,* 23**,** 5934-5936.

FLEGR, J., ZITKOVÁ, S., KODYM, P. & FRYNTA, D. 1996. Induction of changes in human behaviour by the parasitic protozoan Toxoplasma gondii. *Parasitology***,** 49-54.

FUHRMANN, M., BITTNER, T., JUNG, C. K., BURGOLD, S., PAGE, R. M., MITTEREGGER, G., HAASS, C., LAFERLA, F. M., KRETZSCHMAR, H. & HERMS, J. 2010. Microglial Cx3cr1 knockout prevents neuron loss in a mouse model of Alzheimer's disease. *Nat Neurosci,* 13**,** 411-3.

FUJIGAKI, S., SAITO, K., TAKEMURA, M., MAEKAWA, N., YAMADA, Y., WADA, H. & SEISHIMA, M. 2002. L-tryptophan-L-kynurenine pathway metabolism accelerated by Toxoplasma gondii infection is abolished in gamma interferon-gene-deficient mice: Cross-regulation between inducible nitric oxide synthase and indoleamine-2,3-dioxygenase. *Infection and Immunity,* 70**,** 779-786.

FUKUHARA, K., OHNO, A., OTA, Y., SENOO, Y., MAEKAWA, K., OKUDA, H., KURIHARA, M., OKUNO, A., NIIDA, S., SAITO, Y. & TAKIKAWA, O. 2013. NMR-based metabolomics of urine in a mouse model of Alzheimer's disease: identification of oxidative stress biomarkers. *J Clin Biochem Nutr,* 52**,** 133-8.

FULLER TORREY, E. & YOLKEN, R. H. 2013. Toxoplasma oocysts as a public health problem. *Trends Parasitol,* 29**,** 380-4.

GALVAN-RAMIREZ MDE, L., SANCHEZ-OROZCO, L. V., RODRIGUEZ, L. R., RODRIGUEZ, S., ROIG-MELO, E., TROYO SANROMAN, R., CHIQUETE, E. & ARMENDARIZ-BORUNDA, J. 2013. Seroepidemiology of Toxoplasma gondii infection in drivers involved in road traffic accidents in the metropolitan area of Guadalajara, Jalisco, Mexico. *Parasit Vectors,* 6**,** 294.

GASKELL, E. A., SMITH, J. E., PINNEY, J. W., WESTHEAD, D. R. & MCCONKEY, G. A. 2009. A unique dual activity amino acid hydroxylase in Toxoplasma gondii. *PLoS ONE,* 4**,** e4801-e4801.

GATKOWSKA, J., WIECZOREK, M., DZIADEK, B., DZITKO, K. & DLUGONSKA, H. 2012. Behavioral changes in mice caused by Toxoplasma gondii invasion of brain. *Parasitology Research,* 111**,** 53-58.

GHEZZI, P., BIANCHI, M., MANTOVANI, A., SPREAFICO, F. & SALMONA, M. 1984. Enhanced xanthine oxidase activity in mice treated with interferon and interferon inducers. *Biochem Biophys Res Commun,* 119**,** 144-9.

GIGLEY, J. P., BHADRA, R. & KHAN, I. A. 2011. CD8 T cells and toxoplasma gondii: A new paradigm. *Journal of Parasitology Research,* 2011.

GIØRTZ PEDERSEN, M., STEVENS, H. & BØCKER PEDERSEN, C. 2011. Tox oplasma Infection and l ater d evelopm ent of Schizophrenia in M others. *Am J Psychiatry,* 168**,** 814-821.

GONZALEZ, L. E., ROJNIK, B., URREA, F., URDANETA, H., PETROSINO, P., COLASANTE, C., PINO, S. & HERNANDEZ, L. 2007. Toxoplasma gondii infection lower anxiety as measured in the plus-maze and social interaction tests in rats. A behavioral analysis. *Behavioural Brain Research,* 177**,** 70-79.

GRICIUC, A., SERRANO-POZO, A., PARRADO, A. R., LESINSKI, A. N., ASSELIN, C. N., MULLIN, K., HOOLI, B., CHOI, S. H., HYMAN, B. T. & TANZI, R. E. 2013. Alzheimer's disease risk gene CD33 inhibits microglial uptake of amyloid beta. *Neuron,* 78**,** 631-43.

GULINELLO, M., ACQUARONE, M., KIM, J. H., SPRAY, D. C., BARBOSA, H. S., SELLERS, R., TANOWITZ, H. B. & WEISS, L. M. 2010. Acquired infection with Toxoplasma gondii in adult mice results in sensorimotor deficits but normal cognitive behavior despite widespread brain pathology. *Microbes and Infection,* 12**,** 528-537.

HALONEN, S. K., MELZER, T., CRANSTON, H., GRESS, J., MCINNERNEY, K., MAZURIE, A. & DRATZ, E. 2014. Differential gene expression in murine astrocytes infected with virulent (type I) vs . a virulent (type II) strains of Toxoplasma gondii. 5.

HANDFORD, M., RODRIGUEZ-FURLAN, C. & ORELLANA, A. 2006. Nucleotide-sugar transporters: structure, function and roles in vivo. *Braz J Med Biol Res,* 39**,** 1149-58.

HARGRAVE, K. E., WOODS, S., MILLINGTON, O., CHALMERS, S., WESTROP, G. D. & ROBERTS, C. W. 2019. Multi-Omics Studies Demonstrate Toxoplasma gondii-Induced Metabolic Reprogramming of Murine Dendritic Cells. *Front Cell Infect Microbiol,* 9**,** 309.

HARI DASS, S. A. & VYAS, A. 2014. Toxoplasma gondii infection reduces predator aversion in rats through epigenetic modulation in the host medial amygdala. *Molecular Ecology,* 23**,** 6114-6122.

HAY, J., AITKEN, P. P. & GRAHAM, D. I. 1984a. Toxoplasma infection and response to novelty in mice. *Zeitschrift für Parasitenkunde Parasitology Research,* 70**,** 575-588.

HAY, J., AITKEN, P. P., HAIR, D. M., HUTCHISON, W. M. & GRAHAM, D. I. 1984b. The effect of congenital Toxoplasma infection on mouse activity and relative preference for exposed areas over a series of trials. *Annals of Tropical Medicine and Parasitology,* 78**,** 611-618.

HENRIQUEZ, S. A., BRETT, R., ALEXANDER, J., PRATT, J. & ROBERTS, C. W. 2009. Neuropsychiatric disease and Toxoplasma gondii infection. *NeuroImmunoModulation,* 16**,** 122-133.

HERCULANO-HOUZEL, S. 2014. The glia/neuron ratio: how it varies uniformly across brain structures and species and what that means for brain physiology and evolution. *Glia,* 62**,** 1377-91.

HERMES, G., AJIOKA, J. W., KELLY, K. A., MUI, E., ROBERTS, F., KASZA, K., MAYR, T., KIRISITS, M. J., WOLLMANN, R., FERGUSON, D. J. P., ROBERTS, C. W., HWANG, J.-H., TRENDLER, T., KENNAN, R. P., SUZUKI, Y., REARDON, C., HICKEY, W. F., CHEN, L. & MCLEOD, R. 2008. Neurological and behavioral abnormalities, ventricular dilatation, altered cellular functions, inflammation, and neuronal injury in brains of mice due to common, persistent, parasitic infection. *Journal of neuroinflammation,* 5**,** 48-48.

HICKMAN, S. E. & EL KHOURY, J. 2014. TREM2 and the neuroimmunology of Alzheimer's disease. *Biochem Pharmacol,* 88**,** 495-8.

HIDE, G., MORLEY, E. K., HUGHES, J. M., GERWASH, O., ELMAHAISHI, M. S., ELMAHAISHI, K. H., THOMASSON, D., WRIGHT, E. A., WILLIAMS, R. H., MURPHY, R. G. & SMITH, J. E. 2009. Evidence for high levels of vertical transmission in Toxoplasma gondii. *Parasitology,* 136**,** 1877-85.

HILL, D. E., CHIRUKANDOTH, S. & DUBEY, J. P. 2005. Biology and epidemiology of Toxoplasma gondii in man and animals. *Animal Health Research Reviews,* 6**,** 41-61.

HINZE-SELCH, D., DÄUBENER, W., EGGERT, L., ERDAG, S., STOLTENBERG, R. & WILMS, S. 2007. A controlled prospective study of Toxoplasma gondii infection in individuals with schizophrenia: Beyond seroprevalence. *Schizophrenia Bulletin,* 33**,** 782-788.

HIRAHARA, K., POHOLEK, A., VAHEDI, G., LAURENCE, A., KANNO, Y., MILNER, J. D. & O'SHEA, J. J. 2013. Mechanisms underlying helper T-cell plasticity: implications for immune-mediated disease. *J Allergy Clin Immunol,* 131**,** 1276-87.

HIROTA, T. & KISHI, T. 2013. Adenosine hypothesis in schizophrenia and bipolar disorder: A systematic review and meta-analysis of randomized controlled trial of adjuvant purinergic modulators. *Schizophrenia Research,* 149**,** 88-95.

HOLUB, D., FLEGR, J., DRAGOMIRECKÁ, E., RODRIGUEZ, M., PREISS, M., NOVÁK, T., ČERMÁK, J., HORÁČEK, J., KODYM, P., LIBIGER, J., HÖSCHL, C. & MOTLOVÁ, L. B. 2013. Differences in onset of disease and severity of psychopathology between

toxoplasmosis-related and toxoplasmosis-unrelated schizophrenia. *Acta psychiatrica Scandinavica,* 127**,** 227-238.

HONORAT, J. A., KINOSHITA, M., OKUNO, T., TAKATA, K., KODA, T., TADA, S., SHIRAKURA, T., FUJIMURA, H., MOCHIZUKI, H., SAKODA, S. & NAKATSUJI, Y. 2013. Xanthine oxidase mediates axonal and myelin loss in a murine model of multiple sclerosis. *PLoS One,* 8**,** e71329.

HOOGLAND, I. C., HOUBOLT, C., VAN WESTERLOO, D. J., VAN GOOL, W. A. & VAN DE BEEK, D. 2015. Systemic inflammation and microglial activation: systematic review of animal experiments. *J Neuroinflammation,* 12**,** 114.

HOUSE, P. K., VYAS, A. & SAPOLSKY, R. 2011. Predator cat odors activate sexual arousal pathways in brains of toxoplasma gondii infected rats. *PLoS ONE,* 6**,** 8-11.

HOWARD, J. C., HUNN, J. P. & STEINFELDT, T. 2011. The IRG protein-based resistance mechanism in mice and its relation to virulence in Toxoplasma gondii. *Current Opinion in Microbiology,* 14**,** 414-421.

HRDÁ, Š., VOTÝPKA, J., KODYM, P. & FLEGR, J. 2000. TRANSIENT NATURE OF TOXOPLASMA GONDII-INDUCED BEHAVIORAL CHANGES IN MICE. *Journal of Parasitology,* 86**,** 657-657.

HUGHES, D. 2013. Pathways to understanding the extended phenotype of parasites in their hosts. *J Exp Biol,* 216**,** 142-7.

HUNTER, C. A., ABRAMS, J. S., BEAMAN, M. H. & REMINGTON, J. S. 1993. Cytokine mRNA in the central nervous system of SCID mice infected with Toxoplasma gondii: importance of T-cell-independent regulation of resistance to T. gondii. *Infect Immun,* 61**,** 4038-44.

HUNTER, C. A., ROBERTS, C. W. & ALEXANDER, J. 1992. Kinetics of cytokine mRNA production in the brains of mice with progressive toxoplasmic encephalitis. *Eur J Immunol,* 22**,** 2317-22.

HUNTER, C. A. & SIBLEY, L. D. 2012. Modulation of innate immunity by Toxoplasma gondii virulence effectors. *Nature Reviews Microbiology,* 10**,** 766-778.

HUTCHINSON, W. M., BRADLEY, M., CHEYNE, W. M., WELLS, B. W. & HAY, J. 1980. Behavioural abnormalities in Toxoplasma-infected mice. *Annals of tropical medicine and parasitology,* 74**,** 337-45.

HUTCHISON, W. M., DUNACHIE, J. F., SIIM, J. C. & WORK, K. 1969. Life cycle of toxoplasma gondii. *Br Med J,* 4**,** 806.

INNES, E. A. 2010. A brief history and overview of toxoplasma gondii. *Zoonoses and Public Health,* 57**,** 1-7.

ITO, D., IMAI, Y., OHSAWA, K., NAKAJIMA, K., FUKUUCHI, Y. & KOHSAKA, S. 1998. Microglia-specific localisation of a novel calcium binding protein, Iba1. *Brain Res Mol Brain Res,* 57**,** 1-9.

JAMIESON, S. E., CORDELL, H., PETERSEN, E., MCLEOD, R., GILBERT, R. E. & BLACKWELL, J. M. 2009. Host genetic and epigenetic factors in toxoplasmosis. *Mem Inst Oswaldo Cruz,* 104**,** 162-9.

JAMIESON, S. E., DE ROUBAIX, L. A., CORTINA-BORJA, M., TAN, H. K., MUI, E. J., CORDELL, H. J., KIRISITS, M. J., MILLER, E. N., PEACOCK, C. S., HARGRAVE, A. C., COYNE, J. J., BOYER, K., BESSIERES, M. H., BUFFOLANO, W., FERRET, N., FRANCK, J., KIEFFER, F., MEIER, P., NOWAKOWSKA, D. E., PAUL, M., PEYRON, F., STRAY-PEDERSEN, B., PRUSA, A. R., THULLIEZ, P., WALLON, M., PETERSEN, E., MCLEOD, R., GILBERT, R. E. & BLACKWELL, J. M. 2008. Genetic

and epigenetic factors at COL2A1 and ABCA4 influence clinical outcome in congenital toxoplasmosis. *PLoS One,* 3**,** e2285.
JIANG, T., YU, J. T., HU, N., TAN, M. S., ZHU, X. C. & TAN, L. 2014. CD33 in Alzheimer's disease. *Mol Neurobiol,* 49**,** 529-35.
JIANG, Y. T., LI, H. Y., CAO, X. P. & TAN, L. 2018. Meta-analysis of the association between CD33 and Alzheimer's disease. *Ann Transl Med,* 6**,** 169.
JONES, J. L., LOPEZ, A., WILSON, M., SCHULKIN, J. & GIBBS, R. 2001. Congenital toxoplasmosis: a review. *Obstet Gynecol Surv,* 56**,** 296-305.
JOSHI, N. S., CUI, W., CHANDELE, A., LEE, H. K., URSO, D. R., HAGMAN, J., GAPIN, L. & KAECH, S. M. 2007. Inflammation directs memory precursor and short-lived effector CD8(+) T cell fates via the graded expression of T-bet transcription factor. *Immunity,* 27**,** 281-95.
KAŁUŻNA-CZAPLIŃSKA, J., ZURAWICZ, E., STRUCK, W. & MARKUSZEWSKI, M. 2014. Identification of organic acids as potential biomarkers in the urine of autistic children using gas chromatography/mass spectrometry. *Journal of chromatography. B, Analytical technologies in the biomedical and life sciences,* 966**,** 70-76.
KANNAN, G., MOLDOVAN, K., XIAO, J. C., YOLKEN, R. H., JONES-BRANDO, L. & PLETNIKOV, M. V. 2010. Toxoplasma gondii strain-dependent effects on mouse behaviour. *Folia Parasitologica,* 57**,** 151-155.
KAR, N. & MISRA, B. 2004. Toxoplasma seropositivity and depression: a case report. *BMC psychiatry,* 4**,** 1-1.
KEARNEY, C. J., RANDALL, K. L. & OLIARO, J. 2017. DOCK8 regulates signal transduction events to control immunity. *Cell Mol Immunol,* 14**,** 406-411.
KHANDAKER, G. M., COUSINS, L., DEAKIN, J., LENNOX, B. R., YOLKEN, R. & JONES, P. B. 2015. Inflammation and immunity in schizophrenia: implications for pathophysiology and treatment. *The Lancet Psychiatry,* 2**,** 258-270.
KHANDAKER, G. M., ZIMBRON, J., LEWIS, G. & JONES, P. B. 2013. Prenatal maternal infection, neurodevelopment and adult schizophrenia: a systematic review of population-based studies. *Psychol Med,* 43**,** 239-57.
KIM, K. & WEISS, L. M. 2004. Toxoplasma gondii: the model apicomplexan. *Int J Parasitol,* 34**,** 423-32.
KLAREN, V. N. A. & KIJLSTRA, A. 2002. Toxoplasmosis, an overview with emphasis on ocular involvement. *Ocular immunology and inflammation,* 10**,** 1-26.
KLEIN GELTINK, R. I. & PEARCE, E. L. 2019. The importance of methionine metabolism. *Elife,* 8.
KLEIN, R. S., GARBER, C. & HOWARD, N. 2017. Infectious immunity in the central nervous system and brain function. *Nat Immunol,* 18**,** 132-141.
KNIGHT, K. 2013. How Pernicious Parasites Turn Victims Into Zombies. *Journal of Experimental Biology,* 216**,** i-iv.
KOBLANSKY, A. A., JANKOVIC, D., OH, H., HIENY, S., SUNGNAK, W., MATHUR, R., HAYDEN, M. S., AKIRA, S., SHER, A. & GHOSH, S. 2013. Recognition of Profilin by Toll-like Receptor 12 Is Critical for Host Resistance to Toxoplasma gondii. *Immunity,* 38**,** 119-130.
KOCAZEYBEK, B., ONER, Y. A., TURKSOY, R., BABUR, C., CAKAN, H., SAHIP, N., UNAL, A., OZASLAN, A., KILIC, S., SARIBAS, S., ASLAN, M., TAYLAN, A., KOC, S., DIRICAN, A., UNER, H. B., OZ, V., ERTEKIN, C., KUCUKBASMACI, O. & TORUN, M. M. 2009. Higher prevalence of toxoplasmosis in victims of traffic accidents

suggest increased risk of traffic accident in Toxoplasma-infected inhabitants of Istanbul and its suburbs. *Forensic science international,* 187**,** 103-8.

KOOLA, M. M. 2016. Kynurenine pathway and cognitive impairments in schizophrenia: Pharmacogenetics of galantamine and memantine. *Schizophrenia Research: Cognition,* 4**,** 4-9.

KOPPEN, A., KLEIN, J., HOLLER, T. & LOFFELHOLZ, K. 1993. Synergistic effect of nicotinamide and choline administration on extracellular choline levels in the brain. *J Pharmacol Exp Ther,* 266**,** 720-5.

KRISTAL, B. S., VIGNEAU-CALLAHAN, K. E. & MATSON, W. R. 1998. Simultaneous analysis of the majority of low-molecular-weight, redox-active compounds from mitochondria. *Anal Biochem,* 263**,** 18-25.

KRUG, E. C., MARR, J. J. & BERENS, R. L. 1989. Purine metabolism in Toxoplasma gondii. *J Biol Chem,* 264**,** 10601-7.

KUMAR, A., DHULL, D. K., GUPTA, V., CHANNANA, P., SINGH, A., BHARDWAJ, M., RUHAL, P. & MITTAL, R. 2017. Role of Glutathione-S-transferases in neurological problems. *Expert Opin Ther Pat,* 27**,** 299-309.

KUSTOVA, Y., SEI, Y., MORSE III, H. C. & BASILE, A. S. 1998. The Influence of a Targeted Deletion of the IFNγ Gene on Emotional Behaviors. *BRAIN, BEHAVIOR, AND IMMUNITY,* 12**,** 308-324.

LAMBERTON, P. H. L., DONNELLY, C. A. & WEBSTER, J. P. 2008. Specificity of the Toxoplasma gondii-altered behaviour to definitive versus non-definitive host predation risk. *Parasitology,* 135**,** 1143-1150.

LANGE, P. S., LANGLEY, B., LU, P. & RATAN, R. R. 2004. Novel roles for arginase in cell survival, regeneration, and translation in the central nervous system. *J Nutr,* 134**,** 2812S-2817S; discussion 2818S-2819S.

LEE, G. R. 2018. The Balance of Th17 versus Treg Cells in Autoimmunity. *Int J Mol Sci,* 19.

LEE, H. C., MD YUSOF, H. H., LEONG, M. P., ZAINAL ABIDIN, S., SETH, E. A., HEWITT, C. A., VIDYADARAN, S., NORDIN, N., SCOTT, H. S., CHEAH, P. S. & LING, K. H. 2019. Gene and protein expression profiles of JAK-STAT signalling pathway in the developing brain of the Ts1Cje down syndrome mouse model. *Int J Neurosci,* 129**,** 871-881.

LEES, M. P., FULLER, S. J., MCLEOD, R., BOULTER, N. R., MILLER, C. M., ZAKRZEWSKI, A. M., MUI, E. J., WITOLA, W. H., COYNE, J. J., HARGRAVE, A. C., JAMIESON, S. E., BLACKWELL, J. M., WILEY, J. S. & SMITH, N. C. 2010. P2X7 receptor-mediated killing of an intracellular parasite, Toxoplasma gondii, by human and murine macrophages. *J Immunol,* 184**,** 7040-6.

LINDOVÁ, J., NOVOTNÁ, M., HAVLÍČEK, J., JOZÍFKOVÁ, E., SKALLOVÁ, A., KOLBEKOVÁ, P., HODNÝ, Z., KODYM, P. & FLEGR, J. 2006. Gender differences in behavioural changes induced by latent toxoplasmosis. *International Journal for Parasitology,* 36**,** 1485-1492.

LING, V. J., LESTER, D., MORTENSEN, P. B., LANGENBERG, P. W. & POSTOLACHE, T. T. 2011. Toxoplasma gondii seropositivity and suicide rates in women. *The Journal of nervous and mental disease,* 199**,** 440-4.

LOPEZ-LOPEZ, A., GAMEZ, J., SYRIANI, E., MORALES, M., SALVADO, M., RODRIGUEZ, M. J., MAHY, N. & VIDAL-TABOADA, J. M. 2014. CX3CR1 is a modifying gene of survival and progression in amyotrophic lateral sclerosis. *PLoS One,* 9**,** e96528.

MATTHEWS, P. A., SAMUELSSON, A.-M., SEED, P., POMBO, J., OBEN, J. A., POSTON, L. & TAYLOR, P. D. 2011. Fostering in mice induces cardiovascular and metabolic dysfunction in adulthood. *The Journal of physiology,* 589**,** 3969-81.

MCCONKEY, G. A., MARTIN, H. L., BRISTOW, G. C. & WEBSTER, J. P. 2013. Toxoplasma gondii infection and behaviour - location, location, location? *The Journal of experimental biology,* 216**,** 113-9.

MCKENNA, A., HANNA, M., BANKS, E., SIVACHENKO, A., CIBULSKIS, K., KERNYTSKY, A., GARIMELLA, K., ALTSHULER, D., GABRIEL, S., DALY, M. & DEPRISTO, M. A. 2010. The Genome Analysis Toolkit: a MapReduce framework for analyzing next-generation DNA sequencing data. *Genome Res,* 20**,** 1297-303.

MCMASTER, W. R., MORRISON, C. J. & KOBOR, M. S. 2016. Epigenetics: A New Model for Intracellular Parasite-Host Cell Regulation.

MECK, W. H., WILLIAMS, C. L., CERMAK, J. M. & BLUSZTAJN, J. K. 2007. Developmental periods of choline sensitivity provide an ontogenetic mechanism for regulating memory capacity and age-related dementia. *Front Integr Neurosci,* 1**,** 7.

MEYER, U. 2013. Developmental neuroinflammation and schizophrenia. *Progress in Neuro-Psychopharmacology and Biological Psychiatry,* 42**,** 20-34.

MICHAUD, J. P., HALLE, M., LAMPRON, A., THERIAULT, P., PREFONTAINE, P., FILALI, M., TRIBOUT-JOVER, P., LANTEIGNE, A. M., JODOIN, R., CLUFF, C., BRICHARD, V., PALMANTIER, R., PILORGET, A., LAROCQUE, D. & RIVEST, S. 2013. Toll-like receptor 4 stimulation with the detoxified ligand monophosphoryl lipid A improves Alzheimer's disease-related pathology. *Proc Natl Acad Sci U S A,* 110**,** 1941-6.

MILLER, C. M., BOULTER, N. R., IKIN, R. J. & SMITH, N. C. 2009. The immunobiology of the innate response to Toxoplasma gondii.

MONTOYA, J. G. & LIESENFELD, O. Toxoplasmosis. 2004 2004.

MONTOYA, J. G. & ROSSO, F. 2005. Diagnosis and management of toxoplasmosis.

MORIWAKI, Y., YAMAMOTO, T. & HIGASHINO, K. 1999. Enzymes involved in purine metabolism--a review of histochemical localization and functional implications. *Histol Histopathol,* 14**,** 1321-40.

MORTENSEN, P. B., NØRGAARD-PEDERSEN, B., WALTOFT, B. L., SØRENSEN, T. L., HOUGAARD, D., TORREY, E. F. & YOLKEN, R. H. 2007a. Toxoplasma gondii as a Risk Factor for Early-Onset Schizophrenia: Analysis of Filter Paper Blood Samples Obtained at Birth. *Biological Psychiatry,* 61**,** 688-693.

MORTENSEN, P. B., NØRGAARD-PEDERSEN, B., WALTOFT, B. L., SØRENSEN, T. L., HOUGAARD, D. & YOLKEN, R. H. 2007b. Early infections of Toxoplasma gondii and the later development of schizophrenia. *Schizophrenia Bulletin,* 33**,** 741-744.

NAG, N. & BERGER-SWEENEY, J. E. 2007. Postnatal dietary choline supplementation alters behavior in a mouse model of Rett syndrome. *Neurobiol Dis,* 26**,** 473-80.

NGO, C. T., ALM, K. H., METOKI, A., HAMPTON, W., RIGGINS, T., NEWCOMBE, N. S. & OLSON, I. R. 2017. White matter structural connectivity and episodic memory in early childhood. *Dev Cogn Neurosci,* 28**,** 41-53.

NGO, H. M., NGO, E. O., BZIK, D. J. & JOINER, K. A. 2000. Toxoplasma gondii: are host cell adenosine nucleotides a direct source for purine salvage? *Exp Parasitol,* 95**,** 148-53.

NICHOLSON, J. K., LINDON, J. C. & HOLMES, E. 1999. 'Metabonomics': understanding the metabolic responses of living systems to pathophysiological stimuli via multivariate statistical analysis of biological NMR spectroscopic data. *Xenobiotica,* 29**,** 1181-9.

NILSSON, L. K., LINDERHOLM, K. R., ENGBERG, G., PAULSON, L., BLENNOW, K., LINDSTRÖM, L. H., NORDIN, C., KARANTI, A., PERSSON, P. & ERHARDT, S. 2005. Elevated levels of kynurenic acid in the cerebrospinal fluid of male patients with schizophrenia. *Schizophrenia Research,* 80**,** 315-322.

NOTO, A., FANOS, V., BARBERINI, L., GRAPOV, D., FATTUONI, C., ZAFFANELLO, M., CASANOVA, A., FENU, G., DE GIACOMO, A., DE ANGELIS, M., MORETTI, C., PAPOFF, P., DITONNO, R. & FRANCAVILLA, R. 2014. The urinary metabolomics profile of an Italian autistic children population and their unaffected siblings. *J Matern Fetal Neonatal Med,* 27 Suppl 2**,** 46-52.

NOVOTNÁ, M., HANUSOVA, J., KLOSE, J., PREISS, M., HAVLICEK, J., ROUBALOVÁ, K. & FLEGR, J. 2005. Probable neuroimmunological link between Toxoplasma and cytomegalovirus infections and personality changes in the human host. *BMC infectious diseases,* 5**,** 54-54.

PARKER, S. J., ROBERTS, C. W. & ALEXANDER, J. 1991. CD8+ T cells are the major lymphocyte subpopulation involved in the protective immune response to Toxoplasma gondii in mice. *Clin Exp Immunol,* 84**,** 207-12.

PARLOG, A., SCHLUTER, D. & DUNAY, I. R. 2015. Toxoplasma gondii-induced neuronal alterations. *Parasite Immunol,* 37**,** 159-70.

PATTERSON, P. H. 2009. Immune involvement in schizophrenia and autism: etiology, pathology and animal models. *Behav Brain Res,* 204**,** 313-21.

PEARCE, B. D., HUBBARD, S., RIVERA, H. N., WILKINS, P. P., FISCH, M. C., HOPKINS, M. H., HASENKAMP, W., GROSS, R., BLIWISE, N., JONES, J. L., DUNCAN BRADLEY PEARCE, E. D. & DUNCAN, E. 2013. Toxoplasma gondii exposure affects neural processing speed as measured by acoustic startle latency in schizophrenia and controls. *Schizophr Res,* 150**,** 258-261.

PEARCE, E. L. & SHEN, H. 2007. Generation of CD8 T cell memory is regulated by IL-12. *Journal of immunology (Baltimore, Md. : 1950),* 179**,** 2074-2081.

PEJOVIC-MILOVANCEVIC, M. M., MANDIC-MARAVIC, V. D., CORIC, V. M., MITKOVIC-VONCINA, M. M., KOSTIC, M. V., SAVIC-RADOJEVIC, A. R., ERCEGOVAC, M. D., MATIC, M. G., PELJTO, A. N., LECIC-TOSEVSKI, D. R., SIMIC, T. P. & PLJESA-ERCEGOVAC, M. S. 2016. Glutathione S-Transferase Deletion Polymorphisms in Early-Onset Psychotic and Bipolar Disorders: A Case-Control Study. *Lab Med,* 47**,** 195-204.

PENG, J., GUO, K., XIA, J., ZHOU, J., YANG, J., WESTAWAY, D., WISHART, D. S. & LI, L. 2014. Development of isotope labeling liquid chromatography mass spectrometry for mouse urine metabolomics: quantitative metabolomic study of transgenic mice related to Alzheimer's disease. *J Proteome Res,* 13**,** 4457-69.

PETTEGREW, J. W., LEVINE, J. & MCCLURE, R. J. 2000. Acetyl-L-carnitine physical-chemical, metabolic, and therapeutic properties: relevance for its mode of action in Alzheimer's disease and geriatric depression. *Mol Psychiatry,* 5**,** 616-32.

PFEFFERKORN, E. R., ECKEL, M. & REBHUN, S. 1986a. Interferon-gamma suppresses the growth of Toxoplasma gondii in human fibroblasts through starvation for tryptophan. *Mol Biochem Parasitol,* 20**,** 215-24.

PFEFFERKORN, E. R., REBHUN, S. & ECKEL, M. 1986b. Characterization of an indoleamine 2,3-dioxygenase induced by gamma-interferon in cultured human fibroblasts. *J Interferon Res,* 6**,** 267-79.

PICCIO, L., BUONSANTI, C., CELLA, M., TASSI, I., SCHMIDT, R. E., FENOGLIO, C., RINKER, J., 2ND, NAISMITH, R. T., PANINA-BORDIGNON, P., PASSINI, N., GALIMBERTI, D., SCARPINI, E., COLONNA, M. & CROSS, A. H. 2008. Identification of soluble TREM-2 in the cerebrospinal fluid and its association with multiple sclerosis and CNS inflammation. *Brain,* 131**,** 3081-91.

PIFER, R., BENSON, A., STURGE, C. R. & YAROVINSKY, F. 2011. UNC93B1 is essential for TLR11 activation and IL-12-dependent host resistance to Toxoplasma gondii. *Journal of Biological Chemistry,* 286**,** 3307-3314.

PIFER, R. & YAROVINSKY, F. 2011. Innate responses to Toxoplasma gondii in mice and humans. *Trends Parasitol,* 27**,** 388-93.

PINON, J. M., DUMON, H., CHEMLA, C., FRANCK, J., PETERSEN, E., LEBECH, M., ZUFFEREY, J., BESSIERES, M. H., MARTY, P., HOLLIMAN, R., JOHNSON, J., LUYASU, V., LECOLIER, B., GUY, E., JOYNSON, D. H., DECOSTER, A., ENDERS, G., PELLOUX, H. & CANDOLFI, E. 2001. Strategy for diagnosis of congenital toxoplasmosis: evaluation of methods comparing mothers and newborns and standard methods for postnatal detection of immunoglobulin G, M, and A antibodies. *J.Clin.Microbiol.,* 39**,** 2267-2271.

POELCHEN, W., SIELER, D., WIRKNER, K. & ILLES, P. 2001. Co-transmitter function of ATP in central catecholaminergic neurons of the rat. *Neuroscience,* 102**,** 593-602.

PRANDOVSZKY, E., GASKELL, E., MARTIN, H., DUBEY, J. P., WEBSTER, J. P. & MCCONKEY, G. A. 2011. The neurotropic parasite toxoplasma gondii increases dopamine metabolism. *PLoS ONE,* 6**,** e23866-e23866.

RAPPLEY, I., MYERS, D. S., MILNE, S. B., IVANOVA, P. T., LAVOIE, M. J., BROWN, H. A. & SELKOE, D. J. 2009. Lipidomic profiling in mouse brain reveals differences between ages and genders, with smaller changes associated with ??-synuclein genotype. *Journal of Neurochemistry,* 111**,** 15-25.

RASSOULPOUR, A., WU, H. Q., FERRE, S. & SCHWARCZ, R. 2005. Nanomolar concentrations of kynurenic acid reduce extracellular dopamine levels in the striatum. *Journal of Neurochemistry,* 93**,** 762-765.

REMINGTON, J. S., JACK, S., MCLEOD, J. S. & THULLIEZ, P. D. G. 2006. *Infectious diseases of the fetus and newborn infant,* Elsevier Saunders.

RICCIOLINI, R., SCALIBASTRI, M., KELLEHER, J. K., CARMINATI, P., CALVANI, M. & ARDUINI, A. 1998. Role of acetyl-L-carnitine in rat brain lipogenesis: implications for polyunsaturated fatty acid biosynthesis. *J Neurochem,* 71**,** 2510-7.

ROBERT-GANGNEUX, F. & DARDÉ, M.-L. 2012. Epidemiology of and Diagnostic Strategies for Toxoplasmosis INTRODUCTION. 264-296.

ROBERTS, C. W. & ALEXANDER, J. 1992. Studies on a murine model of congenital toxoplasmosis: vertical disease transmission only occurs in BALB/c mice infected for the first time during pregnancy. *Parasitology,* 104 Pt 1**,** 19-23.

ROBERTS, F. & MCLEOD, R. 1999. Pathogenesis of toxoplasmic retinochoroiditis.

ROBERTSON, B., XU, X. J., HAO, J. X., WIESENFELD-HALLIN, Z., MHLANGA, J., GRANT, G. & KRISTENSSON, K. 1997. Interferon-gamma receptors in nociceptive pathways: role in neuropathic pain-related behaviour. *Neuroreport,* 8**,** 1311-1316.

RODRIGUEZ CETINA BIEFER, H., VASUDEVAN, A. & ELKHAL, A. 2017. Aspects of Tryptophan and Nicotinamide Adenine Dinucleotide in Immunity: A New Twist in an Old Tale. *Int J Tryptophan Res,* 10**,** 1178646917713491.

ROGÉRIO DOS SANTOS, A. & ALEX SOARES DE SOUZA, E. A. 2014. The Open Field Test. *Igarss 2014*, 1-5.

RUDDICK, J. P., EVANS, A. K., NUTT, D. J., LIGHTMAN, S. L., ROOK, G. A. W. & LOWRY, C. A. 2006. Tryptophan metabolism in the central nervous system: medical implications. *Expert reviews in molecular medicine,* 8**,** 1-27.

SAEIJ, J. P. J., BOYLE, J. P. & BOOTHROYD, J. C. 2005. Differences among the three major strains of Toxoplasma gondii and their specific interactions with the infected host.

SAKAGUCHI, S. 2000. Regulatory T cells: key controllers of immunologic self-tolerance. *Cell,* 101**,** 455-8.

SALAMONE, J. D. & CORREA, M. 2012. The Mysterious Motivational Functions of Mesolimbic Dopamine.

SANKOWSKI, R., MADER, S. & VALDES-FERRER, S. I. 2015. Systemic inflammation and the brain: novel roles of genetic, molecular, and environmental cues as drivers of neurodegeneration. *Front Cell Neurosci,* 9**,** 28.

SAVIO, L. E. B., DE ANDRADE MELLO, P., DA SILVA, C. G. & COUTINHO-SILVA, R. 2018. The P2X7 Receptor in Inflammatory Diseases: Angel or Demon? *Front Pharmacol,* 9**,** 52.

SCHOLTZOVA, H., CHIANCHIANO, P., PAN, J., SUN, Y., GONI, F., MEHTA, P. D. & WISNIEWSKI, T. 2014. Amyloid beta and Tau Alzheimer's disease related pathology is reduced by Toll-like receptor 9 stimulation. *Acta Neuropathol Commun,* 2**,** 101.

SCHWARCZ, R. & HUNTER, C. A. 2007. Toxoplasma gondii and schizophrenia: Linkage through astrocyte-derived kynurenic acid? *Schizophrenia Bulletin,* 33**,** 652-653.

SCHWARCZ, R., RASSOULPOUR, A., WU, H. Q., MEDOFF, D., TAMMINGA, C. A. & ROBERTS, R. C. 2001. Increased cortical kynurenate content in schizophrenia. *Biological Psychiatry,* 50**,** 521-530.

SCHWARCZ, R. & STONE, T. W. 2017. The kynurenine pathway and the brain: Challenges, controversies and promises. *Neuropharmacology,* 112**,** 237-247.

SCHWARZSCHILD, M. A., AGNATI, L., FUXE, K., CHEN, J. F. & MORELLI, M. 2006. Targeting adenosine A2A receptors in Parkinson's disease. *Trends Neurosci,* 29**,** 647-54.

SCHWIELER, L., LARSSON, M. K., SKOGH, E., KEGEL, M. E., ORHAN, F., ABDELMOATY, S., FINN, A., BHAT, M., SAMUELSSON, M., LUNDBERG, K., DAHL, M.-L., SELLGREN, C., SCHUPPE-KOISTINEN, I., SVENSSON, C., ERHARDT, S. & ENGBERG, G. 2015. Increased levels of IL-6 in the cerebrospinal fluid of patients with chronic schizophrenia - significance for activation of the kynurenine pathway. *Journal of psychiatry & neuroscience : JPN,* 40**,** 126-133.

SHER, A., TOSH, K. & JANKOVIC, D. 2016. Innate recognition of Toxoplasma gondii in humans involves a mechanism distinct from that utilized by rodents. *Cellular & Molecular Immunology advance online publication*.

SIBLEY, L. D., KHAN, A., AJIOKA, J. W. & ROSENTHAL, B. M. 2009. Genetic diversity of Toxoplasma gondii in animals and humans. *Philosophical transactions of the Royal Society of London. Series B, Biological sciences,* 364**,** 2749-61.

SINGH, G. & SEHGAL, R. 2010. Transfusion-transmitted parasitic infections. *Asian journal of transfusion science,* 4**,** 73-7.

SKALLOVA, A., KODYM, P., FRYNTA, D. & FLEGR, J. 2006. The role of dopamine in Toxoplasma-induced behavioural alterations in mice: an ethological and ethopharmacological study. *Parasitology,* 133**,** 525-35.

STAPLES, L. G., MCGREGOR, I. S., APFELBACH, R. & HUNT, G. E. 2008. Cat odor, but not trimethylthiazoline (fox odor), activates accessory olfactory and defense-related brain regions in rats. *Neuroscience,* 151**,** 937-947.

STEIBER, A., KERNER, J. & HOPPEL, C. L. 2004. Carnitine: a nutritional, biosynthetic, and functional perspective. *Mol Aspects Med,* 25**,** 455-73.

STIBBS, H. H. 1985. Changes in brain concentrations of catecholamines and indoleamines in Toxoplasma gondii infected mice. *Ann Trop Med Parasitol,* 79**,** 153-7.

SUKTHANA, Y. 2006. Toxoplasmosis: beyond animals to humans. *Trends in Parasitology,* 22**,** 137-142.

SUZUKI, Y. 2004. Factors determining resistance and susceptibility to infection with Toxoplasma gondii. Boston, MA: Springer US.

TAIT, E. D. & HUNTER, C. A. 2009. Advances in understanding immunity to Toxoplasma gondii. *Mem Inst Oswaldo Cruz, Rio de Janeiro,* 104**,** 201-210.

TANAKA, S., NISHIMURA, M., IHARA, F., YAMAGISHI, J., SUZUKI, Y. & NISHIKAWA, Y. 2013. Transcriptome analysis of mouse brain infected with toxoplasma gondii. *Infection and Immunity,* 81**,** 3609-3619.

TENTER, A. M. 2009. Toxoplasma gondii in animals used for human consumption. *Memórias do Instituto Oswaldo Cruz,* 104**,** 364-369.

TENTER, A. M., HECKEROTH, A. R. & WEISS, L. M. 2000. Toxoplasma gondii: From animals to humans. *International Journal for Parasitology,* 30**,** 1217-1258.

TOMASIK, J., SCHULTZ, T. L., KLUGE, W., YOLKEN, R. H., BAHN, S. & CARRUTHERS, V. B. 2016. Shared immune and repair markers during experimental toxoplasma chronic brain infection and schizophrenia. *Schizophrenia Bulletin,* 42**,** 386-395.

TONIN, A. A., DA SILVA, A. S., CASALI, E. A., SILVEIRA, S. S., MORITZ, C. E., CAMILLO, G., FLORES, M. M., FIGHERA, R., THOME, G. R., MORSCH, V. M., SCHETINGER, M. R., RUE MDE, L., VOGEL, F. S. & LOPES, S. T. 2014. Influence of infection by Toxoplasma gondii on purine levels and E-ADA activity in the brain of mice experimentally infected mice. *Exp Parasitol,* 142**,** 51-8.

TORGERSON, P. R. & MACPHERSON, C. N. L. 2011. The socioeconomic burden of parasitic zoonoses: Global trends. *Veterinary Parasitology,* 182**,** 79-95.

TORREY, E. F., BARTKO, J. J., LUN, Z.-R. & YOLKEN, R. H. 2007. Antibodies to Toxoplasma gondii in patients with schizophrenia: a meta-analysis. *Schizophrenia bulletin,* 33**,** 729-36.

TORREY, E. F. & YOLKEN, R. H. 2003. Toxoplasma gondii and Schizophrenia. *Emerging Infectious Diseases*.

TORREY, E. F. & YOLKEN, R. H. 2007. Editors' introduction: Schizophrenia and toxoplasmosis. *Schizophrenia Bulletin,* 33**,** 727-728.

UENO, N. & LODOEN, M. B. 2015. From the blood to the brain: avenues of eukaryotic pathogen dissemination to the central nervous system. *Curr Opin Microbiol,* 26**,** 53-9.

VAN GISBERGEN, K. P. J. M., GEIJTENBEEK, T. B. H. & VAN KOOYK, Y. 2005. Close encounters of neutrophils and DCs.

VAUDAUX, J. D., MUCCIOLI, C., JAMES, E. R., SILVEIRA, C., MAGARGAL, S. L., JUNG, C., DUBEY, J. P., JONES, J. L., DOYMAZ, M. Z., BRUCKNER, D. A., BELFORT, R., HOLLAND, G. N. & GRIGG, M. E. 2010. Identification of an atypical strain of toxoplasma gondii as the cause of a waterborne outbreak of toxoplasmosis in Santa Isabel do Ivai, Brazil. *The Journal of infectious diseases,* 202**,** 1226-33.

VENEGAS, C. & HENEKA, M. T. 2017. Danger-associated molecular patterns in Alzheimer's disease. *J Leukoc Biol,* 101**,** 87-98.

VINCENTI, J. E., MURPHY, L., GRABERT, K., MCCOLL, B. W., CANCELLOTTI, E., FREEMAN, T. C. & MANSON, J. C. 2015. Defining the Microglia Response during the Time Course of Chronic Neurodegeneration. *J Virol,* 90**,** 3003-17.

VYAS, A. 2015. Mechanisms of Host Behavioral Change in Toxoplasma gondii Rodent Association. *PLOS Pathogens,* 11**,** e1004935-e1004935.

VYAS, A., KIM, S.-K., GIACOMINI, N., BOOTHROYD, J. C. & SAPOLSKY, R. M. 2007. Behavioral changes induced by Toxoplasma infection of rodents are highly specific to aversion of cat odors. *Proceedings of the National Academy of Sciences of the United States of America,* 104**,** 6442-7.

WALSH, R. N. & CUMMINS, R. A. 1976. The Open-Field Test: A Critical Review.

WAN, Y. Y. & FLAVELL, R. A. 2009. How diverse--CD4 effector T cells and their functions. *J Mol Cell Biol,* 1**,** 20-36.

WANG, H., YOLKEN, R. H., HOEKSTRA, P. J., BURGER, H. & KLEIN, H. C. 2011. Antibodies to infectious agents and the positive symptom dimension of subclinical psychosis: The TRAILS study. *Schizophrenia Research,* 129**,** 47-51.

WANG, H. L., WANG, G. H., LI, Q. Y., SHU, C., JIANG, M. S. & GUO, Y. 2006. Prevalence of Toxoplasma infection in first-episode schizophrenia and comparison between Toxoplasma-seropositive and Toxoplasma-seronegative schizophrenia. *Acta Psychiatrica Scandinavica,* 114**,** 40-48.

WANG, J., GAN, Y., HAN, P., YIN, J., LIU, Q., GHANIAN, S., GAO, F., GONG, G. & TANG, Z. 2018. Ischemia-induced Neuronal Cell Death Is Mediated by Chemokine Receptor CX3CR1. *Sci Rep,* 8**,** 556.

WEBSTER, J. P. 1994. The effect of Toxoplasma gondii and other parasites on activity levels in wild and hybrid Rattus norvegicus. *Parasitology,* 109 (Pt 5**,** 583-589.

WEBSTER, J. P., BRUNTON, C. F. & MACDONALD, D. W. 1994. Effect of Toxoplasma gondii upon neophobic behaviour in wild brown rats, Rattus norvegicus. *Parasitology,* 109**,** 37-43.

WEBSTER, J. P., LAMBERTON, P. H. L., DONNELLY, C. A. & TORREY, E. F. 2006. Parasites as causative agents of human affective disorders? The impact of anti-psychotic, mood-stabilizer and anti-parasite medication on Toxoplasma gondii's ability to alter host behaviour. *Proceedings. Biological sciences / The Royal Society,* 273**,** 1023-30.

WEI, T., CHEN, C., HOU, J., XIN, W. & MORI, A. 2000. Nitric oxide induces oxidative stress and apoptosis in neuronal cells. *Biochim Biophys Acta,* 1498**,** 72-9.

WEISS, L. & DUBEY, J. 2009. Toxoplasmosis: a history of clinical observations. *International Journal for Parasitology,* 39**,** 895-901.

WENDTE, J. M., GIBSON, A. K. & GRIGG, M. E. 2011. Population genetics of Toxoplasma gondii: New perspectives from parasite genotypes in wildlife. *Veterinary Parasitology,* 182**,** 96-111.

WILSON, C. B., REMINGTON, J. S., STAGNO, S. & REYNOLDS, D. W. 1980. Development of Adverse Sequelae in Children Born with Subclinical Congenital Toxoplasma Infection. *Pediatrics,* 66.

WILSON, D. C., MATTHEWS, S. & YAP, G. S. 2008. IL-12 signaling drives CD8+ T cell IFN-gamma production and differentiation of KLRG1+ effector subpopulations during Toxoplasma gondii Infection. *J Immunol,* 180**,** 5935-5945.

WILSON, E. H. & HUNTER, C. A. 2004. The role of astrocytes in the immunopathogenesis of toxoplasmic encephalitis.

WOODS, S., SCHROEDER, J., MCGACHY, H. A., PLEVIN, R., ROBERTS, C. W. & ALEXANDER, J. 2013. MAP kinase phosphatase-2 plays a key role in the control of infection with Toxoplasma gondii by modulating iNOS and arginase-1 activities in mice. *PLoS Pathog,* 9**,** e1003535.

WORTH, A. R., LYMBERY, A. J. & THOMPSON, R. C. 2013. Adaptive host manipulation by Toxoplasma gondii: fact or fiction? *Trends Parasitol,* 29**,** 150-5.

WU, H. Q., RASSOULPOUR, A. & SCHWARCZ, R. 2007. Kynurenic acid leads, dopamine follows: A new case of volume transmission in the brain? *J Neural Transm,* 114**,** 33-41.

XIAO, J., JONES-BRANDO, L., TALBOT, C. C. & YOLKEN, R. H. 2011. Differential Effects of Three Canonical Toxoplasma Strains on Gene Expression in Human Neuroepithelial Cells. *Infection and Immunity,* 79**,** 1363-1373.

XU, X.-J., ZHENG, P., REN, G.-P., LIU, M.-L., MU, J., GUO, J., CAO, D., LIU, Z., MENG, H.-Q. & XIE, P. 2014. 2,4-Dihydroxypyrimidine is a potential urinary metabolite biomarker for diagnosing bipolar disorder. *Molecular bioSystems,* 10**,** 813-819.

YAMAMOTO, M., OKUYAMA, M., MA, J. S., KIMURA, T., KAMIYAMA, N., SAIGA, H., OHSHIMA, J., SASAI, M., KAYAMA, H., OKAMOTO, T., HUANG, D. C., SOLDATI-FAVRE, D., HORIE, K., TAKEDA, J. & TAKEDA, K. 2012. A cluster of interferon-gamma-inducible p65 GTPases plays a critical role in host defense against Toxoplasma gondii. *Immunity,* 37**,** 302-13.

YAN, C., ZHANG, B. B., HUA, H., LI, B., ZHANG, B., YU, Q., LI, X. Y., LIU, Y., PAN, W., LIU, X. Y., TANG, R. X. & ZHENG, K. Y. 2015. The dynamics of Treg/Th17 and the imbalance of Treg/Th17 in Clonorchis sinensis-infected mice. *PLoS ONE,* 10**,** e0143217-e0143217.

YAN, T., DING, F. & ZHAO, Y. 2019. Integrated identification of key genes and pathways in Alzheimer's disease via comprehensive bioinformatical analyses. *Hereditas,* 156**,** 25.

YANG, J., CHEN, T., SUN, L., ZHAO, Z., QI, X., ZHOU, K., CAO, Y., WANG, X., QIU, Y., SU, M., ZHAO, A., WANG, P., YANG, P., WU, J., FENG, G., HE, L., JIA, W. & WAN, C. 2013. Potential metabolite markers of schizophrenia. *Mol Psychiatry,* 18**,** 67-78.

YANG, X., LOU, Y., LIU, G., WANG, X., QIAN, Y., DING, J., CHEN, S. & XIAO, Q. 2017. Microglia P2Y6 receptor is related to Parkinson's disease through neuroinflammatory process. *J Neuroinflammation,* 14**,** 38.

YANG, Y., LIU, Z., CERMAK, J. M., TANDON, P., SARKISIAN, M. R., STAFSTROM, C. E., NEILL, J. C., BLUSZTAJN, J. K. & HOLMES, G. L. 2000. Protective effects of prenatal choline supplementation on seizure-induced memory impairment. *J Neurosci,* 20**,** RC109.

YAP, I. K., ANGLEY, M., VESELKOV, K. A., HOLMES, E., LINDON, J. C. & NICHOLSON, J. K. 2010. Urinary metabolic phenotyping differentiates children with autism from their unaffected siblings and age-matched controls. *J Proteome Res,* 9**,** 2996-3004.

YERELI, K., BALCIOĞLU, I. C. & ÖZBILGIN, A. 2006. Is Toxoplasma gondii a potential risk for traffic accidents in Turkey? *Forensic Science International,* 163**,** 34-37.

YIP, L., WOEHRLE, T., CORRIDEN, R., HIRSH, M., CHEN, Y., INOUE, Y., FERRARI, V., INSEL, P. A. & JUNGER, W. G. 2009. Autocrine regulation of T-cell activation by ATP release and P2X7 receptors. *FASEB J,* 23**,** 1685-93.

YOCHUM, C. L., BHATTACHARYA, P., PATTI, L., MIROCHNITCHENKO, O. & WAGNER, G. C. 2010. Animal model of autism using GSTM1 knockout mice and early post-natal sodium valproate treatment. *Behav Brain Res,* 210**,** 202-10.

YOLKEN, R. H., BACHMANN, S., RUSLANOVA, I., LILLEHOJ, E., FORD, G., TORREY, E. F., SCHROEDER, J. & ROUSLANOVA, I. 2001. Antibodies to Toxoplasma gondii in individuals with first-episode schizophrenia. *Clinical infectious diseases : an official publication of the Infectious Diseases Society of America,* 32**,** 842-4.

ZHENG, P., CHEN, J.-J., HUANG, T., WANG, M.-J., WANG, Y., DONG, M.-X., HUANG, Y.-J., ZHOU, L.-K. & XIE, P. 2013a. A Novel Urinary Metabolite Signature for Diagnosing Major Depressive Disorder. *Journal of Proteome Research,* 12**,** 5904-5911.

ZHENG, P., WANG, Y., CHEN, L., YANG, D., MENG, H., ZHOU, D., ZHONG, J., LEI, Y., MELGIRI, N. D. & XIE, P. 2013b. Identification and validation of urinary metabolite biomarkers for major depressive disorder. *Molecular & cellular proteomics : MCP,* 12**,** 207-14.

ZHENG, P., WEI, Y. D., YAO, G. E., REN, G. P., GUO, J., ZHOU, C. J., ZHONG, J. J., CAO, D., ZHOU, L. K. & XIE, P. 2013c. Novel urinary biomarkers for diagnosing bipolar disorder. *Metabolomics,* 9**,** 800-808.

ZHOU, S. L., TAN, C. C., HOU, X. H., CAO, X. P., TAN, L. & YU, J. T. 2019. TREM2 Variants and Neurodegenerative Diseases: A Systematic Review and Meta-Analysis. *J Alzheimers Dis,* 68**,** 1171-1184.

ZHU, J., YAMANE, H. & PAUL, W. E. 2010. Differentiation of effector CD4 T cell populations (*). *Annu Rev Immunol,* 28**,** 445-89.

ZUCHERO, J. B. & BARRES, B. A. 2015. Glia in mammalian development and disease. *Development,* 142**,** 3805-9.

Appendix

Chapter 3

Table 3.1 List of metabolites and their pathways that were detected by pHILLIC Column, C18-PFP Column or Both Column. pHILLIC*** =** metabolites detected by both pHILLIC and C18-PFP Columns in chronic *T.gondii* infection experiment. The metabolites highlight by yellow color corresponding to standard metabolites that used.

	m/z	RT (min)	FORMULA	Putative metabolite	Pathway	Column used
1	329.0524	9.66	C10H12N5O6P	3',5'-Cyclic AMP	Purine metabolism	pHILLIC
2	184.023	39	C5H4N4O4	5-Hydroxyisourate	Purine metabolism	C18-PFP
3	267.0966	9.3	C10H13N5O4	Adenosine	Purine metabolism	pHILLIC*
4	347.0629	14.03	C10H14N5O7P	AMP	Purine metabolism	pHILLIC*
5	251.1018	8.22	C10H13N5O3	Deoxyadenosine	Purine metabolism	pHILLIC
6	443.0242	18.31	C10H15N5O11P2	GDP	Purine metabolism	pHILLIC
7	363.0578	16.98	C10H14N5O8P	GMP	Purine metabolism	pHILLIC
8	522.9904	19.91	C10H16N5O14P3	GTP	Purine metabolism	pHILLIC
9	151.0494	12.62	C5H5N5O	Guanine	Purine metabolism	pHILLIC*
10	283.0916	12.83	C10H13N5O5	Guanosine	Purine metabolism	pHILLIC*
11	136.0385	10.36	C5H4N4O	Hypoxanthine	Purine metabolism	pHILLIC*
12	348.047	15.72	C10H13N4O8P	IMP	Purine metabolism	pHILLIC*
13	268.0807	11.11	C10H12N4O5	Inosine	Purine metabolism	pHILLIC*
14	463.074	18.7	C14H18N5O11P	N6-(1,2-Dicarboxyethyl)-AMP	Purine metabolism	pHILLIC
15	97.9673	18.17	H2O4S	Sulfate	Purine metabolism	pHILLIC
16	168.0283	12.63	C5H4N4O3	Urate	Purine metabolism	pHILLIC
17	152.0334	11.47	C5H4N4O2	Xanthine	Purine metabolism	pHILLIC*
18	306.0262	9.02	C9H11N2O8P	2',3'-Cyclic UMP	Pyrimidine metabolism	C18-PFP
19	403.0182	17.39	C9H15N3O11P2	CDP	Pyrimidine metabolism	pHILLIC
20	323.0518	16.13	C9H14N3O8P	CMP	Pyrimidine metabolism	pHILLIC*
21	482.9844	19.11	C9H16N3O14P3	CTP	Pyrimidine metabolism	pHILLIC
22	243.0855	12.12	C9H13N3O5	Cytidine	Pyrimidine metabolism	pHILLIC*
23	111.0432	5.79	C4H5N3O	Cytosine	Pyrimidine metabolism	C18-PFP
24	104.0109	15.94	C3H4O4	Malonate	Pyrimidine metabolism	pHILLIC

25	156.0171	10.39	C5H4N2O4	Orotate	Pyrimidine metabolism	pHILLIC
26	112.0272	10	C4H4N2O2	Orotate(Fragment)	Pyrimidine metabolism	pHILLIC
27	404.002	16.83	C9H14N2O12P2	UDP	Pyrimidine metabolism	pHILLIC
28	324.0358	15.39	C9H13N2O9P	UMP	Pyrimidine metabolism	pHILLIC*
29	112.0272	8.71	C4H4N2O2	Uracil	Pyrimidine metabolism	pHILLIC*
30	244.0694	9.99	C9H12N2O6	Uridine	Pyrimidine metabolism	pHILLIC*
31	483.9684	18.36	C9H15N2O15P3	UTP	Pyrimidine metabolism	pHILLIC
32	163.0479	6.85	C5H9NO5	4-Hydroxy-L-glutamate	ArginineandProlineMetabolism	C18-PFP
33	217.1063	16.37	C8H15N3O4	N-Acetyl-L-citrulline	arginine biosynthesis III	pHILLIC
34	103.0633	15.75	C4H9NO2	4-Aminobutanoate	Arginine and proline metabolism	pHILLIC*
35	145.0851	5.89	C5H11N3O2	4-Guanidinobutanoate	Arginine and proline metabolism	C18-PFP
36	297.0895	7.41	C11H15N5O3S	5'-Methylthioadenosine	Arginine and proline metabolism	pHILLIC*
37	113.0589	9.93	C4H7N3O	Creatinine	Arginine and proline metabolism	pHILLIC*
38	216.1112	11.74	C9H16N2O4	gamma-Glutamyl-gamma-aminobutyraldehyde	Arginine and proline metabolism	pHILLIC
39	217.1428	23.05	C9H19N3O3	gamma-L-Glutamylputrescine	Arginine and proline metabolism	pHILLIC
40	240.1222	16.48	C10H16N4O3	Homocarnosine	Arginine and proline metabolism	pHILLIC*
41	174.1117	26.75	C6H14N4O2	L-Arginine	Arginine and proline metabolism	pHILLIC*
42	175.0958	15.64	C6H13N3O3	L-Citrulline	Arginine and proline metabolism	pHILLIC*
43	115.0633	13.06	C5H9NO2	L-Proline	Arginine and proline metabolism	pHILLIC*
44	290.1226	17.13	C10H18N4O6	N-(L-Arginino)succinate	Arginine and proline metabolism	pHILLIC
45	246.1329	14.43	C9H18N4O4	N2-(D-1-Carboxyethyl)-L-arginine	Arginine and proline metabolism	pHILLIC
46	232.106	16.56	C9H16N2O5	N2-Succinyl-L-ornithine	Arginine and proline metabolism	pHILLIC
47	189.0638	14.36	C7H11NO5	N-Acetyl-L-glutamate	Arginine and proline metabolism	pHILLIC*
48	174.1005	13.84	C7H14N2O3	N-Acetylornithine	Arginine and proline metabolism	pHILLIC*
49	247.069	17.8	C9H13NO7	N-Succinyl-L-glutamate	Arginine and proline metabolism	pHILLIC
50	211.0358	15.47	C4H10N3O5P	Phosphocreatine	Arginine and proline metabolism	pHILLIC
51	88.1	4.52	C4H12N2	Putrescine	Arginine and proline metabolism	C18-PFP
52	145.1579	4.1	C7H19N3	Spermidine	Arginine and proline metabolism	C18-PFP
53	182.058	8.92	C9H10O4	3-(4-Hydroxyphenyl)lactate	Tyrosine metabolism	pHILLIC
54	180.0425	39.7	C9H8O4	3-(4-Hydroxyphenyl)pyruvate	Tyrosine metabolism	C18-PFP
55	167.0946	11.24	C9H13NO2	3-Methoxytyramine	Tyrosine metabolism	C18-PFP
56	153.0789	7.3	C8H11NO2	Dopamine	Tyrosine metabolism	C18-PFP
57	181.074	13.37	C9H11NO3	L-Tyrosine	Tyrosine metabolism	pHILLIC*
58	191.0582	38.21	C10H9NO3	5-Hydroxyindoleacetate	Tryptophan metabolism	C18-PFP
59	205.0741	39.94	C11H11NO3	Indolelactate	Tryptophan metabolism	C18-PFP
60	208.0849	11.59	C10H12N2O3	L-Kynurenine	Tryptophan metabolism	pHILLIC*
61	204.09	12.06	C11H12N2O2	L-Tryptophan	Tryptophan metabolism	pHILLIC*
62	218.1055	39.24	C12H14N2O2	N-Acetylserotonin	Tryptophan metabolism	C18-PFP
63	176.095	13.5	C10H12N2O	Serotonin	Tryptophan metabolism	C18-PFP

64	250.0622	6.86	C8H14N2O5S	gamma-L-Glutamyl-L-cysteine	Glutathione metabolism	C18-PFP
65	307.0837	14.6	C10H17N3O6S	Glutathione	Glutathione metabolism	pHILLIC*
66	612.1521	17.73	C20H32N6O12S2	Glutathione disulfide	Glutathione metabolism	pHILLIC
67	259.0464	5.52	C6H14NO8P	D-Glucosamine 6-phosphate	Glutamate metabolism	C18-PFP
68	147.0532	14.93	C5H9NO4	L-Glutamate	Glutamate metabolism	pHILLIC*
69	146.0691	15.4	C5H10N2O3	L-Glutamine	Glutamate metabolism	pHILLIC*
70	221.09	12.11	C8H15NO6	N-Acetyl-D-glucosamine	Glutamate metabolism	pHILLIC
71	148.0372	15.43	C5H8O5	(R)-2-Hydroxyglutarate	glutamate degradation	pHILLIC
72	136.0637	24.66	C7H8N2O	1-Methylnicotinamide	Nicotinate and nicotinamide metabolism	pHILLIC
73	144.0422	7.41	C6H8O4	2,3-Dimethylmaleate	Nicotinate and nicotinamide metabolism	pHILLIC
74	152.0585	7.6	C7H8N2O2	N1-Methyl-2-pyridone-5-carboxamide	Nicotinate and nicotinamide metabolism	pHILLIC
75	122.048	7.46	C6H6N2O	Nicotinamide	Nicotinate and nicotinamide metabolism	pHILLIC
76	254.0902	24.44	C11H14N2O5	N-Ribosylnicotinamide	Nicotinate and nicotinamide metabolism	pHILLIC
77	264.1044	4.77	C12H16N4OS	Thiamin	Thiamine metabolism	C18-PFP
78	125.9986	10.74	C2H6O4S	2-Hydroxyethanesulfonate	Taurine and hypotaurine metabolism	pHILLIC*
79	109.0197	5.37	C2H7NO2S	Hypotaurine	Taurine and hypotaurine metabolism	C18-PFP
80	139.9779	18.19	C2H4O5S	Sulfoacetate	Taurine and hypotaurine metabolism	pHILLIC
81	125.0145	15.07	C2H7NO3S	Taurine	Taurine and hypotaurine metabolism	pHILLIC*
82	167.0365	15.78	C3H9N3O3S	Taurocyamine	Taurine and hypotaurine metabolism	pHILLIC
83	536.0443	16.47	C14H22N2O16P2	UDP-D-xylose	Starch and sucrose metabolism	pHILLIC
84	785.1577	11.67	C27H33N9O15P2	FAD	Riboflavin metabolism	pHILLIC
85	376.1382	8.84	C17H20N4O6	Riboflavin	Riboflavin metabolism	pHILLIC
86	90.0314	9.64	C3H6O3	(R)-Lactate	Pyruvate metabolism	pHILLIC
87	167.9824	17.86	C3H5O6P	Phosphoenolpyruvate	Pyruvate metabolism	pHILLIC*
88	154.0031	11.48	C3H7O5P	Propanoyl phosphate	Propanoate metabolis	pHILLIC*
89	226.0953	10.79	C10H14N2O4	Porphobilinogen	Porphyrin and chlorophyll metabolism	C18-PFP
90	85.0892	9.52	C5H11N	Piperidine	piperine biosynthesis	C18-PFP
91	743.0759	17.13	C21H28N7O17P3	NADP+	Photosynthesis	pHILLIC
92	745.0915	17.55	C21H30N7O17P3	NADPH	Photosynthesis	pHILLIC
93	338.0992	16.46	C16H18O8	p-Coumaroyl quinic acid	Phenylpropanoid biosynthesis	pHILLIC
94	172.037	6.14	C7H8O5	3-Dehydroshikimate	Phenylalanine, tyrosine and tryptophan metabolism	C18-PFP
95	166.0632	39.27	C9H10O3	3-(2-Hydroxyphenyl)propanoate	Phenylalanine metabolism	C18-PFP
96	165.079	10.59	C9H11NO2	L-Phenylalanine	Phenylalanine metabolism	pHILLIC
97	207.0898	39.24	C11H13NO3	N-Acetyl-L-phenylalanine	Phenylalanine metabolism	C18-PFP
98	193.0743	39.28	C10H11NO3	Phenylacetylglycine	Phenylalanine metabolism	C18-PFP
99	150.068	4.97	C9H10O2	Phenylpropanoate	Phenylalanine metabolism	pHILLIC

100	191.043	17.44	C6H9NO6	Nitrilotriacetic acid	nitrilotriacetate degradation	pHILLIC
101	180.0457	10.09	C6H12O4S	5-Methylthio-D-ribose	Methionine metabolism	pHILLIC
102	149.0511	11.94	C5H11NO2S	L-Methionine	Methionine metabolism	pHILLIC*
103	165.0459	13.74	C5H11NO3S	L-Methionine S-oxide	Methionine metabolism	pHILLIC*
104	219.0743	14.06	C8H13NO6	O-Succinyl-L-homoserine	Methionine metabolism	pHILLIC*
105	384.1214	14.07	C14H20N6O5S	S-Adenosyl-L-homocysteine	Methionine metabolism	pHILLIC
106	163.0667	11.43	C6H13NO2S	S-Methyl-L-methionine	lysine, threonine and methionine metabolism	C18-PFP
107	146.1055	25.17	C6H14N2O2	L-Lysine	Lysine metabolism	pHILLIC*
108	129.079	5.91	C6H11NO2	L-Pipecolate	Lysine degradation_	C18-PFP
109	127.0633	13.65	C6H9NO2	2,3,4,5-Tetrahydropyridine-2-carboxylate	Lysine degradation	pHILLIC
110	204.1475	4.93	C9H20N2O3	3-Hydroxy-N6,N6,N6-trimethyl-L-lysine	Lysine degradation	C18-PFP
111	145.1102	5.63	C7H15NO2	4-Trimethylammoniobutanoate	Lysine degradation	C18-PFP
112	159.0896	13.06	C7H13NO3	5-Acetamidopentanoate	Lysine degradation	pHILLIC*
113	242.0668	17.58	C6H15N2O6P	5-Phosphonooxy-L-lysine	Lysine degradation	pHILLIC
114	161.1051	13.57	C7H15NO3	L-Carnitine	Lysine degradation	pHILLIC*
115	188.1525	22.66	C9H20N2O2	N6,N6,N6-Trimethyl-L-lysine	Lysine degradation	pHILLIC*
116	188.116	15.33	C8H16N2O3	N6-Acetyl-L-lysine	Lysine degradation	pHILLIC*
117	206.0426	18.4	C7H10O7	2-Hydroxybutane-1,2,4-tricarboxylate	Lysine biosynthesis	pHILLIC
118	188.0321	5.84	C7H8O6	But-1-ene-1,2,4-tricarboxylate	Lysine biosynthesis	C18-PFP
119	203.0794	13.92	C8H13NO5	N2-Acetyl-L-aminoadipate	Lysine biosynthesis	pHILLIC
120	188.1161	13.25	C8H16N2O3	N2-Acetyl-L-lysine	Lysine biosynthesis	pHILLIC
121	276.1322	15.99	C11H20N2O6	N6-(L-1,3-Dicarboxypropyl)-L-lysine	Lysine biosynthesis	pHILLIC
122	249.0861	7.91	C10H19NO2S2	S-Acetyldihydrolipoamide	Alanineandaspartatemetabolism	pHILLIC
123	226.1066	15.98	C9H14N4O3	Carnosine	Alanine and aspartate metabolism	pHILLIC*
124	89.0475	14.92	C3H7NO2	L-Alanine	Alanine and aspartate metabolism	pHILLIC*
125	132.0534	5.21	C4H8N2O3	L-Asparagine	Alanine and aspartate metabolism	C18-PFP
126	133.0375	15.65	C4H7NO4	L-Aspartate	Alanine and aspartate metabolism	pHILLIC*
127	175.0479	14.87	C6H9NO5	N-Acetyl-L-aspartate	Alanine and aspartate metabolism	pHILLIC*
128	203.1158	11.29	C9H17NO4	O-Acetylcarnitine	Alanine and aspartate metabolism	pHILLIC
129	261.1212	13.18	C11H19NO6	Lotaustralin	lotaustralin metabolism	pHILLIC
130	206.0432	7.58	C8H14O2S2	Lipoate	Lipoic acid metabolism	C18-PFP
131	128.0837	5.03	C7H12O2	3-Isopropylbut-3-enoic acid	Limonene and pinene degradation	pHILLIC
132	111.0796	4.57	C5H9N3	1H-Imidazole-4-ethanamine	Histidine metabolism	C18-PFP
133	220.0259	9.05	C6H9N2O5P	3-(Imidazol-4-yl)-2-oxopropyl phosphate	Histidine metabolism	C18-PFP
134	156.0535	11.44	C6H8N2O3	4-Imidazolone-5-propanoate	Histidine metabolism	pHILLIC
135	229.0884	5.71	C9H15N3O2S	Ergothioneine	Histidine metabolism	C18-PFP

136	77.019	6.67	C6H6N2O3	Imidazol-5-yl-pyruvate	Histidine metabolism	pHILLIC
137	155.0694	16.33	C6H9N3O2	L-Histidine	Histidine metabolism	pHILLIC*
138	140.0586	9.87	C6H8N2O2	Methylimidazoleacetic acid	Histidine metabolism	pHILLIC*
139	169.0852	13.4	C7H11N3O2	N(pi)-Methyl-L-histidine	Histidine metabolism	pHILLIC
140	174.0639	11.47	C6H10N2O4	N-Formimino-L-glutamate	Histidine metabolism	pHILLIC
141	559.0716	15.12	C15H23N5O14P2	Phosphoribosyl-AMP	Histidine metabolism	pHILLIC
142	131.0582	5.32	C5H9NO3	5-Aminolevulinate	Glycine, serine and threonine metabolism	C18-PFP
143	117.0789	11.49	C5H11NO2	Betaine	Glycine, serine and threonine metabolism	pHILLIC
144	103.0997	20.48	C5H13NO	Choline	Glycine, serine and threonine metabolism	pHILLIC*
145	131.0693	14.92	C4H9N3O2	Creatine	Glycine, serine and threonine metabolism	pHILLIC*
146	141.0191	16.22	C2H8NO4P	Ethanolamine phosphate	Glycine, serine and threonine metabolism	pHILLIC*
147	117.0538	16.03	C3H7N3O2	Guanidinoacetate	Glycine, serine and threonine metabolism	pHILLIC*
148	104.0111	5.97	C3H4O4	Hydroxypyruvate	Glycine, serine and threonine metabolism	C18-PFP
149	222.0674	17.38	C7H14N2O4S	L-Cystathionine	Glycine, serine and threonine metabolism	pHILLIC
150	105.0426	16.13	C3H7NO3	L-Serine	Glycine, serine and threonine metabolism	pHILLIC
151	119.0583	15	C4H9NO3	L-Threonine	Glycine, serine and threonine metabolism	pHILLIC*
152	185.009	17.87	C3H8NO6P	O-Phospho-L-serine	Glycine, serine and threonine metabolism	pHILLIC
153	488.1074	15.64	C14H26N4O11P2	CDP-choline	Glycerophospholipid metabolism	pHILLIC
154	183.0661	15.27	C5H14NO4P	Choline phosphate	Glycerophospholipid metabolism	pHILLIC*
155	169.0504	14.34	C4H12NO4P	Phosphodimethylethanolamine	Glycerophospholipid metabolism	pHILLIC
156	257.1027	14.73	C8H20NO6P	sn-glycero-3-Phosphocholine	Glycerophospholipid metabolism	pHILLIC*
157	215.056	15.93	C5H14NO6P	sn-glycero-3-Phosphoethanolamine	Glycerophospholipid metabolism	pHILLIC*
158	90.0318	7.24	C3H6O3	Glycerone	Glycerolipid metabolism	C18-PFP
159	172.0142	5.49	C3H9O6P	sn-Glycerol 3-phosphate	Glycerolipid metabolism	C18-PFP
160	573.0874	12.88	C16H25N5O14P2	GDP-3,6-dideoxy-D-galactose	GDP-L-colitose biosynthesis	pHILLIC
161	155.9818	43.01	C2H5O6P	2-Phosphoglycolate	Glyoxylate and dicarboxylate metabolism	C18-PFP
162	185.9929	17.34	C3H7O7P	3-Phospho-D-glycerate	Glycolysis / Gluconeogenesis	pHILLIC
163	180.0634	17.32	C6H12O6	D-Glucose	Glycolysis / Gluconeogenesis	pHILLIC
164	169.998	15.61	C3H7O6P	D-Glyceraldehyde 3-phosphate	Glycolysis / Gluconeogenesis	pHILLIC
165	179.0793	11.5	C6H13NO5	D-Galactosamine	Galactose metabolism	pHILLIC
166	182.0791	14.11	C6H14O6	D-Sorbitol	Fructose and mannose metabolism	pHILLIC
167	589.0823	17.81	C16H25N5O15P2	GDP-L-fucose	Fructose and mannose metabolism	pHILLIC
168	605.0772	18.48	C16H25N5O16P2	GDP-mannose	Fructose and mannose metabolism	pHILLIC
169	244.0347	15.74	C6H13O8P	L-Fucose 1-phosphate	Fructose and mannose metabolism	pHILLIC

170	164.0685	12.18	C6H12O5	L-Rhamnose	Fructose and mannose metabolism	pHILLIC
171	230.0191	15.32	C5H11O8P	D-Ribose 5-phosphate	Pentose phosphate pathway Purine metabolism	pHILLIC*
172	276.0247	18.11	C6H13O10P	6-Phospho-D-gluconate	Pentose phosphate pathway	pHILLIC*
173	200.0085	5.8	C4H9O7P	D-Erythrose 4-phosphate	Pentose phosphate pathway	C18-PFP
174	260.0304	5.7	C6H13O9P	D-Fructose 6-phosphate	Pentose phosphate pathway	C18-PFP
175	196.0583	13.56	C6H12O7	D-Gluconic acid	Pentose phosphate pathway	pHILLIC*
176	290.0403	16.54	C7H15O10P	D-Sedoheptulose 7-phosphate	Pentose phosphate pathway	pHILLIC
177	537.0762	16.89	C14H25N3O15P2	CDP-ribitol	Pentose and glucuronate interconversions	pHILLIC
178	566.0546	16.59	C15H24N2O17P2	UDP-glucose	Pentose and glucuronate interconversions	pHILLIC
179	580.034	19.39	C15H22N2O18P2	UDP-glucuronate	Pentose and glucuronate interconversions	pHILLIC
180	152.0684	13.16	C5H12O5	Xylitol	Pentose and glucuronate interconversions	pHILLIC
181	427.0295	15.48	C10H15N5O10P2	ADP	Oxidative phosphorylation	pHILLIC
182	506.9953	16.91	C10H16N5O13P3	ATP	Oxidative phosphorylation	pHILLIC
183	663.1091	14.46	C21H27N7O14P2	NAD+	Oxidative phosphorylation	pHILLIC*
184	665.1251	13.62	C21H29N7O14P2	NADH	Oxidative phosphorylation	pHILLIC
185	97.9768	16.15	H3O4P	Orthophosphate	Oxidative phosphorylation	pHILLIC
186	217.1314	8.87	C10H19NO4	O-Propanoylcarnitine	Oxidation of Branched Fatty Acids	C18-PFP
187	239.1018	10.35	C9H13N5O3	6-Lactoyl-5,6,7,8-tetrahydropterin	Folate biosynthesis	pHILLIC
188	156.115	4.41	C9H16O2	[FA hydroxy(9:1)] 4-hydroxy-2-nonenal	Fatty aldehydes	pHILLIC
189	118.0629	7.4	C5H10O3	5-Hydroxypentanoate	Fatty Acids and Conjugates	pHILLIC
190	102.068	7.39	C5H10O2	Pentanoate	Fatty Acids and Conjugates	pHILLIC
191	173.08	5.78	C6H11N3O3	5-Guanidino-2-oxopentanoate	D-Arginine and D-ornithine metabolism	C18-PFP
192	134.0215	16.26	C4H6O5	(S)-Malate	Citrate cycle (TCA cycle)	pHILLIC
193	146.0219	6.79	C5H6O5	2-Oxoglutarate	Citrate cycle (TCA cycle)	C18-PFP
194	192.0271	18.11	C6H8O7	Citrate	Citrate cycle (TCA cycle)	pHILLIC*
195	116.0112	10.42	C4H4O4	Fumarate	Citrate cycle (TCA cycle)	C18-PFP
196	118.0266	15.42	C4H6O4	Succinate	Citrate cycle (TCA cycle)	pHILLIC*
197	339.9959	19.26	C6H14O12P2	D-Fructose 1,6-bisphosphate	Carbon fixation	pHILLIC
198	158.0692	16.23	C6H10N2O3	4-Methylene-L-glutamine	C5-Branched dibasic acid metabolism	pHILLIC
199	146.0215	15.79	C5H6O5	Methyloxaloacetate	C5-Branched dibasic acid metabolism	pHILLIC
200	134.0219	6.57	C4H6O5	(R)-Malate	Butanoate metabolism	C18-PFP
201	88.0522	7.41	C4H8O2	Butanoic acid	Butanoate metabolism	pHILLIC
202	214.1318	12.96	C10H18N2O3	Dethiobiotin	Biotin metabolism	pHILLIC
203	216.0407	5.29	C5H13O7P	2-C-Methyl-D-erythritol 4-phosphate	Biosynthesis of steroids	C18-PFP
204	219.1107	8.81	C9H17NO5	Pantothenate	beta-Alanine metabolism	pHILLIC*

205	176.032	14.23	C6H8O6	Ascorbate	Ascorbate and aldarate metabolism	pHILLIC*
206	210.0381	5.43	C6H10O8	D-Glucarate	Ascorbate and aldarate metabolism	C18-PFP
207	614.1468	15.55	C20H31N4O16P	CMP-N-acetylneuraminate	Aminosugars metabolism	pHILLIC
208	179.0793	5.48	C6H13NO5	D-Glucosamine	Aminosugars metabolism	C18-PFP
209	309.1059	13.49	C11H19NO9	N-Acetylneuraminate	Aminosugars metabolism	pHILLIC*
210	607.0815	15.37	C17H27N3O17P2	UDP-N-acetyl-D-glucosamine	Aminosugars metabolism	pHILLIC
211	167.9824	12.96	C3H5O6P	3-Phosphonopyruvate	Aminophosphonate metabolism	pHILLIC
212	111.9925	14.71	CH5O4P	Hydroxymethylphosphonate	Aminophosphonate metabolism	pHILLIC*
213	123.9925	15.27	C2H5O4P	Phosphonoacetaldehyde	Aminophosphonate metabolism	pHILLIC
214	228.1362	4.88	C12H20O4	Traumatic acid	alpha-Linolenic acid metabolism	pHILLIC*
215	161.051	9.03	C6H11NO2S	Allylcysteine	alliin degradation	C18-PFP
216	240.1473	10.34	C12H20N2O3	Slaframine	Alkaloid biosynthesis II	pHILLIC
217	222.0535	39.36	C11H10O5	2-Succinylbenzoate	Ubiquinone biosynthesis	C18-PFP
218	138.0318	42.17	C7H6O3	4-Hydroxybenzoate	Ubiquinone biosynthesis	C18-PFP
219	100.016	7.41	C4H4O3	2-oxobut-3-enanoate	3-methylquinoline degradation	pHILLIC
220	168.0787	4.72	C9H12O3	1,3,5-trimethoxybenzene	1,3,5-trimethoxybenzene biosynthesis	pHILLIC
221	247.1056	13.31	C10H17NO6	Linamarin	linamarin and lotaustralin biosynthesis	pHILLIC
222	433.1372	39.14	C15H24N5O8P	Dihydrozeatin riboside monophosphate	Zeatin biosynthesis	C18-PFP
223	178.0996	41.14	C11H14O2	Eugenol methyl ether	volatile cinnamoic ester biosynthesis	C18-PFP
224	165.0428	40.55	C8H7NO3	4-Pyridoxolactone	Vitamin B6 metabolism	C18-PFP
225	167.0583	8.16	C8H9NO3	Pyridoxal	Vitamin B6 metabolism	pHILLIC
226	247.0245	8.69	C8H10NO6P	Pyridoxal phosphate	Vitamin B6 metabolism	C18-PFP
227	131.0946	11.14	C6H13NO2	L-Leucine	Valine, leucine and isoleucine metabolism	pHILLIC*
228	117.0789	12.84	C5H11NO2	L-Valine	Valine, leucine and isoleucine metabolism	pHILLIC
229	158.0579	39.4	C7H10O4	2-Isopropylmaleate	Valine, leucine and isoleucine biosynthesis	C18-PFP
230	143.131	41.45	C8H17NO	(-)-Hygroline	Unknown	C18-PFP
231	294.1829	4.09	C17H26O4	[6]-Gingerol	Unknown	pHILLIC
232	198.0893	4.88	C10H14O4	1-(3,4-dimethoxylphenyl)ethane-1,2-diol	Unknown	pHILLIC
233	256.1055	9.33	C11H16N2O5	1-(beta-D-Ribofuranosyl)-1,4-dihydronicotinamide	Unknown	pHILLIC
234	343.2722	4.98	C19H37NO4	1,2-dioctanoyl-1-amino-2,3-propanediol	Unknown	pHILLIC
235	508.2797	3.95	C24H45O9P	1-18:2-lysophosphatidylglycerol	Unknown	pHILLIC
236	274.0454	15.44	C7H15O9P	1-Deoxy-D-altro-heptulose 7-phosphate	Unknown	pHILLIC
237	134.0577	7.95	C5H10O4	1-Deoxy-D-xylulose	Unknown	pHILLIC
238	168.0535	7.92	C7H8N2O3	2,3-Diaminosalicylic acid	Unknown	pHILLIC
239	291.0954	13.3	C11H17NO8	2,7-Anhydro-alpha-N-acetylneuraminic acid	Unknown	pHILLIC

240	164.032	12.64	C5H8O6	2-Dehydro-D-xylonate	Unknown	pHILLIC
241	259.1572	5.32	C16H21NO2	2-Heptyl-4-hydroxyquinoline-N-oxide	Unknown	pHILLIC
242	135.0531	9.05	C4H9NO4	2-Hydroxymethylserine	Unknown	C18-PFP
243	242.1518	4.46	C13H22O4	2-isocapryloyl-3R-hydroxymethyl-γ-butyrolactone	Unknown	pHILLIC
244	140.0837	5.03	C8H12O2	2-Methyl-6-oxohepta-2,4-dienal	Unknown	pHILLIC
245	245.1626	37.57	C12H23NO4	2-Methylbutyroylcarnitine	Unknown	C18-PFP
246	117.1153	5.63	C6H15NO	2-Methylcholine	Unknown	C18-PFP
247	415.3296	4.98	C23H45NO5	3-Hydroxyhexadecanoylcarnitine	Unknown	pHILLIC
248	216.0042	9.01	C4H9O8P	3-Phospho-D-erythronate	Unknown	C18-PFP
249	200.095	37.39	C12H12N2O	4-Aminophenyl ether	Unknown	C18-PFP
250	208.1466	40.82	C13H20O2	4-Heptyloxyphenol	Unknown	C18-PFP
251	194.1308	40.18	C12H18O2	4-Hexyloxyphenol	Unknown	C18-PFP
252	246.085	10.21	C9H14N2O6	5-6-Dihydrouridine	Unknown	pHILLIC
253	184.11	38.84	C10H16O3	5-exo-Hydroxy-1,2-campholide	Unknown	C18-PFP
254	241.1063	9.65	C10H15N3O4	5-Methyl-2'-deoxycytidine	Unknown	pHILLIC
255	317.0521	11.35	C9H12N5O6P	7,8-dihydroneopterin 2',3'-cyclic phosphate	Unknown	pHILLIC
256	186.0891	5.02	C9H14O4	7,8-diketopelargonate	Unknown	pHILLIC
257	165.0652	13.51	C6H7N5O	7-Methylguanine	Unknown	pHILLIC
258	395.3039	40.33	C23H41NO4	9,12-Hexadecadienoylcarnitine	Unknown	C18-PFP
259	639.0381	18.73	C15H24N5O17P3	ADPribose 2'-phosphate	Unknown	pHILLIC
260	158.0439	13.86	C4H6N4O3	Allantoin	Unknown	pHILLIC
261	208.1105	41.23	C12H16O3	Benzyl (2R,3S)-2-methyl-3-hydroxybutanoate	Unknown	C18-PFP
262	321.0696	20.5	C11H15NO10	beta-Citryl-L-glutamic acid	Unknown	pHILLIC
263	175.0846	13.58	C7H13NO4	Calystegin B2	Unknown	pHILLIC
264	201.1368	39.38	C10H19NO3	Capryloylglycine	Unknown	C18-PFP
265	369.2879	4.91	C21H39NO4	cis-5-Tetradecenoylcarnitine	Unknown	pHILLIC
266	536.0915	17.61	C31H51N10O22P3S2	CoA-glutathione	Unknown	pHILLIC
267	132.0787	38.23	C6H12O3	D-2-Hydroxyisocaproate	Unknown	C18-PFP
268	160.0848	7.62	C6H12N2O3	Daminozide	Unknown	pHILLIC
269	136.0735	11.03	C5H12O4	D-Apiitol	Unknown	pHILLIC
270	217.179	4.24	C10H23N3O2	Deoxyhypusine	Unknown	C18-PFP
271	202.0845	38.38	C9H14O5	Diethyl 2-methyl-3-oxosuccinate	Unknown	C18-PFP
272	182.071	39.93	C6H15O4P	Diisopropyl phosphate	Unknown	C18-PFP
273	159.1259	13.66	C8H17NO2	DL-2-Aminooctanoicacid	Unknown	pHILLIC
274	242.0193	16.26	C6H11O8P	D-myo-Inositol 1,2-cyclic phosphate	Unknown	pHILLIC*
275	160.1101	41.36	C8H16O3	Ethyl (R)-3-hydroxyhexanoate	Unknown	C18-PFP

276	244.0951	39.74	C12H12N4O2	Flavin	Unknown	C18-PFP
277	116.0109	14.55	C4H4O4	Formylpyruvate	Unknown	pHILLIC
278	214.084	5.03	C20H28O10	Furcatin	Unknown	pHILLIC
279	231.1584	24.19	C10H21N3O3	Gamma-Aminobutyryl-lysine	Unknown	pHILLIC
280	125.1204	7.28	C8H15N	gamma-Coniceine	Unknown	pHILLIC
281	276.0958	17.11	C10H16N2O7	GammaGlutamylglutamicacid	Unknown	pHILLIC
282	275.1118	15.54	C10H17N3O6	Gamma-Glutamylglutamine	Unknown	pHILLIC
283	321.0994	13.16	C11H19N3O6S	gamma-L-Glutamyl-L-cysteinyl-beta-alanine	Unknown	pHILLIC
284	197.0818	13.02	C20H26O8	Glaucarubolone	Unknown	pHILLIC
285	339.012	19.15	C6H15NO11P2	glucosamine-1,6-diphosphate	Unknown	pHILLIC
286	246.0503	12.83	C6H15O8P	Glycerophosphoglycerol	Unknown	pHILLIC
287	273.1944	41.72	C14H27NO4	Heptanoylcarnitine	Unknown	C18-PFP
288	259.1783	39.25	C13H25NO4	Hexanoylcarnitine	Unknown	C18-PFP
289	188.1273	4.72	C7H16N4O2	Homoarginine	Unknown	C18-PFP
290	247.142	11.71	C11H21NO5	Hydroxybutyrylcarnitine	Unknown	pHILLIC
291	246.1368	8.88	C14H18N2O2	Hypaphorine	Unknown	pHILLIC
292	204.0747	5.63	C7H12N2O5	L-beta-aspartyl-L-alanine	Unknown	C18-PFP
293	246.1215	12.03	C10H18N2O5	L-beta-aspartyl-L-leucine	Unknown	C18-PFP
294	189.1114	13.8	C7H15N3O3	L-Homocitrulline	Unknown	pHILLIC
295	195.0898	39.81	C10H13NO3	L-Tyrosine methyl ester	Unknown	C18-PFP
296	159.1259	5.73	C8H17NO2	Methacholine	Unknown	C18-PFP
297	245.1627	8.15	C12H23NO4	N-(octanoyl)-L-homoserine	Unknown	pHILLIC
298	285.096	8.48	C11H15N3O6	N4-Acetylcytidine	Unknown	pHILLIC
299	160.1212	23.97	C7H16N2O2	N6-Methyl-L-lysine	Unknown	pHILLIC*
300	223.1056	13.57	C8H17NO6	N-acetyl -D- glucosaminitol	Unknown	pHILLIC
301	304.0906	17.13	C11H16N2O8	N-Acetyl-aspartyl-glutamate	Unknown	pHILLIC*
302	220.1058	7.04	C8H16N2O5	N-Acetyl-beta-D-glucosaminylamine	Unknown	C18-PFP
303	237.0848	25.57	C8H15NO7	N-Acetyl-D-glucosaminate	Unknown	C18-PFP
304	188.0797	10.69	C7H12N2O4	N-Acetylglutamine	Unknown	pHILLIC
305	197.0802	15.87	C8H11N3O3	N-Acetyl-L-histidine	Unknown	pHILLIC
306	267.0956	17.46	C9H17NO8	Neuraminic acid	Unknown	pHILLIC
307	202.1431	22.21	C8H18N4O2	NG,NG-Dimethyl-L-arginine	Unknown	pHILLIC
308	243.0872	13.05	C23H26N4O8	nocardicin C	Unknown	pHILLIC
309	214.1207	4.62	C23H32N4O4	Nummularine F	Unknown	pHILLIC
310	243.1835	7.33	C13H25NO3	N-Undecanoylglycine	Unknown	pHILLIC*
311	212.0086	12.67	C5H9O7P	Phosphinomethylmalate	Unknown	pHILLIC
312	297.1072	10.19	C11H15N5O5	Psicofuranin	Unknown	pHILLIC
313	334.0666	16.32	C9H19O11P	sn-glycero-3-Phospho-1-inositol	Unknown	pHILLIC

314	231.1108	7.4	C10H17NO5	Suberylglycine	Unknown	pHILLIC
315	383.1076	23.36	C14H17N5O8	Succinyladenosine	Unknown	C18-PFP
316	147.0353	6.56	C5H9NO2S	Thiomorpholine 3-carboxylate	Unknown	C18-PFP
317	192.1153	41.24	C12H16O2	Thymyl acetate	Unknown	C18-PFP
318	243.1472	8.58	C12H21NO4	Tiglylcarnitine	Unknown	pHILLIC
319	271.2152	41.22	C15H29NO3	Tridecanoylglycine	Unknown	C18-PFP
320	271.2511	42.34	C16H33NO2	Undecanoylcholine	Unknown	C18-PFP
321	261.1364	7.39	C15H19NO3	Zinnimidine	Unknown	pHILLIC

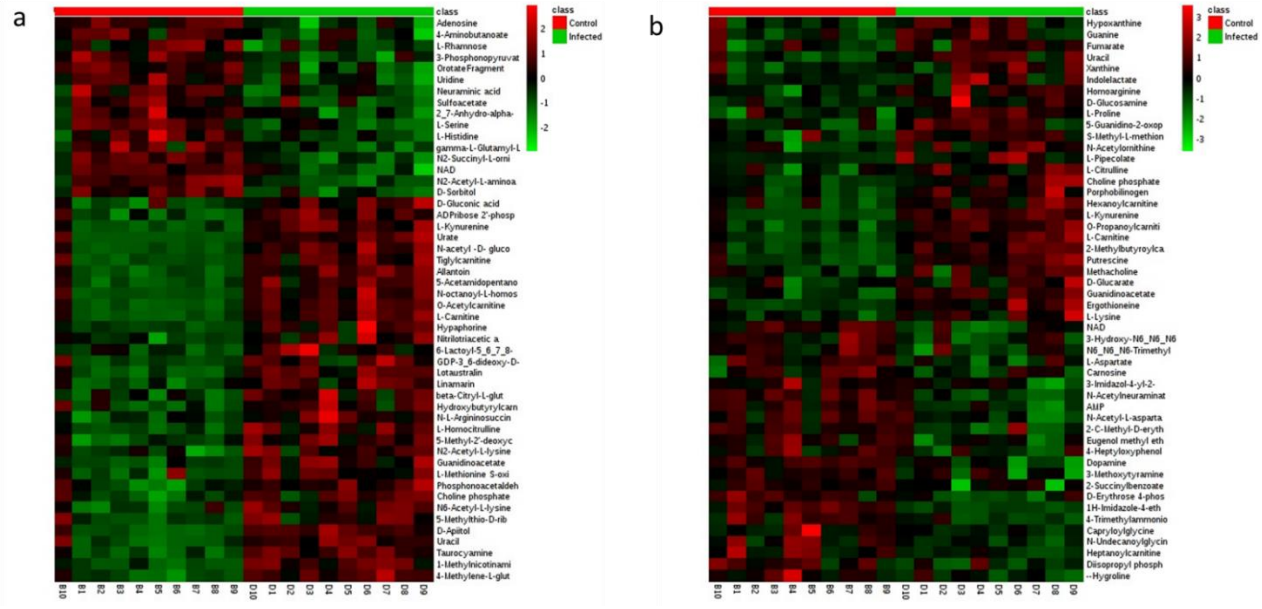

Figure 3.1 Heat map represents the significantly changed metabolites between infected group and corresponding control group according to P-value of student's t-test. (a) pHILLIC Column was used as primary column to detect the metabolites and it was augmented with (b) C18-PFP Column to obtain important missing metabolites. Normalised metabolite abundance (log 2 transformed and row adjustment) are visulaised as a color spectrum scaled from least abundant to highest range is from -3 to 3. Green indicates low expression, while red indicates high expression of the changed metabolites.

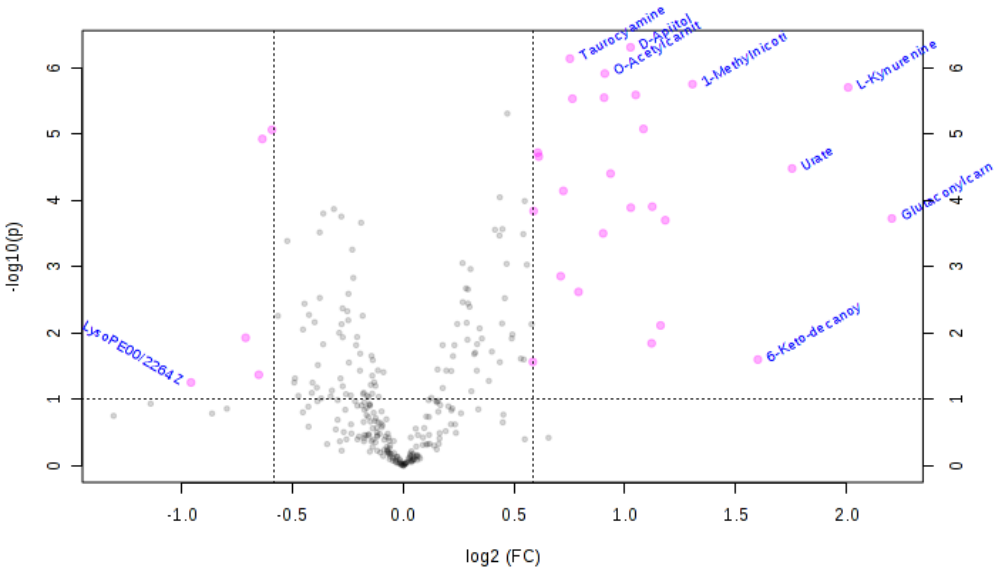

Figure 3.2 Important metabolites selected by volcano plot with log 2 fold change threshold 1.5 and t-tests threshold 0.1(using pHILLIC Column) in chronic *T.gondii* infection experiment. The red circles represent metabolites above the threshold. Note both fold changes and *P*-values are log transformed. The further its position away from the (0, 0), the more significant the feature is.

Table 0.2 Important metabolites identified by volcano plot with pHILLIC Column in chronic *T.gondii* infection experiment.

	Metabolites	**FC**	**log2(FC)**	***P*.value**	**-LOG10(p)**
1	L-Kynurenine	4.0387	2.0139	2.01E-06	5.6961
2	Urate	3.3941	1.763	3.07E-05	4.5128
3	1-Methylnicotinamide	2.4831	1.3122	1.62E-06	5.7895
4	DL-2-Aminooctanoicacid	2.2486	1.169	0.007578	2.1204
5	N-octanoyl-L-homoserine	2.1907	1.1314	0.000112	3.949
6	N-acetyl -D- glucosaminitol	2.1331	1.0929	7.79E-06	5.1084
7	L-Carnitine	2.0793	1.0561	2.43E-06	5.6152
8	D-Apiitol	2.0433	1.0309	4.41E-07	6.3557
9	L-Homocitrulline	1.9216	0.94229	3.31E-05	4.4802
10	O-Acetylcarnitine	1.8874	0.91643	1.13E-06	5.9453
11	Allantoin	1.8839	0.91375	2.25E-06	5.6473
12	Tiglylcarnitine	1.8806	0.91118	0.000286	3.5432
13	Hypaphorine	1.7108	0.77468	0.000469	3.3286
14	Lotaustralin	1.7072	0.77161	2.67E-06	5.574
15	Taurocyamine	1.6924	0.75909	5.39E-07	6.2682
16	5-Acetamidopentanoate	1.5312	0.61464	1.91E-05	4.7189
17	ADP ribose 2'-phosphate	1.513	0.59744	0.000119	3.9236
18	GDP-3_6-dideoxy-D-galactose	1.5012	0.58614	0.006648	2.1773
19	N2-Acetyl-L-aminoadipate	0.66618	-0.58602	1.00E-05	4.998
20	N2-Succinyl-L-ornithine	0.64667	-0.6289	1.31E-05	4.8827
21	6-Gingerol	0.63707	-0.65047	0.046685	1.3308
22	1-Deoxy-D-altro-heptulose 7-phosphate	0.61645	-0.69795	0.011894	1.9247

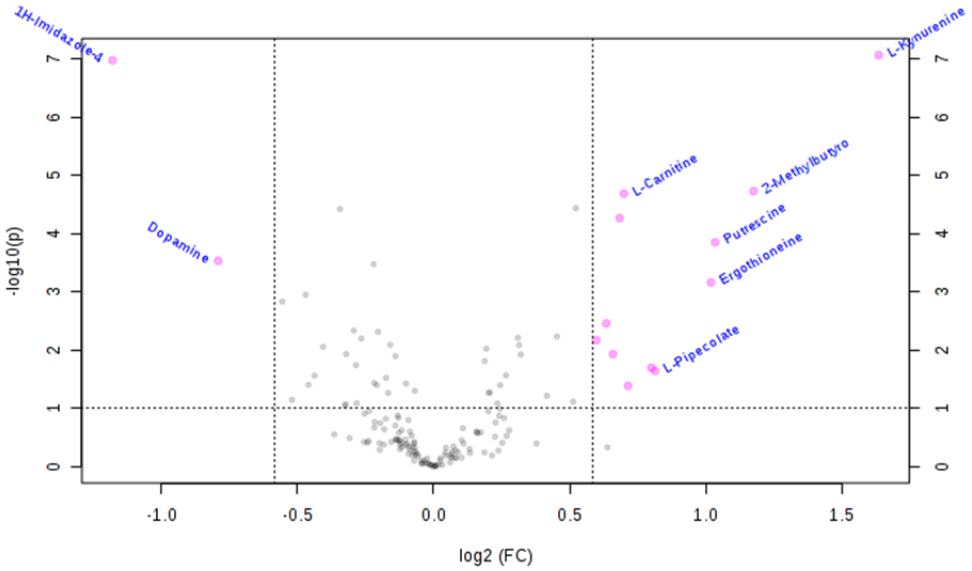

Figure 3.4 Important metabolites selected by volcano plot with log2 fold change threshold 1.5 and t-tests threshold 0.1(using C18-PFP Column) chronic *T.gondii* infection experiment. The red circles represent metabolites above the threshold.

Table 3.3 Important metabolites identified by volcano plot with C18-PFP Column chronic *T.gondii* infection experiment.

	Metabolites	**FC**	**log2(FC)**	***P*.value**	**-LOG10(p)**
1	L-Kynurenine	3.108	1.636	8.69E-08	7.061
2	2-Methylbutyroylcarnitine	2.2599	1.1763	1.88E-05	4.7255
3	Putrescine	2.0498	1.0355	0.0001416	3.849
4	Ergothioneine	2.0276	1.0198	0.0006926	3.1595
5	L-Pipecolate	1.7585	0.81431	0.022741	1.6432
6	Methacholine	1.7417	0.80048	0.02013	1.6962
7	D-Glucosamine	1.6413	0.71484	0.04108	1.3864
8	L-Carnitine	1.6241	0.69963	2.07E-05	4.6841
9	O-Propanoylcarnitine	1.6063	0.68375	5.47E-05	4.2624
10	Hexanoylcarnitine	1.5798	0.6597	0.011749	1.93
11	Porphobilinogen	1.5526	0.63473	0.00349	2.4572
12	Homoarginine	1.5143	0.5987	0.0067768	2.169
13	Dopamine	0.57752	-0.79206	0.0002946	3.5308
14	1H-Imidazole-4-ethanamine	0.44125	-1.1803	1.07E-07	6.9701

Table 3.4 Pathways are ranked by Pathway Perturbation Score (PPS) for chronic infection experiment datasets. Only the 50 top-scoring pathways are included in the table.

	Pathway	PPS
1	tryptophan degradation I (via anthranilate)	1.66
2	tryptophan degradation to 2-amino-3-carboxymuconate semialdehyde	1.44
3	NAD biosynthesis II (from tryptophan)	1.18
4	putrescine biosynthesis III	1.13
5	spermidine biosynthesis I	1.13
6	urate degradation to allantoin	1.11
7	ureide biosynthesis	0.981
8	tryptophan degradation III (eukaryotic)	0.978
9	spermine biosynthesis II	0.93
10	guanosine nucleotides degradation III	0.903
11	allantoin degradation to ureidoglycolate I (urea producing)	0.89
12	urate biosynthesis/inosine 5'-phosphate degradation	0.875
13	adenosine nucleotides degradation II	0.818
14	arginine degradation III (arginine decarboxylase/agmatinase pathway)	0.802
15	putrescine biosynthesis I	0.802
16	putrescine degradation III	0.687
17	heme biosynthesis II	0.635
18	tetrapyrrole biosynthesis II	0.635
19	purine nucleotides degradation II (aerobic)	0.597
20	L-carnitine biosynthesis	0.559
21	dopamine degradation	0.528
22	catecholamine biosynthesis	0.491
23	creatine biosynthesis	0.485
24	asparagine degradation I	0.474
25	asparagine biosynthesis I	0.474
26	creatine-phosphate energy transfer	0.463
27	glutathione redox reactions II	0.451
28	glutathione redox reactions I	0.451
29	histamine biosynthesis	0.432
30	glycine degradation (creatine biosynthesis)	0.43
31	guanine and guanosine salvage II	0.425
32	uracil degradation II (reductive)	0.413
33	citrulline-nitric oxide cycle	0.395
34	glutamine degradation II	0.385

35	aspartate degradation II	0.385
36	adenine and adenosine salvage VI	0.378
37	serine biosynthesis	0.372
38	superpathway of serine and glycine biosynthesis I	0.37
39	glycine biosynthesis I	0.362
40	L-serine degradation	0.362
41	phosphatidylethanolamine biosynthesis I	0.362
42	aspartate biosynthesis	0.356
43	inosine-5'-phosphate biosynthesis II	0.348
44	cysteine biosynthesis/homocysteine degradation	0.344
45	cysteine biosynthesis II	0.344
46	glycine betaine degradation	0.341
47	arginine biosynthesis IV	0.338
48	NAD biosynthesis III	0.336
49	pyrimidine ribonucleosides degradation II	0.33
50	purine ribonucleosides degradation to ribose-1-phosphate	0.329

Chapter 4

4.1 Quality Metrics (Infected vs. Uninfected) in acquired infection experiment.

For inspecting the quality of RNA-Seq data, the 100 most abundant genes are taken from all the samples and heat maps are generated to observe the relation between samples/conditions in acquired infection experiment.

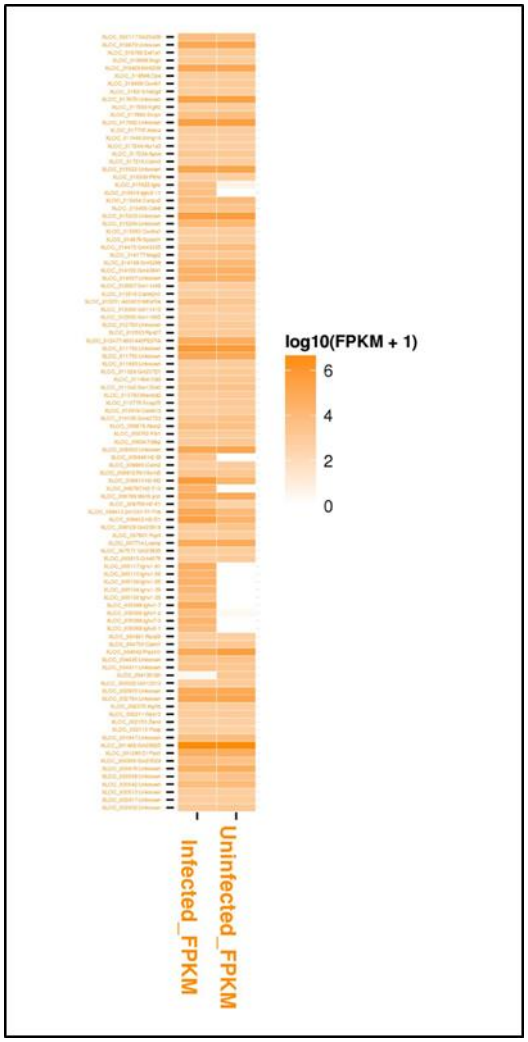

Figure 4.1 Heat map of top 100 differentially expressed genes for infected and uninfected (Control) groups in acquired infection experiment.

4.2 Scatter plots (Infected vs. Uninfected) in acquired infection experiment.

Scatter plots highlight the general similarities and specific outliers between the conditions in the RNA-Seq experiment. They are generated from the expression data for genes using the cummeR-bund package. Scatter plots can be used for inspecting overall quality of RNA-Seq data.

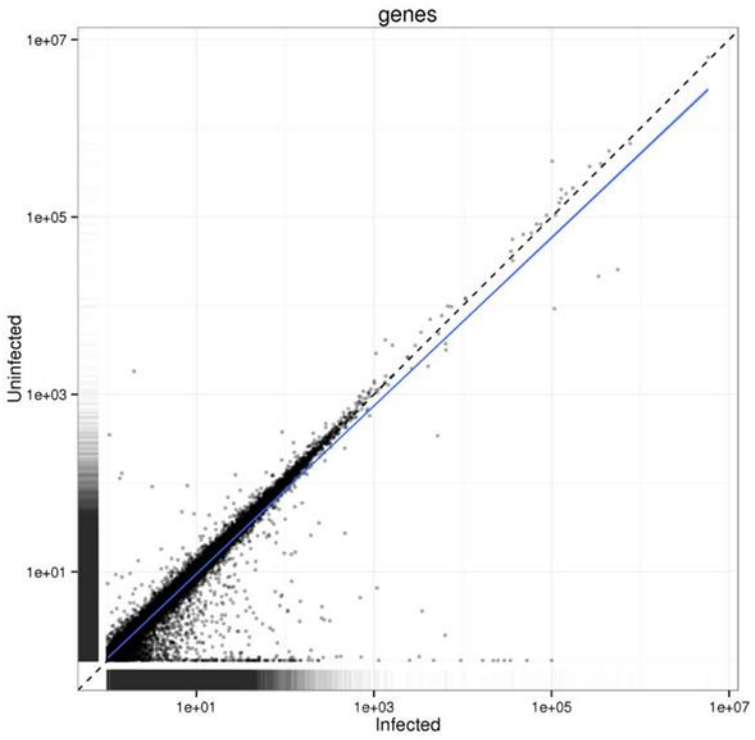

Figure 4.2 Scatter plot for infected group versus Uninfected (control) group in acquired infection experiment. In such a plot gene with equal expression values would line up on the identity line (diagonal), with higher expression values further away from the origin. Points below the diagonal represent genes with higher expression in the acquired infected samples, which plotted on the *x*-axis. Similarly, points above the diagonal represent genes with higher expression values in the control samples, which plotted on the *y*-axis. The further away the point is from the identity line the larger is the difference between its expressions in one group compared with the other.

Table 4.1 All significant genes (FDR of <0.05) upregulated in the acquired *T. gondii* infection experiment.

	Gene	Description	Average FPKM		Fold Change	FDR(q value)
			Infected (n=3)	Uninfected (n=3)		
1	Igkc	immunoglobulin kappa constant	3483.4	2.6	1340.1	0.002
2	Jchain	immunoglobulin joining chain	193.9	0.3	634.3	0.002
3	Zbp1	Z-DNA binding protein 1	20.6	0.1	239.0	0.013
4	H2-Eb1	histocompatibility 2, class II antigen E beta	316.9	1.8	176.5	0.002
5	Cd74	CD74 antigen (invariant polypeptide of major histocompatibility complex, class II antigen-associated)	700.1	4.1	170.7	0.002
6	Gm12250	predicted gene 12250	24.0	0.2	153.1	0.002
7	H2-Aa	histocompatibility 2, class II antigen A, alpha	274.9	1.9	147.1	0.002
8	Gm5970	predicted gene 5970	80.7	0.6	140.5	0.002
9	Iigp1	interferon inducible GTPase 1	80.7	0.6	140.5	0.002
10	H2-Ea-ps	histocompatibility 2, class II antigen E alpha, pseudogene	256.1	2.0	128.1	0.002
11	Cxcl10	chemokine (C-X-C motif) ligand 10	23.6	0.2	99.6	0.002
12	H2-Ab1	histocompatibility 2, class II antigen A, beta 1	258.7	3.0	85.3	0.002
13	Igtp	interferon gamma induced GTPase	145.0	1.8	82.5	0.002
14	Irgm2	immunity-related GTPase family M member 2	145.0	1.8	82.5	0.002
15	Ifi202b	interferon activated gene 202B	4.9	0.1	65.4	0.028
16	Itgax	integrin alpha X	1.8	0.0	62.7	0.037
17	Oasl2	2'-5' oligoadenylate synthetase-like 2	71.5	1.2	60.0	0.002
18	Batf2	basic leucine zipper transcription factor, ATF-like 2	5.5	0.1	58.9	0.002
19	Nlrc5	NLR family, CARD domain containing 5	3.7	0.1	57.5	0.002
20	BC023105	cDNA sequence BC023105	2.9	0.1	52.3	0.017
21	Psmb9	proteasome (prosome, macropain) subunit, beta type 9 (large multifunctional peptidase 2)	66.5	1.3	50.3	0.002
22	Gimap3	GTPase, IMAP family member 3	3.0	0.1	48.7	0.013
23	C3	complement component 3	9.2	0.2	46.1	0.002
24	Gbp2b	guanylate binding protein 2b	38.5	0.8	46.0	0.002

25	Psmb8	proteasome (prosome, macropain) subunit, beta type 8 (large multifunctional peptidase 7)	105.2	2.6	41.2	0.002
26	Ly6a	lymphocyte antigen 6 complex, locus A	147.3	3.6	40.5	0.002
27	Ifi44	interferon-induced protein 44	11.3	0.3	38.9	0.002
28	Hcar2	hydroxycarboxylic acid receptor 2	2.8	0.1	38.1	0.010
29	Ifi44l	interferon-induced protein 44 like	5.2	0.1	34.9	0.002
30	AB124611	cDNA sequence AB124611	4.4	0.1	34.9	0.002
31	Ifi204	interferon activated gene 204	3.6	0.1	34.6	0.002
32	H2-DMb1	histocompatibility 2, class II, locus Mb1	14.2	0.4	33.8	0.002
33	H2-DMb2	histocompatibility 2, class II, locus Mb2	14.2	0.4	33.8	0.002
34	Gbp2	guanylate binding protein 2	35.1	1.1	30.7	0.002
35	Ltb	lymphotoxin B	8.9	0.3	27.8	0.002
36	Spn	sialophorin	1.4	0.1	27.1	0.002
37	Il2rb	interleukin 2 receptor, beta chain	1.4	0.1	26.1	0.002
38	Phf11d	PHD finger protein 11D	3.4	0.1	25.7	0.004
39	Tap1	transporter 1, ATP-binding cassette, sub-family B (MDR/TAP)	28.7	1.1	25.6	0.002
40	Slfn8	schlafen 8	2.4	0.1	25.4	0.002
41	Cd52	CD52 antigen	28.0	1.1	24.6	0.002
42	Serpina3g	serine (or cysteine) peptidase inhibitor, clade A, member 3G	5.3	0.2	23.5	0.024
43	Gbp3	guanylate binding protein 3	46.4	2.0	23.5	0.002
44	Ptprcap	protein tyrosine phosphatase, receptor type, C polypeptide-associated protein	3.6	0.2	23.3	0.028
45	Cd274	CD274 antigen	19.2	0.8	23.2	0.002
46	Slamf8	SLAM family member 8	3.4	0.2	22.4	0.002
47	Lilr4b	leukocyte immunoglobulin-like receptor, subfamily B, member 4B	1.6	0.1	22.2	0.017
48	Lilrb4a	leukocyte immunoglobulin-like receptor, subfamily B, member 4A	1.6	0.1	22.2	0.017
49	Cxcl13	chemokine (C-X-C motif) ligand 13	3.8	0.2	22.1	0.004
50	Oas3	2'-5' oligoadenylate synthetase 3	0.8	0.0	21.9	0.005
51	C4a	complement component 4A (Rodgers blood group)	8.0	0.4	21.7	0.002
52	Mlkl	mixed lineage kinase domain-like	1.3	0.1	21.4	0.005
53	Bst2	bone marrow stromal cell antigen 2	88.7	4.3	20.8	0.002
54	Parp14	poly (ADP-ribose) polymerase family, member 14	7.3	0.4	20.6	0.002
55	Lyz2	lysozyme 2	91.0	4.5	20.3	0.002
56	Hpse	heparanase	5.1	0.3	20.1	0.002
57	Oas1a	2'-5' oligoadenylate synthetase 1A	4.7	0.2	19.9	0.002

58	Ctse	cathepsin E	1.2	0.1	19.5	0.033
59	Gbp7	guanylate binding protein 7	22.2	1.2	19.1	0.002
60	Lag3	lymphocyte-activation gene 3	10.7	0.6	18.8	0.002
61	AI662270	expressed sequence AI662270	2.7	0.1	18.8	0.008
62	Usp18	ubiquitin specific peptidase 18	11.0	0.6	18.7	0.002
63	Gbp5	guanylate binding protein 5	17.5	0.9	18.5	0.002
64	Gimap4	GTPase, IMAP family member 4	4.9	0.3	18.4	0.002
65	Epsti1	epithelial stromal interaction 1 (breast)	3.2	0.2	18.0	0.002
66	B2m	beta-2 microglobulin	470.3	26.2	18.0	0.002
67	Patl2	protein associated with topoisomerase II homolog 2 (yeast)	1.3	0.1	17.9	0.019
68	C4b	complement component 4B (Chido blood group)	42.8	2.4	17.5	0.002
69	AW112010	expressed sequence AW112010	22.6	1.3	16.9	0.002
70	Myo1g	myosin IG	0.9	0.1	16.7	0.023
71	Cytip	cytohesin 1 interacting protein	2.0	0.1	16.6	0.002
72	Irf4	interferon regulatory factor 4	0.9	0.1	16.3	0.002
73	Il18bp	interleukin 18 binding protein	10.0	0.6	16.1	0.002
74	Ifit1	interferon-induced protein with tetratricopeptide repeats 1	9.3	0.6	15.7	0.002
75	Csf2rb	colony stimulating factor 2 receptor, beta, low-affinity (granulocyte-macrophage)	1.4	0.1	15.5	0.002
76	Il1b	interleukin 1 beta	2.8	0.2	15.5	0.002
77	H2-K1	histocompatibility 2, K1, K region	5211.1	340.2	15.3	0.002
78	Ptprc	protein tyrosine phosphatase, receptor type, C	5.1	0.3	15.3	0.002
79	Fgl2	fibrinogen-like protein 2	13.1	0.9	15.2	0.002
80	Cd84	CD84 antigen	3.4	0.2	14.7	0.002
81	Ccr2	chemokine (C-C motif) receptor 2	1.2	0.1	14.6	0.004
82	Apol6	apolipoprotein L 6	1.1	0.1	14.5	0.015
83	Mx1	MX dynamin-like GTPase 1	0.8	0.1	14.2	0.046
84	Ms4a6d	membrane-spanning 4-domains, subfamily A, member 6D	5.6	0.4	14.0	0.002
85	Irf7	interferon regulatory factor 7	15.7	1.1	13.9	0.002
86	Naip2	NLR family, apoptosis inhibitory protein 2	1.0	0.1	13.8	0.002
87	Gbp11	guanylate binding protein 11	10.2	0.7	13.7	0.002
88	Gbp4	guanylate binding protein 4	10.2	0.7	13.7	0.002
89	Gm43302	predicted gene 43302	10.2	0.7	13.7	0.002
90	Ly6c2	lymphocyte antigen 6 complex, locus C2	35.1	2.6	13.4	0.002
91	Acod1	aconitate decarboxylase 1	0.8	0.1	13.3	0.038
92	Irf1	interferon regulatory factor 1	28.4	2.1	13.2	0.002
93	Mpeg1	macrophage expressed gene 1	39.0	3.0	13.1	0.002

94	Oas1b	2'-5' oligoadenylate synthetase 1B	2.0	0.2	13.0	0.004
95	Ms4a6b	membrane-spanning 4-domains, subfamily A, member 6B	5.5	0.4	12.8	0.015
96	Ncf4	neutrophil cytosolic factor 4	3.5	0.3	12.7	0.002
97	Themis2	thymocyte selection associated family member 2	2.1	0.2	12.7	0.002
98	Gm20662	predicted gene 20662	4.9	0.4	12.7	0.002
99	Ip6k1	inositol hexaphosphate kinase 1	4.9	0.4	12.7	0.002
100	Cd79a	CD79A antigen (immunoglobulin-associated alpha)	5.0	0.4	12.6	0.002
101	Slfn9	schlafen 9	1.1	0.1	12.5	0.002
102	Rtp4	receptor transporter protein 4	19.3	1.6	12.0	0.002
103	Cd48	CD48 antigen	4.1	0.3	11.9	0.002
104	Fcgr2b	Fc receptor, IgG, low affinity IIb	6.9	0.6	11.9	0.002
105	Casp4	caspase 4, apoptosis-related cysteine peptidase	1.1	0.1	11.8	0.037
106	Trim30a	tripartite motif-containing 30A	4.7	0.4	11.7	0.002
107	Cd180	CD180 antigen	1.9	0.2	11.7	0.002
108	Tlr9	toll-like receptor 9	1.0	0.1	11.5	0.002
109	Ms4a6c	membrane-spanning 4-domains, subfamily A, member 6C	3.3	0.3	11.4	0.019
110	C1ra	complement component 1, r subcomponent A	3.6	0.3	11.4	0.002
111	Cd86	CD86 antigen	3.2	0.3	11.2	0.002
112	Sp110	Sp110 nuclear body protein	1.8	0.2	11.2	0.002
113	Siglecf	sialic acid binding Ig-like lectin F	0.8	0.1	11.0	0.014
114	Itgb2	integrin beta 2	8.7	0.8	10.9	0.002
115	Gm8995	predicted gene 8995	2.5	0.2	10.8	0.002
116	Oas2	2'-5' oligoadenylate synthetase 2	0.8	0.1	10.7	0.007
117	Ddx60	DEAD (Asp-Glu-Ala-Asp) box polypeptide 60	1.2	0.1	10.6	0.002
118	AU020206	expressed sequence AU020206	6.4	0.6	10.6	0.002
119	Irf8	interferon regulatory factor 8	10.5	1.0	10.5	0.002
120	Il7r	interleukin 7 receptor	1.6	0.2	10.4	0.002
121	Csf2rb2	colony stimulating factor 2 receptor, beta 2, low-affinity (granulocyte-macrophage)	0.9	0.1	10.3	0.002
122	Tlr12	toll-like receptor 12	1.1	0.1	10.1	0.002
123	Acp5	acid phosphatase 5, tartrate resistant	1.3	0.1	10.0	0.004
124	Cd5	CD5 antigen	1.1	0.1	9.9	0.004
125	Gpr84	G protein-coupled receptor 84	1.7	0.2	9.9	0.002
126	Lcp2	lymphocyte cytosolic protein 2	3.8	0.4	9.8	0.002
127	Psd4	pleckstrin and Sec7 domain containing 4	1.2	0.1	9.7	0.002
128	Slc11a1	solute carrier family 11 (proton-coupled divalent metal ion transporters), member 1	4.6	0.5	9.6	0.002

129	Card11	caspase recruitment domain family, member 11	0.5	0.1	9.6	0.014
130	Trim14	tripartite motif-containing 14	1.2	0.1	9.4	0.015
131	Ifit3	interferon-induced protein with tetratricopeptide repeats 3	18.1	1.9	9.4	0.002
132	Ctsc	cathepsin C	16.0	1.7	9.4	0.002
133	Nos2	nitric oxide synthase 2, inducible	0.9	0.1	9.4	0.002
134	Myo1f	myosin IF	3.5	0.4	9.3	0.002
135	Itgal	integrin alpha L	4.9	0.5	9.2	0.002
136	Ptafr	platelet-activating factor receptor	1.5	0.2	9.1	0.002
137	H2-Ob	histocompatibility 2, O region beta locus	0.8	0.1	9.1	0.008
138	Slfn2	schlafen 2	7.0	0.8	9.0	0.002
139	Ifi27l2a	interferon, alpha-inducible protein 27 like 2A	20.2	2.2	9.0	0.002
140	AU020206	expressed sequence AU020206	3.0	0.3	9.0	0.002
141	Gpr35	G protein-coupled receptor 35	0.5	0.1	8.8	0.005
142	Tmem154	transmembrane protein 154	1.0	0.1	8.6	0.002
143	Adora3	adenosine A3 receptor	1.6	0.2	8.6	0.002
144	Samd9l	sterile alpha motif domain containing 9-like	5.9	0.7	8.5	0.002
145	Ptpn18	protein tyrosine phosphatase, non-receptor type 18	2.1	0.2	8.4	0.023
146	Tlr2	toll-like receptor 2	2.8	0.3	8.4	0.002
147	Dock2	dedicator of cyto-kinesis 2	2.6	0.3	8.2	0.008
148	Il12rb1	interleukin 12 receptor, beta 1	4.0	0.5	8.2	0.002
149	C1qc	complement component 1, q subcomponent, C chain	128.6	15.6	8.2	0.002
150	Fcgr1	Fc receptor, IgG, high affinity I	5.8	0.7	8.2	0.002
151	Cnr2	cannabinoid receptor 2 (macrophage)	0.4	0.0	8.2	0.024
152	Il21r	interleukin 21 receptor	1.6	0.2	8.2	0.002
153	Xaf1	XIAP associated factor 1	18.4	2.2	8.2	0.002
154	Ptpn6	protein tyrosine phosphatase, non-receptor type 6	8.3	1.0	8.1	0.002
155	Rasal3	RAS protein activator like 3	1.8	0.2	8.1	0.002
156	Rnf213	ring finger protein 213	14.0	1.7	8.0	0.002
157	Lpxn	leupaxin	1.9	0.2	8.0	0.002
158	Adgre1	adhesion G protein-coupled receptor E1	6.9	0.9	7.9	0.002
159	C1qb	complement component 1, q subcomponent, beta polypeptide	116.4	14.8	7.9	0.002
160	C1qa	complement component 1, q subcomponent, alpha polypeptide	193.1	24.8	7.8	0.002
161	Pik3ap1	phosphoinositide-3-kinase adaptor protein 1	4.5	0.6	7.7	0.002
162	Pld4	phospholipase D family, member 4	11.3	1.5	7.6	0.002

163	Icam1	intercellular adhesion molecule 1	4.5	0.6	7.6	0.002
164	H2-T24	histocompatibility 2, T region locus 24	7.6	1.0	7.6	0.002
165	C3ar1	complement component 3a receptor 1	1.3	0.2	7.6	0.002
166	Il27ra	interleukin 27 receptor, alpha	0.8	0.1	7.6	0.015
167	Siglec1	sialic acid binding Ig-like lectin 1, sialoadhesin	0.5	0.1	7.5	0.002
168	Grap2	GRB2-related adaptor protein 2	0.9	0.1	7.5	0.002
169	Cxcl16	chemokine (C-X-C motif) ligand 16	4.4	0.6	7.4	0.007
170	Trim21	tripartite motif-containing 21	8.1	1.1	7.4	0.002
171	BC035044	cDNA sequence BC035044	1.4	0.2	7.4	0.004
172	9930111J21Rik2	RIKEN cDNA 9930111J21 gene 2	4.2	0.6	7.3	0.002
173	Bcl3	B cell leukemia/lymphoma 3	1.4	0.2	7.3	0.002
174	Tap2	transporter 2, ATP-binding cassette, sub-family B (MDR/TAP)	24.9	3.4	7.2	0.002
175	Lrrc25	leucine rich repeat containing 25	1.0	0.1	7.2	0.021
176	Gpnmb	glycoprotein (transmembrane) nmb	2.2	0.3	7.2	0.002
177	Cysltr2	cysteinyl leukotriene receptor 2	0.6	0.1	7.2	0.002
178	Csf3r	colony stimulating factor 3 receptor (granulocyte)	3.3	0.5	7.0	0.002
179	Ctss	cathepsin S	239.3	34.5	6.9	0.002
180	Rac2	RAS-related C3 botulinum substrate 2	6.4	0.9	6.9	0.002
181	Tmem173	transmembrane protein 173	3.5	0.5	6.8	0.002
182	Lcn2	lipocalin 2	6.8	1.0	6.8	0.002
183	Ccl22	chemokine (C-C motif) ligand 22	0.7	0.1	6.8	0.026
184	Hck	hemopoietic cell kinase	4.3	0.6	6.8	0.002
185	Lgals3bp	lectin, galactoside-binding, soluble, 3 binding protein	34.2	5.1	6.7	0.002
186	Aif1	allograft inflammatory factor 1	12.0	1.8	6.7	0.002
187	Clec4a3	C-type lectin domain family 4, member a3	1.5	0.2	6.6	0.008
188	Lcp1	lymphocyte cytosolic protein 1	14.0	2.1	6.6	0.002
189	Ptpn22	protein tyrosine phosphatase, non-receptor type 22 (lymphoid)	1.0	0.2	6.6	0.002
190	Dtx3l	deltex 3-like, E3 ubiquitin ligase	6.6	1.0	6.5	0.002
191	Tifab	TRAF-interacting protein with forkhead-associated domain, family member B	2.0	0.3	6.4	0.002
192	Neurl3	neuralized E3 ubiquitin protein ligase 3	1.1	0.2	6.4	0.010
193	Gmfg	glia maturation factor, gamma	4.1	0.6	6.4	0.024
194	Hcls1	hematopoietic cell specific Lyn substrate 1	7.8	1.2	6.4	0.002
195	Ifitm3	interferon induced transmembrane protein 3	96.5	15.2	6.4	0.002
196	Vav1	vav 1 oncogene	4.1	0.6	6.3	0.002
197	Plbd1	phospholipase B domain containing 1	1.2	0.2	6.3	0.002

198	Socs1	suppressor of cytokine signaling 1	6.9	1.1	6.2	0.002
199	Parp9	poly (ADP-ribose) polymerase family, member 9	7.7	1.2	6.2	0.002
200	Ikzf1	IKAROS family zinc finger 1	3.0	0.5	6.2	0.002
201	Gsdmd	gasdermin D	3.0	0.5	6.2	0.002
202	Serpina3f	serine (or cysteine) peptidase inhibitor, clade A, member 3F	5.6	0.9	6.2	0.002
203	Serpina3h	serine (or cysteine) peptidase inhibitor, clade A, member 3H	5.6	0.9	6.2	0.002
204	Fcer1g	Fc receptor, IgE, high affinity I, gamma polypeptide	23.3	3.8	6.1	0.002
205	Lgals3	lectin, galactose binding, soluble 3	4.9	0.8	6.0	0.002
206	A530040E14Rik	RIKEN cDNA A530040E14 gene	2.2	0.4	6.0	0.002
207	Tbc1d10c	TBC1 domain family, member 10c	1.1	0.2	5.8	0.010
208	Rhoh	ras homolog family member H	1.5	0.3	5.8	0.002
209	I830077J02Rik	RIKEN cDNA I830077J02 gene	0.6	0.1	5.8	0.005
210	Slc15a3	solute carrier family 15, member 3	4.0	0.7	5.7	0.002
211	Gm20559	predicted gene, 20559	1.9	0.3	5.7	0.002
212	Arhgap30	Rho GTPase activating protein 30	3.3	0.6	5.7	0.002
213	Cryba4	crystallin, beta A4	2.5	0.4	5.7	0.024
214	Serping1	serine (or cysteine) peptidase inhibitor, clade G, member 1	19.0	3.3	5.7	0.002
215	Itgb7	integrin beta 7	3.1	0.5	5.6	0.002
216	Bst1	bone marrow stromal cell antigen 1	0.8	0.1	5.6	0.049
217	P2ry6	pyrimidinergic receptor P2Y, G-protein coupled, 6	3.3	0.6	5.6	0.002
218	Ncf1	neutrophil cytosolic factor 1	8.1	1.5	5.6	0.002
219	Cd300c2	CD300C molecule 2	5.4	1.0	5.6	0.002
220	Il1a	interleukin 1 alpha	1.5	0.3	5.5	0.004
221	Gna15	guanine nucleotide binding protein, alpha 15	1.9	0.4	5.5	0.002
222	Ccl6	chemokine (C-C motif) ligand 6	1.1	0.2	5.5	0.032
223	Ly86	lymphocyte antigen 86	26.9	4.9	5.5	0.002
224	9930111J21Rik1	RIKEN cDNA 9930111J21 gene 1	5.1	0.9	5.4	0.002
225	Gm12185	predicted gene 12185	5.1	0.9	5.4	0.002
226	Hexim2	hexamethylene bis-acetamide inducible 2	1.5	0.3	5.4	0.002
227	Tmed7	transmembrane p24 trafficking protein 7	0.5	0.1	5.4	0.021
228	Pla2g2d	phospholipase A2, group IID	0.8	0.2	5.4	0.023
229	Dram1	DNA-damage regulated autophagy modulator 1	1.0	0.2	5.4	0.002
230	Tbxas1	thromboxane A synthase 1, platelet	1.5	0.3	5.3	0.004
231	Ifih1	interferon induced with helicase C domain 1	3.6	0.7	5.3	0.002
232	Fcgr3	Fc receptor, IgG, low affinity III	18.4	3.5	5.3	0.002

233	Runx1	runt related transcription factor 1	0.6	0.1	5.1	0.002
234	Hmha1	Rho GTPase activating protein 45	2.8	0.5	5.0	0.002
235	Ifi35	interferon-induced protein 35	9.4	1.9	5.0	0.002
236	Tnfsf10	tumor necrosis factor (ligand) superfamily, member 10	2.6	0.5	4.9	0.002
237	Unc93b1	unc-93 homolog B1 (C. elegans)	16.0	3.3	4.9	0.002
238	Rsad2	radical S-adenosyl methionine domain containing 2	2.2	0.4	4.9	0.002
239	Sp100	nuclear antigen Sp100	4.4	0.9	4.9	0.002
240	Spi1	spleen focus forming virus (SFFV) proviral integration oncogene	10.9	2.3	4.8	0.002
241	Casp1	caspase 1	7.7	1.6	4.8	0.002
242	H2-M3	histocompatibility 2, M region locus 3	8.5	1.8	4.8	0.002
243	C1rl	complement component 1, r subcomponent-like	0.6	0.1	4.8	0.028
244	Ifi203	interferon activated gene 203	3.7	0.8	4.8	0.002
245	Mndal	myeloid nuclear differentiation antigen like	3.7	0.8	4.8	0.002
246	Cd40	CD40 antigen	1.2	0.3	4.7	0.005
247	Arhgap9	Rho GTPase activating protein 9	1.6	0.3	4.7	0.004
248	Nckap1l	NCK associated protein 1 like	5.1	1.1	4.7	0.002
249	Cd37	CD37 antigen	5.7	1.2	4.7	0.002
250	Rab20	RAB20, member RAS oncogene family	1.7	0.4	4.7	0.042
251	Fam46c	family with sequence similarity 46, member C	3.2	0.7	4.7	0.002
252	Ddx58	DEAD (Asp-Glu-Ala-Asp) box polypeptide 58	4.5	1.0	4.6	0.002
253	Ncf2	neutrophil cytosolic factor 2	3.1	0.7	4.6	0.002
254	Tnfrsf1b	tumor necrosis factor receptor superfamily, member 1b	2.7	0.6	4.6	0.002
255	Irf9	interferon regulatory factor 9	20.6	4.5	4.6	0.002
256	Rnf31	ring finger protein 31	20.6	4.5	4.6	0.002
257	Irf5	interferon regulatory factor 5	3.3	0.7	4.5	0.002
258	Ccr5	chemokine (C-C motif) receptor 5	4.9	1.1	4.5	0.002
259	Gm44751	predicted gene 44751	0.8	0.2	4.5	0.018
260	Lgals9	lectin, galactose binding, soluble 9	10.9	2.4	4.5	0.002
261	Lpcat2	lysophosphatidylcholine acyltransferase 2	7.7	1.7	4.5	0.002
262	Aim2	absent in melanoma 2	1.6	0.4	4.4	0.002
263	Tmem106a	transmembrane protein 106A	2.0	0.4	4.4	0.002
264	Fam167b	family with sequence similarity 167, member B	2.4	0.5	4.4	0.014
265	Cd36	CD36 molecule	1.7	0.4	4.3	0.002
266	Arl11	ADP-ribosylation factor-like 11	1.2	0.3	4.3	0.034
267	Cd53	CD53 antigen	8.5	2.0	4.3	0.002
268	H2-T22	histocompatibility 2, T region locus 22	18.2	4.2	4.3	0.002

269	Parp12	poly (ADP-ribose) polymerase family, member 12	9.5	2.2	4.3	0.002
270	Pik3cg	phosphatidylinositol-4,5-bisphosphate 3-kinase catalytic subunit gamma	1.1	0.3	4.3	0.002
271	Trim12c	tripartite motif-containing 12C	6.6	1.6	4.2	0.002
272	Klhl6	kelch-like 6	1.7	0.4	4.2	0.002
273	Cyba	cytochrome b-245, alpha polypeptide	24.0	5.7	4.2	0.002
274	Tnfaip8l2	tumor necrosis factor, alpha-induced protein 8-like 2	3.8	0.9	4.2	0.002
275	Gimap9	GTPase, IMAP family member 9	0.9	0.2	4.1	0.038
276	Ifit1bl2	interferon induced protein with tetratricopeptide repeats 1B like 2	0.5	0.1	4.1	0.028
277	Mx2	MX dynamin-like GTPase 2	1.4	0.3	4.1	0.002
278	Zc3hav1	zinc finger CCCH type, antiviral 1	5.8	1.4	4.1	0.002
279	Laptm5	lysosomal-associated protein transmembrane 5	28.7	7.0	4.1	0.002
280	Ifit3b	interferon-induced protein with tetratricopeptide repeats 3B	11.6	2.8	4.1	0.002
281	Tnfrsf13b	tumor necrosis factor receptor superfamily, member 13b	1.6	0.4	4.1	0.004
282	Cd33	CD33 antigen	2.1	0.5	4.0	0.002
283	Casp12	caspase 12	2.7	0.7	4.0	0.002
284	Il10ra	interleukin 10 receptor, alpha	4.0	1.0	4.0	0.002
285	Crybb1	crystallin, beta B1	10.4	2.6	4.0	0.002
286	Trac	T cell receptor alpha constant	5.4	1.4	4.0	0.002
287	Ifit2	interferon-induced protein with tetratricopeptide repeats 2	13.6	3.5	3.9	0.002
288	Dok2	docking protein 2	1.0	0.2	3.9	0.022
289	Hlx	H2.0-like homeobox	0.9	0.2	3.9	0.014
290	Ada	adenosine deaminase	1.3	0.3	3.9	0.013
291	Trem2	triggering receptor expressed on myeloid cells 2	22.1	5.7	3.9	0.002
292	Ifi27	interferon, alpha-inducible protein 27	77.6	20.2	3.8	0.002
293	Tmem119	transmembrane protein 119	22.0	5.7	3.8	0.002
294	Susd3	sushi domain containing 3	1.7	0.4	3.8	0.011
295	Tyrobp	TYRO protein tyrosine kinase binding protein	45.5	12.1	3.8	0.002
296	Map4k1	mitogen-activated protein kinase 1	1.0	0.3	3.8	0.002
297	Herc6	hect domain and RLD 6	9.8	2.6	3.7	0.002
298	Top2a	topoisomerase (DNA) II alpha	1.0	0.3	3.7	0.002
299	Apobec1	apolipoprotein B mRNA editing enzyme, catalytic polypeptide 1	3.6	1.0	3.7	0.002
300	Lat2	linker for activation of T cells family, member 2	2.5	0.7	3.6	0.005
301	Cd44	CD44 antigen	3.1	0.9	3.6	0.002
302	Samhd1	SAM domain and HD domain, 1	11.6	3.2	3.6	0.002

303	Socs3	suppressor of cytokine signaling 3	2.6	0.7	3.6	0.002
304	Birc3	baculoviral IAP repeat-containing 3	1.8	0.5	3.6	0.002
305	Cd300a	CD300A molecule	2.2	0.6	3.6	0.002
306	Syk	spleen tyrosine kinase	1.6	0.4	3.6	0.002
307	Slc7a7	solute carrier family 7 (cationic amino acid transporter, y+ system), member 7	2.6	0.7	3.6	0.026
308	Atf3	activating transcription factor 3	1.4	0.4	3.6	0.011
309	Tapbpl	TAP binding protein-like	8.3	2.3	3.6	0.002
310	Xdh	xanthine dehydrogenase	5.5	1.6	3.5	0.002
311	Tlr6	toll-like receptor 6	0.9	0.2	3.5	0.004
312	Inpp5d	inositol polyphosphate-5-phosphatase D	4.6	1.3	3.5	0.002
313	Akna	AT-hook transcription factor	2.2	0.6	3.5	0.002
314	Gm28177	predicted gene 28177	1.1	0.3	3.5	0.011
315	Stat1	signal transducer and activator of transcription 1	1.1	0.3	3.5	0.011
316	Eif2ak2	eukaryotic translation initiation factor 2-alpha kinase 2	7.2	2.1	3.5	0.002
317	Lgals3bp	lectin, galactoside-binding, soluble, 3 binding protein	1.1	0.3	3.5	0.034
318	Itk	IL2 inducible T cell kinase	0.9	0.3	3.5	0.002
319	Bin2	bridging integrator 2	3.4	1.0	3.4	0.002
320	Plcg2	phospholipase C, gamma 2	2.8	0.8	3.4	0.002
321	Tmem72	transmembrane protein 72	0.6	0.2	3.4	0.011
322	Dok1	docking protein 1	2.6	0.8	3.4	0.002
323	Gbgt1	globoside alpha-1, 3-N-acetylgalactosaminyltransferase 1	1.6	0.5	3.4	0.002
324	Arhgdib	Rho, GDP dissociation inhibitor (GDI) beta	20.2	6.0	3.3	0.002
325	Ctsh	cathepsin H	15.0	4.5	3.3	0.002
326	Plcb2	phospholipase C, beta 2	0.8	0.2	3.3	0.004
327	Cyth4	cytohesin 4	7.1	2.1	3.3	0.002
328	Slamf9	SLAM family member 9	1.6	0.5	3.3	0.041
329	Havcr2	hepatitis A virus cellular receptor 2	1.0	0.3	3.3	0.002
330	Lrmp	lymphoid-restricted membrane protein	1.6	0.5	3.3	0.026
331	Rhbdf2	rhomboid 5 homolog 2	0.8	0.3	3.2	0.011
332	Ube2l6	ubiquitin-conjugating enzyme E2L 6	11.7	3.6	3.2	0.002
333	Parp3	poly (ADP-ribose) polymerase family, member 3	4.3	1.3	3.2	0.002
334	Tlr1	toll-like receptor 1	2.1	0.7	3.2	0.002
335	Stat2	signal transducer and activator of transcription 2	19.4	6.0	3.2	0.002
336	Amica1	junction adhesion molecule like	3.4	1.1	3.2	0.028
337	Capg	capping protein (actin filament), gelsolin-like	3.9	1.2	3.2	0.002

338	Cmtm7	CKLF-like MARVEL transmembrane domain containing 7	7.3	2.3	3.2	0.002
339	Pbx2	pre B cell leukemia homeobox 2	3.0	1.0	3.2	0.005
340	Plek	pleckstrin	9.3	2.9	3.2	0.002
341	Tspo	translocator protein	25.9	8.3	3.1	0.002
342	Cd6	CD6 antigen	2.2	0.7	3.1	0.007
343	Hpgds	hematopoietic prostaglandin D synthase	2.5	0.8	3.1	0.002
344	Csf1r	colony stimulating factor 1 receptor	36.3	11.7	3.1	0.002
345	Lsp1	lymphocyte specific 1	5.9	1.9	3.1	0.002
346	Ifi30	interferon gamma inducible protein 30	5.2	1.7	3.0	0.002
347	Nmi	N-myc (and STAT) interactor	8.1	2.7	3.0	0.002
348	Slc37a2	solute carrier family 37 (glycerol-3-phosphate transporter), member 2	1.1	0.4	3.0	0.002
349	Dock8	dedicator of cytokinesis 8	1.3	0.4	3.0	0.002
350	Arc	activity regulated cytoskeletal-associated protein	79.5	26.7	3.0	0.002
351	Apobec3	apolipoprotein B mRNA editing enzyme, catalytic polypeptide 3	2.2	0.7	3.0	0.004
352	Trim56	tripartite motif-containing 56	4.5	1.5	3.0	0.002
353	Cfb	complement factor B	4.8	1.6	3.0	0.005
354	Gm20547	predicted gene 20547	4.8	1.6	3.0	0.005
355	Clec2d	C-type lectin domain family 2, member d	5.3	1.8	3.0	0.007
356	Prdm1	PR domain containing 1, with ZNF domain	0.7	0.2	2.9	0.015
357	Ggta1	glycoprotein galactosyltransferase alpha 1, 3	2.8	1.0	2.9	0.002
358	Lck	lymphocyte protein tyrosine kinase	4.1	1.4	2.9	0.022
359	Tgm2	transglutaminase 2, C polypeptide	22.8	7.9	2.9	0.002
360	Icosl	icos ligand	3.8	1.3	2.9	0.002
361	Parvg	parvin, gamma	3.6	1.2	2.9	0.002
362	Helz2	helicase with zinc finger 2, transcriptional coactivator	1.0	0.4	2.9	0.002
363	Gm10271	predicted gene 10271	5.8	2.0	2.9	0.002
364	Dhx58	DEXH (Asp-Glu-X-His) box polypeptide 58	2.3	0.8	2.9	0.019
365	Egr2	early growth response 2	3.7	1.3	2.9	0.002
366	Osmr	oncostatin M receptor	1.8	0.6	2.9	0.002
367	Pla1a	phospholipase A1 member A	1.4	0.5	2.8	0.037
368	Snx20	sorting nexin 20	2.0	0.7	2.8	0.005
369	Srgn	serglycin	21.6	7.7	2.8	0.002
370	Cmklr1	chemokine-like receptor 1	1.0	0.4	2.8	0.013
371	Apbb1ip	amyloid beta (A4) precursor protein-binding, family B, member 1 interacting protein	2.5	0.9	2.7	0.004
372	Itgam	integrin alpha M	4.7	1.7	2.7	0.002
373	Gimap6	GTPase, IMAP family member 6	4.4	1.6	2.7	0.004

374	Tram2	translocating chain-associating membrane protein 2	0.6	0.2	2.7	0.023
375	Fes	feline sarcoma oncogene	1.9	0.7	2.7	0.008
376	Slfn5	schlafen 5	3.8	1.4	2.7	0.007
377	Erap1	endoplasmic reticulum aminopeptidase 1	7.0	2.6	2.7	0.002
378	Psmb10	proteasome (prosome, macropain) subunit, beta type 10	65.4	24.4	2.7	0.002
379	Lyn	LYN proto-oncogene, Src family tyrosine kinase	6.0	2.2	2.7	0.002
380	Lrrk1	leucine-rich repeat kinase 1	1.5	0.6	2.7	0.002
381	Nfam1	Nfat activating molecule with ITAM motif 1	1.3	0.5	2.7	0.018
382	Casp8	caspase 8	2.4	0.9	2.6	0.026
383	Gfap	glial fibrillary acidic protein	154.5	58.6	2.6	0.002
384	Selplg	selectin, platelet (p-selectin) ligand	13.5	5.1	2.6	0.002
385	Fgd2	FYVE, RhoGEF and PH domain containing 2	3.5	1.3	2.6	0.004
386	Entpd1	ectonucleoside triphosphate diphosphohydrolase 1	5.6	2.1	2.6	0.002
387	Trim25	tripartite motif-containing 25	3.5	1.3	2.6	0.002
388	Cd14	CD14 antigen	3.1	1.2	2.6	0.023
389	Nod1	nucleotide-binding oligomerization domain containing 1	4.2	1.6	2.6	0.002
390	Hexb	hexosaminidase B	98.9	38.1	2.6	0.002
391	Tgif1	TGFB-induced factor homeobox 1	1.9	0.7	2.6	0.046
392	Vcam1	vascular cell adhesion molecule 1	17.0	6.6	2.6	0.002
393	Adap2	ArfGAP with dual PH domains 2	3.7	1.4	2.6	0.002
394	Olfml3	olfactomedin-like 3	5.6	2.2	2.6	0.002
395	Alox5ap	arachidonate 5-lipoxygenase activating protein	6.2	2.4	2.6	0.018
396	Ly6c1	lymphocyte antigen 6 complex, locus C1	64.1	25.3	2.5	0.002
397	Vwa5a	von Willebrand factor A domain containing 5A	5.0	2.0	2.5	0.002
398	Rab32	RAB32, member RAS oncogene family	1.7	0.7	2.5	0.040
399	Tgfb1	transforming growth factor, beta 1	6.8	2.7	2.5	0.007
400	Mafb	v-maf musculoaponeurotic fibrosarcoma oncogene family, protein B (avian)	9.7	3.9	2.5	0.002
401	Sh3bp2	SH3-domain binding protein 2	2.0	0.8	2.5	0.011
402	Pdzph1	PDZ and pleckstrin homology domains 1	9.4	3.8	2.5	0.007
403	Card6	caspase recruitment domain family, member 6	0.7	0.3	2.5	0.032
404	Fli1	Friend leukemia integration 1	2.8	1.1	2.5	0.002

405	Lacc1	laccase (multicopper oxidoreductase) domain containing 1	1.1	0.4	2.5	0.027
406	Cd68	CD68 antigen	8.3	3.4	2.5	0.002
407	Cx3cr1	chemokine (C-X3-C motif) receptor 1	42.8	17.5	2.4	0.004
408	Hspa1b	heat shock protein 1B	3.6	1.5	2.4	0.002
409	Tlr4	toll-like receptor 4	1.0	0.4	2.4	0.002
410	Stat3	signal transducer and activator of transcription 3	25.9	10.7	2.4	0.002
411	Ly6e	lymphocyte antigen 6 complex, locus E	127.3	53.0	2.4	0.002
412	Serpinb9	serine (or cysteine) peptidase inhibitor, clade B, member 9	7.4	3.1	2.4	0.002
413	Rinl	Ras and Rab interactor-like	2.0	0.8	2.4	0.019
414	B4galt1	UDP-Gal:betaGlcNAc beta 1, 4- galactosyltransferase, polypeptide 1	3.1	1.3	2.4	0.019
415	Tgfbr2	transforming growth factor, beta receptor II	7.8	3.3	2.4	0.002
416	Psme2	proteasome (prosome, macropain) activator subunit 2 (PA28 beta)	26.5	11.2	2.4	0.024
417	Slfn5	schlafen 5	3.2	1.3	2.4	0.002
418	Pik3r5	phosphoinositide-3-kinase regulatory subunit 5	1.1	0.5	2.3	0.028
419	Ccdc88b	coiled-coil domain containing 88B	1.8	0.8	2.3	0.045
420	Ptgs1	prostaglandin-endoperoxide synthase 1	5.0	2.1	2.3	0.002
421	Itpripl1	inositol 1,4,5-triphosphate receptor interacting protein-like 1	1.1	0.5	2.3	0.047
422	Grn	granulin	39.9	17.2	2.3	0.002
423	Arpc1b	actin related protein 2/3 complex, subunit 1B	16.8	7.3	2.3	0.002
424	Thbs1	thrombospondin 1	1.4	0.6	2.3	0.013
425	Vsir	V-set immunoregulatory receptor	6.8	3.0	2.3	0.002
426	Cp	ceruloplasmin	6.1	2.7	2.3	0.004
427	Tor4a	torsin family 4, member A	2.3	1.0	2.3	0.017
428	Tor3a	torsin family 3, member A	10.2	4.5	2.3	0.002
429	Tgfbi	transforming growth factor, beta induced	2.4	1.1	2.2	0.030
430	Blnk	B cell linker	4.6	2.1	2.2	0.017
431	Jak3	Janus kinase 3	2.8	1.2	2.2	0.010
432	Psme1	proteasome (prosome, macropain) activator subunit 1 (PA28 alpha)	73.5	33.4	2.2	0.002
433	Edem1	ER degradation enhancer, mannosidase alpha-like 1	5.4	2.5	2.2	0.002
434	Hk2	hexokinase 2	2.4	1.1	2.2	0.005
435	Pon3	paraoxonase 3	2.0	0.9	2.2	0.007
436	Ptgs2	prostaglandin-endoperoxide synthase 2	3.8	1.7	2.2	0.005
437	Mov10	Moloney leukemia virus 10	2.3	1.1	2.1	0.030

438	Ctsz	cathepsin Z	56.8	26.5	2.1	0.005
439	Nr4a2	nuclear receptor subfamily 4, group A, member 2	13.1	6.1	2.1	0.002
440	Gm43720	predicted gene 43720	4.0	1.9	2.1	0.049
441	Gpc2	glypican 2 (cerebroglycan)	4.0	1.9	2.1	0.049
442	Pim1	proviral integration site 1	4.1	1.9	2.1	0.010
443	Slc12a7	solute carrier family 12, member 7	2.9	1.4	2.1	0.022
444	Itga4	integrin alpha 4	2.4	1.1	2.1	0.008
445	Myd88	myeloid differentiation primary response gene 88	4.4	2.1	2.1	0.046
446	Rab3il1	RAB3A interacting protein (rabin3)-like 1	5.2	2.5	2.1	0.023
447	Fos	FBJ osteosarcoma oncogene	17.1	8.3	2.1	0.002
448	Glipr2	GLI pathogenesis-related 2	3.9	1.9	2.0	0.034
449	Mdfic	MyoD family inhibitor domain containing	3.3	1.6	2.0	0.018
450	Abca9	ATP-binding cassette, sub-family A (ABC1), member 9	2.4	1.2	2.0	0.002
451	Csf1	colony stimulating factor 1 (macrophage)	8.6	4.2	2.0	0.002
452	Arhgap25	Rho GTPase activating protein 25	3.2	1.6	2.0	0.032
453	Fam78a	family with sequence similarity 78, member A	2.5	1.3	2.0	0.008
454	Shisa5	shisa family member 5	47.9	24.5	2.0	0.002
455	Ddr2	discoidin domain receptor family, member 2	2.6	1.3	1.9	0.004
456	Nfatc1	nuclear factor of activated T cells, cytoplasmic, calcineurin dependent 1	2.2	1.1	1.9	0.035
457	Vim	vimentin	69.2	35.9	1.9	0.002
458	P2rx7	purinergic receptor P2X, ligand-gated ion channel, 7	2.3	1.2	1.9	0.014
459	Anxa4	annexin A4	5.4	2.8	1.9	0.029
460	Tnfaip3	tumor necrosis factor, alpha-induced protein 3	2.3	1.2	1.9	0.034
461	Ttr	transthyretin	467.2	245.9	1.9	0.002
462	Pros1	protein S (alpha)	6.4	3.4	1.9	0.004
463	Sdf2l1	stromal cell-derived factor 2-like 1	24.7	13.1	1.9	0.010
464	Sla	src-like adaptor	4.8	2.6	1.9	0.023
465	Txnip	thioredoxin interacting protein	12.5	6.7	1.9	0.002
466	Cflar	CASP8 and FADD-like apoptosis regulator	5.5	3.0	1.9	0.002
467	Tnfrsf1a	tumor necrosis factor receptor superfamily, member 1a	9.1	4.9	1.8	0.015
468	Akap13	A kinase (PRKA) anchor protein 13	3.8	2.1	1.8	0.002
469	Homer1	homer scaffolding protein 1	38.7	21.0	1.8	0.005
470	Fam46a	family with sequence similarity 46, member A	3.3	1.8	1.8	0.030
471	Tlr3	toll-like receptor 3	5.4	3.0	1.8	0.010
472	Myh9	myosin, heavy polypeptide 9, non-muscle	17.2	9.5	1.8	0.002

473	Tifa	TRAF-interacting protein with forkhead-associated domain	9.1	5.0	1.8	0.005
474	Afmid	arylformamidase	9.9	5.5	1.8	0.029
475	Cmpk2	cytidine monophosphate (UMP-CMP) kinase 2, mitochondrial	15.4	8.7	1.8	0.004
476	Ifnar2	interferon (alpha and beta) receptor 2	7.4	4.2	1.8	0.038
477	Itgb5	integrin beta 5	22.9	13.0	1.8	0.002
478	Nfe2l2	nuclear factor, erythroid derived 2, like 2	13.4	7.6	1.8	0.005
479	Creld2	cysteine-rich with EGF-like domains 2	19.5	11.1	1.8	0.013
480	Clic1	chloride intracellular channel 1	22.2	12.7	1.7	0.017
481	Man2b1	mannosidase 2, alpha B1	10.5	6.0	1.7	0.005
482	Nr4a1	nuclear receptor subfamily 4, group A, member 1	33.2	19.3	1.7	0.002
483	Dusp6	dual specificity phosphatase 6	20.6	12.0	1.7	0.007
484	Znfx1	zinc finger, NFX1-type containing 1	17.0	9.9	1.7	0.008
485	Egr1	early growth response 1	84.4	49.4	1.7	0.008
486	Rspo2	R-spondin 2	5.8	3.4	1.7	0.044
487	Tgfbr1	transforming growth factor, beta receptor I	7.0	4.1	1.7	0.017
488	Parp11	poly (ADP-ribose) polymerase family, member 11	7.4	4.4	1.7	0.015
489	Fosl2	fos-like antigen 2	5.9	3.5	1.7	0.019
490	Slc7a11	solute carrier family 7 (cationic amino acid transporter, y+ system), member 11	8.7	5.3	1.6	0.013
491	Mob1a	MOB kinase activator 1A	11.3	6.9	1.6	0.015
492	Irf2	interferon regulatory factor 2	14.2	8.7	1.6	0.028
493	Iqgap1	IQ motif containing GTPase activating protein 1	4.4	2.7	1.6	0.023
494	Nr4a3	nuclear receptor subfamily 4, group A, member 3	9.1	5.6	1.6	0.034
495	Klf10	Kruppel-like factor 10	10.2	6.3	1.6	0.041
496	Lap3	leucine aminopeptidase 3	37.0	23.3	1.6	0.024
497	Tmem123	transmembrane protein 123	11.4	7.2	1.6	0.049
498	Pdia4	protein disulfide isomerase associated 4	27.2	17.3	1.6	0.028
499	Abca1	ATP-binding cassette, sub-family A (ABC1), member 1	6.2	3.9	1.6	0.030
500	Ptbp3	polypyrimidine tract binding protein 3	6.4	4.1	1.6	0.045
501	Ccnd2	cyclin D2	13.4	8.6	1.6	0.039
502	Ighv5-12	immunoglobulin heavy variable 5-12	97.9	0.0	97.9*	0.002
503	Ighv5-1	immunoglobulin heavy variable V5-1	9502.9	0.0	9502.9*	0.002
504	Igkv3-12	immunoglobulin kappa variable 3-12	94.0	0.0	94.0*	0.002
505	Igkv3-5	immunoglobulin kappa chain variable 3-5	94.0	0.0	94.0*	0.002
506	Ighv3-8	immunoglobulin heavy variable V3-8	9.5	0.0	9.5*	0.002

507	Ighv7-1	immunoglobulin heavy variable 7-1	9.1	0.0	9.1*	0.002
508	Igkv16-104	immunoglobulin kappa variable 16-104	86.4	0.0	86.4*	0.002
509	Igkv8-24	immunoglobulin kappa chain variable 8-24	86.3	0.0	86.3*	0.002
510	Igkv6-17	immunoglobulin kappa variable 6-17	85.2	0.0	85.2*	0.002
511	Igkv14-126	immunoglobulin kappa variable 14-126	8.8	0.0	8.8*	0.002
512	Ubd	ubiquitin D	8.6	0.0	8.6*	0.002
513	Ighv8-4	immunoglobulin heavy variable V8-4	8.2	0.0	8.2*	0.002
514	Ighv1-54	immunoglobulin heavy variable V1-54	8.0	0.0	8.0*	0.002
515	Igkv4-68	immunoglobulin kappa variable 4-68	73.2	0.0	73.2*	0.002
516	Igkv3-1	immunoglobulin kappa variable 3-1	71.5	0.0	71.5*	0.002
517	Igkv3-2	immunoglobulin kappa variable 3-2	71.5	0.0	71.5*	0.002
518	Gm31026	predicted gene, 31026	7.5	0.0	7.5*	0.002
519	Igkv9-124	immunoglobulin kappa chain variable 9-124	63.6	0.0	63.6*	0.002
520	Ighv1-2	immunoglobulin heavy variable 1-2	6141.7	0.0	6141.7*	0.002
521	Igkv6-15	immunoglobulin kappa variable 6-15	61.4	0.0	61.4*	0.002
522	Igkv5-48	immunoglobulin kappa variable 5-48	60.4	0.0	60.4*	0.002
523	Ighv2-3	immunoglobulin heavy variable 2-3	6.3	0.0	6.3*	0.046
524	Igkv12-38	immunoglobulin kappa chain variable 12-38	6.1	0.0	6.1*	0.002
525	Igkv1-135	immunoglobulin kappa variable 1-135	57.9	0.0	57.9*	0.002
526	Igkv14-111	immunoglobulin kappa variable 14-111	57.8	0.0	57.8*	0.002
527	Ighv1-81	immunoglobulin heavy variable 1-81	52894.7	0.0	52894.7*	0.002
528	Ighv3-7	immunoglobulin heavy variable V3-7	50.3	0.0	50.3*	0.002
529	Igkv4-50	immunoglobulin kappa variable 4-50	5.3	0.0	5.3*	0.002
530	Ighv8-12	immunoglobulin heavy variable V8-12	49.5	0.0	49.5*	0.002
531	Igkv3-10	immunoglobulin kappa variable 3-10	49.2	0.0	49.2*	0.002
532	Ighv3-6	immunoglobulin heavy variable 3-6	48.1	0.0	48.1*	0.002
533	Igkv3-11	immunoglobulin kappa variable 3-11	4698.5	0.0	4698.5*	0.049
534	Ighv2-2	immunoglobulin heavy variable 2-2	46.2	0.0	46.2*	0.002
535	Ighv5-9	immunoglobulin heavy variable 5-9	46.0	0.0	46.0*	0.002
536	Ighv5-9-1	immunoglobulin heavy variable 5-9-1	46.0	0.0	46.0*	0.002
537	Igkv1-133	immunoglobulin kappa variable 1-133	44.3	0.0	44.3*	0.002
538	Igkv13-84	immunoglobulin kappa chain variable 13-84	43.4	0.0	43.4*	0.002
539	Igkv4-72	immunoglobulin kappa chain variable 4-72	43.3	0.0	43.3*	0.002
540	Igkv6-32	immunoglobulin kappa variable 6-32	43.2	0.0	43.1*	0.002
541	Igkv11-125	immunoglobulin kappa variable 11-125	4.8	0.0	4.8*	0.002
542	Igkv9-129	immunoglobulin kappa variable 9-129	4.5	0.0	4.5*	0.002
543	Iglv3	immunoglobulin lambda variable 3	4.2	0.0	4.2*	0.002
544	Igkv4-51	immunoglobulin kappa chain variable 4-51	4.0	0.0	4.0*	0.002
545	Ighv5-6	immunoglobulin heavy variable 5-6	39.2	0.0	39.2*	0.002

546	Igkv13-85	immunoglobulin kappa chain variable 13-85	38.5	0.0	38.5*	0.002
547	Ighv6-6	immunoglobulin heavy variable 6-6	37.6	0.0	37.6*	0.002
548	Igkv4-91	immunoglobulin kappa chain variable 4-91	37.0	0.0	37.0*	0.002
549	Igkv8-28	immunoglobulin kappa variable 8-28	35.4	0.0	35.4*	0.002
550	Igkv12-89	immunoglobulin kappa chain variable 12-89	35.2	0.0	35.2*	0.002
551	Ighv1-55	immunoglobulin heavy variable 1-55	34399.8	0.0	34399.8*	0.002
552	Ighv10-3	immunoglobulin heavy variable V10-3	32.3	0.0	32.3*	0.002
553	Igkv10-94	immunoglobulin kappa variable 10-94	31.1	0.0	31.1*	0.002
554	Ighv2-6	immunoglobulin heavy variable 2-6	30.2	0.0	30.2*	0.002
555	Igkv3-3	immunoglobulin kappa variable 3-3	3.8	0.0	3.8*	0.002
556	Igkv8-16	immunoglobulin kappa variable 8-16	3.2	0.0	3.2*	0.002
557	Igkv1-132	immunoglobulin kappa variable 1-132	3.1	0.0	3.1*	0.002
558	Ighv1-56	immunoglobulin heavy variable 1-56	29368.4	0.0	29368.4*	0.039
559	Igkv6-13	immunoglobulin kappa variable 6-13	28.9	0.0	29.0*	0.002
560	Ighv5-4	immunoglobulin heavy variable 5-4	28.5	0.0	28.5*	0.002
561	Igkv4-86	immunoglobulin kappa variable 4-86	26.4	0.0	26.4*	0.002
562	H2-Bl	histocompatibility 2, blastocyst	2514.7	0.0	2514.7*	0.002
563	Igkv4-69	immunoglobulin kappa variable 4-69	24.9	0.0	24.9*	0.002
564	Igkv4-80	immunoglobulin kappa variable 4-80	24.9	0.0	24.9*	0.002
565	Ighv1-85	immunoglobulin heavy variable 1-85	24.6	0.0	24.6*	0.002
566	Ighv1-66	immunoglobulin heavy variable 1-66	234.6	0.0	234.6*	0.002
567	Ighv8-8	immunoglobulin heavy variable 8-8	234.5	0.0	234.5*	0.002
568	Igkv3-7	immunoglobulin kappa variable 3-7	22.9	0.0	23.0*	0.002
569	Ighv7-3	immunoglobulin heavy variable 7-3	22087.2	0.0	22087.2*	0.002
570	Ighv7-4	immunoglobulin heavy variable 7-4	22087.2	0.0	22087.2*	0.002
571	Igkv12-98	immunoglobulin kappa variable 12-98	21.4	0.0	21.4*	0.002
572	Igkv8-21	immunoglobulin kappa variable 8-21	200.6	0.0	200.6*	0.002
573	Iglv2	immunoglobulin lambda variable 2	20.0	0.0	20.0*	0.002
574	Trbv13-1	T cell receptor beta, variable 13-1	2.7	0.0	2.7*	0.002
575	Cd8a	CD8 antigen, alpha chain	2.4	0.0	2.4*	0.002
576	Igkv18-36	immunoglobulin kappa chain variable 18-36	2.3	0.0	2.3*	0.007
577	Trbv1	T cell receptor beta, variable 1	2.0	0.0	2.0*	0.002
578	Igkv9-120	immunoglobulin kappa chain variable 9-120	19.6	0.0	19.6*	0.002
579	Igkv17-121	immunoglobulin kappa variable 17-121	19.2	0.0	19.2*	0.002
580	Igkv6-23	immunoglobulin kappa variable 6-23	181.4	0.0	181.4*	0.002
581	Ighv7-2	immunoglobulin heavy variable 7-2	18.6	0.0	18.6*	0.002
582	Ighv1-64	immunoglobulin heavy variable 1-64	18.3	0.0	18.3*	0.002
583	Ighv1-39	immunoglobulin heavy variable 1-39	16743.1	0.0	16743.1*	0.002
584	Igkv6-20	immunoglobulin kappa variable 6-20	15.9	0.0	15.9*	0.002

585	Gm18445	predicted gene, 18445	15.8	0.0	15.8*	0.002
586	Ighv2-5	immunoglobulin heavy variable 2-5	15.1	0.0	15.1*	0.002
587	Igkv3-4	immunoglobulin kappa variable 3-4	149.1	0.0	149.1*	0.002
588	Ighv1-67	immunoglobulin heavy variable V1-67	146.4	0.0	146.4*	0.002
589	Igkv4-74	immunoglobulin kappa variable 4-74	14.6	0.0	14.6*	0.002
590	Igkv17-127	immunoglobulin kappa variable 17-127	14.4	0.0	14.4*	0.002
591	Ighv1-82	immunoglobulin heavy variable 1-82	130.9	0.0	130.9*	0.002
592	Igkv4-63	immunoglobulin kappa variable 4-63	13.0	0.0	13.0*	0.002
593	Ighv1-77	immunoglobulin heavy variable 1-77	124.8	0.0	124.8*	0.002
594	Igkv8-30	immunoglobulin kappa chain variable 8-30	116.9	0.0	116.9*	0.002
595	Ighv1-42	immunoglobulin heavy variable V1-42	1130.7	0.0	1130.7*	0.002
596	Igkv2-137	immunoglobulin kappa chain variable 2-137	112.9	0.0	112.9*	0.002
597	Igkv19-93	immunoglobulin kappa chain variable 19-93	112.6	0.0	112.6*	0.002
598	Ighv8-5	immunoglobulin heavy variable V8-5	11.9	0.0	11.9*	0.002
599	Ighv10-1	immunoglobulin heavy variable 10-1	11.4	0.0	11.4*	0.002
600	Ighv2-4	immunoglobulin heavy variable V2-4	11.1	0.0	11.1*	0.002
601	Igkv2-109	immunoglobulin kappa variable 2-109	105.7	0.0	105.7*	0.002
602	Ighv1-7	immunoglobulin heavy variable V1-7	100403.0	0.0	100403*	0.002
603	Igkv1-88	immunoglobulin kappa chain variable 1-88	10.8	0.0	10.8*	0.002
604	Ighv13-2	immunoglobulin heavy variable 13-2	10.7	0.0	10.7*	0.002
605	Igkv1-99	immunoglobulin kappa variable 1-99	10.5	0.0	10.5*	0.002
606	Igkv4-90	immunoglobulin kappa chain variable 4-90	1.7	0.0	1.7*	0.002
607	Trbv14	T cell receptor beta, variable 14	1.7	0.0	1.7*	0.002
608	Trbv5	T cell receptor beta, variable 5	1.7	0.0	1.7*	0.002
609	Ighv6-7	immunoglobulin heavy variable V6-7	1.6	0.0	1.6*	0.002
610	Glycam1	glycosylation dependent cell adhesion molecule 1	1.5	0.0	1.5*	0.002
611	Igkv9-123	immunoglobulin kappa variable 9-123	1.5	0.0	1.5*	0.002
612	Ms4a1	membrane-spanning 4-domains, subfamily A, member 1	1.1	0.0	1.1*	0.002
613	Igkv4-92	immunoglobulin kappa variable 4-92	0.9	0.0	0.9*	0.014
614	Slamf7	SLAM family member 7	0.9	0.0	0.9*	0.002
615	Cd22	CD22 antigen	0.8	0.0	0.8*	0.002
616	Cd69	CD69 antigen	0.8	0.0	0.8*	0.002
617	Igkv8-26	immunoglobulin kappa variable 8-26	0.7	0.0	0.7*	0.007
618	Klrc1	killer cell lectin-like receptor subfamily C, member 1	0.7	0.0	0.7*	0.002
619	Klrc2	killer cell lectin-like receptor subfamily C, member 2	0.7	0.0	0.7*	0.002
620	Ms4a4d	membrane-spanning 4-domains, subfamily A, member 4D	0.7	0.0	0.7*	0.002
621	9330175E14Rik	RIKEN cDNA 9330175E14 gene	0.7	0.0	0.7*	0.002

622	Il1rn	interleukin 1 receptor antagonist	0.7	0.0	0.7*	0.002
623	H2-Eb2	histocompatibility 2, class II antigen E beta2	0.6	0.0	0.6*	0.002
624	Clec4d	C-type lectin domain family 4, member d	0.6	0.0	0.6*	0.002
625	Tnf	tumor necrosis factor	0.6	0.0	0.6*	0.002
626	Icos	inducible T cell co-stimulator	0.6	0.0	0.6*	0.002
627	Tcrg-C2	T-cell receptor gamma, constant 2	0.5	0.0	0.5*	0.002
628	Pyhin1	interferon activated gene 209	0.5	0.0	0.5*	0.002
629	Ubash3a	ubiquitin associated and SH3 domain containing, A	0.5	0.0	0.5*	0.002

Chapter 6

Table 6.1 List of metabolites and their pathways that were detected by pHILLIC Column, C18-PFP Column or Both Column. pHILLIC* = metabolites detected by both pHILLIC and C18-PFP Columns in congenital study. The metabolites highlight by yellow color corresponding to standard metabolites that used.

	m/z	RT (min)	Formula	Putative metabolite	Pathway	Column used
1	329.0525	9.69	C10H12N5O6P	3',5'-Cyclic AMP	Purine metabolism	pHILLIC*
2	267.0965	9.32	C10H13N5O4	Adenosine	Purine metabolism	pHILLIC*
3	283.0916	12.87	C10H13N5O5	Guanosine	Purine metabolism	pHILLIC*
4	136.0385	10.41	C5H4N4O	Hypoxanthine	Purine metabolism	pHILLIC*
5	348.0471	15.63	C10H13N4O8P	IMP	Purine metabolism	pHILLIC*
6	268.0806	11.14	C10H12N4O5	Inosine	Purine metabolism	pHILLIC*
7	463.0741	18.37	C14H18N5O11P	N6-(1,2-Dicarboxyethyl)-AMP	Purine metabolism	pHILLIC*
8	152.0335	11.48	C5H4N4O2	Xanthine	Purine metabolism	pHILLIC*
9	363.0583	16.87	C10H14N5O8P	GMP	Purine metabolism	pHILLIC*
10	135.0545	9.32	C5H5N5	Adenine	Purine metabolism	pHILLIC*
11	347.0629	13.95	C10H14N5O7P	AMP	Purine metabolism	pHILLIC*
12	559.0713	14.98	C15H23N5O14P2	ADP-ribose	Purine metabolism	pHILLIC
13	158.0439	13.86	C4H6N4O3	Allantoin	Purine metabolism	pHILLIC
14	251.1018	8.35	C10H13N5O3	Deoxyadenosine	Purine metabolism	pHILLIC
15	252.0857	9.78	C10H12N4O4	Deoxyinosine	Purine metabolism	pHILLIC
16	443.0246	18.11	C10H15N5O11P2	GDP	Purine metabolism	pHILLIC
17	151.0494	12.71	C5H5N5O	Guanine	Purine metabolism	pHILLIC
18	168.0283	12.53	C5H4N4O3	Urate	Purine metabolism	pHILLIC
19	364.0425	18.06	C10H13N4O9P	Xanthosine 5'-phosphate	Purine metabolism	pHILLIC
20	284.0757	12.12	C10H12N4O6	Xanthosine	Purine metabolism	pHILLIC
21	522.9909	19.61	C10H16N5O14P3	GTP	Purine metabolism	pHILLIC
22	154.0032	11.45	C3H7O5P	Propanoyl phosphate	Propanoate metabolism	pHILLIC
23	745.0918	17.19	C21H30N7O17P3	NADPH	Photosynthesis	pHILLIC
24	743.0757	16.96	C21H28N7O17P3	NADP+	Photosynthesis	pHILLIC
25	379.1047	7.45	C13H21N3O8S	(R)-S-Lactoylglutathione	Pyruvate metabolism	C18-PFP
26	208.0851	11.17	C10H12N2O3	L-Kynurenine	Tryptophan metabolism	pHILLIC*
27	191.0583	12.81	C10H9NO3	5-Hydroxyindoleacetate	Tryptophan metabolism	pHILLIC
28	204.0899	11.93	C11H12N2O2	L-Tryptophan	Tryptophan metabolism	pHILLIC
29	176.0948	11.64	C10H12N2O	Serotonin	Tryptophan metabolism	C18-PFP
30	323.0518	16.05	C9H14N3O8P	CMP	Pyrimidine metabolism	pHILLIC*

31	243.0855	12.17	C9H13N3O5	Cytidine	Pyrimidine metabolism	pHILLIC*
32	244.0696	10.05	C9H12N2O6	Uridine	Pyrimidine metabolism	pHILLIC*
33	324.0359	15.31	C9H13N2O9P	UMP	Pyrimidine metabolism	pHILLIC*
34	417.0339	15.63	C10H17N3O11P2	2'-Deoxy-5-hydroxy methylcytidine-5'-diphosphate	Pyrimidine metabolism	pHILLIC
35	403.0183	17.25	C9H15N3O11P2	CDP	Pyrimidine metabolism	pHILLIC
36	227.0905	10.7	C9H13N3O4	Deoxycytidine	Pyrimidine metabolism	pHILLIC
37	228.0747	8.39	C9H12N2O5	Deoxyuridine	Pyrimidine metabolism	pHILLIC
38	242.0904	7.54	C10H14N2O5	Thymidine	Pyrimidine metabolism	pHILLIC
39	126.0428	7.52	C5H6N2O2	Thymine	Pyrimidine metabolism	pHILLIC
40	112.0272	8.71	C4H4N2O2	Uracil	Pyrimidine metabolism	pHILLIC
41	404.0022	16.66	C9H14N2O12P2	UDP	Pyrimidine metabolism	pHILLIC
42	128.0586	5.32	C5H8N2O2	5,6-Dihydrothymine	Pyrimidine metabolism	C18-PFP
43	111.0433	5.49	C4H5N3O	Cytosine	Pyrimidine metabolism	C18-PFP
44	165.079	10.56	C9H11NO2	L-Phenylalanine	Phenylalanine metabolism	pHILLIC*
45	147.0531	14.81	C5H9NO4	L-Glutamate	Glutamate metabolism	pHILLIC*
46	145.0852	15.49	C5H11N3O2	4-Guanidinobutanoate	Arginine and proline metabolism	pHILLIC*
47	113.059	9.97	C4H7N3O	Creatinine	Arginine and proline metabolism	pHILLIC*
48	240.1221	16.54	C10H16N4O3	Homocarnosine	Arginine and proline metabolism	pHILLIC*
49	175.0957	15.73	C6H13N3O3	L-Citrulline	Arginine and proline metabolism	pHILLIC*
50	189.0637	14.21	C7H11NO5	N-Acetyl-L-glutamate	Arginine and proline metabolism	pHILLIC*
51	174.1004	13.85	C7H14N2O3	N-Acetylornithine	Arginine and proline metabolism	pHILLIC*
52	174.1117	26.44	C6H14N4O2	L-Arginine	Arginine and proline metabolism	pHILLIC*
53	115.0633	13.12	C5H9NO2	L-Proline	Arginine and proline metabolism	pHILLIC*
54	129.079	7.54	C6H11NO2	N4-Acetylaminobutanal	Arginine and proline metabolism	pHILLIC
55	211.0358	15.38	C4H10N3O5P	Phosphocreatine	Arginine and proline metabolism	pHILLIC
56	290.1225	17.07	C10H18N4O6	N-(L-Arginino)succinate	Arginine and proline metabolism	pHILLIC
57	297.0895	7.46	C11H15N5O3S	5'-Methylthioadenosine	Arginine and proline metabolism	pHILLIC
58	108.5714	4.51	C9H19N3O3	gamma-L-Glutamylputrescine	Arginine and proline metabolism	C18-PFP
59	103.0633	5.2	C4H9NO2	4-Aminobutanoate	Arginine and proline metabolism	C18-PFP
60	88.1001	4.36	C4H12N2	Putrescine	Arginine and proline metabolism	C18-PFP
61	354.1471	4.33	C14H22N6O3S	S-Adenosylmethioninamine	Arginine and proline metabolism	C18-PFP
62	398.137	4.64	C15H22N6O5S	S-Adenosyl-L-methionine	Arginine and proline metabolism	C18-PFP
63	132.0898	23.34	C5H12N2O2	L-Ornithine	D-Arginine and D-ornithine metabolism	pHILLIC*
64	173.0799	5.61	C6H11N3O3	5-Guanidino-2-oxopentanoate	D-Arginine and D-ornithine metabolism	C18-PFP
65	175.048	14.69	C6H9NO5	N-Acetyl-L-aspartate	Alanine and aspartate metabolism	pHILLIC*
66	203.1157	11.35	C9H17NO4	O-Acetylcarnitine	Alanine and aspartate metabolism	pHILLIC*
67	133.0374	15.22	C4H7NO4	L-Aspartate	Alanine and aspartate metabolism	pHILLIC*
68	89.0475	14.99	C3H7NO2	L-Alanine	Alanine and aspartate metabolism	pHILLIC*

69	226.1065	16.03	C9H14N4O3	Carnosine	Alanine and aspartate metabolism	pHILLIC*
70	249.0861	7.94	C10H19NO2S2	S-Acetyldihydrolipoamide	Alanine and aspartate metabolism	pHILLIC
71	132.0533	5.14	C4H8N2O3	L-Asparagine	Alanine and aspartate metabolism	C18-PFP
72	117.0789	12.85	C5H11NO2	L-Valine	Valine, leucine and isoleucine metabolism	pHILLIC*
73	131.0946	8.92	C6H13NO2	L-Leucine	Valine, leucine and isoleucine metabolism	C18-PFP
74	167.0947	20.43	C9H13NO2	3-Methoxytyramine	Tyrosine metabolism	pHILLIC*
75	181.0739	13.26	C9H11NO3	L-Tyrosine	Tyrosine metabolism	pHILLIC*
76	182.058	8.9	C9H10O4	3-(4-Hydroxyphenyl)lactate	Tyrosine metabolism	pHILLIC
77	149.0476	9.38	C8H7NO2	5,6-Dihydroxyindole	Tyrosine metabolism	C18-PFP
78	153.0789	6.78	C8H11NO2	Dopamine	Tyrosine metabolism	C18-PFP
79	131.0693	14.99	C4H9N3O2	Creatine	Glycine, serine and threonine metabolism	pHILLIC*
80	117.0538	16.07	C3H7N3O2	Guanidinoacetate	Glycine, serine and threonine metabolism	pHILLIC*
81	103.0997	20.38	C5H13NO	Choline	Glycine, serine and threonine metabolism	pHILLIC*
82	141.0191	16.26	C2H8NO4P	Ethanolamine phosphate	Glycine, serine and threonine metabolism	pHILLIC
83	119.0583	14.7	C4H9NO3	L-Threonine	Glycine, serine and threonine metabolism	pHILLIC
84	105.0426	16.04	C3H7NO3	L-Serine	Glycine, serine and threonine metabolism	pHILLIC*
85	219.1107	8.82	C9H17NO5	Pantothenate	Pantothenate and CoA biosynthesis	pHILLIC*
86	217.1426	23	C9H19N3O3	beta-Alanyl-L-lysine	beta-Alanine metabolism	pHILLIC
87	176.032	14.11	C6H8O6	Ascorbate	Ascorbate and aldarate metabolism	pHILLIC*
88	307.0836	14.57	C10H17N3O6S	Glutathione	Glutathione metabolism	pHILLIC*
89	250.0623	14.33	C8H14N2O5S	gamma-L-Glutamyl-L-cysteine	Glutamate metabolism	pHILLIC*
90	612.1521	17.62	C20H32N6O12S2	Glutathione disulfide	Glutathione metabolism	pHILLIC
91	146.0691	15.37	C5H10N2O3	L-Glutamine	Glutamate metabolism	pHILLIC*
92	221.0896	5.49	C8H15NO6	N-Acetyl-D-glucosamine	Glutamate metabolism	C18-PFP
93	264.1044	20.98	C12H16N4OS	Thiamin	Thiamine metabolism	pHILLIC*
94	125.0145	15.04	C2H7NO3S	Taurine	Taurine and hypotaurine metabolism	pHILLIC*
95	125.9987	10.72	C2H6O4S	2-Hydroxyethanesulfonate	Taurine and hypotaurine metabolism	pHILLIC
96	785.1574	11.61	C27H33N9O15P2	FAD	Riboflavin metabolism	pHILLIC*
97	376.1382	8.87	C17H20N4O6	Riboflavin	Riboflavin metabolism	pHILLIC
98	687.1491	10.01	C21H35N7O13P2S	Dephospho-CoA	Pantothenate and CoA biosynthesis	pHILLIC
99	358.0968	10.43	C11H23N2O7PS	Pantetheine 4'-phosphate	Pantothenate and CoA biosynthesis	pHILLIC*
100	456.1045	11.72	C17H21N4O9P	FMN	Oxidative phosphorylation	pHILLIC
101	663.1091	14.47	C21H27N7O14P2	NAD+	Oxidative phosphorylation	pHILLIC*
102	665.1249	13.53	C21H29N7O14P2	NADH	Oxidative phosphorylation	pHILLIC
103	506.9956	16.77	C10H16N5O13P3	ATP	Oxidative phosphorylation	pHILLIC
104	427.0295	15.38	C10H15N5O10P2	ADP	Oxidative phosphorylation	pHILLIC
105	97.977	5.47	H3O4P	Orthophosphate	Oxidative phosphorylation	C18-PFP

106	217.1312	8.11	C10H19NO4	O-Propanoylcarnitine	Oxidation of Branched Fatty Acids	C18-PFP
107	152.0586	7.65	C7H8N2O2	N1-Methyl-2-pyridone-5-carboxamide	Nicotinate and nicotinamide metabolism	pHILLIC
108	254.0901	24.47	C11H14N2O5	N-Ribosylnicotinamide	Nicotinate and nicotinamide metabolism	pHILLIC
109	122.048	7.48	C6H6N2O	Nicotinamide	nicotinamide metabolism	pHILLIC*
110	149.0511	11.84	C5H11NO2S	L-Methionine	Methionine metabolism	pHILLIC*
111	384.1213	13.97	C14H20N6O5S	S-Adenosyl-L-homocysteine	Methionine metabolism	pHILLIC*
112	219.074	8.2	C8H13NO6	O-Succinyl-L-homoserine	Methionine metabolism	C18-PFP
113	161.0688	15.2	C6H11NO4	N-Methyl-L-glutamate	Methane metabolism	pHILLIC
114	75.0685	11.32	C3H9NO	Trimethylamine N-oxide	Methane metabolism	pHILLIC
115	159.0896	13.11	C7H13NO3	5-Acetamidopentanoate	Lysine degradation	pHILLIC*
116	161.1051	13.64	C7H15NO3	L-Carnitine	Lysine degradation	pHILLIC*
117	188.1525	22.48	C9H20N2O2	N6,N6,N6-Trimethyl-L-lysine	Lysine degradation	pHILLIC*
118	145.1103	13.75	C7H15NO2	4-Trimethylammoniobutanoate	Lysine degradation	pHILLIC
119	242.0667	17.56	C6H15N2O6P	5-Phosphonooxy-L-lysine	Lysine degradation	pHILLIC
120	129.079	12.72	C6H11NO2	L-Pipecolate	Lysine degradation	pHILLIC
121	127.0633	5.35	C6H9NO2	2,3,4,5-Tetrahydropyridine-2-carboxylate	Lysine degradation	C18-PFP
122	204.1472	4.77	C9H20N2O3	3-Hydroxy-N6,N6,N6-trimethyl-L-lysine	Lysine degradation	C18-PFP
123	145.1103	5.49	C7H15NO2	4-Trimethylammoniobutanoate	Lysine degradation	C18-PFP
124	204.1109	7.55	C8H16N2O4	N6-Acetyl-N6-hydroxy-L-lysine	Lysine degradation	C18-PFP
125	102.1157	4.37	C5H14N2	Cadaverine	Lysine degradation	C18-PFP
126	276.1321	15.95	C11H20N2O6	N6-(L-1,3-Dicarboxypropyl)-L-lysine	Lysine metabolism	pHILLIC
127	160.1212	23.97	C7H16N2O2	N6-Methyl-L-lysine	Lysine metabolism	pHILLIC*
128	203.0795	13.66	C8H13NO5	N2-Acetyl-L-aminoadipate	Lysine biosynthesis	pHILLIC*
129	146.1055	25	C6H14N2O2	L-Lysine	Lysine biosynthesis	pHILLIC*
130	161.0687	5.52	C6H11NO4	L-2-Aminoadipate	Lysine biosynthesis	C18-PFP
131	261.1212	13.15	C11H19NO6	Lotaustralin	lotaustralin biosynthesis	pHILLIC
132	156.0535	11.19	C6H8N2O3	4-Imidazolone-5-propanoate	Histidine metabolism	pHILLIC
133	140.0586	9.68	C6H8N2O2	Methylimidazoleacetic acid	Histidine metabolism	pHILLIC
134	169.0851	13.24	C7H11N3O2	N(pi)-Methyl-L-histidine	Histidine metabolism	pHILLIC
135	229.0883	5.54	C9H15N3O2S	Ergothioneine	Histidine metabolism	C18-PFP
136	125.0953	4.41	C6H11N3	N-Methylhistamine	Histidine metabolism	C18-PFP
137	155.0695	4.72	C6H9N3O2	L-Histidine	Histidine metabolism	C18-PFP
138	185.993	17.09	C3H7O7P	3-Phospho-D-glycerate	Glycolysis / Gluconeogenesis	pHILLIC
139	169.9981	15.52	C3H7O6P	Glycerone phosphate	Glycolysis / Gluconeogenesis	pHILLIC
140	167.9825	17.61	C3H5O6P	Phosphoenolpyruvate	Glycolysis / Gluconeogenesi	pHILLIC
141	215.0559	15.95	C5H14NO6P	sn-glycero-3-Phosphoethanolamine	Glycerophospholipid metabolism	pHILLIC*
142	222.0674	17.35	C7H14N2O4S	Cystathionine	Sulfur metabolism	pHILLIC
143	260.0297	17.41	C6H13O9P	D-Glucose 6-phosphate	Starch and sucrose metabolism	pHILLIC

144	187.1683	4.49	C9H21N3O	N1-Acetylspermidine	spermine and spermidine degradation	C18-PFP
145	169.0504	14.39	C4H12NO4P	Phosphodimethylethanolamine	Glycerophospholipid metabolism	pHILLIC
146	488.1069	5.15	C14H26N4O11P2	CDP-choline	Glycerophospholipid metabolism	C18-PFP
147	257.1025	5.17	C8H20NO6P	sn-glycero-3-Phosphocholine	Glycerophospholipid metabolism	C18-PFP
148	183.0659	5.16	C5H14NO4P	Choline phosphate	Glycerophospholipid metabolism	C18-PFP
149	90.0314	9.69	C3H6O3	Glycerone	Glycerolipid metabolism	pHILLIC
150	172.0136	5.5	C3H9O6P	sn-Glycerol 3-phosphate	Glycerolipid metabolism	C18-PFP
151	180.0635	17.36	C6H12O6	D-Galactose	Galactose metabolism	pHILLIC
152	92.0474	5.5	C3H8O3	Glycerol	Galactose metabolism	C18-PFP
153	589.0823	17.66	C16H25N5O15P2	GDP-L-fucose	Fructose and mannose metabolism	pHILLIC
154	182.0791	14.19	C6H14O6	Mannitol	Fructose and mannose metabolism	pHILLIC
155	239.1015	7.05	C9H13N5O3	Dihydrobiopterin	Folate biosynthesis	C18-PFP
156	231.1469	14.69	C11H21NO4	O-Butanoylcarnitine	Fatty acyl carnitines	C18-PFP
157	240.0238	16.53	C6H12N2O4S2	L-Cystine	Cysteine metabolism	pHILLIC*
158	426.0875	5.2	C13H22N4O8S2	S-glutathionyl-L-cysteine	Cysteine metabolism	C18-PFP
159	200.0797	10.71	C8H12N2O4	Dihydroclavaminic acid	Clavulanic acid biosynthesis	pHILLIC
160	192.0272	18.16	C6H8O7	Citrate	Citrate cycle (TCA cycle)	pHILLIC
161	118.0266	8.51	C4H6O4	Succinate	Citrate cycle (TCA cycle)	C18-PFP
162	339.9963	18.93	C6H14O12P2	D-Fructose 1,6-bisphosphate	Carbon fixation	pHILLIC
163	84.0212	5.66	C4H4O2	3-Butynoate	Butanoate metabolism	C18-PFP
164	214.1315	8.63	C10H18N2O3	Dethiobiotin	Biotin metabolism	C18-PFP
165	75.0321	5.14	C2H5NO2	Glycine	Bile acid biosynthesis	C18-PFP
166	309.106	13.43	C11H19NO9	N-Acetylneuraminate	Aminosugars metabolism	pHILLIC*
167	179.0794	11.57	C6H13NO5	D-Glucosamine	Aminosugars metabolism	pHILLIC
168	607.0815	15.26	C17H27N3O17P2	UDP-N-acetyl-D-glucosamine	Aminosugars metabolism	pHILLIC
169	341.1319	6.09	C12H23NO10	Lactosamine	Aminosugars metabolism	C18-PFP
170	430.0657	15.18	C11H20N4O10P2	CMP-2-aminoethylphosphonate	Aminophosphonate metabolism	pHILLIC
171	111.9925	14.62	CH5O4P	Hydroxymethylphosphonate	Aminophosphonate metabolism	pHILLIC
172	276.0249	17.83	C6H13O10P	6-Phospho-D-gluconate	Pentose phosphate pathway	pHILLIC
173	196.0583	13.5	C6H12O7	D-Gluconic acid	Pentose phosphate pathway	pHILLIC
174	290.0403	16.44	C7H15O10P	D-Sedoheptulose 7-phosphate	Pentose phosphate pathway	pHILLIC
175	260.0296	16.34	C6H13O9P	D-Fructose 6-phosphate	Pentose phosphate pathway	pHILLIC
176	230.0191	15.25	C5H11O8P	D-Ribose 5-phosphate	Pentose phosphate pathway	pHILLIC
177	537.0762	16.74	C14H25N3O15P2	CDP-ribitol	Pentose and glucuronate interconversions	pHILLIC
178	232.0349	15.82	C5H13O8P	D-Ribitol 5-phosphate	Pentose and glucuronate interconversions	pHILLIC
179	152.0684	13.2	C5H12O5	Xylitol	Pentose and glucuronate interconversions	pHILLIC
180	580.0345	19.05	C15H22N2O18P2	UDP-glucuronate	Pentose and glucuronate interconversions	pHILLIC
181	566.0547	16.46	C15H24N2O17P2	UDP-glucose	Pentose and glucuronate interconversions	pHILLIC

182	274.0087	5.87	C6H11O10P	D-Glucuronate 1-phosphate	Pentose and glucuronate interconversions	C18-PFP
183	167.0583	8.21	C8H9NO3	Pyridoxal	Vitamin B6 metabolism	pHILLIC
184	181.0964	10.41	C7H11N5O	6-methyltetrahydropterin	Unknown	pHILLIC*
185	275.1116	15.5	C10H17N3O6	Gamma-Glutamylglutamine	Unknown	pHILLIC*
186	275.1368	13.05	C12H21NO6	Glutarylcarnitine	Unknown	pHILLIC*
187	247.1419	11.79	C11H21NO5	Hydroxybutyrylcarnitine	Unknown	pHILLIC*
188	223.1057	13.65	C8H17NO6	N-acetyl -D- glucosaminitol	Unknown	pHILLIC*
189	304.0908	16.86	C11H16N2O8	N-Acetyl-aspartyl-glutamate	Unknown	pHILLIC*
190	188.0797	10.66	C7H12N2O4	N-Acetylglutamine	Unknown	pHILLIC*
191	204.111	18.24	C8H16N2O4	γ-glutamyl-L-alaninol	Unknown	pHILLIC
192	256.1056	9.38	C11H16N2O5	1-(beta-D-Ribofuranosyl)-1,4-dihydronicotinamide	Unknown	pHILLIC
193	274.0454	15.43	C7H15O9P	1-Deoxy-D-altro-heptulose 7-phosphate	Unknown	pHILLIC
194	281.1123	14.77	C11H15N5O4	1-Methyladenosine	Unknown	pHILLIC
195	521.3483	4.73	C26H52NO7P	1-Oleoylglycerophosphocholine	Unknown	pHILLIC
196	495.3324	4.82	C24H50NO7P	1-Palmitoylglycerophosphocholine	Unknown	pHILLIC
197	245.1626	8.21	C12H23NO4	2-Methylbutyroylcarnitine	Unknown	pHILLIC
198	133.0738	7.46	C5H11NO3	3-nitro-2-pentanol	Unknown	pHILLIC
199	290.0042	18.17	C6H11O11P	3-phosphoglucarate	Unknown	pHILLIC
200	246.0853	10.24	C9H14N2O6	5-6-Dihydrouridine	Unknown	pHILLIC
201	403.0879	17.81	C12H22NO12P	6-(alpha-D-Glucosaminyl)-1D-myo-inositol 1,2-cyclic phosphate	Unknown	pHILLIC
202	282.0964	8.84	C11H14N4O5	8-Oxocoformycin	Unknown	pHILLIC
203	639.0382	18.38	C15H24N5O17P3	ADPribose 2'-phosphate	Unknown	pHILLIC
204	321.0698	20.01	C11H15NO10	beta-Citryl-L-glutamic acid	Unknown	pHILLIC
205	369.2878	4.9	C21H39NO4	cis-5-Tetradecenoylcarnitine	Unknown	pHILLIC
206	96.969	15.34	[H2PO4]-	Dihydrogenphosphate	Unknown	pHILLIC
207	242.0195	17.12	C6H11O8P	D-myo-Inositol 1,2-cyclic phosphate	Unknown	pHILLIC
208	343.2721	4.96	C19H37NO4	Dodecanoylcarnitine	Unknown	pHILLIC
209	555.2694	4.8	C28H37N5O7	EnkephalinL	Unknown	pHILLIC
210	231.1583	24.24	C10H21N3O3	Gamma-Aminobutyryl-lysine	Unknown	pHILLIC
211	218.0902	10.32	C8H14N2O5	gamma-L-Glutamyl-D-alanine	Unknown	pHILLIC
212	321.0993	10.62	C11H19N3O6S	gamma-L-Glutamyl-L-cysteinyl-beta-alanine	Unknown	pHILLIC
213	339.0119	18.84	C6H15NO11P2	glucosamine-1,6-diphosphate	Unknown	pHILLIC
214	246.0504	12.79	C6H15O8P	Glycerophosphoglycerol	Unknown	pHILLIC
215	273.1939	7.43	C14H27NO4	Heptanoylcarnitine	Unknown	pHILLIC
216	259.1783	7.57	C13H25NO4	Hexanoylcarnitine	Unknown	pHILLIC
217	254.1377	15.19	C11H18N4O3	Homoanserine	Unknown	pHILLIC
218	248.0644	17.54	C8H12N2O7	L-beta-aspartyl-L-asparticacid	Unknown	pHILLIC

219	262.08	17.57	C9H14N2O7	L-beta-aspartyl-L-glutamicacid	Unknown	pHILLIC
220	234.0851	15.87	C8H14N2O6	L-beta-aspartyl-L-threonine	Unknown	pHILLIC
221	260.1372	11.65	C11H20N2O5	L-gamma-glutamyl-L-leucine	Unknown	pHILLIC
222	172.0848	12.68	C7H12N2O3	L-prolyl-L-glycine	Unknown	pHILLIC
223	573.2257	4.89	C27H35N5O7S	MET-enkephalin	Unknown	pHILLIC
224	159.1259	13.75	C8H17NO2	Methacholine	Unknown	pHILLIC
225	311.1228	8.94	C12H17N5O5	N2-N2-Dimethylguanosine	Unknown	pHILLIC
226	285.096	8.52	C11H15N3O6	N4-Acetylcytidine	Unknown	pHILLIC
227	190.0952	11.36	C7H14N2O4	N5-acetyl-N5-hydroxy-L-ornithine	Unknown	pHILLIC
228	197.08	10.43	C8H11N3O3	N-Acetyl-L-histidine	Unknown	pHILLIC
229	350.0617	17.22	C9H19O12P	nonulose 9-phosphate	Unknown	pHILLIC
230	218.0497	7.31	C13H11OCl	p-Chlorobenzhydrol	Unknown	pHILLIC
231	212.0087	12.58	C5H9O7P	Phosphinomethylisomalate	Unknown	pHILLIC
232	150.0793	7.45	C8H10N2O	p-nitroso-N,N-dimethylaniline	Unknown	pHILLIC
233	326.151	13.1	C20H22O4	Pulverochromenol	Unknown	pHILLIC
234	171.0296	11.44	C3H10NO5P	serinol phosphate	Unknown	pHILLIC
235	321.0993	13.09	C11H19N3O6S	S-Methyl GSH	Unknown	pHILLIC
236	232.1423	17.47	C10H20N2O4	Spermic acid 2	Unknown	pHILLIC
237	383.1075	14.64	C14H17N5O8	Succinyladenosine	Unknown	pHILLIC
238	174.0165	19.06	C6H6O6	trans-Aconitate	Unknown	pHILLIC
239	308.1253	37.61	C16H20O6	14-Dihydroxycornestin	Unknown	C18-PFP
240	199.157	40.87	C11H21NO2	2-Hexenoylcholine	Unknown	C18-PFP
241	145.0528	37.12	C9H7NO	3-Methyleneoxindole	Unknown	C18-PFP
242	165.065	6.57	C6H7N5O	3-Methylguanine	Unknown	C18-PFP
243	224.0835	38.79	C15H12O2	Flavanone	Unknown	C18-PFP
244	276.0956	5.63	C10H16N2O7	GammaGlutamylglutamicacid	Unknown	C18-PFP
245	233.1261	36.76	C10H19NO5	Hydroxypropionylcarnitine	Unknown	C18-PFP
246	233.1737	4.21	C10H23N3O3	Hypusine	Unknown	C18-PFP
247	133.0196	5.56	C4H7NO2S	L-thiazolidine-4-carboxylate	Unknown	C18-PFP
248	220.1057	6.73	C8H16N2O5	N-Acetyl-beta-D-glucosaminylamine	Unknown	C18-PFP
249	243.1832	40.13	C13H25NO3	N-Undecanoylglycine	Unknown	C18-PFP

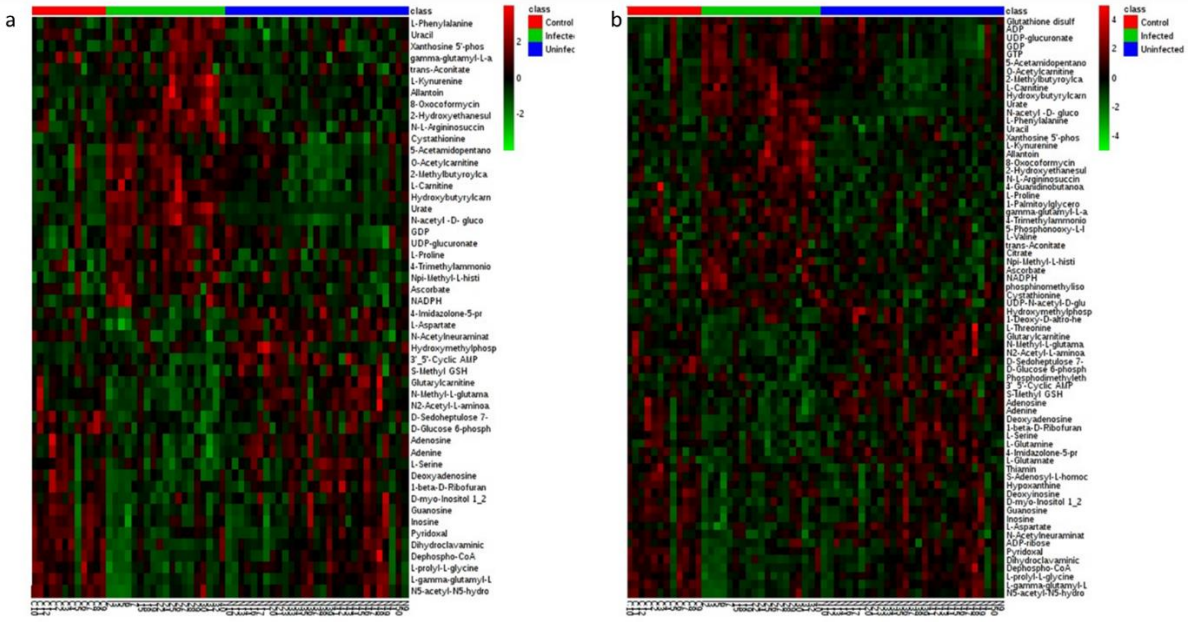

Figure 6.1 Heat map represents the significantly changed metabolites between infected, uninfected groups and corresponding control group according to *P*-value of student's *t*-test. (a) pHILLIC Column was used as primary column to detect the metabolites and it was augmented with (b) C18-PFP Column to obtain important missing metabolites. Normalised metabolite abundance (log 2 transformed and row adjustment) are visulaised as a color spectrum scaled from least abundant to highest range is from -4 to 4. Green indicates low expression, while red indicates high expression of the changed metabolites.

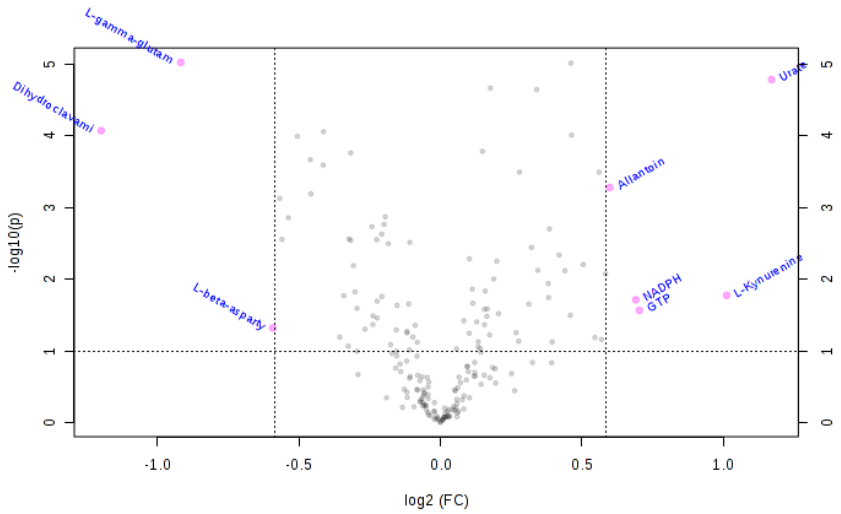

Figure 6.2 Important metabolites selected by volcano plot between control mice group and congenitally infected mice with fold change threshold 1.5 and *t*-tests threshold 0.1 (pHILLIC Column). The red circles represent features above the threshold.

Table 6.2 Important metabolites identified between control mice group and congenitally infected mice by volcano plot (pHILLIC Column).

	Metabolites	**FC (Infected/Control)**	**log2(FC)**	***p*.value**	**-LOG10(p)**
1	Urate	2.2518	1.1711	1.64E-05	4.7851
2	L-Kynurenine	2.0169	1.0122	0.016851	1.7734
3	GTP	1.6285	0.7035	0.027283	1.5641
4	NADPH	1.6144	0.69102	0.019409	1.712
5	Allantoin	1.5143	0.59866	0.0005246	3.2802
6	L-beta-aspartyl-L-threonine	0.66302	-0.59288	0.047871	1.3199
7	L-gamma-glutamyl-L-leucine	0.52911	-0.91837	9.43E-06	5.0254
8	Dihydroclavaminic acid	0.4353	-1.1999	8.47E-05	4.0721

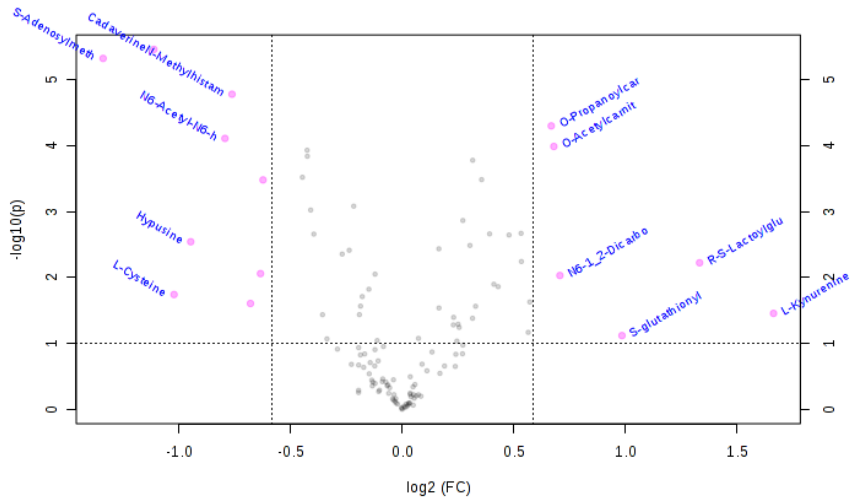

Figure 6.3 Important metabolites selected by volcano plot between control mice group and congenitally infected mice with fold change threshold 1.5 and *t*-tests threshold 0.1 (C18-PFP Column). The red circles represent features above the threshold.

Table 6.3 Important metabolites identified between control mice group and congenitally infected mice by volcano plot (C18-PFP Column).

	Metabolites	**FC (Infected/Control)**	**log2(FC)**	***p*.value**	**-LOG10(p)**
1	L-Kynurenine	3.1658	1.6626	0.035008	1.4558
2	R-S-Lactoylglutathione	2.5165	1.3314	0.005995	2.2222
3	S-glutathionyl-L-cysteine	1.9775	0.98369	0.075897	1.1198
4	N6-1_2-Dicarboxyethyl-AMP	1.6308	0.70559	0.009336	2.0299
5	O-Acetylcarnitine	1.6004	0.67848	0.000104	3.9838
6	O-Propanoylcarnitine	1.5876	0.66681	5.07E-05	4.2952
7	5_6-Dihydroxyindole	0.64867	-0.62443	0.000333	3.477
8	Glutarylcarnitine	0.64364	-0.63567	0.008739	2.0586
9	N1-Acetylspermidine	0.62385	-0.68073	0.024774	1.606
10	N-Methylhistamine	0.5891	-0.76343	1.68E-05	4.7749
11	N6-Acetyl-N6-hydroxy-L-lysine	0.57635	-0.79499	7.84E-05	4.1056
12	Hypusine	0.51824	-0.94831	0.002879	2.5407
13	L-Cysteine	0.49208	-1.023	0.018135	1.7415
14	Cadaverine	0.46219	-1.1134	3.52E-06	5.4541
15	S-Adenosylmethioninamine	0.39478	-1.3409	4.82E-06	5.3171

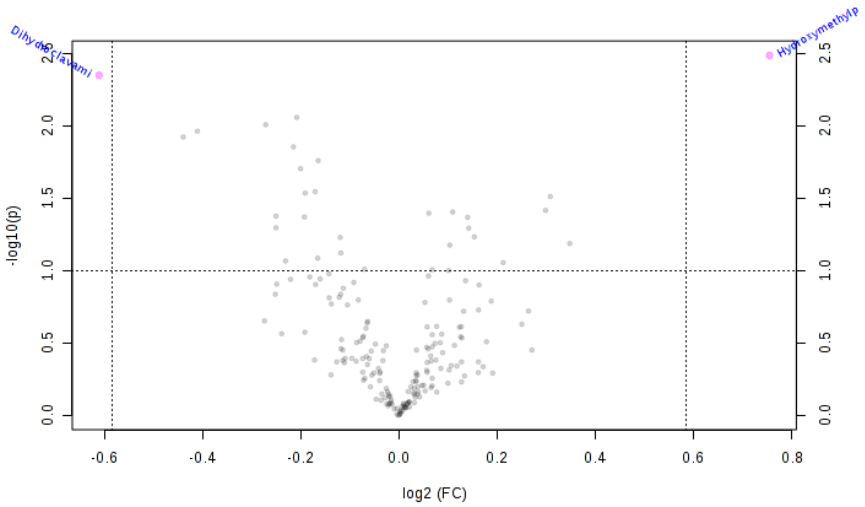

Figure 6.3 Important metabolites selected by volcano plot between control mice group and exposed uninfected mice with fold change threshold 1.5 and t-tests threshold (pHILLIC Column).

Table 6.4 Important metabolites identified between control mice group and exposed uninfected mice by volcano plot (pHILLIC Column).

	Metabolites	**FC (Uninfected/Control)**	**log2(FC)**	***p*.value**	**-LOG10(p)**
1	Hydroxymethylphosphonate	1.6878	0.75512	0.003263	2.4864
2	Dihydroclavaminic acid	0.65495	-0.61054	0.004477	2.349

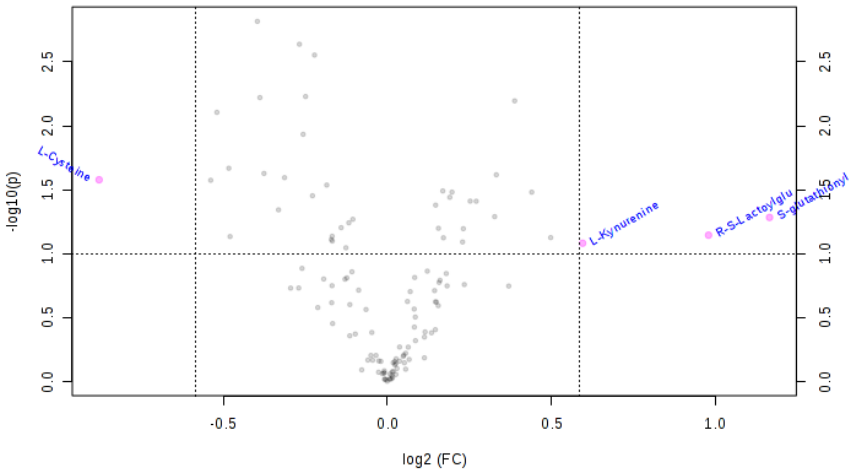

Figure 6.4 Important metabolites selected by volcano plot between control mice group and exposed uninfected mice with fold change threshold 1.5 and t-tests threshold (C18-PFP Column).

Table 6.5 Important metabolites identified between control mice group and exposed uninfected mice by volcano plot (C18-PFP Column).

	Metabolites	**FC (Uninfected/Control)**	**log2(FC)**	***p*.value**	**-LOG10(p)**
1	S-glutathionyl-L-cysteine	2.2439	1.166	0.05199	1.2841
2	R-S-Lactoylglutathione	1.9722	0.97982	0.071557	1.1453
3	L-Kynurenine	1.5112	0.59566	0.082702	1.0825
4	L-Cysteine	0.54344	-0.87981	0.026407	1.5783

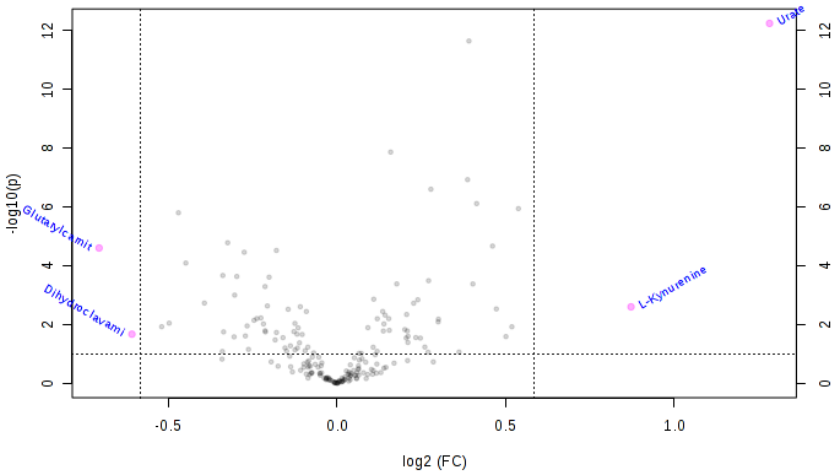

Figure 6.5 Important metabolites selected by volcano plot between congenitally infected mice group and exposed uninfected mice with fold change threshold 1.5 and t-tests threshold (pHILLIC Column).

Table 6.6 Important metabolites identified between congenitally infected mice group and exposed uninfected mice group by volcano plot (pHILLIC Column).

	Metabolites	**FC (Infected/Uninfected)**	**log2(FC)**	***p*.value**	**-LOG10(p)**
1	Urate	2.4337	1.2832	5.62E-13	12.25
2	L-Kynurenine	1.8306	0.87234	0.002504	2.6013
3	Dihydroclavaminic acid	0.65601	-0.60821	0.021272	1.6722
4	Glutarylcarnitine	0.61322	-0.70552	2.48E-05	4.6049

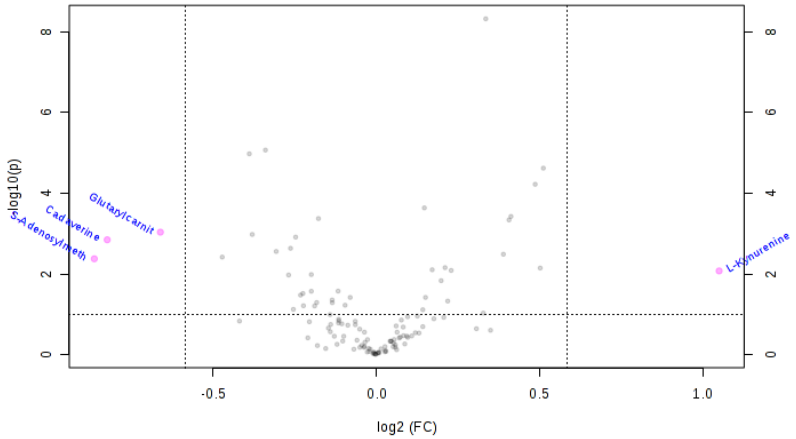

Figure 6.6 Important metabolites selected by volcano plot between congenitally infected mice group and exposed uninfected mice with fold change threshold 1.5 and t-tests threshold (C18-PFP Column).

Table 6.6 Important metabolites identified between congenitally infected mice group and exposed uninfected mice group by volcano plot (C18-PFP Column).

	Metabolites	**FC**	**log2(FC)**	***p*.value**	**-LOG10(p)**
1	L-Kynurenine	2.0708	1.0502	0.008425	2.0744
2	Glutarylcarnitine	0.63201	-0.66198	0.000922	3.0351
3	Cadaverine	0.56452	-0.82489	0.001425	2.8461
4	S-Adenosylmethioninamine	0.54922	-0.86455	0.004213	2.3754

Table 6.7 Pathways are ranked by Pathway Perturbation Score (PPS) for congenital experiment datasets. Only the 50 top-scoring pathways are included in the table.

Pathway	DPPS
tryptophan degradation I (via anthranilate)	1.4
methylglyoxal degradation I	1.35
spermine biosynthesis	1.33
spermidine biosynthesis I	1.33
tryptophan degradation to 2-amino-3-carboxymuconate semialdehyde	1.21
spermine biosynthesis II	1.09
NAD biosynthesis II (from tryptophan)	1.06
urate degradation to allantoin	1.01
molybdenum cofactor (sulfide) biosynthesis	0.983
L-cysteine degradation VI	0.983
L-cysteine degradation III	0.983
tryptophan degradation III (eukaryotic)	0.901
ureide biosynthesis	0.879
glutathione biosynthesis	0.833
GDP-L-fucose biosynthesis I (from GDP-D-mannose)	0.827
1,25-dihydroxyvitamin D3 biosynthesis	0.827
thioredoxin pathway	0.827
wax esters biosynthesis I	0.827
fatty acid β-oxidation IV (unsaturated, even number)	0.827
biosynthesis of prostaglandins	0.827
very long chain fatty acid biosynthesis	0.827
palmitate biosynthesis I (animals)	0.827
uracil degradation II (reductive)	0.827
tetrahydrobiopterin biosynthesis II	0.816
tetrahydrobiopterin biosynthesis I	0.811
urate biosynthesis/inosine 5'-phosphate degradation	0.807
L-arabinose degradation II	0.756
D-glucuronate degradation I	0.756
biosynthesis of corticosteroids	0.756
γ-glutamyl cycle	0.746
nicotine degradation III	0.744
cysteine biosynthesis II	0.728
cysteine biosynthesis/homocysteine degradation	0.728
GDP-L-fucose biosynthesis II (from L-fucose)	0.725

glutathione redox reactions II	0.724
allantoin degradation to ureidoglycolate I (urea producing)	0.701
mevalonate pathway I	0.697
superpathway of cholesterol biosynthesis	0.697
L-cysteine degradation I	0.696
glutathione redox reactions I	0.686
coenzyme A biosynthesis	0.681
nicotine degradation II	0.678
biosynthesis of androgens	0.677
tRNA charging pathway	0.669
guanosine nucleotides degradation III	0.661
histamine degradation	0.659
asparagine biosynthesis I	0.648
trehalose degradation II (trehalase)	0.648
L-glutamine biosynthesis II (tRNA-dependent)	0.648
S-adenosyl-L-methionine biosynthesis	0.648

Chapter 7

7.1 Quality Metrics (Control vs. Infected and Control vs. Uninfected) in congenital infection experiment.

For inspecting the quality of RNA-Seq data, the 100 most abundant genes are taken from all the samples and heat maps are generated to observe the relation between samples/conditions in the congenital experiment.

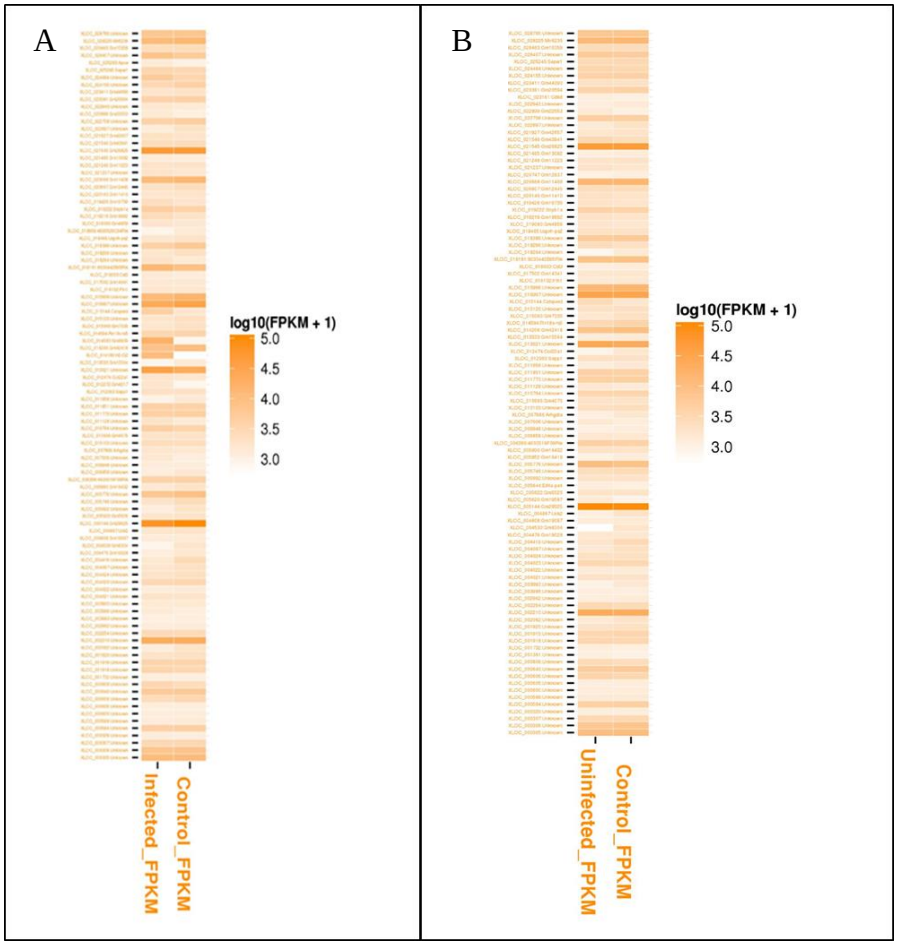

Figure 0.1 Heat map of top 100 differentially expressed genes in congenital infection experiment. (A) The top 100 genes for congenitally infected mice and control group. (B) The top 100 genes for congenitally exposed uninfected group and control group.

7.2 Scatter plots (Control vs. Infected and Control vs. Uninfected) in congenital infection experiment.

Scatter plots highlight the general similarities and specific outliers between the conditions in the RNA-Seq experiment see figure 6.6.

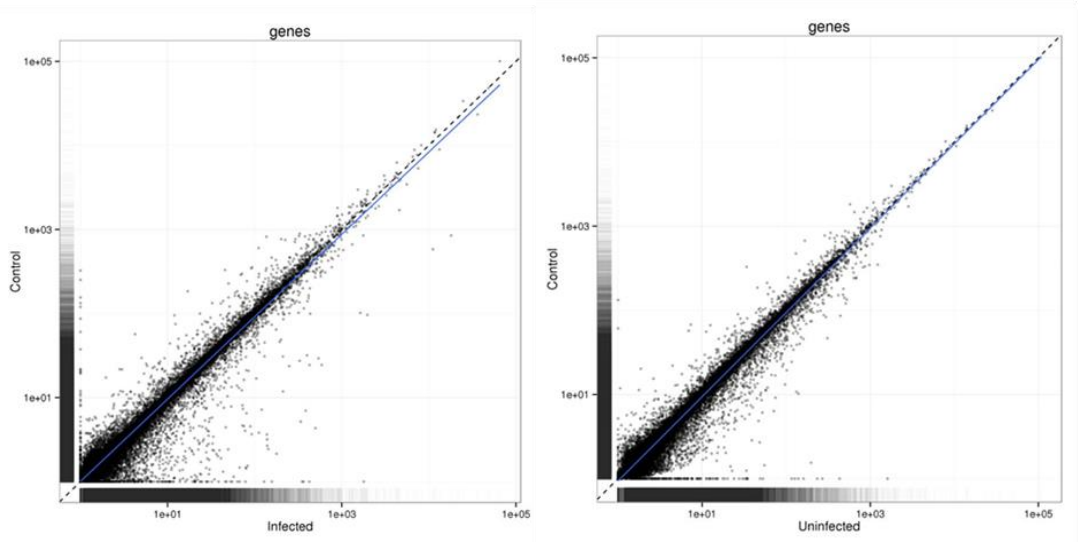

Figure 0.2 Scatter plot of congenital infection experiment. (A) Congenitally infected group versus control group and (B) congenitally exposed uninfected group versus control. In such a plot gene with equal expression values would line up on the identity line (diagonal), with higher expression values further away from the origin. Points below the diagonal represent genes with higher expression in the congenitally infected samples, which plotted on the *x*-axis. Similarly, points above the diagonal represent genes with higher expression values in the control samples, which plotted on the *y*-axis. The further away the point is from the identity line the larger is the difference between its expressions in one group compared with the other.

Table 7.1 All significant genes (FDR of <0.05) upregulated in congenitally infected mice brain with *T. gondii*.

	Gene	Description	Average FPKM		Fold Change	FDR
			Infected (n=3)	Control (n=3)		
1	Ighg1	immunoglobulin heavy constant gamma 1 (G1m marker)	78.8	0.4	182.8	0.002
2	Igkv8-21	immunoglobulin kappa variable 8-21	78.0	0.5	166.0	0.016
3	H2-Eb1	histocompatibility 2, class II antigen E beta	177.0	1.2	153.8	0.002
4	Zbp1	Z-DNA binding protein 1	20.6	0.1	149.5	0.002
5	Cd74	CD74 antigen (invariant polypeptide of major histocompatibility complex, class II antigen-associated)	497.4	3.3	149.1	0.002
6	H2-Ea-ps	histocompatibility 2, class II antigen E alpha, pseudogene	66.2	0.5	139.9	0.002
7	Iigp1	interferon inducible GTPase 1	42.4	0.3	134.1	0.002
8	Ighg2b	immunoglobulin heavy constant gamma 2B	28.8	0.2	127.5	0.002
9	Ccl5	chemokine (C-C motif) ligand 5	23.2	0.2	106.4	0.043
10	Gm12250	predicted gene 12250	19.6	0.2	101.6	0.002
11	H2-Aa	histocompatibility 2, class II antigen A, alpha	142.8	1.4	98.9	0.002
12	Jchain	immunoglobulin joining chain	22.6	0.2	93.9	0.002
13	Gm12185	predicted gene 12185	1.2	0.01	87.3	0.043
14	Cxcl9	chemokine (C-X-C motif) ligand 9	7.0	0.1	85.7	0.002
15	Igha	immunoglobulin heavy constant alpha	138.5	1.7	82.8	0.002
16	Igkc	immunoglobulin kappa constant	337.0	4.2	80.6	0.002
17	Irgm2	immunity-related GTPase family M member 2	109.2	1.4	79.3	0.002
18	Nlrc5	NLR family, CARD domain containing 5	3.6	0.1	66.0	0.002
19	Hcar2	hydroxycarboxylic acid receptor 2	2.4	0.04	58.6	0.034
20	Gbp10	guanylate-binding protein 10	26.8	0.5	58.6	0.002
21	Gm43302	predicted gene 43302	26.8	0.5	58.6	0.002
22	Plac8	placenta-specific 8	6.4	0.1	55.5	0.045
23	H2-DMb1	histocompatibility 2, class II, locus Mb1	9.3	0.2	53.9	0.002
24	F830016B08Rik	RIKEN cDNA F830016B08 gene	2.2	0.04	53.3	0.002
25	H2-Ab1	histocompatibility 2, class II antigen A, beta 1	137.4	2.6	52.0	0.002
26	Gm4841	predicted gene 4841	2.5	0.1	48.5	0.002
27	Batf2	basic leucine zipper transcription factor, ATF-like 2	5.0	0.1	46.8	0.002
28	Ciita	class II transactivator	2.6	0.1	46.4	0.002
29	Oasl2	2'-5' oligoadenylate synthetase-like 2	40.1	0.9	44.8	0.002

30	Cd8a	CD8 antigen, alpha chain	2.0	0.1	38.0	0.002
31	Fcgr4	Fc receptor, IgG, low affinity IV	7.8	0.2	37.7	0.002
32	Psmb9	proteasome (prosome, macropain) subunit, beta type 9 (large multifunctional peptidase 2)	36.8	1.0	36.5	0.002
33	Igkv1-117	immunoglobulin kappa variable 1-117	13.9	0.4	36.2	0.037
34	Ighg3	Immunoglobulin heavy constant gamma 3	12.8	0.4	36.0	0.002
35	Psmb8	proteasome (prosome, macropain) subunit, beta type 8 (large multifunctional peptidase 7)	91.5	2.7	34.3	0.002
36	Tap1	transporter 1, ATP-binding cassette, sub-family B (MDR/TAP)	23.2	0.7	32.5	0.002
37	Ifi44l	interferon-induced protein 44 like	4.8	0.2	32.0	0.002
38	H2-Q6	histocompatibility 2, Q region locus 6	35.4	1.1	31.3	0.002
39	Gbp2b	guanylate binding protein 2b	27.6	0.9	31.2	0.002
40	Ccl12	chemokine (C-C motif) ligand 12	10.1	0.4	26.5	0.002
41	H2-Q4	histocompatibility 2, Q region locus 4	76.7	3.0	25.3	0.002
42	2410017I17Rik	RIKEN cDNA 2410017I17 gene	587.5	23.5	25.0	0.002
43	Ly6a	lymphocyte antigen 6 complex, locus A	88.3	3.5	24.9	0.002
44	Il2rb	interleukin 2 receptor, beta chain	1.1	0.05	24.8	0.002
45	H2-Q5	histocompatibility 2, Q region locus 5	33.0	1.3	24.6	0.002
46	Clec7a	C-type lectin domain family 7, member a	2.3	0.1	24.1	0.002
47	C3	complement component 3	8.0	0.4	22.3	0.002
48	Gm8909	predicted gene 8909	15068.4	685.7	22.0	0.002
49	Cd274	CD274 antigen	15.2	0.7	21.7	0.002
50	Gbp2	guanylate binding protein 2	26.8	1.2	21.7	0.002
51	Ifi204	interferon activated gene 204	2.2	0.1	21.0	0.002
52	H2-T23	histocompatibility 2, T region locus 23	74.4	3.6	20.8	0.002
53	Serpina3g	serine (or cysteine) peptidase inhibitor, clade A, member 3G	4.1	0.2	20.8	0.002
54	Epsti1	epithelial stromal interaction 1 (breast)	2.6	0.1	20.8	0.002
55	H2-M2	histocompatibility 2, M region locus 2	1962.5	95.1	20.6	0.002
56	Ifi44	interferon-induced protein 44	8.5	0.4	20.1	0.002
57	Slfn8	schlafen 8	2.2	0.1	19.7	0.002
58	H2-K1	histocompatibility 2, K1, K region	210.9	10.8	19.5	0.002
59	H2-Q10	histocompatibility 2, Q region locus 10	338.4	17.6	19.2	0.002
60	H2-Bl	histocompatibility 2, blastocyst	540.3	28.3	19.1	0.002
61	H2-DMb2	histocompatibility 2, class II, locus Mb2	5.5	0.3	18.8	0.002
62	Ifi202b	interferon activated gene 202B	3.3	0.2	18.5	0.002
63	H2-K2	histocompatibility 2, K region locus 2	72.7	3.9	18.4	0.002

64	Lat	linker for activation of T cells	1.7	0.1	18.0	0.006
65	Cxcl13	chemokine (C-X-C motif) ligand 13	2.3	0.1	17.7	0.002
66	Gbp3	guanylate binding protein 3	31.8	1.8	17.3	0.002
67	Ccl2	chemokine (C-C motif) ligand 2	2.6	0.2	16.7	0.008
68	Itgax	integrin alpha X	1.6	0.1	16.3	0.002
69	C4a	complement component 4A (Rodgers blood group)	11.3	0.7	16.2	0.043
70	Gm10499	predicted gene 10499	1632.7	100.8	16.2	0.002
71	Cytip	cytohesin 1 interacting protein	1.1	0.1	15.8	0.014
72	Isg15	ISG15 ubiquitin-like modifier	28.6	1.8	15.8	0.002
73	Pou2af1	POU domain, class 2, associating factor 1	0.6	0.04	15.6	0.046
74	AB124611	cDNA sequence AB124611	2.8	0.2	15.6	0.002
75	Ifi27l2a	interferon, alpha-inducible protein 27 like 2A	21.5	1.4	15.3	0.002
76	Gbp5	guanylate binding protein 5	11.4	0.8	14.7	0.002
77	Mzb1	marginal zone B and B1 cell-specific protein 1	3.6	0.2	14.6	0.002
78	Cdkn2a	cyclin-dependent kinase inhibitor 2A	1.9	0.1	14.5	0.042
79	Gbp7	guanylate binding protein 7	14.4	1.0	14.5	0.002
80	Slamf8	SLAM family member 8	2.3	0.2	14.4	0.002
81	Ms4a6c	membrane-spanning 4-domains, subfamily A, member 6C	2.6	0.2	14.4	0.008
82	Gm20662	predicted gene 20662	4.7	0.3	13.7	0.002
83	Ip6k1	inositol hexaphosphate kinase 1	4.7	0.3	13.7	0.002
84	Oas1a	2'-5' oligoadenylate synthetase 1A	3.2	0.2	13.4	0.002
85	Bst2	bone marrow stromal cell antigen 2	45.6	3.4	13.3	0.002
86	Cd5	CD5 antigen	0.8	0.1	13.2	0.010
87	Lcn2	lipocalin 2	3.4	0.3	13.2	0.002
88	B2m	beta-2 microglobulin	397.7	30.8	12.9	0.002
89	Irf7	interferon regulatory factor 7	12.2	1.0	12.8	0.002
90	H2-D1	histocompatibility 2, D region locus 1	327.5	26.4	12.4	0.002
91	Ifit1	interferon-induced protein with tetratricopeptide repeats 1	4.5	0.4	12.3	0.002
92	Usp18	ubiquitin specific peptidase 18	8.5	0.7	12.2	0.002
93	Cd36	CD36 molecule	3.1	0.3	12.2	0.002
94	Gm20478	predicted gene 20478	24.4	2.0	12.1	0.002
95	Irf1	interferon regulatory factor 1	22.4	1.9	11.8	0.002
96	Gimap4	GTPase, IMAP family member 4	3.5	0.3	11.5	0.002
97	C4b	complement component 4B (Chido blood group)	28.6	2.5	11.3	0.002
98	AW112010	expressed sequence AW112010	16.9	1.5	11.3	0.002

99	H2-Q2	histocompatibility 2, Q region locus 2	71.6	6.4	11.3	0.002
100	Parp14	poly (ADP-ribose) polymerase family, member 14	4.6	0.4	11.2	0.002
101	BE692007	expressed sequence BE692007	1.3	0.1	11.1	0.024
102	Ifit3	interferon-induced protein with tetratricopeptide repeats 3	9.9	1.0	10.4	0.002
103	Cd52	CD52 antigen	21.4	2.1	10.3	0.002
104	Acap1	ArfGAP with coiled-coil, ankyrin repeat and PH domains 1	0.6	0.1	10.1	0.046
105	Ly9	lymphocyte antigen 9	2.0	0.2	10.0	0.006
106	Phf11b	PHD finger protein 11B	1.0	0.1	9.9	0.039
107	Phf11d	PHD finger protein 11D	1.5	0.2	9.8	0.002
108	Apol9a	apolipoprotein L 9a	0.7	0.1	9.7	0.014
109	Csf2rb	colony stimulating factor 2 receptor, beta, low-affinity (granulocyte-macrophage)	1.2	0.1	9.6	0.002
110	Dlx1as	distal-less homeobox 1, antisense	5.8	0.6	9.6	0.049
111	Fgl2	fibrinogen-like protein 2	7.1	0.8	9.5	0.002
112	Fam26f	family with sequence similarity 26, member F	1.9	0.2	9.4	0.002
113	Psd4	pleckstrin and Sec7 domain containing 4	0.8	0.1	9.3	0.002
114	Pla2g2d	phospholipase A2, group IID	0.9	0.1	9.3	0.006
115	Casp4	caspase 4, apoptosis-related cysteine peptidase	1.3	0.1	9.2	0.006
116	Ptprcap	protein tyrosine phosphatase, receptor type, C polypeptide-associated protein	2.4	0.3	9.1	0.002
117	Ltb	lymphotoxin B	4.8	0.5	9.1	0.002
118	Il18bp	interleukin 18 binding protein	7.2	0.8	9.1	0.002
119	Tlr12	toll-like receptor 12	1.2	0.1	8.6	0.002
120	Il1b	interleukin 1 beta	2.3	0.3	8.6	0.002
121	Gm13710	predicted gene 13710	0.9	0.1	8.6	0.022
122	Themis2	thymocyte selection associated family member 2	1.3	0.2	8.6	0.002
123	C1ra	complement component 1, r subcomponent A	1.4	0.2	8.4	0.002
124	Plec	plectin	5.3	0.6	8.4	0.002
125	Trim30a	tripartite motif-containing 30A	3.1	0.4	8.2	0.002
126	Csf2rb2	colony stimulating factor 2 receptor, beta 2, low-affinity (granulocyte-macrophage)	0.6	0.1	8.2	0.002
127	Hpse	heparanase	2.4	0.3	8.0	0.002
128	Lag3	lymphocyte-activation gene 3	9.5	1.2	7.9	0.002
129	Ms4a6b	membrane-spanning 4-domains, subfamily A, member 6B	1.7	0.2	7.9	0.002
130	Myo1g	myosin IG	0.9	0.1	7.8	0.030
131	Acp5	acid phosphatase 5, tartrate resistant	1.4	0.2	7.7	0.002
132	Mlkl	mixed lineage kinase domain-like	0.8	0.1	7.7	0.002

133	Ctsw	cathepsin W	1.7	0.2	7.6	0.002
134	Ptprc	protein tyrosine phosphatase, receptor type, C	2.8	0.4	7.5	0.002
135	Serpina3i	serine (or cysteine) peptidase inhibitor, clade A, member 3I	1.7	0.2	7.4	0.016
136	Saa3	serum amyloid A 3	2.3	0.3	7.4	0.030
137	H2-Ob	histocompatibility 2, O region beta locus	1.2	0.2	7.2	0.002
138	Lck	lymphocyte protein tyrosine kinase	2.2	0.3	7.1	0.002
139	Plbd1	phospholipase B domain containing 1	1.4	0.2	7.0	0.002
140	Irf8	interferon regulatory factor 8	9.9	1.4	6.9	0.002
141	Serpina3h	serine (or cysteine) peptidase inhibitor, clade A, member 3H	2.3	0.3	6.9	0.002
142	Lgals3bp	lectin, galactoside-binding, soluble, 3 binding protein	24.1	3.5	6.9	0.002
143	Slfn2	schlafen 2	4.5	0.7	6.8	0.002
144	AU020206	expressed sequence AU020206	7.3	1.1	6.8	0.002
145	Rnf213	ring finger protein 213	1.2	0.2	6.6	0.002
146	Gm15821	predicted gene 15821	43.4	6.6	6.6	0.002
147	Cd180	CD180 antigen	1.5	0.2	6.6	0.002
148	AU020206	expressed sequence AU020206	2.4	0.4	6.5	0.010
149	Oas1b	2'-5' oligoadenylate synthetase 1B	1.6	0.3	6.5	0.002
150	Prl	prolactin	103.3	15.9	6.5	0.002
151	Itgal	integrin alpha L	2.5	0.4	6.5	0.002
152	Gpr84	G protein-coupled receptor 84	1.6	0.2	6.5	0.002
153	Gm8995	predicted gene 8995	1.4	0.2	6.5	0.002
154	Gbp11	guanylate binding protein 11	4.3	0.7	6.4	0.002
155	Trim34b	tripartite motif-containing 34B	0.8	0.1	6.3	0.004
156	Ifitm3	interferon induced transmembrane protein 3	70.2	11.2	6.3	0.002
157	Tap2	transporter 2, ATP-binding cassette, sub-family B (MDR/TAP)	22.2	3.6	6.2	0.002
158	Mpeg1	macrophage expressed gene 1	25.9	4.3	6.0	0.002
159	Frrs1	ferric-chelate reductase 1	1.3	0.2	5.9	0.047
160	Ifi35	interferon-induced protein 35	13.4	2.3	5.9	0.002
161	Trim21	tripartite motif-containing 21	5.0	0.8	5.9	0.002
162	Cd48	CD48 antigen	2.8	0.5	5.7	0.002
163	H2-M3	histocompatibility 2, M region locus 3	10.0	1.8	5.7	0.002
164	Ptpn7	protein tyrosine phosphatase, non-receptor type 7	0.8	0.1	5.6	0.024
165	Nlrp3	NLR family, pyrin domain containing 3	0.8	0.1	5.6	0.008
166	Lcp2	lymphocyte cytosolic protein 2	3.0	0.5	5.6	0.002
167	Pik3ap1	phosphoinositide-3-kinase adaptor protein 1	3.4	0.6	5.5	0.002

168	Hspb2	heat shock protein 2	4.3	0.8	5.5	0.002
169	Rsad2	radical S-adenosyl methionine domain containing 2	1.9	0.3	5.5	0.002
170	Itk	IL2 inducible T cell kinase	0.7	0.1	5.5	0.006
171	Tlr9	toll-like receptor 9	0.9	0.2	5.5	0.004
172	Xaf1	XIAP associated factor 1	11.7	2.2	5.4	0.002
173	Lilr4b	leukocyte immunoglobulin-like receptor, subfamily B, member 4B	1.2	0.2	5.4	0.025
174	Gm8995	predicted gene 8995	1.6	0.3	5.3	0.002
175	Casp1	caspase 1	6.3	1.2	5.3	0.002
176	Slc15a3	solute carrier family 15, member 3	3.6	0.7	5.2	0.002
177	Gh	growth hormone	40.0	7.8	5.1	0.002
178	Gmfg	glia maturation factor, gamma	3.6	0.7	5.1	0.002
179	Siglec1	sialic acid binding Ig-like lectin 1, sialoadhesin	0.8	0.2	5.1	0.006
180	Fam167b	family with sequence similarity 167, member B	2.2	0.4	5.1	0.004
181	Pycard	PYD and CARD domain containing	4.2	0.8	5.1	0.022
182	Tnfsf10	tumor necrosis factor (ligand) superfamily, member 10	2.5	0.5	5.1	0.002
183	Cd86	CD86 antigen	2.7	0.5	5.0	0.002
184	Icam1	intercellular adhesion molecule 1	3.9	0.8	5.0	0.002
185	Cxcl16	chemokine (C-X-C motif) ligand 16	14.4	2.9	5.0	0.002
186	Slc11a1	solute carrier family 11 (proton-coupled divalent metal ion transporters), member 1	4.2	0.8	5.0	0.002
187	Ptpn18	protein tyrosine phosphatase, non-receptor type 18	6.0	1.2	5.0	0.002
188	Isg20	interferon-stimulated protein	3.1	0.6	5.0	0.002
189	Parp9	poly (ADP-ribose) polymerase family, member 9	5.7	1.2	4.9	0.002
190	Serpina3f	serine (or cysteine) peptidase inhibitor, clade A, member 3F	1.7	0.4	4.9	0.002
191	AI662270	expressed sequence AI662270	1.2	0.3	4.9	0.012
192	Il7r	interleukin 7 receptor	1.2	0.3	4.8	0.002
193	C1qc	complement component 1, q subcomponent, C chain	61.7	12.9	4.8	0.002
194	Lgals3bp	lectin, galactoside-binding, soluble, 3 binding protein	1.0	0.2	4.7	0.002
195	Rasal3	RAS protein activator like 3	1.8	0.4	4.7	0.002
196	Sp110	Sp110 nuclear body protein	2.8	0.6	4.7	0.002
197	Cd84	CD84 antigen	2.5	0.5	4.7	0.002
198	Gm12185	predicted gene 12185	0.7	0.2	4.6	0.047
199	Lpxn	leupaxin	1.5	0.3	4.6	0.002
200	Pld4	phospholipase D family, member 4	11.4	2.5	4.6	0.002

201	Neurl3	neuralized E3 ubiquitin protein ligase 3	1.1	0.2	4.6	0.002
202	Hpgds	hematopoietic prostaglandin D synthase	6.3	1.4	4.5	0.002
203	Itgb7	integrin beta 7	1.9	0.4	4.5	0.002
204	Arhgap9	Rho GTPase activating protein 9	1.7	0.4	4.5	0.002
205	Tnfrsf14	tumor necrosis factor receptor superfamily, member 14 (herpesvirus entry mediator)	1.5	0.3	4.5	0.002
206	Gm44935	RIKEN cDNA A930037H05 gene	2.7	0.6	4.5	0.019
207	Hck	hemopoietic cell kinase	4.0	0.9	4.5	0.002
208	Ifit3b	interferon-induced protein with tetratricopeptide repeats 3B	6.9	1.5	4.5	0.002
209	Dtx3l	deltex 3-like, E3 ubiquitin ligase	4.9	1.1	4.4	0.002
210	Ptpn22	protein tyrosine phosphatase, non-receptor type 22 (lymphoid)	0.9	0.2	4.4	0.002
211	Ptpn6	protein tyrosine phosphatase, non-receptor type 6	6.2	1.4	4.4	0.002
212	Ncf4	neutrophil cytosolic factor 4	3.1	0.7	4.4	0.002
213	Itgb2	integrin beta 2	6.7	1.5	4.4	0.002
214	H2-T24	histocompatibility 2, T region locus 24	6.6	1.5	4.4	0.002
215	Fcgr1	Fc receptor, IgG, high affinity I	4.9	1.1	4.3	0.002
216	Zfp773	zinc finger protein 773	1.0	0.2	4.3	0.002
217	Ly6c2	lymphocyte antigen 6 complex, locus C2	9.7	2.2	4.3	0.002
218	C1qa	complement component 1, q subcomponent, alpha polypeptide	128.9	30.0	4.3	0.002
219	Trim14	tripartite motif-containing 14	1.2	0.3	4.3	0.002
220	Aif1	allograft inflammatory factor 1	8.9	2.1	4.3	0.002
221	Adgre1	adhesion G protein-coupled receptor E1	5.7	1.3	4.3	0.002
222	C1qb	complement component 1, q subcomponent, beta polypeptide	84.1	19.8	4.2	0.002
223	Gzmk	granzyme K	1.3	0.3	4.2	0.002
224	Gm42743	predicted gene 42743	0.5	0.1	4.2	0.014
225	H19	H19, imprinted maternally expressed transcript	1.3	0.3	4.2	0.002
226	Ctss	cathepsin S	199.6	47.9	4.2	0.002
227	Lyz2	lysozyme 2	27.1	6.5	4.2	0.002
228	Cd79a	CD79A antigen (immunoglobulin-associated alpha)	1.2	0.3	4.2	0.004
229	Socs1	suppressor of cytokine signaling 1	5.4	1.3	4.1	0.002
230	Klhl6	kelch-like 6	1.7	0.4	4.1	0.002
231	Cryba4	crystallin, beta A4	2.6	0.6	4.1	0.002
232	Myo1f	myosin IF	3.4	0.8	4.1	0.002
233	Fyb	FYN binding protein	3.0	0.7	4.1	0.002
234	Tbxas1	thromboxane A synthase 1, platelet	1.6	0.4	4.0	0.002

235	Hcls1	hematopoietic cell specific Lyn substrate 1	6.7	1.7	4.0	0.002
236	Tmem106a	transmembrane protein 106A	1.5	0.4	4.0	0.002
237	Gna15	guanine nucleotide binding protein, alpha 15	2.5	0.6	4.0	0.002
238	Ptafr	platelet-activating factor receptor	1.2	0.3	4.0	0.002
239	P2ry6	pyrimidinergic receptor P2Y, G-protein coupled, 6	3.7	0.9	4.0	0.002
240	Arg1	arginase, liver	1.5	0.4	3.9	0.002
241	Dock2	dedicator of cyto-kinesis 2	2.0	0.5	3.9	0.002
242	Fcgr2b	Fc receptor, IgG, low affinity IIb	1.8	0.5	3.9	0.004
243	Parp12	poly (ADP-ribose) polymerase family, member 12	9.1	2.3	3.9	0.002
244	H2-DMa	histocompatibility 2, class II, locus DMa	19.0	4.9	3.9	0.002
245	Gsdmd	gasdermin D	3.1	0.8	3.9	0.002
246	Bcl3	B cell leukemia/lymphoma 3	1.0	0.3	3.8	0.002
247	Ncf1	neutrophil cytosolic factor 1	8.5	2.2	3.8	0.002
248	Ube2l6	ubiquitin-conjugating enzyme E2L 6	10.2	2.7	3.8	0.002
249	Crybb1	crystallin, beta B1	10.4	2.7	3.8	0.002
250	Tmem173	transmembrane protein 173	3.6	1.0	3.8	0.002
251	Mx2	MX dynamin-like GTPase 2	1.2	0.3	3.8	0.002
252	Ly86	lymphocyte antigen 86	25.0	6.7	3.7	0.002
253	Tapbpl	TAP binding protein-like	7.1	1.9	3.7	0.002
254	Samd9l	sterile alpha motif domain containing 9-like	3.1	0.9	3.7	0.002
255	Il10ra	interleukin 10 receptor, alpha	4.3	1.2	3.7	0.002
256	Casp12	caspase 12	2.7	0.7	3.6	0.002
257	Vav1	vav 1 oncogene	3.6	1.0	3.6	0.002
258	Serping1	serine (or cysteine) peptidase inhibitor, clade G, member 1	12.4	3.5	3.5	0.002
259	Arl11	ADP-ribosylation factor-like 11	0.9	0.3	3.5	0.014
260	Ccdc88b	coiled-coil domain containing 88B	1.7	0.5	3.5	0.002
261	Rab20	RAB20, member RAS oncogene family	1.9	0.6	3.5	0.029
262	Clec4a3	C-type lectin domain family 4, member a3	1.2	0.3	3.5	0.002
263	Il1a	interleukin 1 alpha	1.4	0.4	3.5	0.002
264	Ifi27	interferon, alpha-inducible protein 27	64.1	18.5	3.5	0.002
265	Xdh	xanthine dehydrogenase	4.8	1.4	3.5	0.002
266	BC035044	cDNA sequence BC035044	1.7	0.5	3.5	0.002
267	Cd33	CD33 antigen	3.1	0.9	3.4	0.008
268	Havcr2	hepatitis A virus cellular receptor 2	2.3	0.7	3.4	0.002
269	Ifih1	interferon induced with helicase C domain 1	3.0	0.9	3.4	0.002
270	Unc93b1	unc-93 homolog B1 (C. elegans)	13.1	3.9	3.4	0.002

271	Plcb2	phospholipase C, beta 2	1.0	0.3	3.3	0.002
272	Sp100	nuclear antigen Sp100	3.6	1.1	3.3	0.002
273	Rhoh	ras homolog family member H	1.1	0.3	3.3	0.004
274	Ms4a6d	membrane-spanning 4-domains, subfamily A, member 6D	3.6	1.1	3.3	0.002
275	Lst1	leukocyte specific transcript 1	7.3	2.2	3.3	0.002
276	Lrrc25	leucine rich repeat containing 25	1.1	0.3	3.3	0.004
277	4930599N23Rik	RIKEN cDNA 4930599N23 gene	0.6	0.2	3.3	0.014
278	Ikzf1	IKAROS family zinc finger 1	2.4	0.7	3.3	0.002
279	Fcgr3	Fc receptor, IgG, low affinity III	14.4	4.4	3.3	0.002
280	Hmha1	Rho GTPase activating protein 45	2.9	0.9	3.2	0.002
281	Ddx58	DEAD (Asp-Glu-Ala-Asp) box polypeptide 58	3.1	1.0	3.2	0.002
282	Cd300c2	CD300C molecule 2	4.9	1.5	3.2	0.002
283	H2-T22	histocompatibility 2, T region locus 22	13.3	4.1	3.2	0.002
284	Pomc	pro-opiomelanocortin-alpha	8.6	2.7	3.2	0.002
285	Arhgap30	Rho GTPase activating protein 30	2.4	0.8	3.2	0.002
286	Lgals3	lectin, galactose binding, soluble 3	3.0	1.0	3.2	0.002
287	Tlr2	toll-like receptor 2	2.4	0.7	3.2	0.002
288	Susd3	sushi domain containing 3	1.9	0.6	3.2	0.002
289	Top2a	topoisomerase (DNA) II alpha	1.1	0.4	3.2	0.022
290	Slfn9	schlafen 9	1.1	0.3	3.2	0.002
291	Il12rb1	interleukin 12 receptor, beta 1	3.2	1.0	3.1	0.002
292	Ighj1	immunoglobulin heavy joining 1	4.6	1.5	3.1	0.002
293	Lgals9	lectin, galactose binding, soluble 9	23.8	7.6	3.1	0.002
294	Dmrtb1	DMRT-like family B with proline-rich C-terminal, 1	2.7	0.9	3.1	0.002
295	Trim12c	tripartite motif-containing 12C	4.1	1.3	3.1	0.002
296	Fcer1g	Fc receptor, IgE, high affinity I, gamma polypeptide	21.4	7.0	3.1	0.002
297	Laptm5	lysosomal-associated protein transmembrane 5	49.5	16.1	3.1	0.002
298	Nckap1l	NCK associated protein 1 like	4.9	1.6	3.1	0.002
299	Naip2	NLR family, apoptosis inhibitory protein 2	0.7	0.2	3.1	0.002
300	Lcp1	lymphocyte cytosolic protein 1	11.0	3.6	3.1	0.002
301	Avp	arginine vasopressin	44.6	14.6	3.1	0.002
302	Pbx2	pre B cell leukemia homeobox 2	2.9	1.0	3.1	0.002
303	Tifab	TRAF-interacting protein with forkhead-associated domain, family member B	1.9	0.6	3.1	0.002
304	Fermt3	fermitin family member 3	3.7	1.2	3.0	0.022
305	Zc3hav1	zinc finger CCCH type, antiviral 1	4.9	1.6	3.0	0.002

306	Plin4	perilipin 4	1.6	0.5	2.9	0.002
307	Fam46c	family with sequence similarity 46, member C	1.9	0.6	2.9	0.002
308	Trim34a	tripartite motif-containing 34A	0.8	0.3	2.9	0.046
309	Ifi30	interferon gamma inducible protein 30	5.9	2.0	2.9	0.002
310	Apobec1	apolipoprotein B mRNA editing enzyme, catalytic polypeptide 1	2.8	1.0	2.9	0.002
311	Lat2	linker for activation of T cells family, member 2	2.3	0.8	2.9	0.002
312	9930111J21Rik2	RIKEN cDNA 9930111J21 gene 2	2.3	0.8	2.9	0.002
313	Tnfaip8l2	tumor necrosis factor, alpha-induced protein 8-like 2	3.4	1.2	2.8	0.002
314	Irf5	interferon regulatory factor 5	3.9	1.4	2.8	0.002
315	Bin2	bridging integrator 2	4.8	1.7	2.8	0.002
316	Ccl6	chemokine (C-C motif) ligand 6	1.9	0.7	2.8	0.002
317	Nmi	N-myc (and STAT) interactor	7.9	2.8	2.8	0.002
318	Klrg2	killer cell lectin-like receptor subfamily G, member 2	0.7	0.3	2.8	0.049
319	Herc6	hect domain and RLD 6	5.0	1.8	2.8	0.002
320	Ccrl2	chemokine (C-C motif) receptor-like 2	1.6	0.6	2.7	0.002
321	Mki67	antigen identified by monoclonal antibody Ki 67	0.6	0.2	2.7	0.002
322	Eif2ak2	eukaryotic translation initiation factor 2-alpha kinase 2	5.5	2.0	2.7	0.002
323	Batf3	basic leucine zipper transcription factor, ATF-like 3	1.8	0.6	2.7	0.049
324	Aim2	absent in melanoma 2	1.6	0.6	2.7	0.002
325	Arhgdib	Rho, GDP dissociation inhibitor (GDI) beta	18.6	6.8	2.7	0.002
326	Pdzph1	PDZ and pleckstrin homology domains 1	7.0	2.6	2.7	0.002
327	Tspo	translocator protein	19.9	7.4	2.7	0.002
328	Catsperd	cation channel sperm associated auxiliary subunit delta	4582.0	1699.0	2.7	0.022
329	Procr	protein C receptor, endothelial	1.5	0.6	2.7	0.002
330	Tyrobp	TYRO protein tyrosine kinase binding protein	23.5	8.8	2.7	0.002
331	Gm10271	predicted gene 10271	3.6	1.4	2.7	0.002
332	Lrg1	leucine-rich alpha-2-glycoprotein 1	1.3	0.5	2.7	0.016
333	Tmem119	transmembrane protein 119	24.9	9.4	2.6	0.002
334	Samhd1	SAM domain and HD domain, 1	9.9	3.7	2.6	0.002
335	Il6ra	interleukin 6 receptor, alpha	3.8	1.4	2.6	0.035
336	Cd40	CD40 antigen	0.8	0.3	2.6	0.037
337	Ncf2	neutrophil cytosolic factor 2	3.2	1.2	2.6	0.002
338	Cd37	CD37 antigen	4.7	1.8	2.6	0.002
339	Tgm2	transglutaminase 2, C polypeptide	11.9	4.6	2.6	0.002

340	Rpl13a	ribosomal protein L13A	2.8	1.1	2.6	0.024
341	Alox5ap	arachidonate 5-lipoxygenase activating protein	8.3	3.2	2.6	0.002
342	Rab32	RAB32, member RAS oncogene family	1.5	0.6	2.6	0.002
343	Trim25	tripartite motif-containing 25	3.3	1.3	2.6	0.002
344	Dok1	docking protein 1	2.4	0.9	2.6	0.002
345	Cyba	cytochrome b-245, alpha polypeptide	19.2	7.5	2.6	0.002
346	Pik3cg	phosphatidylinositol-4,5-bisphosphate 3-kinase catalytic subunit gamma	0.9	0.4	2.5	0.002
347	Fgd2	FYVE, RhoGEF and PH domain containing 2	3.9	1.6	2.5	0.002
348	Apobec3	apolipoprotein B mRNA editing enzyme, catalytic polypeptide 3	2.1	0.8	2.5	0.002
349	Lsp1	lymphocyte specific 1	4.3	1.7	2.5	0.002
350	Clec2d	C-type lectin domain family 2, member d	4.6	1.8	2.5	0.002
351	Cdk1	cyclin-dependent kinase 1	1.1	0.4	2.5	0.046
352	Lair1	leukocyte-associated Ig-like receptor 1	2.2	0.9	2.5	0.002
353	Rnf31	ring finger protein 31	10.5	4.2	2.5	0.002
354	Icosl	icos ligand	3.4	1.4	2.5	0.002
355	Cyth4	cytohesin 4	6.7	2.7	2.5	0.002
356	Csf3r	colony stimulating factor 3 receptor (granulocyte)	2.7	1.1	2.5	0.002
357	Tnfrsf1b	tumor necrosis factor receptor superfamily, member 1b	2.8	1.1	2.4	0.002
358	Plcg2	phospholipase C, gamma 2	2.7	1.1	2.4	0.002
359	Capg	capping protein (actin filament), gelsolin-like	4.6	1.9	2.4	0.002
360	Birc3	baculoviral IAP repeat-containing 3	1.6	0.7	2.4	0.002
361	Trac	T cell receptor alpha constant	3.8	1.6	2.4	0.002
362	Ccno	cyclin O	0.8	0.3	2.4	0.024
363	Lpcat2	lysophosphatidylcholine acyltransferase 2	6.3	2.6	2.4	0.002
364	Pla1a	phospholipase A1 member A	1.1	0.5	2.4	0.010
365	Psme1	proteasome (prosome, macropain) activator subunit 1 (PA28 alpha)	53.6	22.3	2.4	0.002
366	Ighm	immunoglobulin heavy constant mu	11.7	4.9	2.4	0.002
367	Ifit2	interferon-induced protein with tetratricopeptide repeats 2	8.4	3.5	2.4	0.002
368	Entpd1	ectonucleoside triphosphate diphosphohydrolase 1	11.2	4.7	2.4	0.002
369	Cmtm7	CKLF-like MARVEL transmembrane domain containing 7	7.1	3.0	2.4	0.002
370	Slc12a7	solute carrier family 12, member 7	2.4	1.0	2.4	0.002
371	St14	suppression of tumorigenicity 14 (colon carcinoma)	1.0	0.4	2.4	0.002
372	Psmb10	proteasome (prosome, macropain) subunit, beta type 10	46.3	19.6	2.4	0.002

373	Parvg	parvin, gamma	3.1	1.3	2.4	0.002
374	Brca1	breast cancer 1, early onset	1.1	0.5	2.4	0.046
375	Abcc3	ATP-binding cassette, sub-family C (CFTR/MRP), member 3	1.3	0.6	2.3	0.002
376	Fes	feline sarcoma oncogene	2.2	0.9	2.3	0.002
377	Nod1	nucleotide-binding oligomerization domain containing 1	5.0	2.1	2.3	0.002
378	Syk	spleen tyrosine kinase	1.3	0.6	2.3	0.002
379	Ido1	indoleamine 2,3-dioxygenase 1	3.3	1.4	2.3	0.008
380	Parp3	poly (ADP-ribose) polymerase family, member 3	4.5	1.9	2.3	0.002
381	Sh3bp2	SH3-domain binding protein 2	1.8	0.8	2.3	0.002
382	Ctsh	cathepsin H	15.7	6.9	2.3	0.002
383	Gfap	glial fibrillary acidic protein	217.8	96.6	2.3	0.002
384	Erap1	endoplasmic reticulum aminopeptidase 1	5.4	2.4	2.3	0.002
385	Socs3	suppressor of cytokine signaling 3	2.0	0.9	2.2	0.002
386	Nfam1	Nfat activating molecule with ITAM motif 1	1.5	0.7	2.2	0.002
387	Trem2	triggering receptor expressed on myeloid cells 2	13.9	6.3	2.2	0.002
388	Kcnk6	potassium inwardly-rectifying channel, subfamily K, member 6	1.6	0.7	2.2	0.002
389	Stat2	signal transducer and activator of transcription 2	13.3	6.0	2.2	0.002
390	Cd53	CD53 antigen	7.3	3.3	2.2	0.002
391	Akna	AT-hook transcription factor	2.2	1.0	2.2	0.002
392	Casp8	caspase 8	2.9	1.3	2.2	0.002
393	Agpat2	1-acylglycerol-3-phosphate O-acyltransferase 2 (lysophosphatidic acid acyltransferase, beta)	1.2	0.6	2.2	0.035
394	Adap2	ArfGAP with dual PH domains 2	3.8	1.8	2.2	0.002
395	Tlr1	toll-like receptor 1	1.5	0.7	2.2	0.002
396	Srgn	serglycin	13.8	6.4	2.2	0.002
397	Csf1r	colony stimulating factor 1 receptor	38.4	17.8	2.2	0.002
398	Dusp2	dual specificity phosphatase 2	1.1	0.5	2.1	0.045
399	Tnfaip2	tumor necrosis factor, alpha-induced protein 2	2.4	1.2	2.1	0.002
400	Ano2	anoctamin 2	2.4	1.1	2.1	0.004
401	Snx20	sorting nexin 20	3.0	1.4	2.1	0.002
402	Rinl	Ras and Rab interactor-like	1.8	0.8	2.1	0.002
403	Rhbdf2	rhomboid 5 homolog 2	1.0	0.5	2.1	0.046
404	Trim56	tripartite motif-containing 56	4.1	2.0	2.1	0.002
405	B4galt1	UDP-Gal:betaGlcNAc beta 1,4-galactosyltransferase, polypeptide 1	2.8	1.3	2.1	0.002

406	Psme2	proteasome (prosome, macropain) activator subunit 2 (PA28 beta)	44.5	21.3	2.1	0.002
407	Pik3r5	phosphoinositide-3-kinase regulatory subunit 5	1.2	0.6	2.1	0.002
408	Selplg	selectin, platelet (p-selectin) ligand	21.4	10.3	2.1	0.002
409	Gpr160	G protein-coupled receptor 160	1.1	0.5	2.1	0.035
410	Myd88	myeloid differentiation primary response gene 88	4.2	2.0	2.1	0.002
411	Grn	granulin	42.7	20.7	2.1	0.002
412	Nuak2	NUAK family, SNF1-like kinase, 2	1.0	0.5	2.1	0.012
413	Cx3cr1	chemokine (C-X3-C motif) receptor 1	18.8	9.1	2.1	0.002
414	Upp1	uridine phosphorylase 1	2.8	1.4	2.1	0.004
415	Mafb	v-maf musculoaponeurotic fibrosarcoma oncogene family, protein B (avian)	7.7	3.7	2.1	0.002
416	Jak3	Janus kinase 3	2.8	1.4	2.1	0.002
417	Pstpip1	proline-serine-threonine phosphatase-interacting protein 1	1.6	0.8	2.1	0.022
418	Hhex	hematopoietically expressed homeobox	1.9	0.9	2.0	0.006
419	Irak4	interleukin-1 receptor-associated kinase 4	1.5	0.7	2.0	0.004
420	Casp7	caspase 7	2.0	1.0	2.0	0.002
421	Rgl2	ral guanine nucleotide dissociation stimulator-like 2	53.7	26.6	2.0	0.002
422	Tapbp	TAP binding protein	53.7	26.6	2.0	0.002
423	Zbtb22	zinc finger and BTB domain containing 22	53.7	26.6	2.0	0.002
424	Fli1	Friend leukemia integration 1	3.3	1.7	2.0	0.002
425	Itgam	integrin alpha M	5.3	2.7	2.0	0.002
426	Cmklr1	chemokine-like receptor 1	1.3	0.7	2.0	0.006
427	Tlr4	toll-like receptor 4	1.1	0.6	2.0	0.002
428	Cd44	CD44 antigen	1.8	0.9	2.0	0.002
429	Tnfrsf1a	tumor necrosis factor receptor superfamily, member 1a	11.1	5.6	2.0	0.002
430	Tnfrsf13b	tumor necrosis factor receptor superfamily, member 13b	1.1	0.6	2.0	0.049
431	Aspg	asparaginase	1.3	0.7	1.9	0.019
432	Zfp217	zinc finger protein 217	1.1	0.6	1.9	0.002
433	Ly6e	lymphocyte antigen 6 complex, locus E	99.8	51.5	1.9	0.002
434	Nfkb2	nuclear factor of kappa light polypeptide gene enhancer in B cells 2, p49/p100	2.4	1.2	1.9	0.002
435	Cd14	CD14 antigen	3.2	1.7	1.9	0.004
436	Edn1	endothelin 1	1.9	1.0	1.9	0.012
437	Lyn	LYN proto-oncogene, Src family tyrosine kinase	6.6	3.5	1.9	0.002
438	Serpinb6b	serine (or cysteine) peptidase inhibitor, clade B, member 6b	1.5	0.8	1.9	0.021

439	Hexb	hexosaminidase B	106.5	56.4	1.9	0.002
440	Cd4	CD4 antigen	3.8	2.0	1.9	0.002
441	Stat3	signal transducer and activator of transcription 3	22.3	11.9	1.9	0.002
442	Ptgs1	prostaglandin-endoperoxide synthase 1	5.9	3.2	1.9	0.002
443	Adrb2	adrenergic receptor, beta 2	1.5	0.8	1.9	0.037
444	Cebpb	CCAAT/enhancer binding protein (C/EBP), beta	17.2	9.3	1.8	0.002
445	Oxt	oxytocin	20.2	11.0	1.8	0.017
446	Lacc1	laccase (multicopper oxidoreductase) domain containing 1	1.5	0.8	1.8	0.035
447	Ctsz	cathepsin Z	46.0	25.1	1.8	0.012
448	Pros1	protein S (alpha)	7.1	3.9	1.8	0.002
449	Txnip	thioredoxin interacting protein	14.0	7.6	1.8	0.002
450	Cd68	CD68 antigen	7.0	3.9	1.8	0.019
451	Adora2a	adenosine A2a receptor	24.0	13.1	1.8	0.002
452	Lrrc10b	leucine rich repeat containing 10B	16.6	9.1	1.8	0.002
453	Gm43549	predicted gene 43549	5.7	3.1	1.8	0.002
454	Gm43720	predicted gene 43720	5.2	2.9	1.8	0.002
455	Gpc2	glypican 2 (cerebroglycan)	5.2	2.9	1.8	0.002
456	Rin3	Ras and Rab interactor 3	1.3	0.7	1.8	0.024
457	Serpinb9	serine (or cysteine) peptidase inhibitor, clade B, member 9	5.2	2.9	1.8	0.002
458	Gimap6	GTPase, IMAP family member 6	4.3	2.4	1.8	0.002
459	Mfng	MFNG O-fucosylpeptide 3-beta-N-acetylglucosaminyltransferase	3.1	1.7	1.8	0.008
460	Glipr2	GLI pathogenesis-related 2	4.1	2.2	1.8	0.002
461	Helz2	helicase with zinc finger 2, transcriptional coactivator	1.0	0.5	1.8	0.006
462	Vwa5a	von Willebrand factor A domain containing 5A	7.0	3.9	1.8	0.002
463	Matn4	matrilin 4	7.8	4.3	1.8	0.002
464	Mcm3	minichromosome maintenance complex component 3	1.7	1.0	1.8	0.010
465	Ripk2	receptor (TNFRSF)-interacting serine-threonine kinase 2	2.1	1.2	1.8	0.006
466	BC064078	cDNA sequence BC064078	3.7	2.1	1.8	0.043
467	Osmr	oncostatin M receptor	1.6	0.9	1.8	0.006
468	Cebpa	CCAAT/enhancer binding protein (C/EBP), alpha	8.4	4.8	1.8	0.002
469	Sh3rf2	SH3 domain containing ring finger 2	2.2	1.2	1.7	0.004
470	Tor3a	torsin family 3, member A	7.5	4.3	1.7	0.002
471	Epyc	epiphycan	2.7	1.6	1.7	0.040
472	Tnnt1	troponin T1, skeletal, slow	12.5	7.3	1.7	0.004

473	Rab3il1	RAB3A interacting protein (rabin3)-like 1	6.4	3.7	1.7	0.002
474	Fam105a	family with sequence similarity 105, member A	6.4	3.8	1.7	0.002
475	Stom	stomatin	7.3	4.4	1.7	0.002
476	Vcam1	vascular cell adhesion molecule 1	13.2	7.9	1.7	0.002
477	Relb	avian reticuloendotheliosis viral (v-rel) oncogene related B	4.1	2.5	1.7	0.027
478	Tgfb1	transforming growth factor, beta 1	5.7	3.5	1.6	0.025
479	Prkd2	protein kinase D2	2.3	1.4	1.6	0.016
480	Siglech	sialic acid binding Ig-like lectin H	5.8	3.6	1.6	0.002
481	Gpr88	G-protein coupled receptor 88	55.0	33.8	1.6	0.002
482	Afmid	arylformamidase	10.0	6.1	1.6	0.002
483	Gm20708	predicted gene 20708	10.0	6.1	1.6	0.002
484	Vsir	V-set immunoregulatory receptor	6.1	3.8	1.6	0.002
485	Csf1	colony stimulating factor 1 (macrophage)	8.0	4.9	1.6	0.002
486	Tgfbr1	transforming growth factor, beta receptor I	8.1	5.0	1.6	0.002
487	Man2b1	mannosidase 2, alpha B1	12.2	7.6	1.6	0.002
488	Cebpd	CCAAT/enhancer binding protein (C/EBP), delta	6.8	4.2	1.6	0.017
489	Map3k14	mitogen-activated protein kinase kinase kinase 14	2.0	1.3	1.6	0.019
490	Spata13	spermatogenesis associated 13	5.6	3.5	1.6	0.002
491	Vwa5a	von Willebrand factor A domain containing 5A	1.5	0.9	1.6	0.035
492	Fmnl3	formin-like 3	4.4	2.8	1.6	0.002
493	Gpr6	G protein-coupled receptor 6	7.5	4.7	1.6	0.019
494	Olfml3	olfactomedin-like 3	5.7	3.6	1.6	0.004
495	Tcirg1	T cell, immune regulator 1, ATPase, H+ transporting, lysosomal V0 protein A3	6.3	3.9	1.6	0.012
496	Ucp2	uncoupling protein 2 (mitochondrial, proton carrier)	45.8	28.8	1.6	0.002
497	Tnfaip3	tumor necrosis factor, alpha-induced protein 3	1.7	1.1	1.6	0.043
498	Fam46a	family with sequence similarity 46, member A	3.4	2.1	1.6	0.006
499	Slco2b1	solute carrier organic anion transporter family, member 2b1	10.6	6.7	1.6	0.014
500	Cp	ceruloplasmin	5.7	3.6	1.6	0.043
501	Sla	src-like adaptor	4.2	2.7	1.6	0.012
502	Actn2	actinin alpha 2	3.9	2.5	1.6	0.014
503	Rgs9	regulator of G-protein signaling 9	21.3	13.5	1.6	0.002
504	Sipa1	signal-induced proliferation associated gene 1	6.1	3.8	1.6	0.006
505	Tifa	TRAF-interacting protein with forkhead-associated domain	11.3	7.1	1.6	0.017

506	Anxa3	annexin A3	9.1	5.8	1.6	0.039
507	Edem1	ER degradation enhancer, mannosidase alpha-like 1	4.8	3.1	1.6	0.004
508	Cmpk2	cytidine monophosphate (UMP-CMP) kinase 2, mitochondrial	13.6	8.7	1.6	0.002
509	Shisa5	shisa family member 5	36.0	23.0	1.6	0.004
510	Tgfbr2	transforming growth factor, beta receptor II	7.6	4.9	1.6	0.002
511	Clic5	chloride intracellular channel 5	2.8	1.8	1.6	0.006
512	Stxbp2	syntaxin binding protein 2	4.4	2.8	1.6	0.004
513	Capn3	calpain 3	8.0	5.1	1.6	0.006
514	Ganc	glucosidase, alpha; neutral C	8.0	5.1	1.6	0.006
515	Ets1	E26 avian leukemia oncogene 1, 5' domain	4.6	3.0	1.5	0.002
516	Cpne7	copine VII	10.9	7.1	1.5	0.012
517	Foxo6	forkhead box O6	9.2	6.0	1.5	0.008
518	Cflar	CASP8 and FADD-like apoptosis regulator	5.1	3.3	1.5	0.004
519	Vwf	Von Willebrand factor	2.3	1.5	1.5	0.014
520	Ppp1r1b	protein phosphatase 1, regulatory (inhibitor) subunit 1B	151.9	99.7	1.5	0.002
521	Ppp1r18	protein phosphatase 1, regulatory subunit 18	3.9	2.5	1.5	0.021
522	Rem2	rad and gem related GTP binding protein 2	10.2	6.7	1.5	0.040
523	Slfn5	schlafen 5	3.2	2.1	1.5	0.027
524	Hs3st4	heparan sulfate (glucosamine) 3-O-sulfotransferase 4	15.6	10.4	1.5	0.016
525	Zfp366	zinc finger protein 366	2.0	1.3	1.5	0.049
526	Serpina3n	serine (or cysteine) peptidase inhibitor, clade A, member 3N	18.2	12.2	1.5	0.012
527	Clic1	chloride intracellular channel 1	17.5	11.8	1.5	0.024
528	Gm5552	predicted gene 5552	21.3	14.4	1.5	0.022
529	Prom1	prominin 1	11.2	7.6	1.5	0.008
530	Drd1	dopamine receptor D1	10.4	7.0	1.5	0.014
531	Vasp	vasodilator-stimulated phosphoprotein	8.5	5.8	1.5	0.039
532	Itgb5	integrin beta 5	25.4	17.3	1.5	0.002
533	Pald1	phosphatase domain containing, paladin 1	4.3	2.9	1.5	0.046
534	Klf2	Kruppel-like factor 2 (lung)	8.8	6.0	1.5	0.049
535	Zfp36l2	zinc finger protein 36, C3H type-like 2	12.3	8.4	1.5	0.008
536	Ly6c1	lymphocyte antigen 6 complex, locus C1	31.0	21.2	1.5	0.017
537	Parp11	poly (ADP-ribose) polymerase family, member 11	6.3	4.3	1.5	0.025
538	Junb	jun B proto-oncogene	56.1	38.8	1.4	0.002
539	Gng7	guanine nucleotide binding protein (G protein), gamma 7	83.0	57.4	1.4	0.002

540	Pnpla2	patatin-like phospholipase domain containing 2	14.5	10.1	1.4	0.017
541	Crym	crystallin, mu	34.8	24.2	1.4	0.017
542	Drd2	dopamine receptor D2	12.2	8.6	1.4	0.024
543	Miat	myocardial infarction associated transcript (non-protein coding)	7.6	5.3	1.4	0.022
544	Syndig1l	synapse differentiation inducing 1 like	18.2	12.7	1.4	0.008
545	Pabpc1	poly(A) binding protein, cytoplasmic 1	67.8	47.7	1.4	0.004
546	Rcn1	reticulocalbin 1	19.7	13.9	1.4	0.008
547	Ogfr	opioid growth factor receptor	18.3	12.9	1.4	0.019
548	Ccnd2	cyclin D2	13.1	9.2	1.4	0.008
549	Trafd1	TRAF type zinc finger domain containing 1	19.1	13.5	1.4	0.021
550	Lap3	leucine aminopeptidase 3	38.7	27.4	1.4	0.008
551	Nfkbia	nuclear factor of kappa light polypeptide gene enhancer in B cells inhibitor, alpha	17.8	12.7	1.4	0.047
552	Tmem158	transmembrane protein 158	46.8	33.3	1.4	0.016
553	Sgk1	serum/glucocorticoid regulated kinase 1	52.9	38.0	1.4	0.016
554	Rasd2	RASD family, member 2	49.8	35.9	1.4	0.012
555	Cmtm6	CKLF-like MARVEL transmembrane domain containing 6	12.2	8.8	1.4	0.047
556	Ctso	cathepsin O	14.7	10.7	1.4	0.045
557	Apcdd1	adenomatosis polyposis coli down-regulated 1	16.3	11.9	1.4	0.035
558	Pde10a	phosphodiesterase 10A	28.5	20.9	1.4	0.016
559	Vim	vimentin	51.5	37.7	1.4	0.022
560	Penk	preproenkephalin	123.6	91.6	1.4	0.035
561	Hpca	hippocalcin	319.2	240.0	1.3	0.029
562	Ighv3-7	immunoglobulin heavy variable V3-7	362.76	0	362.8*	0.002
563	Ighv1-23	immunoglobulin heavy variable V1-23	127.24	0	127.2*	0.002
564	Ighv7-4	immunoglobulin heavy variable 7-4	66.232	0	66.2*	0.002
565	Cd36	CD36 molecule	62.432	0	62.4*	0.002
566	Ighv8-11	immunoglobulin heavy variable V8-11	51.655	0	51.7*	0.002
567	Ighj3	immunoglobulin heavy joining 3	46.688	0	46.7*	0.002
568	Igkv4-79	immunoglobulin kappa variable 4-79	31.287	0	31.3*	0.002
569	Igkv4-55	immunoglobulin kappa variable 4-55	30.922	0	30.9*	0.002
570	Ighv5-1	immunoglobulin heavy variable V5-1	28.409	0	28.4*	0.002
571	Ighv1-15	immunoglobulin heavy variable 1-15	26.965	0	27.0*	0.002
572	Igkv4-70	immunoglobulin kappa chain variable 4-70	23.142	0	23.1*	0.002
573	Ighv8-12	immunoglobulin heavy variable V8-12	22.513	0	22.5*	0.002
574	Ighv8-8	immunoglobulin heavy variable 8-8	19.763	0	19.8*	0.002

575	Igkv8-24	immunoglobulin kappa chain variable 8-24	19.503	0	19.5*	0.002
576	Ighv2-3	immunoglobulin heavy variable 2-3	19.382	0	19.4*	0.002
577	Ighv14-2	immunoglobulin heavy variable 14-2	18.354	0	18.4*	0.002
578	Ighv3-8	immunoglobulin heavy variable V3-8	12.283	0	12.3*	0.002
579	Hk3	hexokinase 3	11.608	0	11.6*	0.002
580	Ighv3-6	immunoglobulin heavy variable 3-6	10.716	0	10.7*	0.002
581	Igkv11-125	immunoglobulin kappa variable 11-125	9.8226	0	9.8*	0.002
582	Ighv5-4	immunoglobulin heavy variable 5-4	9.6361	0	9.6*	0.002
583	Igkv19-93	immunoglobulin kappa chain variable 19-93	9.5507	0	9.6*	0.002
584	Igkv14-111	immunoglobulin kappa variable 14-111	9.3332	0	9.3*	0.002
585	Ighv14-3	immunoglobulin heavy variable V14-3	9.2427	0	9.2*	0.002
586	Ighv1-2	immunoglobulin heavy variable 1-2	8.6623	0	8.7*	0.002
587	Igkv12-98	immunoglobulin kappa variable 12-98	8.2157	0	8.2*	0.002
588	Igkv5-48	immunoglobulin kappa variable 5-48	7.7549	0	7.8*	0.002
589	Igkv4-91	immunoglobulin kappa chain variable 4-91	7.5363	0	7.5*	0.002
590	Igkv12-89	immunoglobulin kappa chain variable 12-89	7.1016	0	7.1*	0.002
591	Prss36	protease, serine 36	6.7912	0	6.8*	0.002
592	Ighv9-1	immunoglobulin heavy variable 9-1	6.029	0	6.0*	0.002
593	Ripk3	receptor-interacting serine-threonine kinase 3	5.6406	0	5.6*	0.002
594	Ighv2-6	immunoglobulin heavy variable 2-6	5.4818	0	5.5*	0.002
595	Ighv6-6	immunoglobulin heavy variable 6-6	4.8594	0	4.9*	0.002
596	Ly6i	lymphocyte antigen 6 complex, locus I	4.5933	0	4.6*	0.002
597	Gm15056	predicted gene 15056	4.4147	0	4.4*	0.002
598	Ighv3-1	immunoglobulin heavy variable 3-1	4.2816	0	4.3*	0.002
599	Igkv4-53	immunoglobulin kappa variable 4-53	4.2122	0	4.2*	0.002
600	Ighv2-9	immunoglobulin heavy variable 2-9	4.1406	0	4.1*	0.002
601	Ighv1-7	immunoglobulin heavy variable V1-7	4.0322	0	4.0*	0.002
602	Gm19585	predicted gene, 19585	4.028	0	4.0*	0.002
603	Tram2	translocating chain-associating membrane protein 2	3.7758	0	3.8*	0.002
604	Igkv1-88	immunoglobulin kappa chain variable 1-88	3.5103	0	3.5*	0.002
605	Ighv2-2	immunoglobulin heavy variable 2-2	3.2643	0	3.3*	0.002
606	Ighv5-9-1	immunoglobulin heavy variable 5-9-1	3.2483	0	3.2*	0.002
607	Igkv1-133	immunoglobulin kappa variable 1-133	3.2212	0	3.2*	0.002
608	Ighv5-12	immunoglobulin heavy variable 5-12	3.2161	0	3.2*	0.002
609	Igkv4-86	immunoglobulin kappa variable 4-86	3.1689	0	3.2*	0.002
610	Igkv2-137	immunoglobulin kappa chain variable 2-137	3.1416	0	3.1*	0.002

611	Ighv1-67	immunoglobulin heavy variable V1-67	3.1029	0	3.1*	0.002
612	Card11	caspase recruitment domain family, member 11	3.0604	0	3.1*	0.002
613	Ighv2-5	immunoglobulin heavy variable 2-5	3.0488	0	3.0*	0.002
614	Cd226	CD226 antigen	2.9088	0	2.9*	0.002
615	Ighv4-1	immunoglobulin heavy variable 4-1	2.8127	0	2.8*	0.002
616	F830016B08Rik	RIKEN cDNA F830016B08 gene	2.7413	0	2.7*	0.002
617	Gm4951	predicted gene 4951	2.6254	0	2.6*	0.002
618	Slfn9	schlafen 9	2.5991	0	2.6*	0.002
619	Igkv9-120	immunoglobulin kappa chain variable 9-120	2.4928	0	2.5*	0.002
620	C1s2	complement component 1, s subcomponent 2	2.2522	0	2.3*	0.002
621	Ighv14-1	immunoglobulin heavy variable 14-1	2.2388	0	2.2*	0.002
622	Ighv13-2	immunoglobulin heavy variable 13-2	2.1537	0	2.2*	0.002
623	Ighv1-50	immunoglobulin heavy variable 1-50	2.0933	0	2.1*	0.002
624	Ighv1-4	immunoglobulin heavy variable 1-4	2.0252	0	2.0*	0.002
625	Ighv10-1	immunoglobulin heavy variable 10-1	1.8939	0	1.9*	0.002
626	Arhgap8	Rho GTPase activating protein 8	1.8536	0	1.9*	0.002
627	Mir146	microRNA 146	1.8509	0	1.9*	0.002
628	F830016B08Rik	RIKEN cDNA F830016B08 gene	1.8306	0	1.8*	0.002
629	Grap2	GRB2-related adaptor protein 2	1.7886	0	1.8*	0.002
630	Gm43291	predicted gene, 30211	1.6908	0	1.7*	0.002
631	Il18r1	interleukin 18 receptor 1	1.6891	0	1.7*	0.002
632	Ighv7-3	immunoglobulin heavy variable 7-3	1.6751	0	1.7*	0.002
633	Ubash3a	ubiquitin associated and SH3 domain containing, A	1.5583	0	1.6*	0.002
634	Ighv1-66	immunoglobulin heavy variable 1-66	1.4273	0	1.4*	0.002
635	Trbv1	T cell receptor beta, variable 1	1.4075	0	1.4*	0.002
636	Igkv3-2	immunoglobulin kappa variable 3-2	1.395	0	1.4*	0.002
637	Mir146	microRNA 146	1.3074	0	1.3*	0.002
638	Mcpt2	mast cell protease 2	1.2943	0	1.3*	0.002
639	Igkv2-112	immunoglobulin kappa variable 2-112	1.2895	0	1.3*	0.002
640	Slamf1	signaling lymphocytic activation molecule family member 1	1.2808	0	1.3*	0.002
641	Gm44257	predicted gene, 44257	1.2625	0	1.3*	0.010
642	Clec5a	C-type lectin domain family 5, member a	1.2312	0	1.2*	0.002
643	Irf4	interferon regulatory factor 4	1.2258	0	1.2*	0.002
644	Ighv7-2	immunoglobulin heavy variable 7-2	1.2037	0	1.2*	0.002
645	Mcpt1	mast cell protease 1	1.1724	0	1.2*	0.002
646	Gm43291	predicted gene, 30211	1.0998	0	1.1*	0.002

647	Irgm1	immunity-related GTPase family M member 1	1.0472	0	1.0*	0.002
648	Vhl-ps1	von Hippel-Lindau tumor suppressor-like, pseudogene 1	1.0294	0	1.0*	0.002
649	H2-Eb2	histocompatibility 2, class II antigen E beta2	0.9923	0	1.0*	0.002
650	Cd226	CD226 antigen	0.8913	0	0.9*	0.002
651	Klrk1	killer cell lectin-like receptor subfamily K, member 1	0.8777	0	0.9*	0.002
652	Slamf7	SLAM family member 7	0.8315	0	0.8*	0.008
653	Slfn8	schlafen 8	0.8303	0	0.8*	0.002
654	Il2rb	interleukin 2 receptor, beta chain	0.8159	0	0.8*	0.002
655	Iglv3	immunoglobulin lambda variable 3	0.811	0	0.8*	0.002
656	Gm2564	predicted gene 2564	0.8009	0	0.8*	0.002
657	Olfr56	olfactory receptor 56	0.7622	0	0.8*	0.002
658	9330175E14Rik	RIKEN cDNA 9330175E14 gene	0.7218	0	0.7*	0.002
659	Dexi	dexamethasone-induced transcript	0.6427	0	0.6*	0.002
660	Gpr132	G protein-coupled receptor 132	0.6181	0	0.6*	0.002
661	Ikzf3	IKAROS family zinc finger 3	0.5331	0	0.5*	0.002
662	Mcm10	minichromosome maintenance 10 replication initiation factor	0.5124	0	0.5*	0.002
663	Pyhin1	interferon activated gene 209	0.4508	0	0.5*	0.002